Institut für Erd-und Umweltwissenschaften
Mathematisch-Naturwissenschaftliche Fakultät
Universität Potsdam

DFG GRK 1364
Interactions between Tectonics, Climate and the Biosphere in the African-Asian Monsoonal Region

Quantifying crystalline exhumation in the Himalaya

Franziska Daniela Helena Wilke

Kumulative Dissertation
zur Erlangung des akademischen Grades "doctor rerum naturalium"
(Dr. rer. nat.)
in der Wissenschaftsdisziplin "Mineralogie/Petrologie"

Potsdam, im Februar 2010

Published online at the
Institutional Repository of the University of Potsdam:
URL http://opus.kobv.de/ubp/volltexte/2010/4313/
URN urn:nbn:de:kobv:517-opus-43138
http://nbn-resolving.org/urn:nbn:de:kobv:517-opus-43138

Abstract

In 1915, Alfred Wegener published his hypotheses of plate tectonics that revolutionised the world for geologists. Since then, many scientists have studied the evolution of continents and especially the geologic structure of orogens: the most visible consequence of tectonic processes. Although the morphology and landscape evolution of mountain belts can be observed due to surface processes, the driving force and dynamics at lithosphere scale are less well understood despite the fact that rocks from deeper levels of orogenic belts are in places exposed at the surface. In this thesis, such formerly deeply-buried (ultra-) high-pressure rocks, in particular eclogite facies series, have been studied in order to reveal details about the formation and exhumation conditions and rates and thus provide insights into the geodynamics of the most spectacular orogenic belt in the world: the Himalaya. The specific area investigated was the Kaghan Valley in Pakistan (NW Himalaya).

Following closure of the Tethyan Ocean by ca. 55-50 Ma, the northward subduction of the leading edge of India beneath the Eurasian Plate and subsequent collision initiated a long-lived process of intracrustal thrusting that continues today. The continental crust of India – granitic basement, Paleozoic and Mesozoic cover series and Permo-Triassic dykes, sills and lavas – has been buried partly to mantle depths. Today, these rocks crop out as eclogites, amphibolites and gneisses within the Higher Himalayan Crystalline between low-grade metamorphosed rocks (600-640°C/ ca. 5 kbar) of the Lesser Himalaya and Tethyan sediments. Beside tectonically driven exhumation mechanisms the channel flow model, that describes a denudation focused ductile extrusion of low viscosity material developed in the middle to lower crust beneath the Tibetan Plateau, has been postulated. To get insights into the lithospheric and crustal processes that have initiated and driven the exhumation of this (ultra-) high-pressure rocks, mineralogical, petrological and isotope-geochemical investigations have been performed. They provide insights into 1) the depths and temperatures to which these rocks were buried, 2) the pressures and temperatures the rocks have experienced during their exhumation, 3) the timing of these processes 4) and the velocity with which these rocks have been brought back to the surface.

In detail, through microscopical studies, the identification of key minerals, microprobe analyses, standard geothermobarometry and modelling using an effective bulk rock composition it has been shown that published exhumation paths are incomplete. In particular, the eclogites of the northern Kaghan Valley were buried to depths of 140-100 km (36-30 kbar) at 790-640°C. Subsequently, cooling during decompression (exhumation)

towards 40-35 km (17-10 kbar) and 630-580°C has been superseded by a phase of reheating to about 720-650°C at roughly the same depth before final exhumation has taken place. In the southern-most part of the study area, amphibolite facies assemblages with formation conditions similar to the deduced reheating phase indicate a juxtaposition of both areas after the eclogite facies stage and thus a stacking of Indian Plate units.

Radiometric dating of zircon, titanite and rutile by U-Pb and amphibole and micas by Ar-Ar reveal peak pressure conditions at 47-48 Ma. With a maximum exhumation rate of 14 cm/a these rocks reached the crust-mantle boundary at 40-35 km within 1 Ma. Subsequent exhumation (46-41 Ma, 40-35 km) decelerated to ca. 1 mm/a at the base of the continental crust but rose again to about 2 mm/a in the period of 41-31 Ma, equivalent to 35-20 km. Apatite fission track (AFT) and (U-Th)/He ages from eclogites, amphibolites, micaschists and gneisses yielded moderate Oligocene to Miocene cooling rates of about 10°C/Ma in the high altitude northern parts of the Kaghan Valley using the mineral-pair method. AFT ages are of 24.5±3.8 to 15.6±2.1 Ma whereas apatite (U-Th)/He analyses yielded ages between 21.0±0.6 and 5.3±0.2 Ma. The southern-most part of the Valley is dominated by younger late Miocene to Pliocene apatite fission track ages of 7.6±2.1 and 4.0±0.5 Ma that support earlier tectonically and petrologically findings of a juxtaposition and stack of Indian Plate units. As this nappe is tectonically lowermost, a later distinct exhumation and uplift driven by thrusting along the Main Boundary Thrust is inferred.

A multi-stage exhumation path is evident from petrological, isotope-geochemical and low temperature thermochronology investigations. Buoyancy driven exhumation caused an initial rapid exhumation: exhumation as fast as recent normal plate movements (ca. 10 cm/a). As the exhuming units reached the crust-mantle boundary the process slowed down due to changes in buoyancy. Most likely, this exhumation pause has initiated the reheating event that is petrologically evident (e.g. glaucophane rimmed by hornblende, ilmenite overgrowth of rutile). Late stage processes involved widespread thrusting and folding with accompanied regional greenschist facies metamorphism, whereby contemporaneous thrusting on the Batal Thrust (seen by some authors equivalent to the MCT) and back sliding of the Kohistan Arc along the inverse reactivated Main Mantle Thrust caused final exposure of these rocks. Similar circumstances have been seen at Tso Morari, Ladakh, India, 200 km further east where comparable rock assemblages occur. In conclusion, as exhumation was already done well before the initiation of the monsoonal system, climate dependent effects (erosion) appear negligible in comparison to far-field tectonic effects.

Zusammenfassung

Seit der von Alfred Wegener 1915 postulierten Hypothese der Plattentektonik haben viele Forscher Anstrengungen unternommen die Entstehungsgeschichte und den geologischen Aufbau von Gebirgen nachzuvollziehen. Oberflächennahe Abläufe sind ansatzweise verstanden, während Prozesse im Erdinneren weit weniger bekannt sind. Informationen hierüber können jedoch aus den Gesteinen, ihren Mineralen und wiederum deren chemischen Komponenten gewonnen werden, da diese die Entstehung und Entwicklung der Gebirgsbildung "miterlebt", und wichtige Informationen gespeichert haben. In dieser Arbeit wurden dazu exemplarisch (Ultra-) Hochdruckgesteine ((U-)HP), sogenannte Eklogite, und deren Umgebungsgesteine aus dem nordwestlichen Himalaja, insbesondere aus dem Kaghan Tal in Pakistan untersucht um den Exhumationsprozess von tief subduzierten Krustengesteinen im allgemeinen, und im Hinblick auf mögliche klimabedingte Einflüsse, besser zu verstehen.

Die Bildung des Himalajas ist auf die Versenkung, eines südlich der eurasischen Platte angesiedelten Ozeans, der Tethys, und die nachfolgende Kollision Indiens mit dem Eurasischen Kontinent vor und seit etwa 50-55 Millionen Jahre zurück zu führen. Dabei wurden kalter, dichter Ozeanboden und leichtere Krustensegmente rasch in große Tiefen subduziert. Heute sind diese Hochdruck- und ultra Hochdruckgesteine in einigen Bereichen des Himalaja zwischen schwach metamorph überprägten (600-640°C/ca. 5 kbar) Gesteinen und alten Sedimenten der Tethys aufgeschlossen. Anhand von petrographischen, mineral-chemischen, petrologischen und isotopen-geochemischen Untersuchungen dieser (Ultra) Hochdruckgesteine konnte ich zeigen, dass 1) die Gesteine in über 100 km Tiefe also bis in den Erdmantel vordrangen, 2) sie bei ihrem Aufstieg in Krustenbereiche von 40-35 km zuerst von 790-640°C auf 630-580°C abgekühlten um danach wieder auf 720-650°C aufgeheizt zu werden, sie 3) innerhalb von 700.000 Jahren um mindestens 60 km Richtung Erdoberfläche exhumiert wurden und somit 4) Geschwindigkeiten von 9-14 cm pro Jahr erreichten, die der normaler Plattengeschwindigkeiten (>10 cm/a) entspricht, wobei sich 5) dieser Prozess ab 40-35 km auf 0.1-0.2 cm/a stark verlangsamte und auch 6) ab einer Tiefe von 6 km bis zur Erdoberfläche keine, z. B. niederschlagsbedingt, erhöhte Abkühlungsrate zu erkennen ist.

Eine schnelle initiale Exhumierung erfolgte durch den Dichteunterschied von leichtem, subduzierten Krustengestein zum dichteren Mantel. Dieser Prozess kam an der Krusten-Mantel-Grenze nahezu zum erliegen, einhergehend mit einer sekundären Aufheizung des Gesteins und wurde, jedoch weit weniger schnell, durch die Kollision der beiden Kontinente Eurasien und Indien und dadurch bedingte Überschiebungen, Faltungen und gravitative Abschiebungen fortgesetzt, die Gesteine zur Oberfläche transportiert und dort freigelegt. Eine erosions- und damit klimabedingte Beschleunigung oder gar gänzlich davon abhängige kontinuierliche Exhumation konnte in dieser Region des Himalajas nicht bestätigt werden. Vielmehr belegen die Daten eine mehrstufige Exhumation wie sie auch im Tso Morari Gebiet (NW Indien) angenommen wird, für weitere Ultrahochdruckareale wie, z. B. das Kokchetav Massif (Kasachstan), den Dabie Shan (China) oder den europäischen Varisziden (z. B. Böhmisches Massiv) jedoch noch geklärt werden muss, um generell gültige Mantel- und Krustenprozesse abzuleiten.

Danksagung

In diesem kurzen Abschnitt möchte ich gerne allen Menschen danken, die mir während der Zeit der Doktorarbeit mit Rat & Tat, Zuspruch & Kritik und Geduld & Ansporn zur Seite standen.

Primär gilt mein persönlicher Dank Patrick O'Brien der mich immer wieder auf die richtigen Bahnen lenkte, mich über Stunden am Mikroskop und in Diskussionen Petrologie und Petrographie von Eklogiten lehrte um sich dann letztlich doch noch mit rezenter Tektonik und Klima auseinanderzusetzen. Uwe Altenberger danke ich für sein unerschütterliches Verständnis, seine Motivation, seine wiederbelebende Ruhe und für diverse Espressozeremonien.

Besonderen Dank gebührt auch Martin Timmerman und Matthias Konrad-Schmolke für Diskussionen in allen Stadien dieser Arbeit und Roland Oberhänsli für Hilfe in "politischen" Fragen und die Einsicht, dass man sich Stress nur immer selbst macht.

Katrin Rehak, Annett Junginger, Astrid Riemann, Gabriela Marcano, Julia Nckel und Saswati Sarkar danke ich herzlich für die arbeitsreichen, aber dennoch aufheiternden und in allen Lebenslagen "süßen" Stunden in unserem gemeinsamen Büro. Lydia Olaka, Manuela Borchert, Henry Wichura, Esther Fußeis, Alexandra Roy, Veronica Torres Acosta und Amaury Pourteau sage ich Dank für gelegentliche Besuche in der zweiten Etage, für tiefgründige Gespräche auf dem Weg zur und in der Uni und für den guten Zusammenhalt während diverser Exkursionen.

Axel Gerdes von der Universität Frankfurt gebührt Dank für lehr- und wortreiche Stunden an der Laser–ICP-MS, Christine Fischer für ihre Ideen zu Preparationstechniken, Martin Ziemann für die dunklen Stunden am Ramanspektrometer, Masafumi Sudo für die Einweisung in die Geheimnisse der Ar-Ar Messung, Gerold Zeilinger für Diskussionen rund um Tektonik und Spaltspuren und Ed Sobel für das geduldige Einarbeiten in die Präparation von Apatiten und das Auszählen der Spaltspuren in denselbigen.

Bei der deutschen Forschungsgemeinschaft (DFG) und dem gesamten Graduiertenkolleg (GK 1364) um Manfred Strecker möchte ich mich für die Finanzierung dieser Arbeit und den damit in Zusammenhang stehenden gemeinschaftlichen Unternehmungen (Exkusionen, Konferenzen, Tagungen) bedanken, die meinen Horizont geologisch wie interkulturel stark erweitert haben.

Contents

Mihi enim liber non videtur, qui non aliquando nihil agit. (Cicero)

1. Introduction

Orogenic belts are essentially a product of subduction–collision processes generally accompanied by partial loss of lithosphere (Ernst, 2001). In the so-called Pacific–type, found in circum–Pacific orogenic belts, long-term subduction of oceanic crust into the mantle is linked to the formation of an accretionary prism within which high-pressure (HP) metamorphism of ocean floor–, trench– and fore-arc sequences reaches blueschist and locally low-temperature eclogite facies conditions. In contrast, Alpine–type orogenic belts involve consumption of an intervening oceanic plate followed by the approach and collision of a continent, microcontinent, or island arc. In some cases, the leading edge of the colliding body may be dragged down to mantle depths leading to high– or even ultra high-pressure (UHP) metamorphism of felsic continental material, although such relatively low density material is generally rapidly exhumed (Ernst, 2001). This simplified but nonetheless generally valid mechanism for compressional mountain belts raises questions about the rates and mechanisms of exhumation processes pertaining to UHP metamorphic complexes now recognised worldwide (e.g. European Variscides; Dabie Shan/Sulu, China; NW Himalaya).

At least two models have been proposed for continental collisions producing UHP rocks in general and for the Himalayan belt in particular. In one model (Chemenda et al., 2000), the buoyancy of the subducted crustal material results in the separation of the upper to middle crustal material from its underlying more basic and thus denser lower crust and upper mantle. Such a process leads to stacking of upper crustal material, jamming of the subduction zone and perhaps even to the formation of a local tear in the lithosphere, which could lead to slab break-off. Subsequent convergence would thus involve a shallower angle of subduction. In addition, upwelling of asthenospheric mantle due to slab break-off causes short-lived heating of the lowermost crustal units. This type of subduction-collision model predicts UHP rock units tectonically uppermost in a crustal-stacked sequence above units that never experienced UHP conditions. Syncompressional initiation of normal faults and back sliding of formerly stacked nappes will force a continuous ascent and emergence of deeply buried rocks (e.g. Patriat&Achache, 1984; Chemenda et al., 2000; Ernst, 2001; Treloar et al., 2003).

A second group of models is based on the general observation in the central Himalaya (e.g. Le Fort, 1975) that high-grade crystalline units occur between an overlying much lower grade sequence, separated by a normal fault, and an underlying

mostly lower-grade unit that exhibits an inverse metamorphic gradient up towards the bounding thrust plane known as the Main Central Thrust (MCT). This situation has been interpreted as showing ductile extrusion of the high-grade units between these bounding faults. Further, the crystalline sequences at depth are interpreted to be channelised between more rigid upper and lower crustal bodies. Such so-called channel-flow models have gained popularity in recent years especially since the publication of a number of numerical simulations of subduction–collision channel-flow processes by the Halifax group (Beaumont et al., 2001; 2004; Warren et al., 2008; Beaumont et al., 2009). An important aspect of the channel-flow extrusion models is the necessity for enhanced erosion at the extrusion front induced by the effect of the monsoon which itself is controlled by the tectonic barrier caused by the uplift of the Tibetan Plateau to the north of the exposed crystalline sequences. Also important for the channel-flow models is the presence of partial melt in the crystalline sequences, which requires a time interval between the start of crustal stacking and the attainment of temperatures necessary for anatexis in the Indian plate middle and upper crustal rocks. Important to recognise in both models is the transition from subduction–related to collision–related processes, and thus from generally low dT/dP to high dT/dP metamorphic conditions, which commonly causes multi-stage metamorphic overprints and thus makes reconstruction of P–T paths difficult.

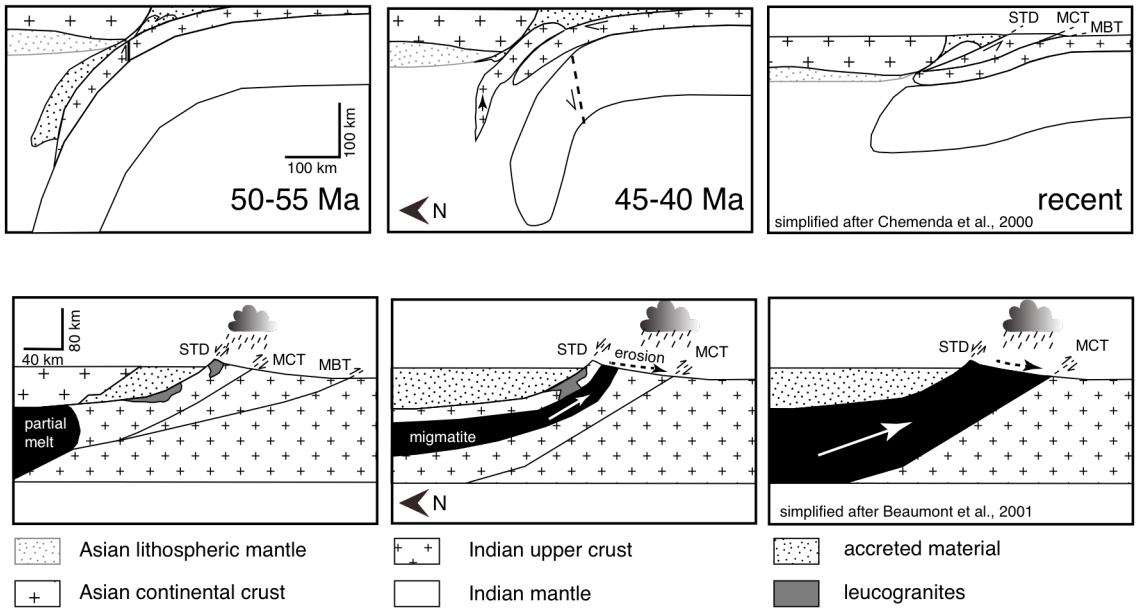

The ability to constrain exhumation paths and mechanisms of deeply buried rocks (England & Holland, 1979; Ernst et al., 1997; Davis & von Blanckenburg, 1995;

Chemenda et al., 2000; Liou et al., 2004; Warren et al., 2008; Beaumont et al., 2009) is always dependent on the temporal change of physical conditions. Unfortunately, the scarcity of complete data for the large-scale pattern of maximum metamorphic grade, age of metamorphic stages, cooling and exhumation rates introduces large uncertainties in geological models and reconstructions. Especially problematic is the dating of high pressure stages in HP and UHP rocks which is limited by problems such as: (1) the multi-stage evolution of these rocks, often resulting in multiple generations or partial resetting of datable minerals (DiVincenzo et al., 2003; Villa et al., 2000); (2) the presence of excess argon in the important index mineral phengite thus preventing a meaningful interpretation (Blankenburg et al., 1989; Boundy et al., 1997; Sherlock & Arnaud, 1999); and (3) the common difficulty of directly linking the age of datable minerals to a discrete part of the metamorphic history (Dahl, 1996; Villa, 1997; Cherniak et al., 2000; Harrison et al., 2009). The determination of a reliable pressure–temperature–time path requires the integration of detailed petrography, microprobe analysis (including compositional zoning information), geothermobarometry, thermodynamic forward modelling (to incorporate fractionation and zoning information) and isotope analysis of phases recording age information from both high- and low-pressure stages.

The question of whether climatic conditions can influence tectonic processes and thus control the rate of exhumation, can only be answered with detailed information about the style and time scale of exhumation as well as the temporal and spatial changes in precipitation, relief and fluvial vs. glacial processes. In this project, I combined a study of the petrology, isotope geochemistry and thermochronology of (ultra) high-pressure rocks in order to quantify the short- and long-term exhumation processes that have taken place during the Tertiary in the tectonically active and climatically influenced Himalayan mountain belt, in particular in the Kaghan Valley, Pakistan, north-west Himalaya. This thesis presents new findings concerning (1) the multi-stage pressure-temperature-time path of eclogites and their hosts in the Higher Himalayan Crystalline nappes, (2) the accompanied exhumation rates, and (3) subsequent tectonic implications.

Chapter 2 focuses on the different metabasite types that have been sampled in the Upper Kaghan Valley. Five distinct types were identified based on micro-structural differences and variations in the degree of alteration. Bulk rock major-, trace- and rare

earth element analysis was undertaken in order to determine the protoliths. Furthermore, I studied in detail the macro- and microscopic textures and structures to characterise mineral parageneses and mineral reactions and thus delineate the retrograde as well as prograde history. Important was the confirmation of the presence of the high-pressure polymorph of SiO_2, coesite, in some samples as the simple occurrence of this phase indicates ultra high-pressure conditions. This was undertaken by *in-situ* micro-Raman spectroscopy. These ultra high-pressure conditions have been further confirmed both by standard geothermobarometry using actual mineral compositions as well as in phase diagrams, using internally consistent thermodynamic data, modelled on the basis of an effective bulk rock composition. Besides addressing the geochemical and petrological evolution of the different protoliths, the conditions of metamorphism, the preservation potential of the rocks and the distinct growth episodes of minerals, I also discuss the possibility whether the deduced formation and exhumation processes of these ultra high-pressure metamorphic series are comparable to those postulated for similar rocks elsewhere in the Himalaya.

In chapter 3, I present Ar-Ar and U-Pb radiometric ages on accessory and rock forming minerals. The dating program was integrated with the petrological and petrographical investigations and carried out in order to obtain information about the time span and velocities of distinguishable stages of the exhumation path. The timing and duration of peak metamorphism, subsequent exhumation and partial relaxation prior to final exposure have also been determined. Subsequently, I constructed a relatively well-constrained pressure-temperature-time path for the Kaghan rocks. The resulting path was compared to that expected from the regional tectonic context. The new and previously published ages are critically discussed with regard to closure temperatures, partial resetting and fluid-induced relaxation of isotopic systems. Finally, the causes of the changes in exhumation rates are addressed and compared to recently derived models and existing theories.

In chapter 4, I present results about the low-temperature history of the rocks from the Upper Kaghan Valley from both high (4300 m) and relatively low (3200 m) altitudes. Apatite fission track analyses were carried out in combination with zircon and apatite U-Th/He analyses on UHP and HP eclogites and gneisses. By comparing the results of both dating methods I was able to quantify the cooling rates for the ultimate exhumation stages, from depths of about 2 to 6 km, to their present surface exposure

level. These ages have been related to both tectonic events in the study area, previously investigated ages and tectonics in neighbouring areas and possible climatic controls.

Each chapter constitutes an individual, yet related manuscript that has either been published, submitted or is in the process of being submitted. Chapter 2 ("Multi-stage history in different eclogite types from the Pakistan Himalaya and implications for exhumation processes" by Franziska D.H Wilke, Patrick J. O'Brien, Uwe Altenberger, Matthias Konrad-Schmolke, M. Ahmed Khan) has been published in Lithos in 2010, already online since August 2009. Chapter 3 ("The multistage exhumation history of the Kaghan Valley UHP series, NW Himalaya, Pakistan from U-Pb and $^{40}Ar/^{39}Ar$ ages" by Franziska D.H. Wilke, Patrick J. O'Brien, Axel Gerdes, Martin J. Timmerman, Masafumi Sudo, M. Ahmed Khan) was submitted to the European Journal of Mineralogy in October 2009. Chapter 4 ("Apatite fission track and (U-Th)/He ages from the Higher Himalayan Crystallines, Kaghan Valley, Pakistan: implications for an Eocene Plateau and Oligocene to Pliocene exhumation" by Franziska D.H. Wilke, Edward R. Sobel, Patrick J. O´Brien) will be submitted soon to The International Journal of Earth Sciences. In chapter 5, I summarise the final results and present some specific as well as more general conclusions. The Appendix lists the analytical methods and additional data to those collected during this study, but which have not been incorporated in any of the manuscripts.

Each manuscript represents a co-operation with a number of colleges, apart from the initiation and realisation of the articles by myself. All laboratory work has been done by me except the (U-Th)/He analyses which were performed by Daniel Stockli (Kansas, USA). M. Ahmed Khan guided the excursion in Pakistan while Patrick O'Brien, Roland Oberhänsli and Robert Reinisch sampled the rocks. With kind assistance of Patrick O'Brien, each manuscript was checked carefully. Uwe Altenberger monitored the geochemistry part and Matthias Konrad-Schmolke helped a lot during the thermodynamic modelling. Martin Timmerman, Masafumi Sudo Axel Gerdes and Edward Sobel supervised my laboratory work and taught me raw data reduction.

2. Multi-stage reaction history in different eclogite types from the Pakistan Himalaya and implications for exhumation processes

Abstract

Metabasites were sampled from rock series of the subducted margin of the Indian Plate, the so-called Higher Himalayan Crystalline, in the Upper Kaghan Valley, Pakistan. These vary from corona dolerites, cropping out around Saif-ul-Muluk in the south, to coesite-eclogite close to the suture zone against rocks of the Kohistan arc in the north. Bulk rock major- and trace- element chemistry reveals essentially a single protolith as the source for five different eclogite types, which differ in fabric, modal mineralogy as well as in mineral chemistry. The study of newly-collected samples reveals coesite (confirmed by in situ Raman spectroscopy) in both garnet and omphacite. All eclogites show growth of amphiboles during exhumation. Within some coesite-bearing eclogites the presence of glaucophane cores to barroisite is noted whereas in most samples porphyroblastic sodic-calcic amphiboles are rimmed by more aluminous calcic amphibole (pargasite, tschermakite, edenite). Eclogite facies rutile is replaced by ilmenite which itself is commonly surrounded by titanite. In addition, some eclogite bodies show leucocratic segregations containing phengite, quartz, zoisite and/or kyanite. The important implication is that the complex exhumation path shows stages of initial cooling during decompression (formation of glaucophane) followed by re-heating: a very similar situation to that reported for the coesite-bearing eclogite series of the Tso Morari massif, India, 450 km to the south-east.

2.1. Introduction

The subduction of Tethys and subsequent collision of India with Asia is well evidenced in the record of crustal thickening, magmatism, multi-stage metamorphism, exhumation and finally extension (back sliding) in rocks of the former margin of the Indian Plate (e.g., Treloar & Searle, 1993; Khan et al., 2000). Although the main metamorphism of the crystalline complexes of the Indian Plate is of amphibolite to granulite facies there are numerous eclogite facies rocks recognised as an integral part of the sequences thus

pointing to a more complex evolution that is only partly preserved (Guillot et al., 1997; de Sigoyer et al., 1997; Lombardo et al., 2000; Lombardo & Rolfo, 2000; O'Brien et al., 2001). These volumetrically-minor eclogite bodies reveal a much greater part of the metamorphic history than their strongly overprinted hosts and are a key to the understanding of rates and magnitudes of dynamic processes active during deep collision and exhumation of continental crust in this archetypal collision orogen (Chemenda et al., 2000; Massonne & O'Brien, 2003; Guillot et al., 2003; Treloar et al., 2003).

The significance of high- (HP) and ultrahigh-pressure (UHP) metamorphism for the understanding of the Himalayan evolution has come about as a result of detailed petrological and geochemical studies initiated in the 1990's in Kaghan Valley, NW Pakistan (Pognante & Spencer, 1991) and Tso Morari, NE India (Guillot et al., 1995; de Sigoyer et al., 1997). Subsequent intensified investigation of the geochemical, petrological and geochronological features of the eclogites and related host rocks (Tonarini et al., 1993; de Sigoyer et al., 2000; Lombardo et al., 2000; Fontan et al., 2000; Kaneko et al., 2003; Treloar et al., 2003; Parrish et al., 2006; Rehman et al., 2007; Guillot et al., 2008) and especially the discovery of coesite, firstly in Kaghan Valley (O'Brien et al., 2001) and shortly after in Tso Morari (Sachan et al., 2004), have revolutionised ideas about the Himalayan subduction–collision process (e.g. Chemenda et al., 2000). The deduced pressure-temperature-time paths for both Kaghan and Tso Morari eclogites show many similarities (Massonne & O'Brien, 2003; Parrish et al., 2006; Guillot et al., 2008). The timing of coesite-grade metamorphism, the initial exhumation at cm/a rates, and the cooling below apatite fission track temperatures before the age of peak metamorphism in the typical Higher Himalayan crystalline series of the central Himalaya are remarkably similar. However, there are distinct differences even within a single eclogite-bearing area in the compositions of post-peak pressure amphiboles, garnet compositional zoning patterns, garnet and omphacite grain size, degree of preservation of protolith texture, and in proportions of Ca-rich phases such as epidote, carbonates and titanite. In recent publications on the Kaghan Valley (Rehman et al., 2007, 2008) there is also a great discrepancy between the exhumation path presented for pelitic rocks and that already deduced from the eclogites (Lombardo et al., 2000; O'Brien et al., 2001). Here we present the results of a new, detailed geochemical and petrological investigation of macroscopically different eclogite types from a wide area

of the Kaghan Valley with the aim of testing the validity of the existing, contrasting, pressure-temperature-time paths for the area. In addition, the possibility that eclogites in different nappe units show contrasting evolutions will also be investigated.

2.2. Geologic Setting

Eclogite facies rocks in northern Pakistan occur in the upper Kaghan and Neelum Valleys (Fig. 2.1) as part of the so-called Higher Himalayan Crystallines (HHC). This high-grade metamorphic sequence, part of the Indian plate, is bounded to the north by the Indus Suture (Main Mantle Thrust, MMT) from the mafic/ultramafic rocks of the Kohistan Island Arc, and to the south by the Batal Thrust from lower-grade sequences generally attributed to the Lesser Himalaya (Fig. 2.1). Three main units, which have firstly been described by Chaudhry & Ghazanfar (1987); Greco et al. (1989) and Greco & Spencer (1993), can be identified in the HHC; a basement complex made of metagranite and paragneiss, which is overlain by two sequences of meta-sedimentary cover rocks, a first predominantly metapelite–greywacke-bearing unit and a second stratigraphically younger series with marbles, schists and amphibolites. On the basis of a comparison with unmetamorphosed units in Kashmir, the carbonate-rich sequence is interpreted as Permo-Mesozoic platform cover and the mafic bodies, dykes, sills and lava flows correspond to the extensive Panjal Trap magmatism (Wadia, 1931; Greco & Spencer, 1993).

The large-scale structure in the Upper Kaghan Valley is of a stack of thrust sheets (Treloar et al., 2003; Kaneko et al., 2003). In the north, basement and first cover units structurally overlie rocks belonging to the second cover whereas in the south, at Saif-ul-Muluk, a further basement-bearing unit is tectonically lowermost. East–west-trending open folds of this stacked sequence dominate the present day structural picture but a series of older isoclinal folds are recognised within the basement/first cover unit. The carbonate-rich units of the second cover thus appear as a series of domes protruding through the older sequences and not, as depicted by Kaneko et al. (2003), as a unit structurally overlying basement/first cover. Later deformation related to the exhumation of the high-grade units is reflected by a pervasive north-directed extensional shearing, at high structural levels, close to the MMT (Burg et al., 1996; Treloar et al., 2003). This latter stage is well evidenced by folds involving albite porphyroblasts (often several cm

in length) representing a pervasive greenschist facies overprint in pelitic, granitic and basic rocks.

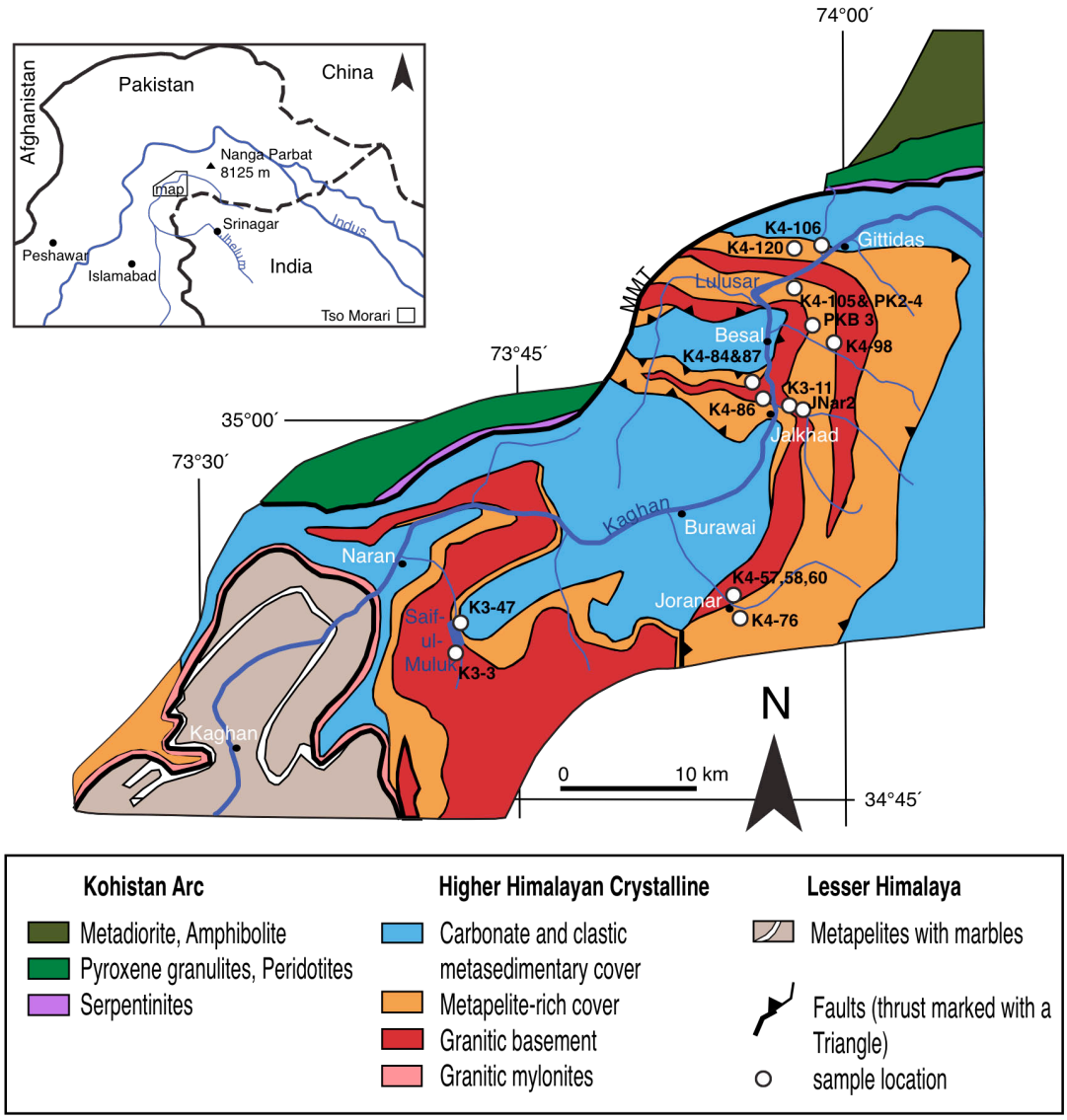

Fig. 2.1. Simplified geological map of upper Kaghan Valley, north Pakistan (modified after Greco & Spencer, 1993; Lombardo et al., 2000) showing locations of investigated eclogites. Inset map shows the regional location.

A regional gradient in metamorphic grade (dominantly high amphibolite facies with garnet, staurolite, kyanite and only very locally sillimanite in metapelites) is postulated by Rehman et al. (2007, 2008), based on a three-nappe structure for Upper Kaghan with the eclogite-bearing unit located between eclogite-free over- and underlying units. However, the tectonic pattern of Rehman et al. (2007, 2008) is inconsistent with several other mapping studies (e.g. Chaudhry & Ghazanfar, 1987;

Treloar et al., 2003; Parrish et al., 2006), which indicate that the eclogite-bearing unit is uppermost. In the eclogites, now seen to be more extensive than previously realised, the much larger collection of material shows that fresh or strongly retrograded samples occur throughout the area with a rough relationship between size of body, position in the body and degree of retrogression. An obvious difference in formation conditions of the eclogites in the northern part of the area is not apparent and will be discussed in detail later. However, further south, near Naran and between Naran and Burawai, many metabasites preserve magmatic textures with only minor corona growth of garnet and no breakdown of plagoclase as would be expected for the conditions reached by the metabasites in the north. The implication is that there is a structural break between the basement units in the north and south.

2. 3. Eclogites and coronitic metabasites of the Kaghan Valley

Several macroscopically distinct eclogite types were identified in the field. In the following section the key petrographic features of these eclogite types will be outlined.

2.3.1 Coarse grained, skarn-like eclogites

The most conspicuous garnet–clinopyroxene rocks in the Kaghan Valley are the skarn-like eclogites (mapped as ultramafic bodies) first recognised by Chaudhry & Ghazanfar (1987), and later studied in more detail by Pognante & Spencer (1991). Typical for this generally unaltered eclogite type are large, dark red garnets several cm in diameter set in a matrix of dark green clinopyroxene (Fig. 2.2A). Some varieties show quartz veins with cm-sized titanite (PKB3) or rutile (K4-60) crystals. Garnet contains abundant inclusions of clinopyroxene (partly replaced by hornblende), rutile (partly replaced by ilmenite and titanite), large idiomorphic titanites, and minor quartz and zircon. Many of these rocks also show irregular patches and streaks of garnetite (Fig. 2.2B), within which lightly-coloured, up to 0.1 mm garnet cores occur in a darker, net-like garnet matrix: minor rutile is the only other phase in such areas. In some examples garnet aggregates, showing pale cores and sharply-bounded, irregularly-shaped darker margins to individual grains, form a net-like structure around pyroxene domains. Matrix clinopyroxene, mostly 0.5 to 1 mm in length, and with minor inclusions of quartz, shows an irregular breakdown to fine-grained (innermost) or coarse-grained (outermost) symplectites of secondary clinopyroxene and plagioclase (with or without magnetite) or

is replaced by hornblende. Some samples show abundant apatite as ca. 0.5 mm grains or clusters. Amphibole appears to be secondary with texturally earliest being olive-green hornblende and later rims or fracture fills comprising more aluminous, hence bluer varieties. This eclogite variety occurs in Purbinar (settlement Kaar) (PKB3), between Besal and Lake Lulusar, and in Joranar (K4-60&76).

2.3.2 Medium- to coarse-grained eclogites with inherited magmatic fabrics

This variety of eclogite represents the transition between corona dolerites and skarn-like eclogites. Typical for this type are clusters and networks of anhedral, irregularly- zoned garnet or skeletal coronas of garnet, with a range in size from 0.1 up to 1.5 mm which roughly pseudomorph the original feldspar fabric. Omphacite is 0.2-0.8 mm in longest dimension showing an irregular breakdown to fine and coarse-grained symplectites of clinopyroxene, amphibole and plagioclase. The inclusion content in omphacite varies between almost inclusion-free (with only minor quartz and rutile) to inclusion-rich varieties with an evenly-distributed dusting of fine-grained rutile. In addition, amphibole exists as large (cm-sized), green, poikilitic porphyroblasts, which are notably browner around rutile and ilmenite inclusions. Small (0.1 mm) nematoblastic amphibole in oriented clusters occurs together with epidote minerals (up to 0.5 mm), biotite, albite and quartz and represents a later retrogression. Accessory minerals are apatite, as ca. 0.8 mm grains, and large rutile grains (up to 2 mm), mostly in chains or cluster, partly replaced by ilmenite. Eclogites in Joranar (K4-57 & -58) belong to this group.

2.3.3 Layered, clinozoisite and epidote bearing eclogites with leucocratic segregations

These generally strongly foliated and retrogressed eclogites exhibit a fine-grained, dark green to gray matrix, red garnet-rich layers, and cm-sized black amphiboles overgrowing this fabric (Fig. 2.2C). The macroscopically visible layers comprise alternating garnet–omphacite–symplectite, garnet–amphibole–symplectite and garnet-biotite–clinozoisite assemblages. Elongate omphacite, epidote minerals, and garnet bands, conspicuous around the margins of the large clinozoisites (Fig. 2.2D), define the foliation. In addition, the rock is cut by light-coloured veinlets containing phengite, albite, kyanite and locally also cm-sized rutile grains. In the microscope, garnet is generally 0.25 mm or less, pale pink, anhedral and mostly inclusion free. Relicts of omphacite occur mainly as tiny inclusions in clinozoisite although locally primary coarse omphacite-bearing bands are still preserved. Matrix omphacite, mostly smaller

than 1 mm, contains minor inclusions of quartz or rutile needles, and is randomly replaced to varying degrees by fine-grained symplectites of pyroxene, amphibole and albite or large porphyroblastic amphiboles. Amphibole exists in several generations: as inclusions in clinozoisite; as large, pale green porphyroblastic grains with partly retrograded outer rims; in rough and fine symplectites after matrix omphacite and as euhedral nematoblastic amphibole of up to 0.1 mm in the leucocratic segregations. Phengite, up to 1 mm, occurs as inclusion in zoisite and in leucocratic sheets, partially transformed to lepidoblastic biotite and albite symplectites (Fig. 2.2G). Clinozoisite occurs as lense- or lath- like individuals within chain- or boudin-like structures. Grains up to 0.7 mm in length show the complete range of an eclogite mineral assemblage as inclusions whereas the foliation of the inclusions often differs from that defined by the same phases in the matrix. Epidote commonly appears as up to 2 mm long aggregates containing garnet, minor symplectised pyroxene and amphibole. Rutile, up to 2 mm in diameter, is partly replaced by ilmenite, which is itself rimmed by titanite. Apatite (mm-sized) occurs also. Leucocratic sheets of up to 1 cm thickness, most probably products of aqueous fluid migrations under HP conditions, contain quartz, zoisite (up to 2.5 mm), phengite, kyanite, and secondary biotite and albite after phengite. (Fig.2.2E, F). This eclogite type crops out in Gittidas Nala (K4-105, PK2-4), in Purbinar (settlement Kaar) (K4-98) and north (K4-84/87) and west of Jalkhad (J Nar 2).

2.3.4 Coesite-bearing UHP eclogites with secondary glaucophane and barrosite

The glaucophane- and coesite-bearing, commonly very fresh eclogites exhibit a massive, fine-grained (<1 mm) matrix with red garnet and dark green omphacite. Overgrowing this early fabric are larger (>1 mm) dark amphiboles. Anhedral, optically-zoned garnets (Fig. 2.2H) up to 0.8 mm in diameter sit within a weakly defined foliation formed by elongate omphacite, phengite and chains of rutile. Garnet contains tiny inclusions of rutile, minor quartz/ coesite, graphite and zircon. Omphacite is up to 1 mm in length and mostly inclusion poor, whereas some grains look dusty due to evenly distributed fine-grained rutile. Phengite, in 0.5 mm laths, is surrounded by a thin biotite-bearing breakdown rim. Amphiboles with a conspicuous lilac core and a dark green rim form small poikiloblasts (Fig. 2.2H) partly enclosing the earlier phases. Coesite occurs as inclusions in omphacite and garnet, showing in both cases the typical radiating network of fractures and partial breakdown to quartz. Coesite inclusions (Fig. 2.2I) are best preserved in omphacite and

so far only one example has been found in garnet. Some of the glaucophane-bearing eclogites also contain the carbonate minerals magnesite and dolomite as matrix phases, apparently in equilibrium with the high-pressure assemblage, as well as ankerite as inclusions in garnet. Rutile, partly replaced by titanite, domains of pyrite/ chalcopyrite transformed to hematite, magnetite and goethite and a small amounts of epidote/clinozoisite, apatite and zircon are accessory phases. Coesite eclogites occur only a few hundred metres from the Indus Suture Zone north and northwest of Gittidas: at Saleh di Baihk (K4-106) as boulders close to the road and in situ at Saleh Gali (K4-120).

2.3.5 Very fine-grained eclogite

An unusual very fine-grained eclogite type exhibits a pale lilac hue in hand specimen whereby non-retrograded portions show only a very subtle red and green colouration. In the microscope, garnet is generally less than 100 μm, optically zoned, anhedral to semi-euhedral with locally inclusions of graphite and rutile in their interiors (Fig. 2.2J). Matrix omphacite, in places as aggregates of tiny, 20 μm grains, is mostly replaced to varying degrees by amphibole–clinopyroxene–plagioclase symplectites and secondary green amphiboles. Three generations of amphiboles occur. Yellow-green porphyroblastic amphibole grains significantly larger than primary phases randomly overgrow the fabric, a second variety occurs in symplectites and the youngest variant is found in late cross-cutting veins. Rutile is about 10-20 μm in diameter and rimmed by titanite whereas fine distributed titanite and graphite give thin sections a dusty appearance. This eclogite type has been found within the metasediments close to Jalkhad in Jalkhad Nar (K3-11).

2.3.6 Coronitic metabasites

In addition to the eclogites exists a further metabasite variety exhibiting coronitic growth of garnet around plagioclase and recrystallisation of clinopyroxene. A wide variety of textures can be observed from only slightly modified magmatic rocks to completely recrystallised garnet+clinopyroxene+plagioclase+quartz±hornblende assemblages which pseudomorph the magmatic texture (Figs. 2.2K, L). The presence of stable plagioclase in the most recrystallised samples indicates a high-pressure amphibolite/granulite facies rather than eclogite facies conditions for these rocks. These coronitic metadolerites are found on both sides of lake Saif-ul-Muluk, in the area between Naran and Burawai, significantly further south than the outcrops of eclogite (Fig. 2.1) and have also been noted in the neighbouring Neelum Valley (Fontan et al., 2000).

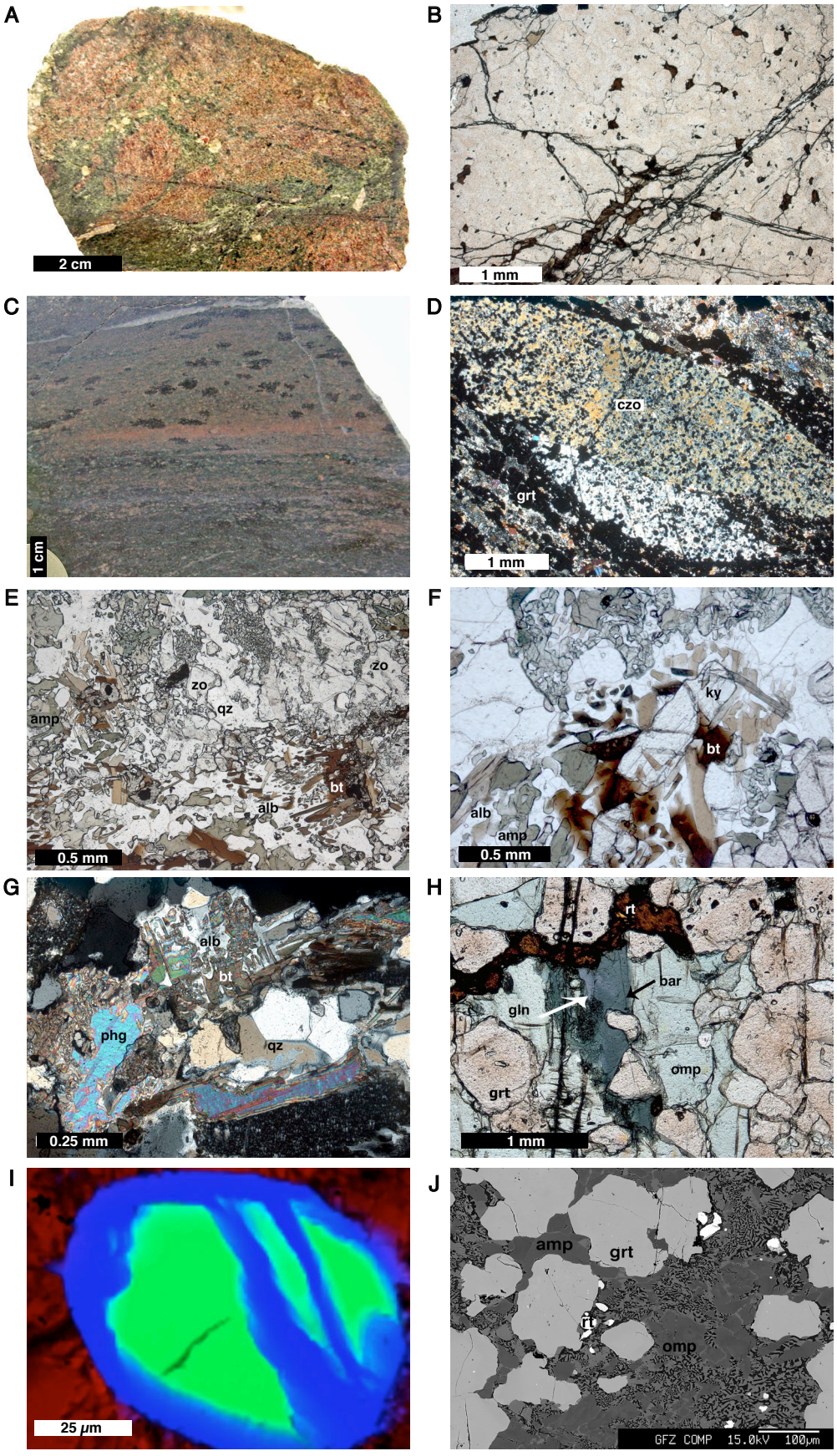
A
2 cm
B
1 mm
C
1 cm
D
czo
grt
1 mm
E
zo
zo
qz
amp
bt
alb
0.5 mm
F
ky
bt
alb
amp
0.5 mm
G
alb
bt
phg
qz
0.25 mm
H
rt
bar
gln
omp
grt
1 mm
I
25 µm
J
amp
grt
rt
omp
GFZ COMP 15.0kV 100µm

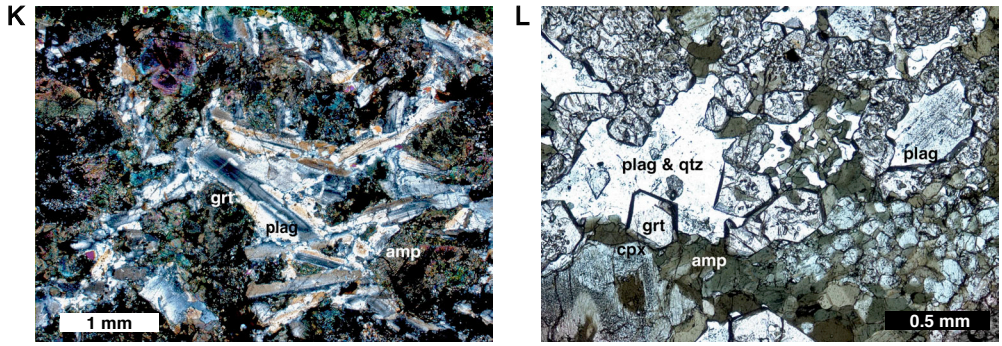

Fig. 2.2. A-L Textural features of the various eclogites. A Several cm-sized dark red garnets and cm-sized white titanite (ttn) grains set in a matrix of dark green clinopyroxene. Hand specimen, PKB3. B Cluster of zoned garnets (garnetite), showing pale inclusion rich cores with sharply-bounded, irregularly-shaped darker margins. Darker grains are rutile. Photomicrograph, plane polars, K4-76. C Strongly foliated and retrogressed eclogite containing a green to grey matrix (epidote and symplectite), layers of red garnet and large secondary black amphibole porphyroblasts. Hand specimen, K4-105. D Lens-like, inclusion-rich (mostly omphacite and garnet) clinozoisite (czo) crystal wrapped by bands of fine-grained garnet (grt) defining the strong foliation. Photomicrograph, crossed nicols, PK2-4. E Zoisite (zo) and quartz (qz) forming leucocratic segregations. Euhedral nematoblastic amphibole (amp) is restricted to such zones. Lepidoblastic biotite (bt) is secondary. Rutile is rimmed by ilmenite, which is itself surrounded by titanite. Photomicrograph, plane polars, K4-87. F Kyanite (ky) in a leucocratic segregation surrounded by biotite (bt). Photomicrograph, plane polars, PK2-4. G Phengite (phg) in a leucocratic segregation partially replaced by a biotite (bt) – albite (alb) intergrowth. Photomicrograph, crossed nicols, J Nar2. H Optically-zoned garnet, fresh omphacite, chains of rutile and lilac glaucophane core to dark green barroisite. Vertical cracks relate to a later greenschist facies overprint. Photomicrograph, plane polars, K4-120. I Colour-coded Raman map showing coesite (green) rimmed and crosscut by quartz (blue) hosted in omphacite. K4-106. J Anhedral to semi-euhedral garnet (grt) sit in a very fine grained matrix of omphacite (omp: dark grey) relicts, replaced by symplectites of secondary clinopyroxene (medium grey), plagioclase (black) and amphibole. Porphyroblastic amphibole (amp) overgowth the matrix. BSE-image, K3-11. K Plagioclase laths preserving an original magmatic texture in metadolerite. Photomicrograph, crossed nicols, K3-3. L Garnet chains filled with quartz inclusions in metadolerite. Photomicrograph, plane polars, K3-47.

2.4. Mineral chemistry

In the following section the chemistry of major minerals and their breakdown products will be outlined. Analyses were obtained using a 4 spectrometer Cameca SX100 electron microprobe at the GeoForschungsZentrum (GFZ) Potsdam operating at 15 kV and 20 nA with a 2-10 μm beam. Counting time were 10-30 s on peaks and half-peak on background, synthetic and natural standards were used. Representative point analyses are given in Table 2.1-2.4.

2.4.1 Garnet

In addition to differences in grain size, distribution, texture, colour and inclusion density the garnet in the investigated samples shows variation in composition and in zoning pattern (Table 2.1; Fig. 2.3). Garnets from skarn-type eclogites and the rocks with inherited magmatic fabric (in both cases generally coarse-grained) are iron rich ($Alm_{60}Prp_{16}Sps_1Grs_{18}$) and show essentially homogeneous cores overgrown by smaller rims with increasing Prp, X_{Mg} and Sps associated with decreasing Ca content (Fig. 2.3A). In contrast, garnets in the epidote-bearing eclogites show a strong compositional zoning pattern with abrupt changes. In the inclusion-rich cores, garnets are Fe rich and Ca poor ($Alm_{55}Prp_{22}Sps_1Grs_{19}$) and only minor variation exists within cores of a single sample. These cores are surrounded by homogeneous overgrowths showing higher Ca and lower Fe with a sharp, step-like compositional change existing between the two zones (Figs. 2.3 B, C &-D). In some examples three distinct zones are visible (Fig. 2.3B). Garnets in UHP- and very fine-grained eclogites are characterised by a complex multipart zoning (Figs. 2.3 E, F). Small, irregular-shaped Fe+Ca-rich cores are surrounded by a zone with lower Ca and higher Fe+Mg, which is itself surrounded, by a wider zone with highest Fe and equal Ca and Mg. This outer zone is criss-crossed by vein-like structures, well depicted in the compositional map of Fig. 2.4, showing higher Ca and lower Fe+Mg as is usual for the outermost zones of such grains.

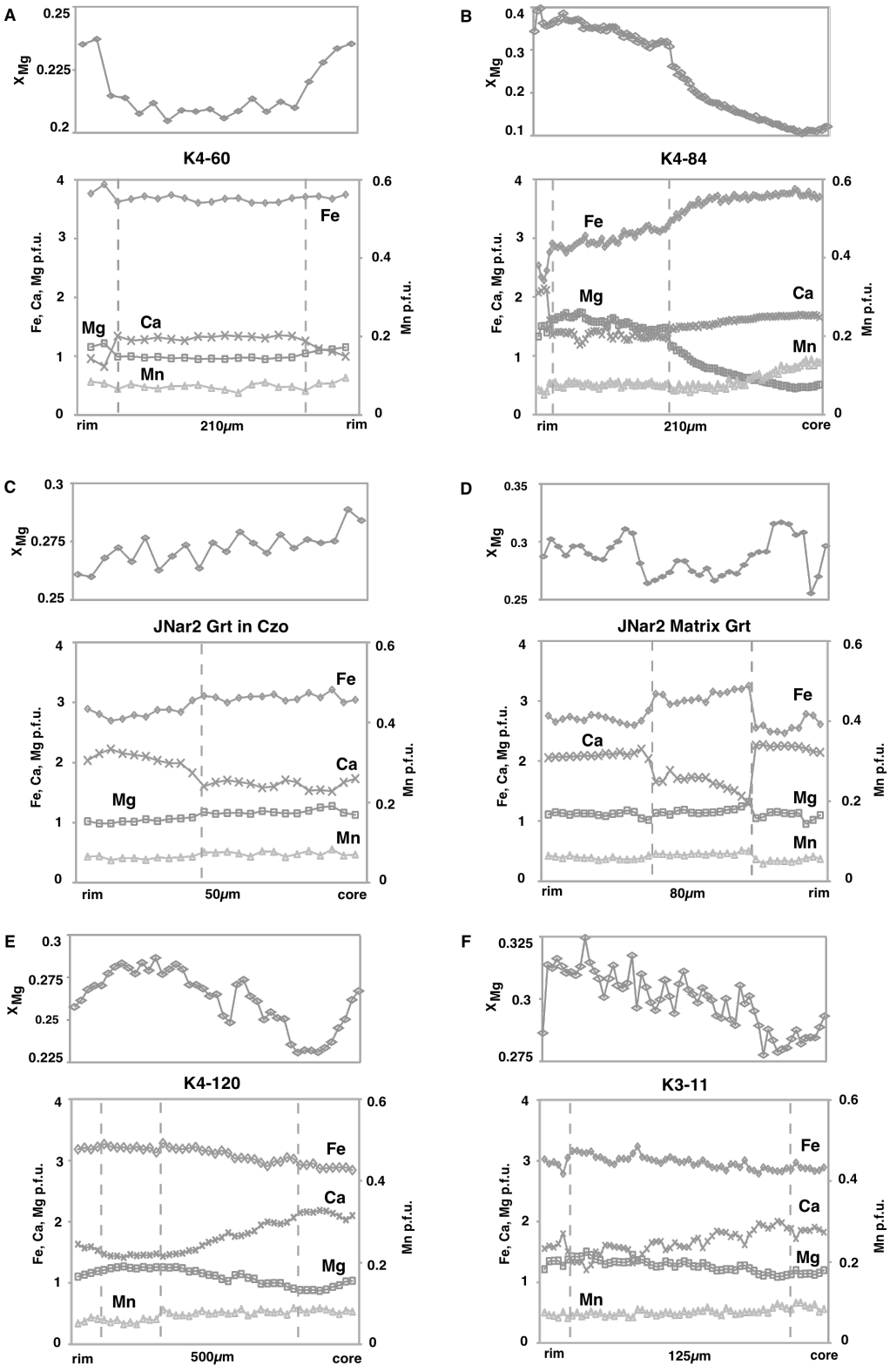

Fig. 2.3. A-F Garnet compositional zoning profiles, show rim to rim or rim to core variations of Ca, Fe, Mg and Mn calculated per 24 oxygens. Distances in μm are given below the horizontal axes. X_{Mg}*= Mg/(Mg+*Fe^{2+}*) See text for details.*

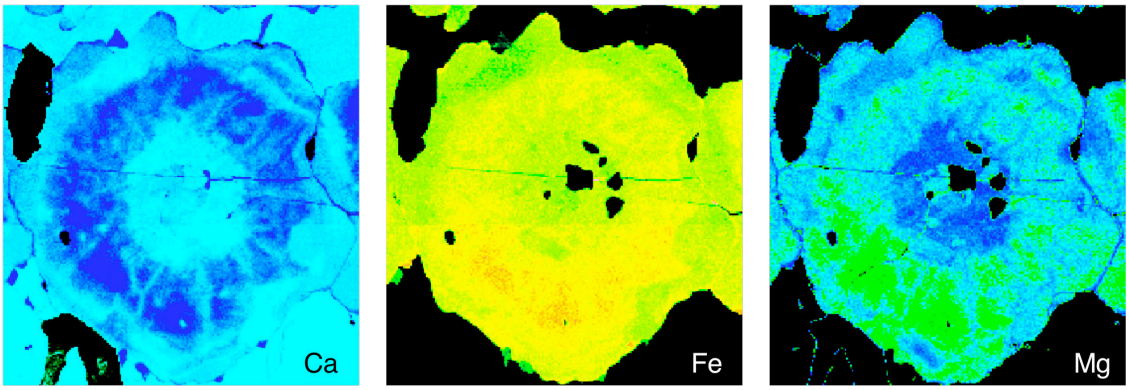

Fig. 2.4. Qualitative compositional map of garnet zoning in UHP eclogites (K4-120). Element concentrations (rainbow scale) rise from dark blue (low) to red (high).

2.4.2 Clinopyroxene

Omphacite is an essential constituent of all the eclogites, but a large variation in grain size, modal abundance, inclusions and degree of breakdown is obvious. Jadeite content varies between 12 and 45 mol% for texturally eclogite facies clinopyroxene (Table 2.2; Fig. 2.5). In most samples this omphacite has been partially replaced by symplectitic intergrowths of secondary, less jadeitic clinopyroxene intergrown with plagioclase and commonly also amphibole. The skarn-like eclogites show lowest jadeite contents (generally below 20 mol%) whereas in the other coarse-grained eclogites even the secondary symplectitic clinopyroxene has a jadeite content above 20 mol% (Fig. 2.5). Epidote- and coesite-bearing eclogites contain matrix omphacites with X_{Jd} between 0.30 and 0.39 — tiny omphacites included in large clinozoisite porphyroblasts show a similar range — whereas secondary, symplectitic clinopyroxene especially in the epidote-rich varieties coexists with magnetite and has a significantly higher aegirine content (around 20 mol%). Conspicuously, the highest jadeite contents, up to 45 mol%, have been found in the tiny matrix omphacites of the very fine-grained eclogite (Table 2.2; Fig. 2.5).

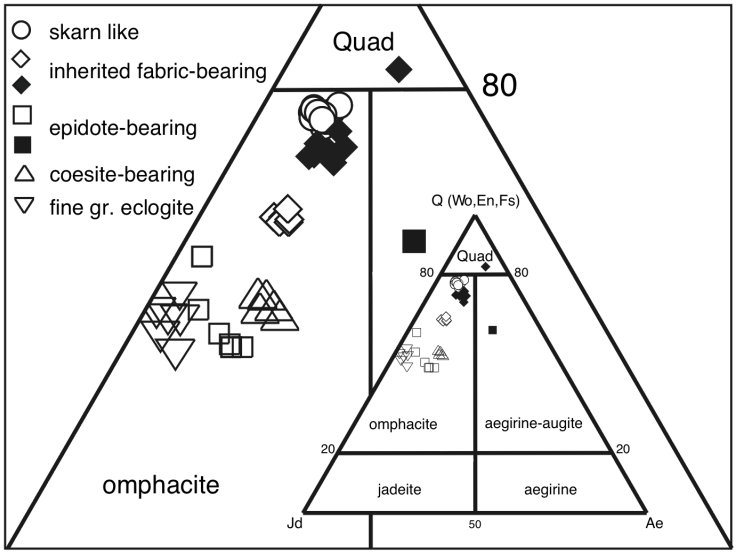

Fig. 2.5. Clinopyroxene analyses plotted in the Jd-Aeg-Quad (Quad: Ca-Mg-Fe pyroxene area) triangular diagram after Morimoto (1988). Open symbols represent primary omphacites whereas filled symbols are for secondary (symplectite) clinopyroxene.

2.4.3 Amphibole

Amphibole is a major phase in almost all studied samples and occurs in a number of compositional and textural modifications. The main varieties are calcic and sodic-calcic amphiboles but locally also sodic amphiboles occur. Different amphibole varieties may exist in a single sample as well as in a single zoned grain (Table 2.3; Figs. 2.6A, B). Coarse-grained eclogites contain mainly large porphyroblasts of barroisite or edenite/pargasite/Mg-hastingsite but inclusions in garnet and zone rims of such amphiboles adjacent to garnet are generally more aluminous. In comparison, large poikilitic amphibole porphyroblasts in epidote-bearing eclogites show a barroisite core and a rim of pargasite or tschermakite whereas tiny grains and inclusions in clinozoisite are edenite (Fig. 2.6A). Symplectitic amphiboles tend to be edenitic or pargasitic in composition. Noticeable in many of these samples is a conspicuous brown halo around rutile inclusions marked by a 2- to 4-fold increase in TiO_2 content. Amphiboles in UHP eclogites are unusual in that they contain irregular patches of lilac glaucophane (already noticed by Lombardo et al., 2000) in the core surrounded by barroisite (Fig. 2.6C) and with a thin outer rim of magnesio-hornblende. A typical example of core-rim compositional variation for such an amphibole is depicted in Fig. 2.6D. Fine-grained eclogites contain less-aluminous amphiboles than the other eclogite types with the typical porphyroblasts plotting in the barroisite to Mg-katophorite fields.

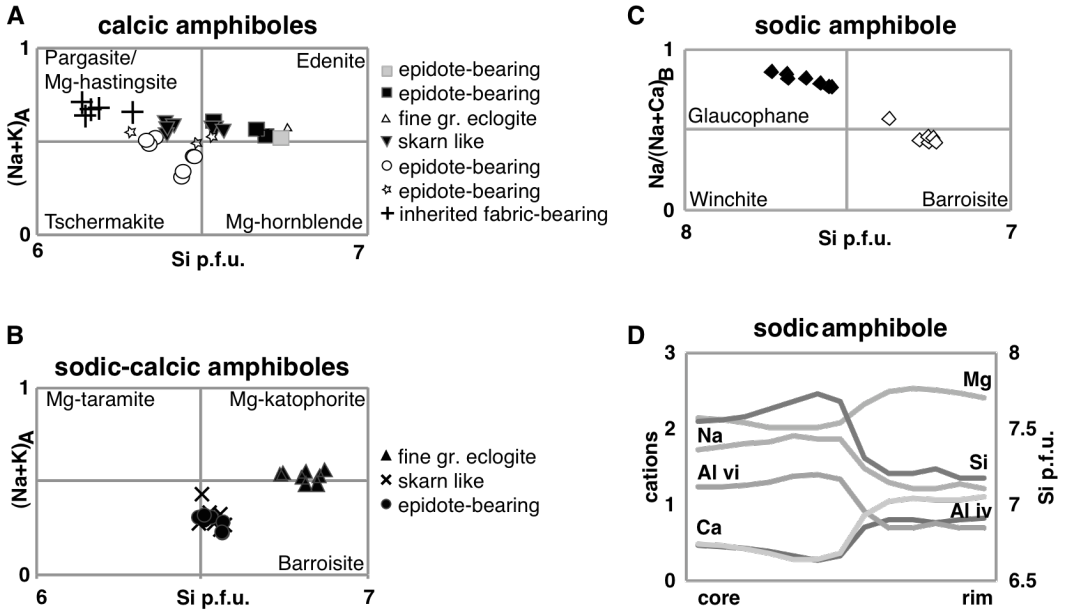

Fig. 2.6. A-D Representative plots of amphibole analyses. Different symbols indicate porphyroblastic amphiboles (black filled symbols), rims of porphyroblasts (open symbols), symplectitic types (small open symbols) and inclusions in clinozoisite (grey filled box). Each symbol (square, triangle, etc.) represents analyses from one sample. C and D are for coesite+glaucophane-bearing eclogite (K4-120) with D showing a typical core–rim compositional profile.

2.4.4 Epidote minerals

As a common phase in the eclogite facies assemblage, fairly homogeneous epidote and clinozoisite (Table 2.4) occur as elongate lenses or individual grains. Eclogites with preserved magmatic texture contain zoisite most probably indicating the local influence of former magmatic Ca-plagioclase. The large clinozoisites overgrowing the eclogite fabric and preserving garnet and omphacite as inclusions are generally also unzoned. An additional epidote variety occurs in the leucocratic segregation zones where it is typically idiomorphic and optically and compositionally zoned to more Fe-rich rims. An important observation is the presence of feathery-textured quartz as inclusions in epidote of samples from the area of the coesite-bearing eclogites, which could represent pseudomorphs after coesite.

2.4.5 Mica phases

Phengite, grown during the UHP/HP-stage and in leucocratic sheets, is the dominant mica phase in the studied samples. Primary phengite is relatively homogeneous within a single sample with composition generally plotting between 3.44 and 3.55 Si p.f.u. (based on 11 oxygens), with low Ti but significant (around 5 mol%) paragonite content. In contrast, white micas in the leucocratic pockets contain lower Si in cores and are zoned to even lower Si values at the rim (Table 2.4). Breakdown of phengite produced phlogopite or biotite (Table 2.4).

2.4.6 Plagioclase

Plagioclase is only found as a secondary phase in the eclogites where it occurs in symplectites after omphacite intergrown with amphiboles and clinopyroxene and in leucocratic segregations together with biotite, phengite, kyanite and zoisite. Symplectite plagioclase is generally more sodic (albite-oligoclase) than the plagioclase of the segregation pockets (andesine)(Table 2.4).

sample	K4-60	K4-60	K4-76	K4-57	K4-98	K4-98	K4-84	K4-84	K4-84	JNar2	JNar2	JNar2	JNar2	PK2-4	K4-120b	K4-120	K4-120	K3-11	K3-11
wt%/position	core	rim	general	general	core	shell	core	shell	rim	incl core	incl rim	matrix core	matrix rim	rim	core	shell	rim	core	rim
SiO_2	37.84	38.28	38.08	38.32	39.98	38.70	37.34	38.61	38.70	38.60	38.24	38.49	38.74	38.66	38.48	38.56	38.53	38.73	38.79
TiO_2	0.13	0.04	0.06	0.10	0.05	0.03	0.11	0.02	0.05	0.14	0.10	0.10	0.09	0.11	0.04	0.08	0.06	0.07	0.03
Al_2O_3	20.46	20.94	21.35	21.15	21.79	21.95	20.20	21.32	21.43	21.54	21.50	21.69	21.93	21.68	21.39	21.34	21.11	21.59	22.23
Cr_2O_3	<0.01	0.02	0.02	0.02	0.07	0.06	0.04	<0.01	0.02	0.04	0.01	0.03	0.04	0.04	0.01	0.01	0.02	0.05	<0.01
FeO	28.63	29.50	24.79	26.09	21.60	21.85	28.28	22.39	19.01	21.71	24.96	24.02	20.43	22.80	22.64	25.50	25.31	22.81	22.47
MgO	4.15	4.94	5.80	5.23	9.26	9.88	1.95	7.43	6.38	4.28	5.16	4.90	5.05	6.70	3.76	5.45	4.76	4.66	5.56
MnO	0.59	0.72	0.69	0.29	0.35	0.35	0.88	0.44	0.39	0.43	0.60	0.53	0.39	0.54	0.41	0.59	0.61	0.42	0.59
CaO	7.85	5.94	8.96	8.34	7.79	7.06	10.65	9.16	13.75	13.42	9.17	10.36	13.68	9.23	13.09	8.90	9.79	11.72	10.97
Na_2O	0.01	0.02	<0.01	0.04	<0.01	<0.01	<0.01	<0.01	<0.01	0.03	0.01	0.03	0.01	n.d.	0.03	0.06	0.01	0.03	0.02
Sum	99.66	100.38	99.74	99.57	99.89	99.88	99.45	99.37	99.72	100.20	99.73	100.13	100.37	99.77	99.85	100.49	100.19	100.07	100.65
Si	5.99	6.00	5.92	6.00	5.92	5.87	5.98	5.96	5.93	5.97	5.97	5.97	5.94	5.96	5.99	5.97	6.00	6.00	5.95
Al	3.82	3.87	3.91	3.90	3.90	3.92	3.81	3.87	3.87	3.93	3.95	3.97	3.96	3.95	3.93	3.89	3.87	3.94	4.02
Ti	0.02	<0.01	0.01	0.01	0.01	<0.01	0.01	<0.01	0.01	0.02	0.01	0.01	0.01	0.01	0.01	0.01	0.01	0.01	<0.01
Cr	<0.01	<0.01	<0.01	<0.01	0.01	0.01	0.01	-	<0.01	<0.01	<0.01	<0.01	0.01	0.01	<0.01	<0.01	<0.01	0.01	<0.01
Fe^{2+}	3.61	3.75	3.00	3.33	2.52	2.44	3.58	2.68	2.17	2.70	3.16	3.04	2.49	2.83	2.87	3.13	3.18	2.92	2.79
Fe^{3+}	0.18	0.12	0.22	0.08	0.23	0.33	0.21	0.21	0.26	0.11	0.10	0.07	0.13	0.11	0.08	0.17	0.11	0.04	0.09
Mg	0.98	1.15	1.34	1.22	2.10	2.23	0.46	1.71	1.46	0.99	1.20	1.13	1.15	1.54	0.87	1.26	1.10	1.08	1.27
Mn	0.08	0.10	0.09	0.04	0.04	0.04	0.12	0.06	0.05	0.06	0.08	0.07	0.05	0.07	0.05	0.08	0.08	0.05	0.08
Ca	1.33	1.00	1.49	1.40	1.27	1.15	1.83	1.51	2.26	2.22	1.53	1.72	2.25	1.53	2.18	1.48	1.63	1.95	1.80
Na	<0.01	0.01	-	0.01	-	-	-	-	-	0.01	<0.01	0.01	<0.01	-	0.01	0.02	<0.01	0.01	<0.01
X_{Mg}	0.214	0.235	0.309	0.268	0.454	0.478	0.115	0.390	0.401	0.268	0.275	0.271	0.317	0.352	0.233	0.287	0.258	0.270	0.313
Alm	60.2	62.5	50.6	55.6	42.5	41.6	59.8	44.9	36.6	45.2	52.9	51.0	41.9	47.5	48.0	52.7	53.0	48.7	47.0
Adr	4.6	3.0	5.7	2.0	5.7	8.4	5.1	5.3	6.7	2.8	2.4	1.8	3.3	2.7	2.0	4.3	2.9	1.0	2.4
Grs	17.6	13.6	19.5	21.3	15.5	11.0	25.2	20.1	31.3	34.4	23.2	26.9	34.4	22.7	34.5	20.5	24.3	31.3	28.0
Prp	16.3	19.2	22.7	20.4	35.4	38.1	7.8	28.7	24.5	16.6	20.1	19.0	19.4	25.8	14.6	21.2	18.4	18.0	21.4
Sps	1.3	1.6	1.5	0.6	0.8	0.8	2.0	1.0	0.8	0.9	1.3	1.2	0.9	1.2	0.9	1.3	1.3	0.9	1.3

Table 2.1. Representative garnet analyses. n.d.=not determined. Normalised to 24[O], ferric iron calculated by charge balance. X_{Mg}= Mg/(Fe^{2+}+Mg)

sample	K4-60	K4-57	K4-76 p	K4-76 s	K4-98 p	K4-84 s	PK2-4 p	PK2-4 s	JNar 2	K4-120	K3-11
SiO_2	55.21	53.81	52.67	51.81	54.84	52.75	54.85	52.87	56.13	54.29	56.86
TiO_2	0.04	0.17	0.26	0.27	0.14	0.11	0.04	0.11	0.05	0.12	0.06
Al_2O_3	6.53	8.90	8.89	6.62	9.08	7.97	10.29	7.98	10.48	9.31	11.52
Cr_2O_3	0.05	<0.01	0.05	0.02	0.02	0.05	0.07	0.05	<0.01	0.04	0.05
FeO	9.30	9.36	8.58	9.41	4.92	8.57	7.04	7.57	4.67	7.95	2.46
MgO	8.20	8.48	8.15	9.53	9.62	9.27	7.66	10.17	8.55	8.22	8.85
MnO	0.03	0.02	0.06	0.06	0.02	0.04	0.03	0.04	0.01	0.04	<0.01
CaO	13.67	14.29	15,28	17.92	15.53	16.31	12.02	16.21	13.96	13.28	13.92
Na_2O	6.64	5.83	5.34	3.68	5.50	4.88	7.13	4.87	6.95	6.35	7.15
K_2O	<0.01	n.d.	<0.01	<0.01	n.d.	n.d.	<0.01	n.d.	n.d.	<0.01	n.d.
Sum	99.68	100.86	99.28	99.33	99.67	99.94	99.13	99.87	100.80	99.60	100.87
Si	2.00	1.94	1.92	1.91	1.97	1.91	1.97	1.91	1.98	1.96	1.99
Al^{IV}	<0.01	0.06	0.08	0.09	0.03	0.09	0.03	0.09	0.02	0.04	0.01
Al^{VI}	0.28	0.32	0.31	0.20	0.35	0.26	0.41	0.25	0.41	0.35	0.46
Ti	<0.01	<0.01	0.01	0.01	<0.01	<0.01	<0.01	<0.01	<0.01	<0.01	<0.01
Cr	<0.01	<0.01	<0.01	<0.01	<0.01	<0.01	<0.01	<0.01	<0.01	<0.01	<0.01
Fe^{2+}	0.09	0.12	0.13	0.16	0.09	0.09	0.10	0.06	0.05	0.12	0.04
Fe^{3+}	0.19	0.15	0.13	0.13	0.05	0.17	0.11	0.17	0.08	0.12	0.03
Mg	0.44	0.46	0.44	0.52	0.51	0.50	0.41	0.55	0.45	0.44	0.46
Mn	<0.01	<0.01	<0.01	<0.01	0.00	<0.01	<0.01	<0,01	<0.01	<0.01	<0.01
Ca	0.53	0.55	0.60	0.71	0.60	0.63	0.46	0.63	0.53	0.51	0.52
Na	0.47	0.41	0.38	0.26	0.38	0.38	0.50	0.34	0.47	0.44	0.48
X_{Mg}	0.82	0.79	0.77	0.77	0.85	0.84	0.80	0.91	0.89	0.79	0.92
Xjd	0.28	0.25	0.25	0.13	0.33	0.18	0.39	0.17	0.39	0.32	0.45
Xaeg	0.19	0.15	0.13	0.13	0.05	0.17	0.11	0.18	0.08	0.12	0.04
Quad	0.53	0.54	0.55	0.66	0.59	0.58	0.48	0.57	0.50	0.52	0.50

Table 2.2. Representative omphacite analyses. n.d.=not determined. Normalised to 6[O]. Ferric iron calculated by charge balance. X_{Mg}=Mg/(Fe^{2+}+Mg). p=primary; s=secondary

sample	PKB3	K4-60	K4-57	K4-76	K4-105	K4-105	PK2-4	PK2-4	K4-120b	K4-120b	K4-106	K3-11
wt%/type	pargasite	barroisite	Mg-hastingsite	Mg-hastingsite	barroisite	tschermakite	edenite	pargasite	glaucophane	barroisite	barroisite	barroisite
SiO_2	43.02	45.25	42.07	42.19	45.86	45.16	45.56	43.08	55.74	52.05	50.24	48.55
TiO_2	1.29	0.51	0.57	1.21	1.14	1.84	0.75	0.65	0.09	0.09	0.20	0.34
Al_2O_3	12.86	10.45	14.02	13.43	12.00	12.23	12.40	15.35	10.93	10.64	9.99	12.08
Cr_2O_3	0.02	0.02	0.02	<0.01	n.d.	<0.01	0.02	0.08	<0.01	0.04	0.07	0.01
FeO	15.97	16.77	16.90	16.16	11.60	10.31	12.52	10.42	12.84	14.67	12.91	9.41
MnO	0.03	0.09	0.04	0.04	0.05	0.01	0.02	0.03	0.02	0.07	0.04	0.01
MgO	10.36	12.00	10.53	11.03	13.98	14.14	13.08	12.76	9.61	10. 20	12.66	14.25
CaO	11.01	8.55	11.35	11.48	9.67	10.08	11.65	11.62	3.15	7.36	8.43	8.84
Na_2O	2.62	3.05	2.23	2.56	2.92	3.14	2.13	2.59	5.95	4.45	3.66	3.98
K_2O	0.50	0.49	1.60	0.86	0.37	0.15	0.67	0.24	0.06	0.23	0.22	0.40
Sum	97.66	97.26	99.33	98.95	97.57	97.06	98.80	96.82	98.39	99.80	98.42	97.86
Si	6.36	6.54	6.15	6.17	6.52	6.47	6.53	6.26	7.74	7.34	7.14	6.85
Al^{IV}	1.64	1.46	1.85	1.83	1.48	1.53	1.47	1.74	0.26	0.66	0.86	1.15
T	*8.00*	*8.00*	*8.00*	*8.00*	*8.00*	*8.00*	*8.00*	*8.00*	*8.00*	*8.00*	*8.00*	*8.00*
Al^{VI}	0.60	0.32	0.57	0.48	0.53	0.54	0.62	0.89	1.53	1.11	0.82	0.86
Ti	0.14	0.06	0.06	0.13	0.12	0.20	0.08	0.07	0.01	0.01	0.02	0.04
Fe^{3+}	0.43	1.43	0.67	0.60	0.89	0.59	0.40	0.31	0.10	0.03	0.24	0.39
Cr	<0.01	<0.01	<0.01	<0.01	<0.01	<0.01	<0.01	0.01	-	<0.01	0.01	<0.01
Mg	2.28	2.58	2.30	2.40	2.96	3.02	2.79	2.76	1.99	2.14	2.68	3.00
Fe^{2+}	1.55	0.60	1.40	1.37	0.49	0.65	1.10	0.95	1.37	1.70	1.23	0.72
Mn	<0.01	0.01	0.01	<0.01	0.01	<0.01	<0.01	<0.01	-	-	-	<0.01
C	*5.00*	*5.00*	*5.00*	*5.00*	*5.00*	*5.00*	*5.00*	*5.00*	*5.00*	*5.00*	*5.00*	*5.00*
Fe	-	-	-	-	-	-	-	-	0.02	-	0.06	-
Mn	-	-	-	-	-	-	-	-	<0.01	0.01	<0.01	-
Ca	1.74	1.32	1.78	1.80	1.47	1.55	1.79	1.81	0.47	1.11	1.28	1.34
Na	0.26	0.68	0.22	0.20	0.53	0.45	0.21	0.19	1.50	0.88	0.65	0.66
B	*2.00*	*2.00*	*2.00*	*2.00*	*2.00*	*2.00*	*2.00*	*2.00*	*2.00*	*2.00*	*2.00*	*2.00*
Na in A	0.49	0.18	0.41	0.52	0.28	0.42	0.38	0.54	0.10	0.34	0.36	0.42
K in A	0.10	0.09	0.19	0.16	0.07	0.03	0.12	0.04	0.01	0.04	0.04	0.07
A	*0.59*	*0.27*	*0.60*	*0.68*	*0.34*	*0.45*	*0.50*	*0.58*	*0.11*	*0.38*	*0.40*	*0.50*
sum	15.59	15.27	15.60	15.68	15.34	15.45	15.63	15.58	15.11	15.38	15.40	15.50
X_{Mg}	0.60	0.81	0.62	0.64	0.86	0.82	0.72	0.74	0.59	0.56	0.67	0.81

Table 2.3. Selected amphibole analysis. n.d.=not determined. Calculation is based on 23[O] with Fe^{2+}/Fe^{3+}calculation after charge balance assuming 13 cations excluding Ca, Na, K (except for K4-120 & K4-106 where Fe^{3+} is calculated by charge balance after normalisation to 15 excluding K, Na_A). Cations calculated after Leake et al., 1997. X_{Mg}= $Mg/(Fe^{2+}+Mg)$

sample	K4-76 Phl	K4-57 Phl	JNar2 Bt	PK2-4 Phl	JNar2 Phg core	JNar2 Phg rim	K4-120d Phg	sample	K4-76 Plag	JNar2 Plag	Pk2-4 Plag	PK2-4 Plag	sample	JNar2 Zo rim	JNar2 Zo core	PK2-4 Czo	K4-120 Ep
SiO_2	36.16	36.88	39.14	37.63	51.14	49.37	51.35	SiO_2	63.48	62.00	62.64	60.05	SiO_2	39.88	39.95	38.85	38.30
TiO_2	4.05	3.77	1.58	3.21	0.65	0.50	0.71	TiO_2	<0.01	0.03	0.02	0.01	TiO_2	0.11	0.07	0.07	0.15
Al_2O_3	15.53	15.74	23.83	17.86	28.27	31.15	25.37	Al_2O_3	22.30	23.38	23.56	25.32	Al_2O_3	31.45	31.91	27.86	23.62
Cr_2O_3	0.09	<0.01	<0.01	<0.01	<0.01	<0.01	<0.01	FeO	0.06	0.12	0.29	0.24	Cr_2O_3	0.04	0.02	<0.01	n.d.
FeO	16.50	15.67	10.71	13.14	1.54	1.51	3.25	MnO	<0.01	<0.01	0.02	<0.01	FeO	1.86	1.48	7.30	11.61
MgO	13.41	13.84	10.90	14.89	3.88	2.81	3.83	CaO	3.75	4.98	3.91	6.97	MnO	<0.01	0.01	0.05	0.05
MnO	0.02	<0.01	0.07	0.03	<0.01	<0.01	0.04	Na_2O	10.19	9.42	9.96	8.29	CaO	23.71	23.57	23.20	23.09
CaO	0.02	0.04	0.08	0.08	0.04	0.09	<0.01	K_2O	0.22	0.18	0.22	0.08	Na_2O	0.04	<0.01	<0.01	0.04
Na_2O	0.08	0.09	0.23	0.37	0.30	0.34	0.26	Sum	100.01	100.11	100.41	100.96	K_2O	<0.01	<0.01	0.01	0.01
K_2O	9.16	9.56	9.65	9.41	10.41	10.51	10.73						Sum	97.08	97.00	97.35	96.86
Sum	95.02	95.58	96.20	96.62	96.22	96.27	95.54										
													Si	3.25	3.26	3.07	3.12
Si	2.73	2.76	2.79	2.74	3.36	3.25	3.44	Si	2.81	2.75	2.77	2.66	Al	2.99	3.03	2.59	2.25
Al^{IV}	1.27	1.24	1.21	1.26	0.64	0.75	0.66	Al	1.17	1.22	1.23	1.32	Ti	0.01	<0.01	<0.01	0.01
Al^{VI}	0.11	0.14	0.79	0.27	1.55	1.67	1.44	Ti	<0.01	<0.01	<0.01	<0.01	Fe^{3+}	0.13	0.10	0.48	0.79
Ti	0.23	0.21	0.08	0.18	0.03	0.02	0.04	Fe	<0.01	<0.01	0.01	0.01	Mn	0.00	<0.01	<0.01	<0.01
Cr	0.01	<0.01	<0.01	<0.01	<0.01	<0.01	<0.01	Mn	<0.01	<0.01	<0.01	<0.01	Ca	2.07	2.06	1.96	2.02
Fe	1.04	0.98	0.64	0.80	0.08	0.08	0.18	Ca	0.18	0.24	0.18	0.33	Na	<0.01	<0.01	<0.01	0.01
Mg	1.51	1.54	1.16	1.61	0.38	0.28	0.38	Na	0.88	0.81	0.85	0.71	K	<0.01	<0.01	<0.01	<0.01
Mn	<0.01	<0.01	<0.01	<0.01	<0.01	<0.01	<0.01	K	0.01	0.01	0.01	<0.01	Sum	8.44	8.45	8.10	8.19
Ca	<0.01	<0.01	0.01	0.01	<0.01	0.01	<0.01	An	16.7	22.4	17.6	31.6	Al_2Fe (mol%)	0.13	0.10	0.82	3.23
Na	0.01	0.01	0.03	0.05	0.04	0.04	0.03	Ab	82.1	76.6	81.2	68.0	$Fe^{3+}/Al+Fe^{3+}$	0.04	0.03	0.16	0.26
K	0.88	0.91	0.88	0.87	0.87	0.88	0.92	Kfs	1.2	1.0	1.2	0.4					
X_{Fe}	0.41	0.39	0.36	0.33	0.18	0.23	0.32										
X_{Mg}	0.59	0.61	0.64	0.67	0.82	0.77	0.68										

Table 2.4. Selected microprobe analysis of primary and secondary mica phases, plagioclase and epidote minerals .n.d.=not determined. Normalisation based on 11oxygens for mica, 8 oxygens for plagioclase and 12.5 for epidote minerals. Al_2 Fe=Fe/(Al-2) (Franz et al., 1995)).

2.5. Whole rock geochemistry

Major and trace element analyses for the five different eclogite groups are presented in Table 2.5. Analyses for major and trace elements were obtained using a Phillips PW-2400 X-ray fluorescence (XRF) spectrometer at the GeoForschungs-Zentrum Potsdam and the Geochemical Laboratory of the Institute of Geosciences in Mainz using internationally accepted rock standards yielding a determined precision better than 1–3% for major elements (depending on concentrations levels) and 2–3% for trace elements. The H_2O and CO_2 contents were analysed by quantitative high-temperature decomposition with an Elemental CHN analyser. Rare earth elements (REE) were determined by inductively coupled plasma–optical emission spectrometer (ICP-OES, Vista MPX) at the Geochemical Laboratory of the University of Potsdam. Sample preparation involved Na_2O_2 standard fusion and dilution techniques for dissolving rock powders into solution (Zuleger et al. 1988). Analytical precision was checked with international reference standards and found to be better than 12%.

eclogite type wt. %	SiO_2	TiO_2	Al_2O_3	Fe_2O_3(tot)	MnO	MgO	CaO	Na_2O	K_2O	P_2O_5	CO_2	H_2O	Sum	
coesite-bearing	48.03	2.85	13.20	14.25	0.21	6.53	10.29	2.65	0.91	0.29	0.09	1.09	100.39	
fine-grained	49.56	2.14	13.89	14.44	0.21	6.23	10.28	2.02	0.09	0.16	0.05	0.67	99.74	
inherited fabrics	48.27	2.75	12.47	16.78	0.26	5.27	9.86	2.50	0.75	0.25	0.06	1.02	100.26	
epidote-bearing	51.58	2.50	13.58	13.56	0.16	3.93	11.81	1.71	0.09	0.26	0.05	0.67	99.91	
skarn-like eclogite	39.62	5.94	14.99	21.46	0.26	4.83	11.00	0.89	0.07	0.04	n.d.	n.d.	99.68	
ppm	La	Ce	Pr	Nd	Sm	Eu	Gd	Tb	Dy	Ho	Er	Tm	Yb	Lu
coesite-bearing	12.9	30.5	3.7	20.1	5.4	1.9	6.5	1.1	6.3	1.2	3.5	0.5	3.0	0.4
fine-grained	6.0	14.3	1.7	9.8	3.0	1.1	5.1	0.9	6.2	1.2	3.6	0.6	3.2	0.5
inherited fabrics	15.3	37.1	4.8	21.6	6.8	2.1	8.3	1.3	8.7	1.8	5.2	0.8	4.9	0.7
epidote-bearing	23.8	52.5	6.5	29.8	7.1	2.1	7.8	1.3	7.3	1.5	4.0	0.6	3.5	0.5
skarn-like eclogite	0.9	4.0	0.7	4.4	2.9	1.6	7.5	1.3	12.1	2.5	7.2	1.0	6.3	0.9
ppm	Ba	Cr	Nb	Rb	Sr	V	Y	Zn	Zr					
coesite-bearing	127	170	18	33	137	400	39	96	159					
fine-grained	3	60	13	3	58	428	35	90	139					
inherited fabrics	37	<10	15	2	340	342	41	85	216					
epidote bearing	118	39	15	22	133	526	46	272	193					
skarn-like eclogite	<20	45	65	<3	32	528	65	119	210					

Table 2.5. Major- and trace-elements of the different eclogite types. n.d.= not determined.

2.5.1 Results

According to the classification of Winchester & Floyd (1977), based on contents of the relatively immobile high field strength elements Zr, Ti, Nb and Y (Fig. 2.7A), the eclogites are all of subalkaline to alkaline basaltic composition (assuming magmatic precursors). The maximum SiO_2 and Cr concentration of 51.6 wt.% and 170 ppm, respectively, are characteristic for the tholeiitic series according to the classification of Middlemost (1975). The non-skarn eclogites have total iron (as ferric) concentrations in the range 13.6 to 16.8 wt.%, low to moderate MgO (3.9–6.5 wt.%), mg# values of 23–31

(mg# = 100*Mg/(Mg + Fe_{tot}) for SiO_2 concentrations between 48 and 52 wt.%, and TiO_2 concentrations in the range 2.1–2.8 wt.% which are significantly higher than for modern subduction-related magmas (see compilation of modern analogues by Verma, 2006). Vanadium contents are 340–530 ppm but Ti/V is greater than 30, exceeding the limit of modern subduction-related basic melts significantly (Shervais, 1982). With one exception Cr concentrations are <110 ppm indicating that the melts parental to the eclogites could not have been in equilibrium with a mantle peridotite, and must have undergone pyroxene and spinel fractionation during their magmatic evolution. In contrast, the high Al_2O_3 (15.0 wt.%), total iron (as ferric) of 21.5 wt.%, TiO_2 (5.9 wt.%) and Nb (65 ppm) but low Na_2O (0.89 wt.%) and mg# (18) values of the skarn-like eclogites clearly distinguish them from the other eclogite samples.

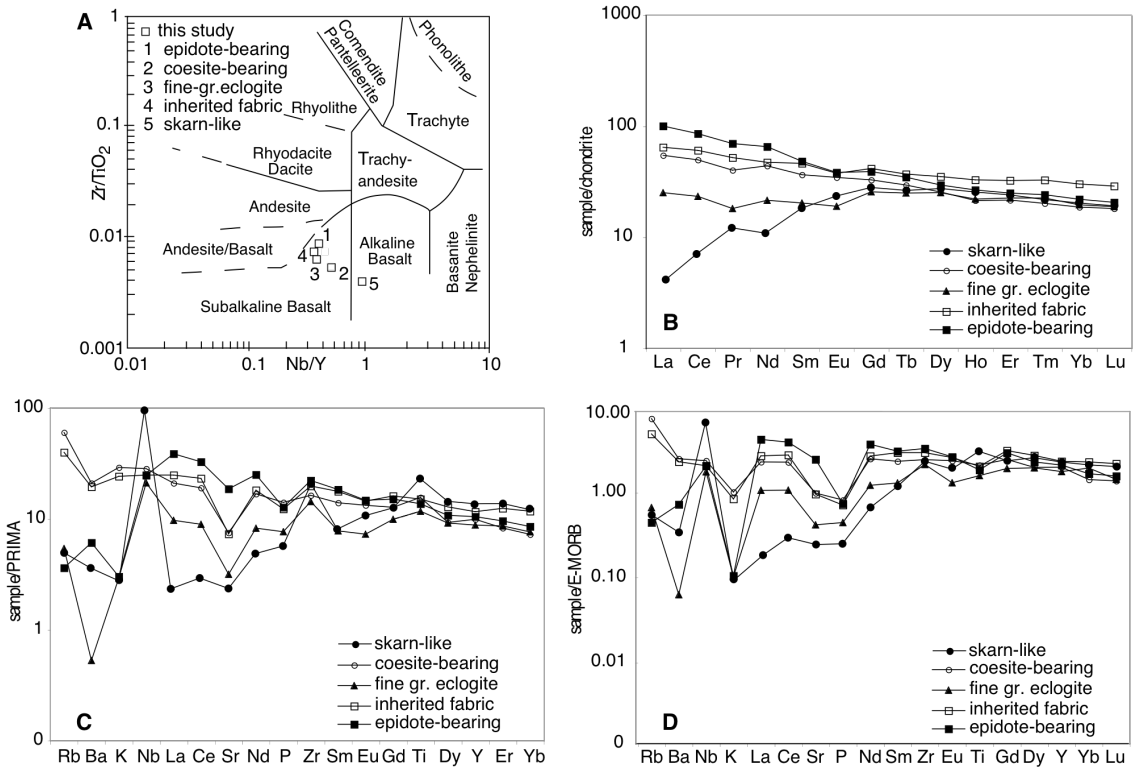

Fig. 2.7. A-D Geochemical discrimination plots for the different eclogites. A after Winchester & Floyd (1977). B Chondrite-normalised REE abundances (after McDonough & Sun, 1995). C and D show incompatible elements normalized to (C) primitive mantle (PRIMA) (after Hofmann, 1988) and (D) enriched mid-ocean ridge basalt (E-MORB) (after Sun & McDonough, 1989).

In order to evaluate possible melt-generating and -modifying processes in a qualitative way, the measured incompatible elements were plotted normalised to chondrite

(Fig. 2.7B: McDonough & Sun, 1995) primitive mantle (Fig. 2.7C: Hofmann, 1988), and E-MORB (Fig. 2.7D: Sun & McDonough, 1989). Three metabasic samples show similar behaviour with a moderate chondrite-normalized LREE enrichment (Fig. 2.7B) as expressed by chondrite-normalized La/Yb ratios between 2.1 and 4.6 and La/Sm ratios between 1.4 and 2.1. The fine-grained eclogite, despite comparable major and most minor element concentrations to those of the other eclogite types, shows significantly different trace element patterns with lower LREE contents, and La/Yb (1.3) and La/Sm (1.2) values similar to those of transitional mid-ocean ridge basalts (T-MORB, Schilling et al., 1983). The skarn-like eclogite is characterised by low LREE (La/Yb and La/Sm= 0.1) and displays a N-MORB like pattern (Fig. 2.7B).

Primitive mantle-normalised multi-element plots (Fig. 2.7C) show a pronounced enrichment in LIL elements and the lack of any Nb anomaly. The most significant anomaly of the metabasic samples is the PRIMA-normalized negative Sr anomaly, resulting from low concentrations, with an average of 140 ppm**.**

2.6. Metamorphic conditions and evolution

sample	Peak Grt X_{Mg} X_{Ca}	Cpx X_{Mg} X_{Jd}	Phg core X_{Mg} Si p.f.u.	Phg rim X_{Mg} Si p.f.u.	Amp secondary X_{Mg}	Plag secondary X_{An}	K_DGrt-Cpx Fe-Mg	Grt-Cpx T[°C] P[kbar]	lnKGrt-Phg-Cpx core Fe-Mg	Grt-Phg-Cpx T[°C] P[kbar]	K_DGrt-Phg Fe-Mg	Grt-Phg T[°C] P[kbar]	Amp-Plag T[°C] P[kbar]
K4-120	0.21	0.41	0.67					698		690		790	
	0.25	0.32	3.44				9.42	36	1.92	33	5.23	30	
K4-106	0.29	0.43						740					
	0.25	0.45					7.80	30					
K4-98	0.20	0.43						749					
	0.38	0.33					6.01	30					
PK2-4	0.26	0.42						764					654
	0.26	0.39			0.49	17.81	7.22	30					12
													717
					0.48	31.56							12
JNar2	0.18	0.43		0.75						690		763	
	0.35	0.39		3.25					4.77	33	7.12	33	
JNar2	0.19	0.43	0.78					703		690		759	
	0.38	0.37	3.43				13.54	36	2.66	36	8.10	36	
K4-84	0.29	0.41						721					
	0.25	0.18					8.33	30					
K3-11	0.21	0.43						641					
	0.30	0.45					13.50	30					
K4-58	0.19	0.38						659					
	0.19	0.22					8.12	30					
K4-57	0.20	0.40						644					
	0.23	0.26					10.28	30					
K4-76	0.23	0.38						746					
	0.25	0.25					7.58	30					
PKB3	0.15	0.37						707					
	0.29	0.15					9.91	30					

Table 2.6. Amalgamated mineral compositions and P-Testimates. Grt-Cpx: T from Krogh (1988) for given nominal P; Grt-Phg-Cpx: method of Carswell et al., 1997; Grt-Phg: calculation of Green & Hellman (1982); Amp-Plag: calculated after Holland & Blundy (1994).
X_{Mg}=Mg/Mg+Fe^{2+}+Ca+Mn; X_{Ca}=Ca/Ca+Fe^{2+}+Mg+Mn; X_{An}=Ca/Ca+Na+K

The petrographic descriptions and characteristic mineral compositions of the studied eclogites make it apparent that no single equilibrium assemblage is present in a sample. Instead, compositional zoning and reaction textures, especially with the evolution of different amphibole generations, allow an insight into the possible P-T path followed by the Kaghan eclogites. The peak-pressure parageneses in the eclogites are all plagioclase-free and garnet+omphacite+rutile-bearing. Additional phases such as phengite, quartz

(locally coesite), carbonate(s), and epidote occur in various proportions in the assemblages pre-dating amphibole growth. Standard conventional geothermobarometers for these assemblages are the garnet–clinopyroxene (Krogh, 1988), and garnet–phengite (Green & Hellman, 1982) Fe–Mg exchange thermometers and the garnet–clinopyroxene–phengite (Carswell et al., 1997) geobarometer which, together with the univariant coesite=quartz reaction for the samples with preserved coesite relics, allow a broad delimitation of metamorphic conditions.

The compositional profiles for garnet (Figs. 2.3 & 4) show significant variation in both Ca content and X_{Mg}. We interpret garnet cores with generally lowest X_{Mg} and high Ca (in some cases also high Mn) as belonging to part of the prograde evolution and have interpreted outer parts of grains (not necessarily the rims which in most cases show effects of decompression and resorption of garnet) with a plateau at maximum X_{Mg} as representing the peak eclogite facies stage. Based on this assumption for peak-pressure eclogite garnet composition, and taking the most jadeite-rich omphacite (Table 2.6), we deduced temperatures in the range 640-790°C for pressures in the range 30-36 kbar (Table 2.6, Fig. 2.8). Garnet–phengite thermometry, using the same garnet combined with the most silicic phengite, yielded a similar range (Table 2.6). For the selected phengite-bearing eclogites the pressures deduced by the garnet–clinopyroxene–phengite geobarometer plot above the coesite=quartz univariant curve (as already pointed out by O'Brien et al., 2001).

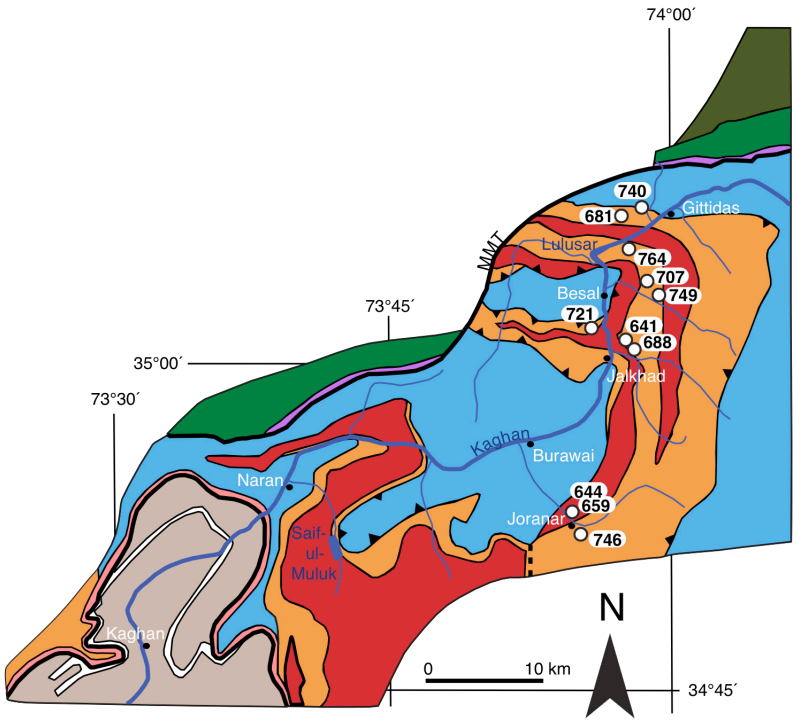

Fig. 2.8. Spatial distribution of temperatures (°C) at 30 kbar derived by standard geothermometry for studied eclogites, using Grt-Cpx (Krogh, 1988). Further methods and details are presented in Table 2.6 and Fig. 2.1.

A significant new observation was the presence of glaucophane cores to sodic–calcic amphoboles in coesite-bearing eclogites. Porphyroblastic amphiboles post-dating the peak-pressure assemblage are characteristic for these eclogites and the presence of glaucophane has important consequences for possible exhumation paths. In order to investigate the possible growth conditions for glaucophane in these rocks we constructed phase diagrams for the effective bulk composition of the rock (i.e. taking the fractionation effect of the zoned garnet into consideration: Spear, 1988; Konrad-Schmolke et al., 2005) using the software Perple_X07, the thermodynamic data of the internally consistent and up-dated dataset of Holland & Powell (1998) and the solid-solution models (in file solut_07) of Dale et al. (2005: amphibole), Fuhrman & Lindsley (1988: feldspar), Berman (1990: garnet), Holland et al. (1998: chlorite), Holland & Powell (1990: phengite), Holland & Powell (1998: epidote) and Holland & Powell (1996: omphacite).

For the petrographically-determined amphibole-free eclogite facies stage, taking into consideration the Si per formula unit (p.f.u.) in phengite, pressures in the coesite field (above 30 kbar) were deduced at around 700°C: values consistent with the results from conventional geothermobarometry (Fig. 2.9). The subsequent growth of glaucophane in

the rock, monitored by the Na content on the A-site [Na(A)] in amphibole, requires conditions around 580-630°C at 10-17 kbar i.e., indicating significantly lower temperatures following a major amount of decompression. The observation that glaucophane-cored porphyroblasts enclose ragged omphacite relicts, points to breakdown of eclogite facies pyroxene in the presence of water at this stage. Surrounding the glaucophane cores are amphiboles of sodic-calcic (barroisite) or calcic (magnesiohornblende) composition. The growth of these second-stage amphiboles requires a significant reheating from the conditions required for glaucophane. This is supported by temperatures derived from conventional amphibole-plagioclase thermometry (Holland & Blundy, 1994) of 650-720°C at around 12 kbar (Table 2.6; Fig. 2.9), taking the plagioclase composition from amphibole-plagioclase intergrowths and with the replacement of rutile by ilmenite. The resultant PT-path from this approach (Fig. 2.9) shows cooling during decompression from peak (coesite-field) pressures at mantle depths followed by a heating stage at normal crustal depths remarkably similar to the path proposed for Tso Morari coesite-bearing eclogites by de Sigoyer et al. (1997).

2.7. Discussion and conclusions

In the last decade, field studies have significantly extended the number of eclogite bodies known from the Upper Kaghan Valley. Together with the results of mapping of the neighbouring Neelum Valley (Fontan et al., 2000) it is clear that eclogite facies metabasites are generally small bodies, representing former dykes, sills and flows, but are widespread. Although significant variation in degree of retrogression can exist within a single metabasite body, it is still possible to assign all the eclogites to one of five major textural types. Analysis of major and trace element compositions showed, despite textural differences, that all investigated samples are subalkaline/alkaline basalts showing tholeiitic affinity and, apart from the very fine-grained and skarn-like type, exhibiting similar behaviour in REE thus strongly suggesting a genetic relation between the investigated samples. Minor differences in the REE pattern probably reflect different amounts of contamination during the emplacement in the continental crust. The deduced major and trace element trends, with key values such as high TiO_2 and Nb contents exclude a subduction-related origin whereas normalised La/Sm (1.25-2.0), La/Yb (1.3-4.6) as well as Zr >>100 ppm, are essentially the same as those recognized for rift tholeiites and within-plate volcanism elsewhere (e.g. Deniel et al., 1994; Pearce & Norry,

1979; Verma, 2006) but, most importantly, also for analyses of non-metamorphosed Panjal Trap continental flood basalts (Bhat et al., 1981; Chauvet et al., 2008) with which the Kaghan metabasites have long been correlated (Papritz & Rey, 1989; Greco & Spencer, 1993; Spencer et al., 1995).

Despite the close similarity in bulk chemistry, other possibilities to explain the difference in eclogite appearance are the metamorphic PT-path or, alternatively, the protolith grain size (fine-grained, possibly hydrothermally-altered basalt versus coarse-grained less-altered dolerite or gabbro). The calculated equilibrium conditions for the different eclogite types do not show significant variation despite the fact that samples are widely spaced. It is highly likely that a continuation of the coesite-eclogite unit exists further north, still buried below Kohistan. The presence of coesite in eclogites only from the northern-most locations, close to the contact with the Kohistan arc, could merely be a problem of preservation potential in the other locations. Significantly, the garnet–clinopyroxene–phengite barometer, the prospecting tool used to locate the first coesite-bearing eclogite (O'Brien et al., 2001), yields coesite-field pressure conditions for samples collected much further south (Fig. 2.1) where no evidence for the former presence of coesite exists. This strongly suggests that a much larger area of the Upper Kaghan experienced pressures of around 30 kbar and that either evidence for the former presence of coesite has been completely obliterated or, alternatively, that these rocks underwent no significant garnet and/or clinopyroxene growth at eclogite facies conditions such that there was no potential for trapping of coesite inclusions at high pressures. This latter alternative has been discussed for Norwegian eclogites by Konrad-Schmolke et al. (2008) and explained with reference to bulk-element fractionation (reflected in distinct compositional zoning patterns in garnets) during episodic rather than continuous garnet growth along a PT path. The important point is that slightly different parageneses and mineral compositions can be derived from the same protolith dependent on subtle variations in growth episodes of major minerals that, as long as non-equilibrated (i.e. zoned) phases exist, thus modifies the effective reacting bulk composition.

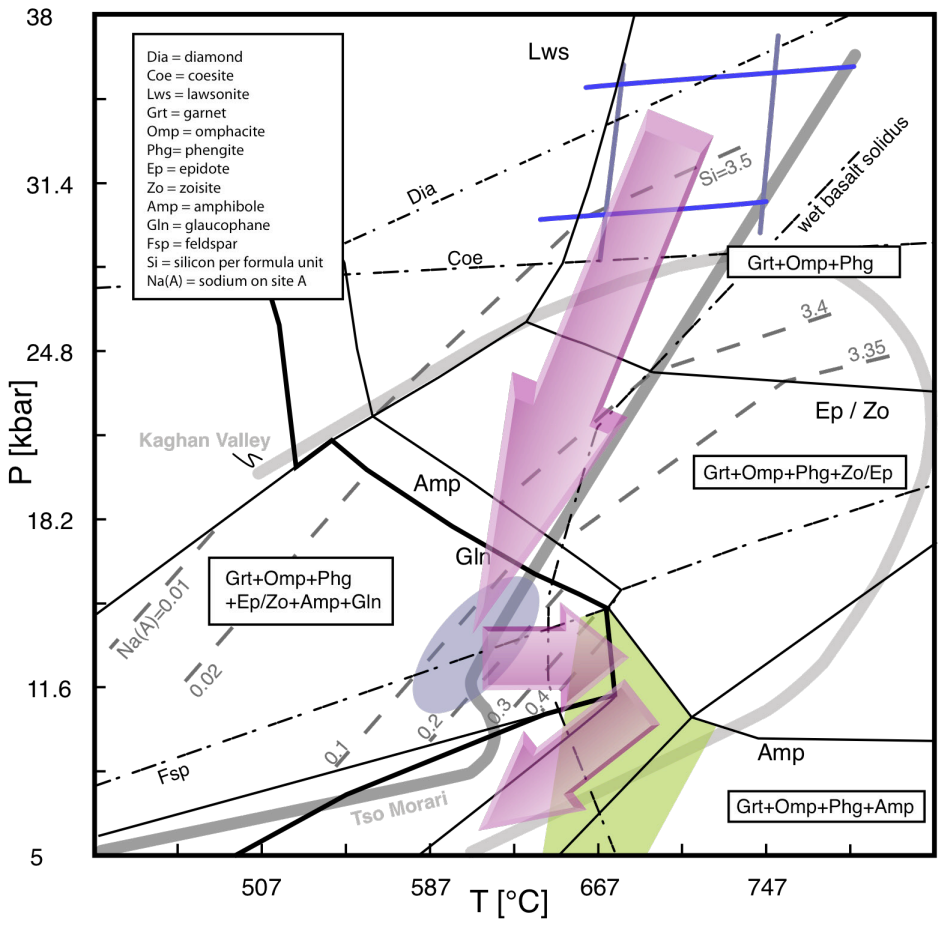

Fig. 2.9. Phase diagram for garnet-fractionated bulk rock chemistry of the UHP eclogite (K4-120) calculated with Perple_X. Plotted are Si content in phengite (p.f.u.) and Na on A-site in amphibole. Also plotted are the water-saturated basalt solidus (Lambert & Wyllie, 1972) and Graphite-Diamond curve (Kennedy & Kennedy, 1976). Coe-Qtz and Alb=Jd+Qtz equilibria are calculated within the phase diagram calculation. The ellipse indicates the field for the measured glaucophane composition whereas the grey-shaded area denotes the limits from corner Amp-Plag barometry. Large arrows show our preferred PT-path. Published PT-paths for Kaghan Valley (Rehman et al., 2008) and for Tso Morari coesite eclogites (Guillot et al., 2008) are shown for comparison.

Pressure-temperature-time information for the Kaghan Valley metamorphic rocks exists from several previous studies. Peak metamorphic conditions for eclogites were derived by O'Brien et al. (2001: 27-29 kbar; 690-750°C), Kaneko et al. (2003: 27-32 kbar; 700-770°C) and Rehman et al. (2007: 757-786°C; 28.6±0.4kbar; 2008: 28kbar; 762±46°C). A significant contrast exists between proposed decompression paths. Kaneko et al. (2003) show a clockwise PT-path with slight cooling during decompression (to 655±55°C; 11±1.4 kbar) whereas Rehman et al. (2008), based on the interpretation of

assemblages in metapelites, suggested a distinct heating to 859±59°C at pressures around 18 kbar (high-pressure granulite facies) before subsequent cooling. This latter path is inconsistent with the presence of secondary glaucophane (as described by Lombardo et al. (2000) or in this work for the first time in coesite-bearing samples) or the survival of sharp compositional zoning profiles in garnet of several eclogites: features requiring relatively low temperatures following the peak. Although heating at lower pressures occurred it is likely that this was only a short-lived episode superimposed on a rapid exhumation path. Significantly, the S-shaped PT-path deduced here for the Kaghan eclogites (Fig. 2.9) is remarkably similar to that presented for the Tso Morari unit (de Sigoyer et al., 1997; Guillot et al., 1997; Guillot et al., 2008). This comparison is strengthened when the timescale of exhumation for these two areas is compared (Massonne & O'Brien, 2003; Treloar et al., 2003; Parrish et al., 2006). In both cases the exhumation from deep mantle to normal crustal depths occurs at rates of several cm per year before slowing to more normal mm per year rates thus suggesting a change in exhumation mechanism between these two stages. It is likely, based on the short time period between ocean closure and peak metamorphism of the subducted Indian Plate at coesite-eclogite conditions that the generally fine-grained nature of the eclogites, as well as the net-like garnet microstructure in many samples, is a product of nucleation–growth kinetics from variably altered protoliths.

The leucocratic segregations recognised in some of the eclogites are comparable with features documented from other eclogite locations around the world (e.g. Becker et al., 1999; Hermann et al., 2006). Such quartz-rich zones containing minerals such as phengite, zoisite, kyanite and rutile have been interpreted as products of metasomatic fluid flow driven by dehydration reactions in the metabasites and their surrounding pelitic gneisses (Spandler & Hermann, 2006; Castelli et al., 1998). In some eclogites there are distinct lens-like bodies of quartz-garnet-phengite-rutile fels most probably derived in the same manner. The possibility of a derivation by melting (e.g. Liebscher et al., 2007) is unlikely due to the complete absence of albite-rich plagioclase in the Kaghan examples although the PT-path for the rocks certainly passed through the necessary wet melting conditions.

In comparison to the metabasites with an obvious, despite retrogressive overprint, eclogite facies evolution, meta-dolerites which crop out in the southern-most part of the study area show no indication that plagioclase was unstable and thus, despite the growth

of metamorphic garnet coronas, probably experienced at most amphibolite facies conditions. Metabasic rocks with relicts of magmatic intergranular textures and growth of amphibole–garnet–biotite–chlorite-bearing assemblages were described by Fontan et al. (2000) from the SW Kalapani unit in the adjacent Neelum Valley. Formation conditions of 650-750°C at 8-9 kbar are consistent with the deduced third stage of metamorphism (producing pargasite, plagioclase and ilmenite) in the eclogite series (at 650-720°C at 12 kbar (Table 2.6, Fig. 2.9). The metamorphic conditions for the metadolerites are thus convergent with those of retrogression in the eclogite series and indicate a tectonic juxtaposition of these units after the eclogite facies stage. Such stacking of Indian Plate basement–cover units is well known further west in Pakistan (Treloar et al., 2003, DiPietro et al., 1993) where more extensive mapping has been undertaken, and is also a fundamental aspect of the subduction–exhumation models for ultrahigh-pressure metamorphic series (e.g. Chemenda et al., 2000; O'Brien, 2001).

2.8. Acknowledgements

We would like to thank Stéphane Guillot and Ian Buick for their helpful reviews and comments on the manuscript. This work received financial support from the Graduate School 1364, funded by the German Science Foundation (DFG). We thank Robert Reinisch for some of the samples and Roland Oberhänsli for helpful discussions. Excellent thin sections were prepared by Christine Fischer and microprobe analysis was supported by Oona Appelt (GFZ Potsdam). We are grateful to Antje Musiol (Potsdam) und Nora Groshopf (Mainz), for their chemical laboratory work.

3. The multistage exhumation history of the Kaghan Valley UHP series, NW Himalaya, Pakistan from U-Pb and $^{40}Ar/^{39}Ar$ ages

Abstract

Amphibole and mica $^{40}Ar/^{39}Ar$ ages as well as zircon, rutile and titanite U-Pb geochronology for rocks of the Higher Himalayan Crystalline (Indian Plate) in the Upper Kaghan Valley, Pakistan allow distinction of a multistage exhumation history. An Eocene age for peak pressure metamorphism has been obtained by phengite $^{40}Ar/^{39}Ar$ (47.25±0.26 Ma) and zircon U-Pb (47.25±0.43 and 47.42±0.25 Ma) from cover and basement gneisses. A very short-lived metamorphic peak and rapid cooling is documented by an amphibole $^{40}Ar/^{39}Ar$ age of 46.65±0.24 Ma and a rutile U-Pb age of 44.1±1.3 Ma from eclogites. Phengite and biotite ages from cover and basement sequences metamorphosed during the Himalayan orogeny are 34.47±0.20 to 28.07±0.22 Ma whereas youngest biotites, yielding 23.55±0.14 and 21.72±0.24 Ma, probably reflect Argon partial resetting due to enhanced hydrothermal activity related to exhumation of the nearby Nanga Parbat massif. The amphibole age, together with those derived from phengite and zircon demonstrate a rate of initial exhumation of 143-86 mm/a i.e. an extremely rapid transport of the Indian Plate continental crust from ultra-high pressure (UHP) conditions back to crustal levels (47-46 Ma, 140-40 km). Subsequent exhumation (46-41 Ma, 40-35 km) slowed to about 1 mm/a at the base of the continental crust but increased again during the late stage, toward slightly higher exhumation rates of ca. 2 mm/a (41-34 Ma, 35-20 km) indicating a change from buoyancy driven exhumation at mantle depths to compression forces related to continent-continent collision and accompanied crustal folding, thrusting and stacking that finally exposed the former deeply-buried rocks.

3.1. Introduction

A spectacular record of crustal thickening, magmatism, multi-stage metamorphism, exhumation and extension, reflecting the subduction of Tethys and subsequent collision of India with Asia, is especially evident in rocks of the former margin of the Indian Plate exposed in NW Pakistan (e.g., Treloar & Searle, 1993; Khan et al., 2000). Although the

main rock types of the crystalline complexes of the Indian Plate are clastic and carbonate-rich metapelites that cover the granitic basement, numerous volumetrically-minor mafic rocks have been recognised. These locally preserve eclogite facies assemblages which reveal an important part of the initial, deep crustal subduction metamorphic history whereas their host gneisses mainly preserve evidence of later dynamic, recrystallisation processes, linked to exhumation- and collision-related metamorphism.

Several workers have attempted to quantify the timing of the metamorphic evolution and the exhumation velocity of the Kaghan Valley. Tonarini et al. (1993), investigating a single eclogite sample, obtained values for peak metamorphism at 49±6 Ma (Sm-Nd, garnet-clinopyroxene) and subsequent cooling ages of 43±1 Ma (Rb-Sr, phengite) and 39-40 Ma (U-Pb, rutile) and referred to the cooling rate as "rapid". Dating by the U-Pb method of zircon (46.4±0.1, 46.2±0.7 and 44±3 Ma: Parrish et al., 2006; Kaneko et al., 2003 and Spencer & Gebauer, 1996, respectively) for the ultrahigh-pressure (UHP) stage, and titanite (46.4 Ma, Parrish et al., 2006) and rutile (44.1±1 Ma, Treloar et al., 2003) for texturally younger (although still high pressure) vein minerals confirm this pattern. Earlier studies suggested 47±3 Ma for peak metamorphism at Naran (Smith et al., 1994: zircon SHRIMP) as well as in Swat valley (further west) whereas the later amphibolite facies overprint was dated at 35-44 Ma (Chamberlain et al., 1991: Ar-Ar, hornblende). From the adjacent Neelum Valley, $^{40}Ar/^{39}Ar$ dating of amphibole and micas points to an early cooling at about 40 Ma followed by Oligocene (29-32 Ma) and Miocene (17 Ma) ages interpreted as cooling through medium to low-grade metamorphic conditions (Fontan et al. 2000). Similar cooling ages were reported from Indian Plate rocks near Besham (Indus Valley west of Kaghan) for hornblende (35±4 Ma), muscovite (24 Ma), and biotite (29-22 Ma) using K-Ar, Ar-Ar and Rb-Sr methods (Treloar & Rex, 1990).

In the eclogite-bearing series of Tso Morari (Ladakh, India) ages for the peak pressure metamorphism of 55±17 and 55±12 Ma (U-Pb: allanite and Lu-Hf: garnet–rutile–pyroxene, respectively), subsequent glaucophane-bearing assemblage of 55±7 Ma (Sm-Nd: garnet–glaucophane–rutile), amphibolite facies overprint of 45-48 Ma (Sm-Nd, Rb-Sr, $^{40}Ar/^{39}Ar$ methods for garnet–amphibole–rutile, phengite–apatite–rutile and phengite, respectively) determined by de Sigoyer et al. (2000) and late cooling through the partial annealing zone (PAZ) of 300-200°C determined by zircon fission track (ZFT) ages of 35-45 Ma (Schlup et al., 2003) reveal a multistage exhumation. Sigoyer et

al. (2000) suggested a two stage exhumation history with an initial rate of >5 mm/a later slowing to about 1.2 mm/a. However, diffusion modelling of sharp compositional steps in garnet indicates a much narrower time window and thus significantly higher initial rates of at least 23-45 mm/a (O'Brien & Sachan, 2000; Massonne & O'Brien, 2003). These rates fit the age constraints (considering the uncertainties) from de Sigoyer et al. (2000). Similar initial rapid exhumation (30-80 mm/a "or more") was proposed for Kaghan eclogites by Parrish et al. (2006) based on U-Pb ages for zircon, allanite and titanite. In this work we attempt to constrain the exhumation history of the petrographically-determined (Wilke et al., 2009) multistage metamorphic evolution of the Kaghan eclogites and related rocks by a combined U-Pb (zircon, rutile and titanite) and $^{40}Ar/^{39}Ar$ (amphibole and micas) investigation.

3.2. Geological setting

High-grade metamorphic rocks in northern Pakistan occur in the upper Kaghan and Neelum Valleys (Fig. 3.1) as part of the so-called Higher Himalayan Crystalline (HHC) series. This part of the Indian plate is bounded to the north by the Indus Suture (Main Mantle Thrust, MMT) from the mafic/ultramafic rocks of the Kohistan Island Arc, and to the south by the Batal Thrust from lower-grade sequences generally attributed to the Lesser Himalaya (Fig. 3.1). Three main units can be identified in the HHC: a basement complex made of metagranite and paragneiss, which is overlain by two sequences of meta-sedimentary cover rocks: an early Palaeozoic, predominantly metapelite–greywacke-bearing unit with minor mafic lenses including the Naran and Lulusar Formations and a second stratigraphically younger series with marbles, garnet-staurolite-kyanite schists and amphibolites which is lithologically identical to the Alpurai sequence in the Swat Valley (Chaudhry & Ghazanfar, 1987; Greco et al., 1989; Greco & Spencer, 1993; DiPietro et al., 1993). By comparison with unmetamorphosed units in Kashmir, the carbonate-rich sequence is interpreted as Permo-Mesozoic platform cover and the mafic bodies as dykes, sills and lava flows corresponding to the extensive Panjal Trap magmatism (Wadia, 1931; Greco & Spencer, 1993) of Permo-Triassic age. Isotope studies (e.g., Argles et al., 2003) reveal that some of the high grade metamorphic rocks of the HHC (i.e., the cover units) correspond to Tethyan Series rocks of the Central Himalaya which generally are of very low grade thus indicating a significant difference in

the tectonometamorphic evolution of the NW Himalaya compared to that of the rest of the belt.

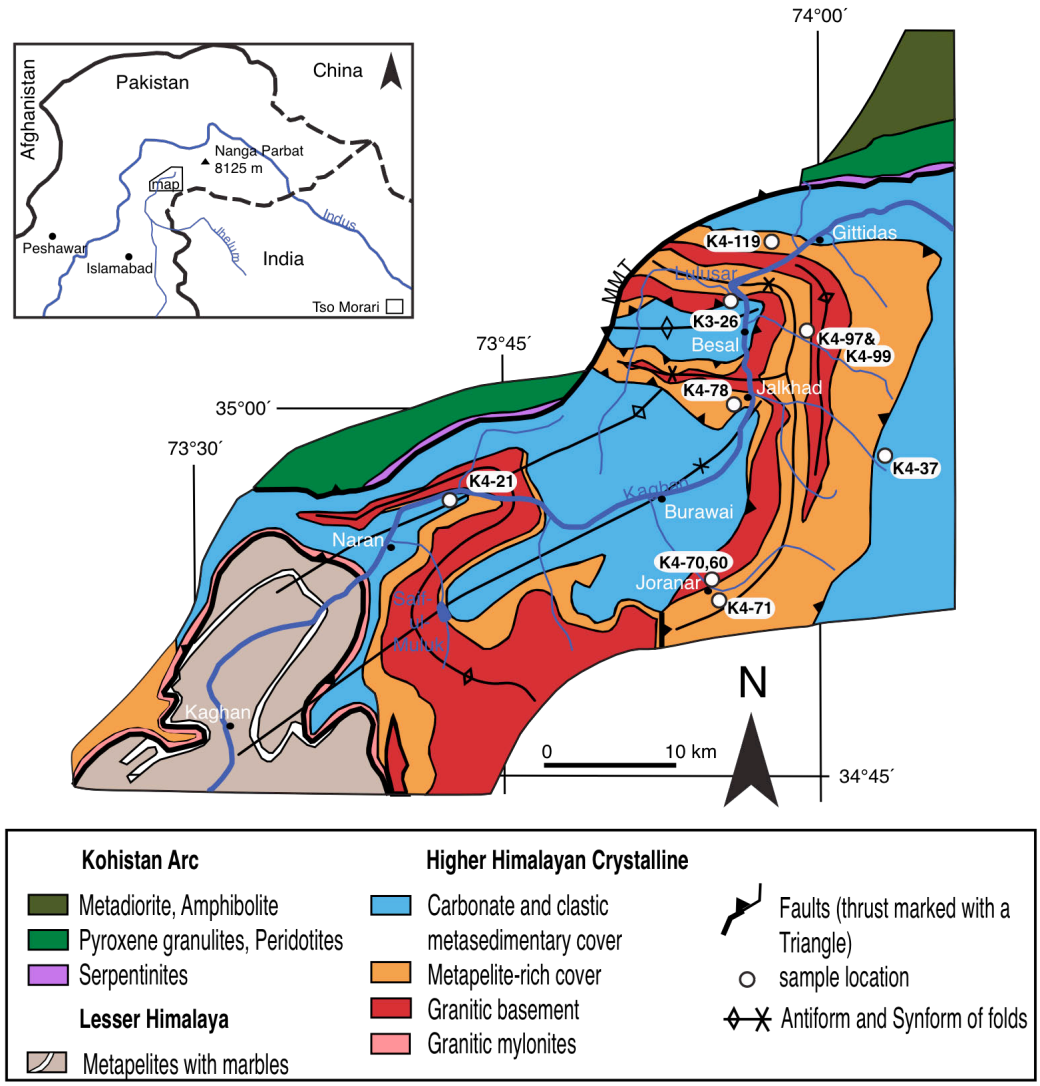

Fig. 3.1. Simplified geological map of upper Kaghan Valley, north Pakistan (modified after Greco & Spencer, 1993; Lombardo et al., 2000; Treloar et al., 2003) showing locations of dated samples. Inset map shows the regional location.

The large-scale structure in the Upper Kaghan Valley (Fig. 3.1) is represented by recumbent fold nappes and isoclinal folds pre-dating the stacking of thrust sheets (Treloar et al., 1989; Greco & Spencer, 1993). Subsequent northwest–southeast-oriented open folds were followed by east–west-trending large-wavelength and -amplitude folds, indicating an anticlockwise rotation of convergence (Greco et al., 1989; Treloar et al., 1989; DiPietro & Lawrence, 1991). Deformation related to the exhumation of high-grade units is reflected in a top-side-north extensional shearing visible by down-dip stretching

lineation of amphiboles on shear surfaces, at high structural levels close to the MMT (Burg et al., 1996; Kazmi & Jan, 1997; Treloar et al., 2003). This latter stage is well evidenced by folds involving albite porphyroblasts (often several cm in length) representing a greenschist facies overprint, in pelitic, granitic and basic rocks, of former amphibolite- to eclogite facies assemblages. Cooling ages of 42-40 Ma for amphibole (Chamberlain et al., 1991; Smith et al., 1994) predating the stack of thrust sheets and the related regional metamorphism: suggesting a very narrow time-window for the exhumation from eclogite- to amphibolite facies conditions (Treloar et al., 2003). Extension controlled by the MMT had finished by the early Miocene (Burg et al., 1996; Anczkiewicz et al., 2001).

3.3. Sample description, petrography and mineral chemistry

3.3.1. Analytical techniques

In the following section, the location, petrography and mineral chemistry of investigated samples is outlined (Table 3.1). Minerals separated for $^{40}Ar/^{39}Ar$-geochronology have been characterised by electron microprobe using a 4 spectrometer Cameca SX100 at the GeoForschungsZentrum (GFZ) Potsdam operating at 15 kV and 20 nA with a 2-10 µm beam. Counting time were 10-30 s on peaks and half this on backgrounds. Synthetic and natural standards were used. Representative point analyses are given in Table 3.2.

3.3.2. Results

Sample K4-119 is a quartz-phengite schist forming layers in coesite-eclogite from the first, metapelite-rich cover unit in Saleh Gali, near Gittidas. The rock, also containing minor allanite, apatite and rutile, is probably the result of metasomatism and fluid flow driven by dehydration reactions in the metabasites at eclogite facies conditions as noted in eclogites elsewhere (Spandler & Hermann, 2006; Hermann et al., 2006). Analysed were unstrained phengites, up to 500 µm in length, only partly transformed to biotite and plagioclase at their margins, exhibiting high and relatively homogeneous Si contents of around 3.4 Si per formula unit (p.f.u.) indicative of high pressure conditions (Table 3.2, Fig. 3.7).

sample	lithology	relation to eclogites	mineral assamblage	size of separated minerals [µm]	number of grains measured			Ar-Ar Age [Ma]			
					Ar-Ar			plateau age		apparent age	
				grain size [µm]	biotite	phengite	amphibole	phengite	biotite	biotite	amphibole
K4-21	garnet gneiss	host rock	quartz, feldspar, garnet, amphibole, biotite, graphite, ilmenite, calcite	125-250	8				28.07		
K4-37	gneiss	host rock	garnet, white mica, quartz, plagioclase, biotite, allanite, rutile, apatite, tourmaline	125-250	8	8		31.77		21.72	
K4-70	gneiss	host of metabasites	amphibole, biotite, garnet, quartz, plagioclase, feldspar, epidote minerals, titanite, apatite	125-250	8				29.57		
K4-97 (Kaar2)	quartz vein	in eclogitic body	phengite, quartz, biotite, plagioclase, epidote, titanite, apatite	250-500 & >1cm	3–4	8, 1		34.47, 47.48	28.25		
K4-99	eclogite		garnet, omphacit, amphibole, plagioclase, biotite, epidote, quartz, TiO_2 phases, apatite	125-250	8		10		23.55		46.65
K4-119	gneiss	between eclogite bodies	phengite, quartz, allanite, biotite, apatite, rutile	250-500		3–4		47.25			
					U-Pb			U-Pb Age [Ma]			
					zircon	rutile	titanite				
K3-26	garnet-orthogneiss	host of metabasites	garnet, biotite, feldspar, plagioclase, quartz, allanite, apatite, zircon	≥200	2			47.25			
K4-60	eclogite		garnet, omphacite, amphibole,plagioclase, quartz, rutile (TiO_2 phases), zircon	≥100		7		44.05			
K4-71	garnet-amphibolite		garnet, amphibole, quartz, epidote minerals, albite, rutile, titanite	≥60			2	41.30			
K4-78	garnet-orthogneiss	host of metabasites	garnet, biotite, feldspar, plagioclase, quartz, allanite, apatite, zircon	≥100	14			47.42			

Table 3.1. Sample description, mineral content with details as well as size, amount and results of measured minerals.

sample	K4-21		K4-37		K4-37		K4-70		K4-97		K4-97		K4-99		K4-119		K4-99	
	Biotite rim	core	Phengite rim	core	Biotite rim	core	Biotite rim	core	Phengite rim	core	Biotite rim	core	Biotite rim	core	Phengite rim	core	Pargasite rim	core
SiO_2	38.58	38.80	49.00	48.97	34.66	34.83	36.39	36.10	48.13	48.53	36.85	36.56	35.20	34.95	50.20	50.16	41.24	38.16
TiO_2	3.02	3.43	0.91	0.96	2.78	2.73	2.91	2.91	1.00	0.95	3.04	2.95	3.24	3.12	0.63	0.65	0.67	0.28
Al_2O_3	18.68	18.17	30.59	30.54	17.75	17.68	18.84	18.78	30.08	29.72	18.27	18.12	19.60	19.83	26.47	26.48	16.82	22.78
FeO	15.19	15.08	3.15	3.22	27.62	27.50	22.05	21.61	4.66	4.49	21.78	22.29	18.59	17.96	4.45	4.29	16.47	16.87
MgO	12.92	13.03	1.58	1.61	3.98	4.12	8.01	7.90	1.71	1.64	8.14	8.01	10.14	10.21	3.04	3.08	9.28	6.75
MnO	<0.01	0.02	<0.01	0.04	0.08	0.14	0.41	0.43	0.02	0.03	0.17	0.18	0.07	0.12	<0.01	0.04	0.11	0.15
CaO	0.10	<0.01	<0.01	<0.01	0.05	<0.01	0.10	0.01	0.03	<0.01	0.07	<0.01	0.09	0.02	<0.01	<0.01	10.57	10.14
Na_2O	0.16	0.22	0.40	0.42	0.08	0.10	0.07	0.08	0.27	0.30	0.06	0.10	0.08	0.06	0.28	0.21	3.18	3.76
K_2O	8.28	8.71	10.32	10.26	8.63	9.13	9.02	9.38	10.43	10.62	8.54	9.34	8.62	9.35	10.49	10.51	1.04	0.30
Sum	96.92	97.45	95.94	96.02	95.62	96.22	97.79	97.19	96.33	96.27	96.92	97.54	95.62	95.63	95.56	95.42	99.37	99.19
Si	2.788	2.795	3.259	3.256	2.731	2.733	2.721	2.719	3.221	3.249	2.764	2.747	2.647	2.633	3.380	3.380	Si 6.043	5.597
Al^{IV}	1.212	1.205	0.741	0.744	1.269	1.267	1.279	1.281	0.779	0.751	1.236	1.253	1.353	1.367	0.620	0.620	Al^{IV} 1.957	2.403
Al^{VI}	0.379	0.338	1.656	1.649	0.379	0.368	0.381	0.386	1.594	1.594	0.379	0.352	0.384	0.393	1.481	1.483	**T 8.000**	**8.000**
Ti	0.164	0.186	0.045	0.048	0.165	0.161	0.163	0.165	0.050	0.048	0.171	0.167	0.183	0.177	0.032	0.033	Al^{VI} 0.947	1.534
Fe	0.918	0.909	0.175	0.179	1.820	1.804	1.379	1.361	0.261	0.251	1.366	1.401	1.169	1.131	0.250	0.242	Ti 0.074	0.030
Mg	1.392	1.400	0.157	0.159	0.468	0.482	0.893	0.887	0.170	0.164	0.910	0.897	1.136	1.147	0.306	0.310	Fe^{3+} 0.283	0.243
Mn	–	0.001	–	0.002	0.005	0.009	0.026	0.028	0.001	0.002	0.011	0.011	0.004	0.008	–	0.002	Mg 2.028	1.476
Ca	0.008	–	–	–	0.004	–	0.008	<0.001	0.002	–	0.006	–	0.007	0.002	–	–	Fe^{2+} 1.667	1.717
Na	0.022	0.030	0.052	0.053	0.012	0.015	0.010	0.011	0.036	0.039	0.009	0.015	0.011	0.008	0.037	0.027	Mn –	–
K	0.763	0.801	0.875	0.870	0.867	0.913	0.860	0.901	0.890	0.907	0.817	0.895	0.827	0.898	0.901	0.904	**C 5.000**	**5.000**
X_{Fe}	0.397	0.394	0.527	0.529	0.796	0.789	0.607	0.606	0.605	0.605	0.600	0.610	0.507	0.497	0.450	0.439	Mg –	–
																	Fe 0.068	0.108
																	Mn 0.013	0.018
																	Ca 1.659	1.593
																	Na 0.260	0.280
																	B 2.000	**2.000**
																	Na_A 0.644	0.789
																	K_A 0.194	0.057
																	A 0.838	**0.846**

Table 3.2. Representative mica and amphibole analyses.
Normalisation based on 11oxygens for mica. Calculation for amphibole is based on 23[O] with Fe^{2+}/Fe^{3+} calculation after charge balance assuming 15 cations excluding Na_A & K. Cations calculated after Leake et al., 1997. $X_{Fe}=Fe^{2+}/(Fe^{2+}+Mg)$. Chlorine contents are under detection limit.

Eclogite **sample K4-99** comes from Purbinar (settlement Kaar), SE of Besal, where large mafic bodies occur in basement gneisses. The rock contains garnet, omphacite (up to 37 mol% jadeite), secondary pargasitic amphibole as well as biotite and plagioclase

replacing amphibole along with accessory epidote, quartz, apatite and rutile rimmed by ilmenite and titanite. Amphibole porphyroblasts are relatively aluminous in the core (Ferroan Pargasite: Si = 5.6, Al^{vi} = 1.53 per 23 oxygens) and show significantly lower Al, and higher Si, Ti and K (Pargasite) in overgrowths or at the rim (Table 3.2; Fig. 3.2) diagnostic for higher temperatures and K-bearing fluids. Biotite is very homogeneous but shows a slight K depletion towards the rim that may be indicative for preliminary retrogression to chlorite.

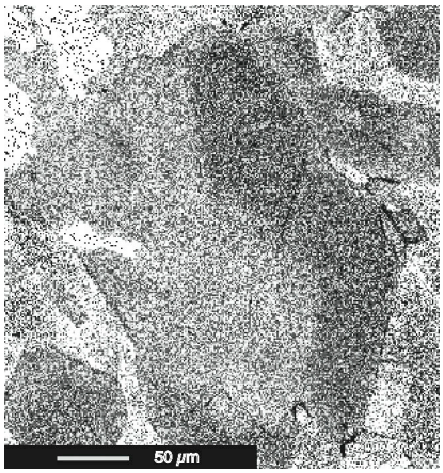

Fig. 3.2. Qualitative compositional map of amphibole zoning (K4-99) showing the Ca/K ratio distribution that drops from gray to black.

The **samples K4-97 and Kaar2** are different segments of a quartz-phengite vein in amphibolitised eclogite from Purbinar (settlement Kaar). In Kaar2, cm-sized phengite is essentially unaltered whereas K4-97 phengite is enveloped by a thick intergrowth of biotite+plagioclase and shows Si contents of 3.2-3.3 p.f.u. diagnostic for post-peak pressure conditions (Table 3.2). Biotite shows minor depletion of K towards the rim indicating incipient retrogressive chlorite growth.

Fine-grained orthogneiss **sample K4-78**, from southwest of Jalkhad, contains mainly quartz, plagioclase and K-feldspar along with garnet, biotite, apatite and red-brown allanite as well as numerous euhedral, up to 150 µm long, partly inclusion-rich, zircon grains.

Sample K4-71 is a fine-grained garnet amphibolite from the first, metapelite-rich cover from Joranar, SE of Burawai. The euhedral, optically zoned and rutile inclusion-rich (mainly in the core) garnets are set in a matrix of green amphibole and epidote minerals or in quartz rich veins. Poikiloblastic clinozoisite, in places with kyanite, has overgrown the

former fabric. Secondary titanites, often with inherited rutile cores, are ≥60 μm in diameter.

Coarse-grained orthogneiss **sample K4-70** is divided into a darker part with amphibole, biotite, garnet, plagioclase, quartz and titanite, and a lighter part containing feldspar, quartz, garnet, amphibole and biotite: minor epidote minerals and apatite occur in both parts. Only the mafic part of this sample was used for biotite separation. The unstrained biotites show no significant compositional variation from core to rim apart from a weak depletion in K, diagnostic for preliminary retrogression (Table 3.2).

Sample K4-60 is a coarse grained eclogite from within the granitic basement around Joranar. Dark red garnets are several cm in diameter set in a matrix of dark green omphacite, partly replaced by symplectites of secondary clinopyroxene and plagioclase with or without hornblende. Rutile grains (up to 150 μm), partly replaced by ilmenite and titanite, represent the dominant accessory minerals: quartz and zircon are minor.

Strongly foliated paragneiss **sample K4-37** contains skeletal garnet in a phengite-quartz matrix overgrown by large plagioclase porphyroblasts: biotite is minor and partly replaces phengite. The rock was collected from SE of Jalkhad at the pass Nurinar Gali (locally Nuri top) from the second, carbonate and clastic metasedimentary cover unit. Accessory phases are allanite, rutile, apatite and tourmaline. Phengite shows a homogeneous Si content of 3.25 p.f.u. diagnostic for post-peak pressure conditions whereas biotite reveals a slight depletion of K at the grain rims that point to initial retrogression to chlorite.

Sample K4-21 is a garnet-rich paragneiss belonging to the metasedimentary second cover and represents the host rock to several metabasites that occur around Naran. The rock contains quartz, feldspar, orthoamphibole, biotite and up to 0.5 cm garnet along with abundant graphite, ilmenite and calcite and minor sulphides and Fe-oxides. Biotite shows again preliminary retrogression at the rim.

From the south side of lake Lulusar, garnet-bearing orthogneiss **sample K3-26** was collected. This rock contains garnet, red-brown (Ti-rich) biotite, quartz, plagioclase, K-feldspar, apatite and allanite as well as numerous euhedral, up to 250 μm long zircon grains.

3.4. U-Pb chronology

3.4.1. Analytical techniques

Laser-ICP-MS U-Th-Pb analyses of separated zircon, titanite and rutile mounted in epoxy were performed using a Thermo-Scientific Element II sector field instrument coupled to a New Wave UP-213 UV-Laser system located at the Department of Geoscience, Goethe University, Frankfurt. Prior and after analysis, polished zircon grains were examined using catholuminescence (CL) imaging on a Leica DMRX with a CLmk4 and on a Jeol microprobe JXA-8900 to reveal internal structures, inclusions and guide laser beam positioning (Fig. 3.3). Analytical data were acquired in time-resolved pulse counting mode with over 810 mass scans during 20 s background measurement followed by 23 s of sample ablation. The zircons, titanites and rutiles were analysed using 16-60 µm spot sizes depending on mineral structure. The penetration depth of the laser pit was typically around 15-25 µm. The signal was tuned for maximum sensitivity for Pb and U while keeping oxide production, monitored as $^{254}UO/^{238}U$, well below 1%. Laser-induced elemental fractionation and instrumental mass discrimination during zircon, titanite and rutile analyses were adjusted using reference minerals GJ-1 (zircon: Jackson et al., 2005) and R10 (rutile: Luvizotto et al., 2009), respectively. The Plešovice zircon (Sláma et al., 2008) was analysed as external reference standard (Table 3.3). Raw data were processed offline using an Excel© spreadsheet within which corrections for common Pb, background signal and time dependent elemental fractionation of U-Pb have been considered. All uncertainties are quoted at the 2σ level and are reported as quadratic addition of external reproducibility obtained from standard zircon of each analytical sequence (n=6 to 12) and the within run precision of each individual analysis. For more details see Gerdes & Zeh (2006, 2009).

3.4.2. Results

Two zircons from an orthogneiss (K3-26), fourteen zircons of a gneiss sample (K4-78), two titanites of a garnet-amphibolite (K4-71) and seven dark rutile crystals (eclogite K4-60) have been analysed. Details are presented in Tables 3.1 & 3.3. The CL-images of zircons (Fig. 3.3) reveal a quite homogeneous zircon population dominated by euhedral to subhedral grains. Inherited, most likely magmatic light cores are characterised by broad planar- and sector-zoned domains whereas finely spaced, indistinct oscillatory or patchy overgrowths were interpreted to be of metamorphic origin; both stages are reflected in the

Concordia diagrams (Fig. 3.4). Bright luminescent outermost rims were also recognised but have been seen to be to fine for measurements. The magmatic core age for sample K3-26 is weakly defined at 276 +37/-39 Ma, giving the highest Th/U ratio (Table 3.3), whereas the lower intercept at 47.25±0.43 Ma (Fig. 3.4b) corresponds to the age of the overgrowth rim (Th/U << 0.2). Ages plotting between these two are discordant, pointing possibly to a loss of daughter isotopes or, most likely, to a mixture of both zones by overlap of the laser spot. Similar results have been found for sample K4-78 (Figs. 3.3; 3.4c&d): the core age is roughly determined at 303±20 Ma, whereas the lower intercept at 47.42±0.25 Ma is derived from ablation pits in the zircon rim, yielding extremely low Th/U ratios.

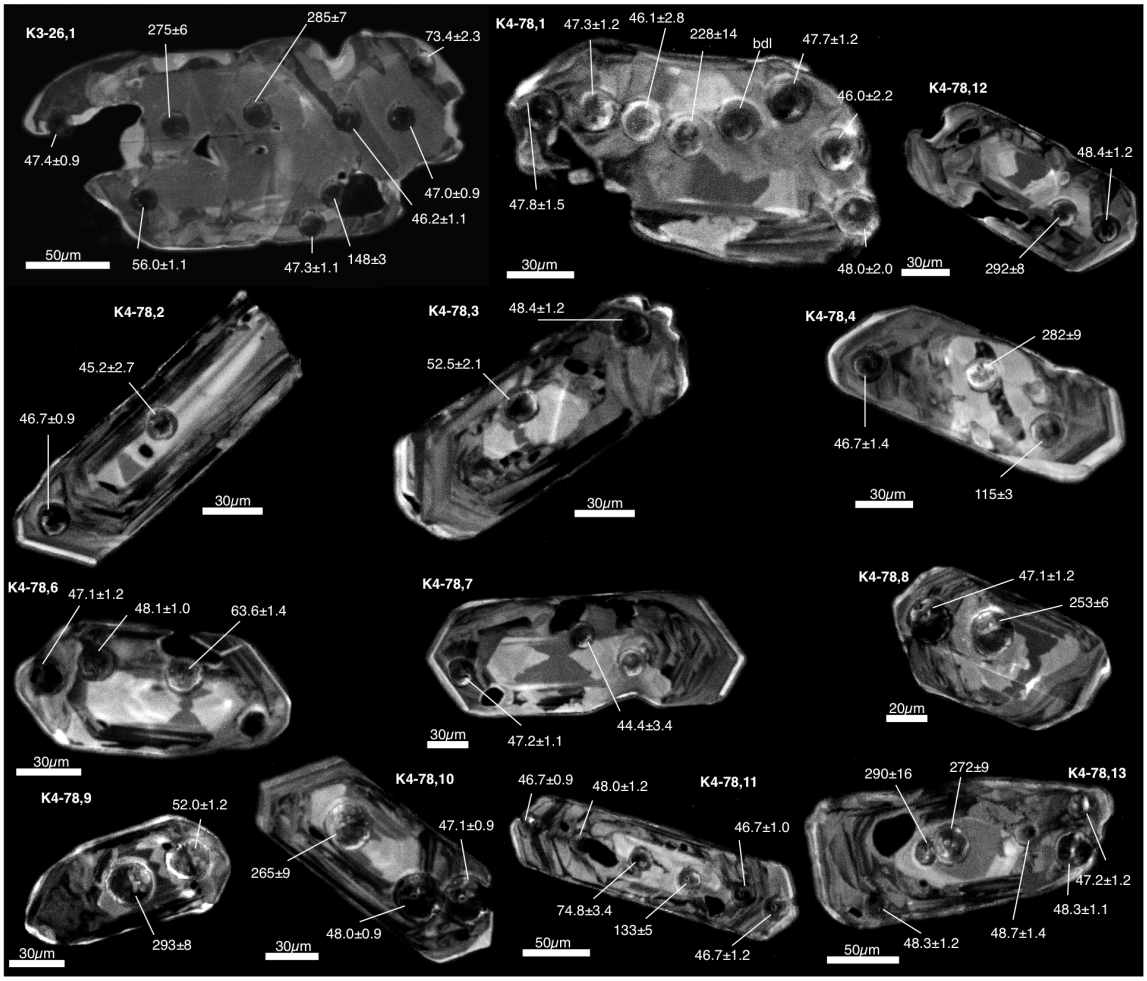

Fig. 3.3. Cathodoluminescence images of representative zircons from sample K3-26 and K4-78. Light idiomorphic cores are surrounded by darker overgrowths. LA-ICP-MS spot $^{206}Pb/^{238}U$ ages (Ma) are reported with 2σ uncertainties. See Table 3.3 for details.

		^{207}Pb [a]	U [b]	Pb [b]	Th [b]	^{206}Pb	^{206}Pb [c]	±2 σ	^{207}Pb [c]	±2 σ	Rho [d]	^{207}Pb [c]	±2 σ	Age (Ma) ^{206}Pb	±2 σ	^{207}Pb	±2 σ
	grain	(cps)	(ppm)	(ppm)	U	^{204}Pb	^{238}U	(%)	^{235}U	(%)		^{206}Pb	(%)	^{238}U		^{235}U	
K3-26	1r	699	515	3.5	0.015	1927	0.007369	2.3	0.04739	6.3	0.37	0.04664	5.8	47.3	1.1	47.0	2.9
	1r1	1710	361	7.7	0.082	4408	0.02327	2.2	0.1673	3.8	0.59	0.05214	3.1	148	3	157	6
	1c	666	523	3.4	0.010	1952	0.007195	2.5	0.04548	5.3	0.46	0.04585	4.7	46.2	1.1	45.2	2.4
	1c1	887	665	4.5	0.012	2481	0.007313	2.0	0.04820	5.5	0.36	0.04780	5.2	47.0	0.9	47.8	2.6
	1c2	1095	122	5.1	0.38	2796	0.04517	2.7	0.3280	4.6	0.58	0.05266	3.8	285	7	288	12
	1r2	1181	630	5.2	0.030	3331	0.008719	1.9	0.05730	4.9	0.40	0.04766	4.5	56.0	1.1	56.6	2.7
	1r3	1511	150	6.1	0.72	3920	0.04361	2.2	0.3117	3.8	0.58	0.05183	3.1	275	6	275	9
	1c3	1300	846	5.8	0.006	3702	0.007382	2.0	0.04805	4.4	0.46	0.04721	3.9	47.4	0.9	47.6	2.0
	1r4	2450	1013	11	0.020	4242	0.01145	3.2	0.07757	4.3	0.74	0.04914	2.9	73.4	2.3	75.9	3.2
	2r	3004	954	13	0.16	8233	0.01511	2.8	0.1022	4.0	0.68	0.04906	3.0	96.7	2.7	98.8	3.8
	2c	3924	1077	18	0.24	10525	0.01778	7.8	0.1229	8.3	0.94	0.05013	2.8	114	9	118	9
	2c1	6738	1196	31	0.27	17680	0.02726	2.8	0.1926	3.9	0.73	0.05124	2.7	173	5	179	6
	2c2	2523	836	13	0.340	4749	0.01557	3.8	0.1046	5.0	0.77	0.04872	3.2	99.6	3.8	101	5
	2r1	1817	1268	8.8	0.008	5034	0.007585	3.4	0.05036	5.1	0.66	0.04815	3.9	48.7	1.6	49.9	2.5
	2r2	1277	933	6.3	0.014	3051	0.007400	1.8	0.04805	4.6	0.40	0.04710	4.2	47.5	0.9	47.7	2.2
K4-78	13c	1636	127	5.8	0.29	2776	0.04606	5.6	0.3374	9.3	0.60	0.05314	7.4	290	16	295	24
	13c	2444	93	4.5	0.57	2031	0.04309	3.5	0.3089	5.6	0.62	0.05199	4.4	272	9	273	14
	13r	1790	430	3.0	0.042	3837	0.007514	2.2	0.04888	3.9	0.57	0.04719	3.2	48.3	1.1	48.5	1.9
	13r	1656	923	6.3	0.052	6651	0.007356	2.6	0.04756	5.7	0.45	0.04689	5.1	47.2	1.2	47.2	2.6
	13m	1761	982	6.8	0.023	7262	0.007584	2.9	0.04776	5.4	0.54	0.04568	4.5	48.7	1.4	47.4	2.5
	13r	1585	854	6.0	0.050	6235	0.007521	2.6	0.04965	8.7	0.29	0.04789	8.3	48.3	1.2	49.2	4.2
	11r	1753	998	6.6	0.015	5488	0.007268	2.5	0.04697	6.6	0.38	0.04687	6.1	46.7	1.2	46.6	3.0
	11m	1780	1044	6.9	0.025	7313	0.007272	2.2	0.04596	4.7	0.48	0.04584	4.1	46.7	1.0	45.6	2.1
	11c	3667	660	17	0.25	13212	0.02086	3.5	0.1504	5.4	0.64	0.05228	4.2	133	5	142	7
	11c	1670	578	7.5	0.22	4808	0.01 167	4.5	0.07859	6.7	0.67	0.04885	5.0	74.8	3.4	76.8	5.0
	11r	1388	746	6.0	0.024	4184	0.007480	2.5	0.05075	8.5	0.29	0.04921	8.1	48.0	1.2	50.3	4.2
	11r	1673	1008	6.7	0.025	5407	0.007271	2.0	0.04586	5.1	0.40	0.04574	4.6	46.7	0.9	45.5	2.3
	12r	1808	1014	7.0	0.027	4949	0.007541	2.5	0.04948	5.0	0.50	0.04759	4.3	48.4	1.2	49.0	2.4
	12c	1257	103	4.7	0.21	4446	0.04641	2.6	0.3407	12	0.21	0.05324	12.1	292	8	298	32
	1r	997	573	3.9	0.008	3974	0.007477	4.1	0.04873	30	0.14	0.04727	30.1	48.0	2.0	48	14
	1r	1519	728	4.8	0.007	4817	0.007165	4.7	0.05869	46	0.10	0.05941	45.5	46.0	2.2	58	26
	1r	840	486	3.4	0.031	3317	0.007426	2.6	0.04886	6.5	0.40	0.04772	5.9	47.7	1.2	48.4	3.1
	1c	1489	158	5.4	0.31	5177	0.03597	6.2	0.2688	10	0.63	0.05419	7.7	228	14	242	21
	1r	1297	735	5.1	0.039	4787	0.007177	6.0	0.04630	6.6	0.92	0.04679	2.6	46.1	2.8	46.0	3.0
	1r	1772	983	6.8	0.034	6547	0.007372	2.5	0.04749	4.6	0.53	0.04672	3.9	47.3	1.2	47.1	2.1
	1r	1882	506	3.5	0.024	7528	0.007447	3.1	0.04833	5.5	0.56	0.04708	4.6	47.8	1.5	47.9	2.6
	5r	1910	1180	8.0	0.027	3904	0.007385	2.5	0.04736	4.6	0.54	0.04651	3.9	47.4	1.2	47.0	2.1
	5c	2306	221	9.2	0.17	6714	0.04297	2.2	0.3064	10	0.23	0.05171	9.3	271	6	271	23
	6r	1602	987	6.6	0.021	6361	0.007328	2.6	0.04794	5.6	0.47	0.04745	5.0	47.1	1.2	47.5	2.6
	6r	1321	826	5.7	0.046	3853	0.007492	2.0	0.04747	3.7	0.54	0.04595	3.1	48.1	1.0	47.1	1.7
	6r	1643	751	7.1	0.062	6487	0.009913	2.1	0.06518	5.4	0.40	0.04769	4.9	63.6	1.4	64.1	3.4
	7r	1611	1016	6.9	0.026	3309	0.007352	2.3	0.04747	3.6	0.63	0.04683	2.8	47.2	1.1	47.1	1.7
	7r	1464	777	5.6	0.05	4640	0.006917	7.7	0.05196	10	0.79	0.05448	5.9	44.4	3.4	51.4	4.9
	4r	1594	1041	6.9	0.024	4696	0.007278	3.1	0.04648	4.8	0.64	0.04632	3.7	46.7	1.4	46.1	2.2
	4c	2217	533	9.2	0.12	5765	0.01798	2.9	0.1270	4.5	0.63	0.05120	3.5	115	3	121	5
	4c	7641	733	36	0.58	27780	0.04474	3.2	0.3195	3.9	0.81	0.05180	2.3	282	9	282	10
	3r	1748	1120	7.7	0.026	7115	0.007534	2.5	0.04807	3.6	0.68	0.04628	2.7	48.4	1.2	47.7	1.7
	3r	1480	790	6.4	0.057	3361	0.008176	4.0	0.05314	6.8	0.59	0.04714	5.5	52.5	2.1	52.6	3.5
	2r	1721	1120	7.5	0.030	6806	0.007275	2.0	0.04777	5.3	0.38	0.04762	4.9	46.7	0.9	47.4	2.5
	2r	1197	799	5.4	0.042	2554	0.007032	6.0	0.04685	10	0.61	0.04832	7.9	45.2	2.7	46.5	4.5
	8r	1416	395	2.7	0.06	5393	0.007332	2.6	0.04583	4.2	0.62	0.04534	3.2	47.1	1.2	45.5	1.9
	8c	2895	141	5.7	0.22	6205	0.04003	2.6	0.2870	6.6	0.39	0.05199	6.1	253	6	256	15
	9c	1695	458	3.5	0.039	4793	0.008092	2.3	0.05216	4.2	0.54	0.04675	3.6	52.0	1.2	51.6	2
	9c	2910	127	6.2	0.37	10830	0.04646	2.7	0.3242	4.5	0.60	0.05061	3.6	293	8	285	11
	10r	1681	483	3.3	0.06	6461	0.007338	2.0	0.04742	3.1	0.64	0.04686	2.4	47.1	0.9	47.0	1.4
	10r	1433	394	2.8	0.08	3626	0.007470	1.9	0.04812	3.1	0.61	0.04671	2.4	48.0	0.9	47.7	1.4
	10c	3874	383	17	0.34	12890	0.04193	3.3	0.3025	5.2	0.64	0.05233	4.0	265	9	268	12
	14r	1359	893	6.3	0.060	5329	0.007470	2.6	0.04572	4.0	0.64	0.04438	3.1	48.0	1.2	45.4	1.8
	14r	1238	830	5.7	0.08	4797	0.007273	2.6	0.04505	4.3	0.60	0.04493	3.5	46.7	1.2	44.7	1.9
	14c	2606	1230	11.4	0.050	5382	0.009776	1.9	0.06433	3.6	0.53	0.04773	3.1	62.7	1.2	63.3	2.2
	14c	4583	834	20.6	0.18	13188	0.02545	2.2	0.1814	4.5	0.50	0.05171	3.9	162	4	169	7

	grain	^{207}Pb [a] (cps)	U [b] (ppm)	Pb [b] (ppm)	Th/U [b]	$^{206}Pb/^{204}Pb$	$^{206}Pb/^{238}U$ [c]	±2 σ (%)	$^{207}Pb/^{235}U$ [c]	±2 σ (%)	Rho [d]	$^{207}Pb/^{206}Pb$ [c]	±2 σ (%)	Age (Ma) $^{206}Pb/^{238}U$	±2 σ	Age (Ma) $^{207}Pb/^{235}U$	±2 σ
K4-60	Rt1	283	7.6	0.05	0.019	bdl	0.006814	4.3	0.0494	15	0.28	0.0526	15	43.8	1.9	48.9	7.3
	Rt1	359	8.5	0.06	0.003	bdl	0.006912	4.8	0.0476	12	0.41	0.0499	11	44.4	2.1	47.2	5.5
	Rt3	322	7.4	0.06	0.050	bdl	0.007159	6.7	0.0451	12	0.54	0.0457	10	46.0	3.1	44.8	5.4
	Rt2	244	6.9	0.04	<0.001	bdl	0.006683	6.2	0.0467	13	0.49	0.0507	11	42.9	2.6	46.4	5.7
	Rt4	224	6.0	0.04	0.011	bdl	0.006697	5.8	0.0418	11	0.54	0.0452	9.1	43.0	2.5	41.5	4.4
	Rt4	285	7.1	0.06	0.049	bdl	0.007574	10	0.0526	14	0.73	0.0504	9.9	48.6	5.1	52.1	7.4
	Rt5	237	7.1	0.04	0.012	bdl	0.006212	12	0.0432	16	0.76	0.0504	11	39.9	4.9	42.9	6.8
	Rt6	226	6.0	0.04	0.005	bdl	0.007106	8.7	0.0483	15	0.59	0.0493	12	45.6	4.0	47.9	6.9
	Rt7	229	6.8	0.05	0.005	bdl	0.007213	8.2	0.0434	13	0.62	0.0436	10	46.3	3.8	43.1	5.6
K4-71	Ttn1a	1579	49	0.44	0.063	1351	0.00684	13	0.0508	21	0.61	0.0538	17	44	6	50	10
	Ttn1b	1756	45	0.41	0.056	1308	0.00806	30	0.0624	41	0.74	0.0561	28	52	16	61	25
	Ttn1c	1737	48	0.41	0.039	1544	0.00671	16	0.0553	35	0.46	0.0598	32	43	7	55	19
	Ttn2a	1393	35	0.33	0.005	963	0.00654	18	0.0425	21	0.87	0.0471	11	42	8	42	9
	Ttn2b	1282	31	0.23	0.005	1300	0.00502	40	0.0283	42	0.94	0.0409	14	32	13	28	12
	Ttn2d	1303	34	0.27	0.004	932	0.00577	26	0.0398	37	0.72	0.0500	25	37	10	40	14
GJ-1 (n=12) [e]		14548	240	21	0.030	25283	0.09860	1.4	0.8205	1.8	0.69	0.06035	1.1	606	8	608	8
R10 (n=6) [e]		10215	43	7.5	<0.001	10385	0.1848	1.8	1.925	1.6	0.65	0.07551	2.6	1093	18	1090	11
Plesovice (n=7) [e]		22458	679	35	0.10	29907	0.05393	1.9	0.3955	1.7	0.86	0.05319	0.8	339	6	338	5

Table 3.3. Results of U-Th-Pb LA-ICP-MS analyses of zircon from sample K3-26, rutile from K4-60 and titanite from K4-71 as well as reference minerals GJ-1, R10 and the Plesovice zircon.

[a] Within run background-corrected meanPb^{207} signal in counts per second (cps).

[b] U and Pb content and Th/U ratio were calculated relative to GJ-1 and R10 reference, respectively, and are accurate to ±20% due to heterogeneity in reference minerals, matrix effects and analytical uncertainty of the LA-ICP-MS method.

[c] corrected for background and within-run Pb/U fractionation and subsequently normalised to GJ-1zircon and R10 rutile (ID-TIMS value/measured value), respectively. $^{207}Pb/^{235}U$ calculated using $^{207}Pb/^{206}Pb/(^{238}U/^{206}Pb \times 1/137.88)$. Uncertainties propagated following Gerdes & Zeh (2006, 2009)

[d] Rho is the error correlation defined as $err\,^{206}Pb/^{238}U$ / $err\,^{207}Pb/^{235}U$. Note that $^{207}Pb/^{235}U$ uncertainty is a quadratic addition of the $^{206}Pb/^{238}U$ and $^{207}Pb/^{206}Pb$ uncertainties.

[e] mean of 6-12 analyses; uncertainties quoted as relative standard deviations. Spots size = 30 μm for GJ-1 and Plesoive zircon and 60 μm for rutile R10.

Bdl: below detection limit. The detection limit of ^{204}Pb is controlled by the abundance of the interfering isotope ^{204}Hg, which exist as impurity in Ar and He gas and how precise it can be estimated. The mean ^{204}Hg (= measured ^{202}Hg multiplied by the natural mass bias corrected $^{202}Hg/^{204}Hg$) detected as gas blank prior each analysis is around 245 ±10 cps. (1 standard deviation) limiting the level of detection of ^{204}Pb to around 10-18 cps. No $^{206}Pb/^{204}Pb$ was reported when the ^{204}Pb was below this level as the resulting ratios will be only minimum estimates.

The Concordia ages (MSWD = 1.6) for rutiles are 44.1±1.3 Ma whereas metamorphically younger titanites yielded 41.3±4.7 Ma (Figs. 3.4e,f). Rutiles and titanites did not show age differences between cores and outermost parts of the grains, but higher uncertainties are related to the lower uranium content compared to the zircons. Nevertheless, all analyses can be interpreted as concordant.

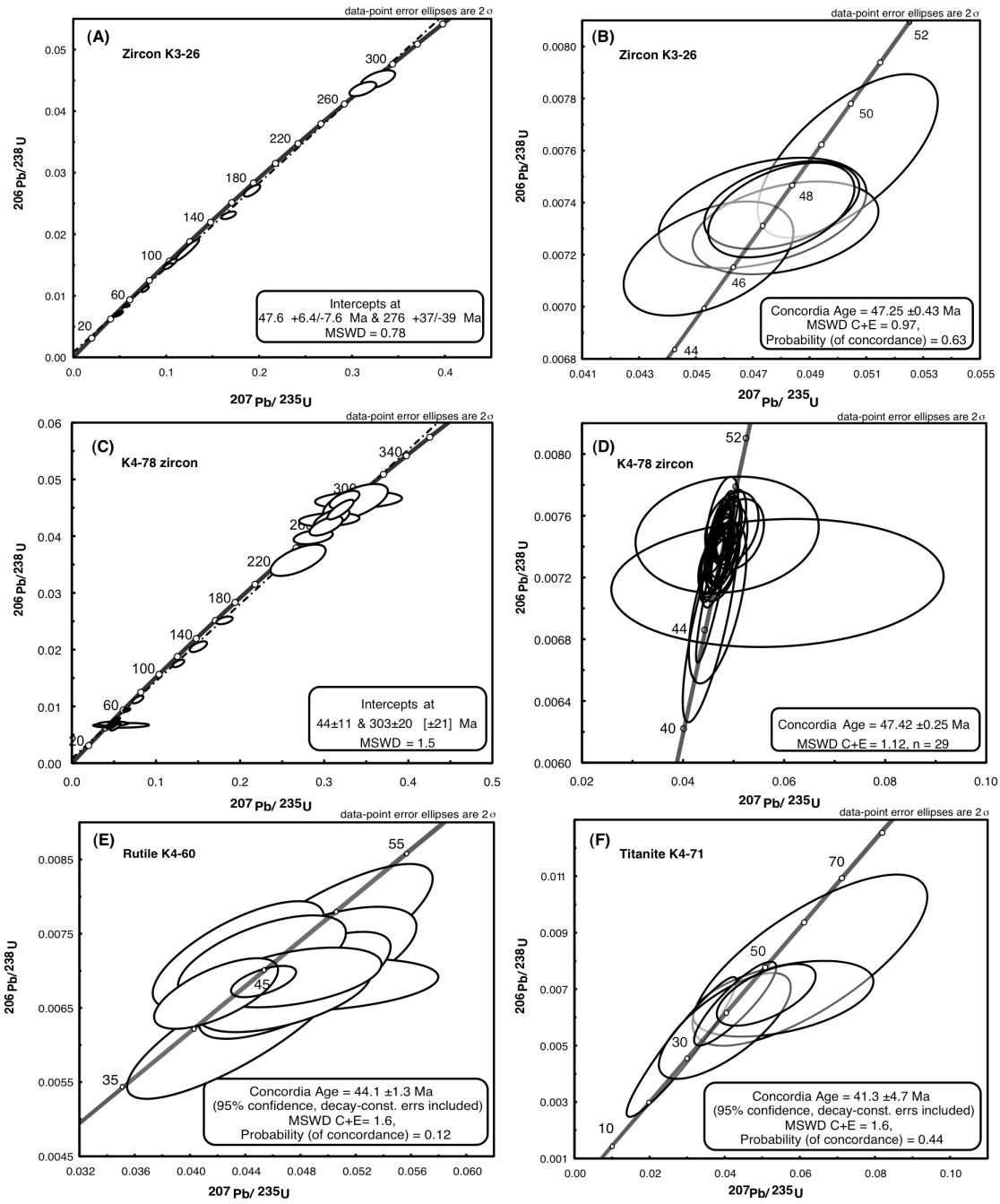

Fig. 3.4. A-F $^{206}Pb/^{238}U$ vs. $^{207}Pb/^{235}U$ concordia plots. Errors are 2σ. $MSWD_{C+E}$: Mean square weighted deviation of concordance and equivalence. Zircons from K3-26 (orthogneiss) (A) and K4-78 (B) with close-ups in C and D. E represents Rutile from K4-60 (eclogite) and F Titanite from K4-71 (amphibolitised eclogite).

3.5. $^{40}Ar/^{39}Ar$ dating

3.5.1. Analytical techniques

Samples were crushed and sieved (Table 3.1) and micas of 125 to 250 µm and 250 to 500 µm in diameter were separated by magnetic methods. The grain size fractions were washed and purified by handpicking under a binocular microscope, wrapped in aluminium foil, and placed in a sample capsule made of 5N (99.999% pure) aluminium. The sample capsule was wrapped in 0.5 mm thick cadmium foil and irradiated for 96 h in position 6 of the ICI (In Core Irradiation) system in the Geesthacht Neutron Facility (GeNF) at FRG-1, GKSS research centre at Geesthacht (Germany). The neutron flux variation over the length of the sample capsule was monitored by Fish Canyon Tuff Sanidine (FC3 sanidine) provided by the Geological Survey of Japan where an age of 27.5 Ma was determined (Uto *et al.,* 1997, Ishizuka 1998; Ishizuka *et al.,* 2002) that is consistent with that of 27.51 Ma obtained by first-principle measurements of K and radiogenic Ar by Lanphere & Dalrymple (2000) and Lanphere & Baadsgaard (2001). The uncertainty in the *J* value is estimated at 0.4% based on 4 earlier irradiations. The $^{40}Ar/^{39}Ar$ analyses were performed at the argon geochronology laboratory of the University of Potsdam, which uses a New Wave laser ablation system with a 50 W CO_2 laser (wavelength 10.6 µm) for gas extraction. The gas fractions were extracted by heating the separates for 1 min with a continuous laser beam defocused to a diameter similar to that of the sample. The gas is purified for 10 min in an ultra-high vacuum line using SAES getters and a cold trap kept at ca. -100°C. After purification the argon gas is analysed using a Micromass 5400 noble gas mass spectrometer with a high sensitivity and an ultra-low background. The mass spectrometer is fitted with an electron multiplier pulse counting system suitable for analysing small amounts of argon. Blanks were run at the start of each session and after every three unknowns. The blank level of the system including mass spectrometer and the extraction line is currently 1.5×10^{-14} ml STP for ^{36}Ar, 1.2×10^{-15} ml STP for ^{37}Ar, 3.1×10^{-15} ml STP or ^{38}Ar, 3.3×10^{-15} ml STP for ^{39}Ar and 3.8×10^{-12} ml STP for ^{40}Ar (STP: standard temperature and pressure).

The raw data were corrected for background contributions, mass discrimination (using the composition of atmospheric argon), and the decay of the neutron-induced nuclides produced during irradiation. Interference correction factors were obtained by analysing CaF_2 and K_2SO_4 irradiated together with the samples, and the average values

are: $(^{36}Ar/^{37}Ar)_{Ca}= (4.225\pm0.167)x10^{-4}$, $(^{39}Ar/^{37}Ar)_{Ca}= (8.922\pm0.153)x10^{-4}$, $(^{38}Ar/^{39}Ar)_{K}= (1.719\pm0.018)x10^{-2}$, and $(^{40}Ar/^{39}Ar)_{K}= (4.670\pm 0.672)x10^{-3}$. Data reduction was carried out following Uto et al. (1997). The accuracy of the method and J values have been confirmed by the analyses of biotite K/Ar standards Sori93 (Sudo et al., 1998: 92.6±0.6 Ma) and HD-B1 (Hess & Lippolt, 1994: 24.21±0.32 Ma) which were routinely included in each irradiation. The analytical data, J-values and heating steps are listed in Table 3.4. The uncertainties on the total-gas ages include the uncertainty in the irradiation parameter (*J*) and are shown on 2σ levels. In view of the complex geological history of the samples and the possible influence of $^{37}Ar/^{39}Ar$ (e.g. Kelley et al., 1986; Villa et al., 1997), Ca/K ratios (Figs. 3.5 a-j) and age vs. Ca/K correlation diagrams (Figs. 3.6 a,b) are also included. Due to the cadmium shielding employed at GKSS the levels of $^{38}Ar_{Cl}$, produced via thermal neutron activation of ^{37}Cl, are very low to zero. Hence, we could not use $^{38}Ar_{Cl}/^{39}Ar_{K}$ ratios to trace chlorine-rich components.

3.5.2. Results

The gas release spectra for the six Kaghan Valley samples have similar patterns in which minimum gas fractions released at lowest temperatures yield lowest apparent ages, with large uncertainties, that stabilise to plateaux at higher temperatures (Table 3.4). The number and size of the grains analysed are listed in Table 3.1. Plateau ages include ≥ 3 gas fractions that overlap within 2σ analytical uncertainty, and represent ≥50% of the total ^{39}Ar released (McDougall & Harrison, 1999; and references therein). Isotope correlation ages ("isochron ages") were calculated using the plateau-defining gas fractions, following York (1969). Due to the low amounts of ^{39}Ar released from sample K4-37 biotite and the absence of overlap for sample K4-99 amphibole, only "forced plateaux" can be presented for these samples. Plateau ages and forced plateau ages are calculated (after corrections) by dividing the sum of the plateau defining steps by the sum of their errors (Uto et al., 1997). Except for two outliers with low radiogenic argon yield ($^{40}Ar^*$ <50%, Table 3.4), the paucity of alteration effects is corroborated by the high $^{40}Ar^*$ yields that show no distinct correlation with their apparent ages for the majority of gas fractions (in particular for the plateau-defining gas fractions) (Table 3.4). Except for one value, noise to sample ratios for ^{36}Ar are 1.5-43.7 for the individual plateau-defining gas fractions.

Laser output [W]	$^{40}Ar/^{39}Ar$			$^{37}Ar/^{39}Ar$			$^{36}Ar/^{39}Ar$ (x10 $^{-3}$)			K/Ca	$^{40}Ar^{*}$ (%)	$^{39}Ar_K$ frac. (%)	$^{40}Ar^{*}/^{39}Ar_K$			Age(±2σ)(Ma)		
K4-119 Phg	*C08062*	J=	0.00199															
0.014	1003.37	±	3.33	0.280	±	0.116	3349.08	±	17.47	2.10	1.37	0.21	13.75	±	4.02	48.71	±	28.10
0.018	26.73	±	0.04	0.009	±	0.004	41.86	±	0.27	64.34	53.72	6.51	14.36	±	0.08	50.83	±	0.70
0.02	16.41	±	0.01	0.003	±	0.001	9.01	±	0.06	178.77	83.79	18.09	13.75	±	0.02	48.71	±	0.40
0.022	14.11	±	0.03	0.002	±	0.001	2.68	±	0.03	352.74	94.39	35.71	13.32	±	0.03	47.19	±	0.44
0.024	14.51	±	0.04	0.004	±	0.003	3.72	±	0.06	137.35	92.43	13.91	13.41	±	0.04	47.51	±	0.46
0.026	13.67	±	0.03	0.005	±	0.004	1.27	±	0.03	117.72	97.25	11.93	13.29	±	0.03	47.09	±	0.42
0.028	13.66	±	0.05	0.006	±	0.010	1.82	±	0.06	91.56	96.07	6.64	13.12	±	0.05	46.51	±	0.50
0.03	13.50	±	0.04	0.009	±	0.003	1.67	±	0.04	69.14	96.34	7.01	13.00	±	0.04	46.09	±	0.46
K4-99 Amp	*C08055*	J=	0.00198															
0.02	97.82	±	0.25	0.24	±	0.06	298.21	±	0.98	2.49	9.95	7.73	9.73	±	0.19	34.50	±	1.36
0.022	25.63	±	0.06	0.15	±	0.04	73.34	±	0.37	4.03	31.12	3.56	9.78	±	0.11	34.68	±	0.78
0.026	19.13	±	0.03	1.75	±	0.07	23.33	±	0.19	0.34	65.26	9.64	12.56	±	0.06	44.39	±	0.56
0.03	15.91	±	0.05	2.55	±	0.05	6.34	±	0.06	0.23	89.42	32.90	1317	±	0.05	46.55	±	0.52
0.032	14.73	±	0.03	2.87	±	0.05	4.10	±	0.07	0.20	94.09	27.13	13.61	±	0.04	48.06	±	0.46
0.034	14.72	±	0.02	2.61	±	0.06	4.20	±	0.13	0.22	93.62	12.64	13.44	±	0.04	47.49	±	0.48
0.038	16.42	±	0.06	3.40	±	0.51	15.91	±	0.37	0.17	74.30	6.58	12.40	±	0.14	43.86	±	1.02
K4-99 Bt	*C08054*	J=	0.00199															
0.012	17940.21	±	396.55	0.775	±	0.689	62293.81	±	1381.44	0.76	-2.61	0.08	-467.83	±	-36.81	-4798.93	±	-3780.32
0.014	1237.67	±	11.53	0.161	±	0.132	4271.44	±	39.85	3.65	-1.98	0.39	-24.53	±	-1.24	-90.18	±	-9.36
0.016	82.04	±	0.16	0.014	±	0.036	260.99	±	0.70	41.96	6.00	4.54	4.92	±	0.15	17.55	±	1.08
0.018	23.36	±	0.02	0.004	±	0.005	57.67	±	0.18	161.83	27.04	17.51	6.31	±	0.05	22.51	±	0.42
0.02	16.24	±	0.02	0.037	±	0.010	32.40	±	0.17	15.74	41.07	16.68	6.67	±	0.05	23.76	±	0.40
0.024	14.38	±	0.01	0.084	±	0.011	26.34	±	0.06	7.01	45.96	17.19	6.61	±	0.02	23.55	±	0.24
0.028	11.42	±	0.02	0.057	±	0.010	16.32	±	0.05	10.33	57.83	15.18	6.60	±	0.02	23.53	±	0.24
0.032	9.97	±	0.03	0.042	±	0.008	11.54	±	0.12	14.03	65.86	11.45	6.57	±	0.04	23.40	±	0.34
0.038	10.36	±	0.02	0.112	±	0.011	11.32	±	0.07	5.25	67.82	14.22	7.02	±	0.03	25.02	±	0.28
0.044	13.22	±	0.08	0.176	±	0.021	16.31	±	0.45	3.35	63.70	2.76	8.42	±	0.15	29.95	±	1.06
K4-97 Bt	*C08059*	J=	0.00197															
0.012	8787.52	±	188.73	0.0284	±	0.1363	29998.36	±	647.16	20.71	-0.88	0.06	-76.99	±	-18.79	-296.91	±	-157.56
0.014	834.67	±	10.86	0.0254	±	0.0327	2808.76	±	36.77	23.11	0.56	0.77	4.69	±	1.85	16.58	±	13.02
0.016	60.46	±	0.05	0.0002	±	0.0011	183.51	±	0.48	2467.17	10.30	7.43	6.23	±	0.14	22.02	±	0.96
0.018	15.20	±	0.01	0.0027	±	0.0020	24.65	±	0.10	221.13	52.07	25.69	7.91	±	0.03	27.92	±	0.32
0.02	9.89	±	0.005	0.0002	±	0.0026	6.33	±	0.04	3475.81	81.08	32.68	8.01	±	0.01	28.28	±	0.24
0.022	10.16	±	0.02	0.0047	±	0.0036	6.95	±	0.12	124.52	79.78	14.47	8.11	±	0.04	28.60	±	0.34
0.024	11.57	±	0.04	0.0111	±	0.0145	12.19	±	0.14	53.13	68.86	6.26	7.96	±	0.05	28.10	±	0.40
0.028	11.22	±	0.02	0.0094	±	0.0119	11.18	±	0.15	62.44	70.55	7.36	7.91	±	0.05	27.92	±	0.40
0.032	10.32	±	0.04	0.0174	±	0.0273	8.35	±	0.14	33.80	76.11	3.98	7.85	±	0.05	27.72	±	0.42
0.036	11.42	±	0.04	0.0535	±	0.0701	11.68	±	0.43	11.00	69.83	1.30	7.97	±	0.13	28.13	±	0.96
K4-97 Phg	*C08060*	J=	0.00198															
0.014	130.83	±	0.58	0.258	±	0.072	400.58	±	5.58	2.28	9.55	0.70	12.49	±	1.59	44.00	±	11.08
0.018	15.98	±	0.02	0.006	±	0.002	20.92	±	0.14	94.64	61.31	29.20	9.80	±	0.04	34.59	±	0.42
0.02	10.49	±	0.03	0.006	±	0.004	2.37	±	0.07	98.87	93.33	30.51	9.79	±	0.03	34.55	±	0.36
0.022	10.34	±	0.01	0.009	±	0.008	2.11	±	0.09	64.13	93.98	22.64	9.72	±	0.03	34.31	±	0.34
0.026	10.09	±	0.02	0.003	±	0.011	1.88	±	0.14	213.00	94.50	12.73	9.53	±	0.04	33.67	±	0.40
0.03	10.15	±	0.05	0.049	±	0.049	2.84	±	0.57	11.92	91.79	2.67	9.32	±	0.18	32.93	±	1.26
0.036	10.66	±	0.09	0.018	±	0.087	2.92	±	0.56	32.36	91.94	1.55	9.80	±	0.19	34.62	±	1.34
K4-97 Phg (Kaar2)		*C05092*	J=	0.00218														
0.012	807.89	±	11.28	0.150	±	0.441	2683.5	±	43.4	3.91	1.85	0.29	14.92	±	6.50	57.86	±	49.60
0.014	41.34	±	0.13	0.006	±	0.020	99.3	±	0.7	106.38	29.03	7.31	12.00	±	0.20	46.68	±	1.76
0.016	24.38	±	0.07	0.009	±	0.008	41.0	±	0.3	65.72	50.36	18.71	12.28	±	0.09	47.74	±	1.08
0.018	19.97	±	0.02	0.005	±	0.005	25.6	±	0.2	122.44	62.12	32.80	12.40	±	0.07	48.22	±	0.98
0.02	15.69	±	0.04	0.0003	±	0.006	12.3	±	0.2	1952.73	76.74	18.98	12.04	±	0.07	46.82	±	0.94
0.022	13.25	±	0.04	0.004	±	0.007	5.2	±	0.2	136.77	88.38	20.81	11.71	±	0.07	45.57	±	0.94
0.026	17.35	±	0.09	0.104	±	0.096	18.0	±	2.0	5.63	69.44	1.10	12.05	±	0.60	46.86	±	4.66
K4-70 Bt	*C08061*	J=	0.00196															
0.012	5190.35	±	37.66	0.977	±	0.280	17692.98	±	135.51	0.60	-0.73	0.18	-37.84	±	-13.18	-138.71	±	-100.46
0.014	335.61	±	0.96	0.070	±	0.020	1127.30	±	5.10	8.41	0.75	2.49	2.50	±	1.18	8.80	±	8.28
0.016	34.26	±	0.02	0.008	±	0.002	88.79	±	0.34	75.07	23.43	22.24	8.03	±	0.10	28.11	±	0.72
0.018	12.30	±	0.02	0.022	±	0.006	12.87	±	0.34	26.26	69.10	8.07	8.50	±	0.10	29.74	±	0.74
0.02	11.31	±	0.02	0.010	±	0.003	9.79	±	0.13	57.67	74.43	17.73	8.42	±	0.04	29.46	±	0.36
0.022	11.62	±	0.04	0.005	±	0.009	10.18	±	0.21	125.91	74.12	12.71	8.61	±	0.07	30.13	±	0.54
0.026	10.85	±	0.01	0.001	±	0.002	8.18	±	0.12	1142.30	77.73	20.05	8.44	±	0.04	29.53	±	0.36
0.03	11.15	±	0.02	0.001	±	0.004	9.35	±	0.17	947.22	75.22	10.11	8.39	±	0.05	29.36	±	0.42
0.036	11.16	±	0.08	0.014	±	0.018	9.16	±	0.20	43.11	75.76	6.41	8.46	±	0.09	29.60	±	0.68
K4-37 Phg	*C08053*	J=	0.00199															
0.012	373.94	±	10.74	0.2924	±	0.4623	1241.99	±	47.72	2.01	1.86	0.05	6.97	±	9.90	24.86	±	70.12
0.016	49.89	±	0.18	0.0012	±	0.0053	142.52	±	0.88	476.13	15.58	2.44	7.77	±	0.25	27.69	±	1.76
0.02	11.53	±	0.05	0.0001	±	0.0004	8.25	±	0.10	7027.03	78.85	36.02	9.09	±	0.05	32.35	±	0.46
0.022	9.31	±	0.02	0.0036	±	0.0009	1.22	±	0.05	163.53	96.13	29.48	8.95	±	0.03	31.86	±	0.32
0.024	9.22	±	0.09	0.0094	±	0.0022	1.38	±	0.12	62.48	95.59	11.27	8.81	±	0.10	31.37	±	0.72
0.028	9.21	±	0.02	0.0051	±	0.0012	1.28	±	0.08	115.06	95.90	20.75	8.83	±	0.03	31.43	±	0.34
K4-37 Bt	*C08052*	J=	0.00199															
0.010	1934.09	±	2681.01	175.805	±	293.276	3517.96	±	5363.53	0.00	47.39	0.00	1086.98	±	1961.66	2078.72	±	4454.42
0.016	601.15	±	2.56	0.012	±	0.016	2051.67	±	11.98	49.75	-0.85	6.66	-5.11	±	-2.57	-18.47	±	-18.62
0.020	25.67	±	0.11	0.003	±	0.001	69.49	±	0.35	227.18	19.99	31.28	5.13	±	0.11	18.35	±	0.82
0.022	22.95	±	0.05	0.005	±	0.004	57.67	±	0.15	117.10	25.74	16.13	5.91	±	0.03	21.10	±	0.28
0.024	37.54	±	0.06	0.007	±	0.005	108.48	±	0.45	81.53	14.62	11.24	5.49	±	0.13	19.62	±	0.92
0.026	26.40	±	0.04	0.008	±	0.008	69.25	±	0.20	77.01	22.50	10.51	5.94	±	0.06	21.22	±	0.44
0.030	15.19	±	0.02	0.006	±	0.007	30.86	±	0.14	100.32	39.95	13.69	6.07	±	0.04	21.67	±	0.36
0.032	11.45	±	0.06	0.019	±	0.023	18.00	±	0.36	31.41	53.56	4.29	6.13	±	0.12	21.90	±	0.84
0.038	9.74	±	0.05	0.013	±	0.019	11.81	±	0.17	45.03	64.18	6.22	6.25	±	0.06	22.33	±	0.48
K4-21 Bt	*C08068*	J=	0.00195															
0.014	6388.76	±	433.11	5.4177	±	1.1205	21926.50	±	1503.28	0.11	-1.41	0.03	-90.28	±	-69.41	-348.77	±	-591.62
0.018	49.05	±	0.12	0.0215	±	0.0170	140.68	±	0.40	27.39	15.26	20.50	7.48	±	0.12	26.10	±	0.84
0.02	14.59	±	0.06	0.0042	±	0.0051	21.60	±	0.19	141.42	56.28	18.23	8.21	±	0.07	28.62	±	0.54
0.022	11.73	±	0.02	0.0002	±	0.0016	12.24	±	0.20	3065.22	69.16	14.80	8.11	±	0.06	28.27	±	0.48
0.026	10.53	±	0.03	0.0001	±	0.0012	8.65	±	0.12	4364.23	75.72	19.17	7.97	±	0.05	27.79	±	0.38
0.03	9.08	±	0.04	0.0040	±	0.0081	3.59	±	0.11	146.79	88.32	13.64	8.02	±	0.05	27.96	±	0.40
0.036	8.86	±	0.04	0.0305	±	0.0067	3.26	±	0.17	19.32	89.18	11.11	7.90	±	0.06	27.54	±	0.48
0.04	9.32	±	0.13	0.0552	±	0.0529	4.78	±	0.42	10.66	84.93	2.52	7.92	±	0.17	27.60	±	1.22

Table 3.4. Results of ^{40}Ar / ^{39}Ar analyses. Errors are given at the 2σ confidence level. K/Ca=($^{37}Ar_{Ca}$ / $^{39}Ar_K$)/1.7.

3.5.2.1. Sample K4-119

Phengite: Step one comprises 0.21% of the ^{39}Ar and also has the highest Ca/K ratio (Table 3.4), which is attributed to minor K depletion due to alteration. Steps two and three

have lower apparent ages and also lower Ca/K ratios: an artefact of continuing alteration. The 4th step comprises >35% of the ^{39}Ar, has the lowest amount of Ca and its 47.19±0.22 Ma apparent age probably reflects the true age of the phengite. The next steps show inverse correlation of increasing Ca/K with decreasing apparent age. Nonetheless, steps 4 to 6 define a 47.25±0.26 Ma plateau age (Fig. 3.5a). The 47.16±0.58 Ma inverse isotope correlation age is similar, and yields a 308±20 ^{36}Ar/^{40}Ar intercept that overlaps that of air (295).

3.5.2.2. Sample K4-99

Amphibole: The Ca/K vs. apparent ages correlate linearly, except for step seven (Fig. 3.5c). The Ca/K ratios for sample K4-99 are much higher reflecting the higher Ca concentrations of amphibole compared to micas. The Ca/K vs. age correlation for both amphibole and biotite from sample K4-99 (Fig. 3.6a) reveals that the first two, low Ca/K steps represent fine-grained biotite overgrowths (ca. 34.63 Ma) degassing at low heating temperatures, as supported by thin section examination. This apparent age is similar to the 34.47±0.20 Ma age of phengite sample K4-97 but ~10 Ma older than the 23.55±0.14 Ma biotite age for the same sample. Fig. 3.2 shows the spatial distribution of Ca/K for one amphibole crystal, revealing an older Ca-rich core surrounded by a K-enriched rim. This is consistent with the microprobe data (Table 3.2) that show that the texturally oldest amphibole with the highest Na_{M4} occurs in the core, reflecting formation under relatively high pressures (Villa et al., 2000). Step 3 shows a low Ca/K ratio that point to the contribution of a younger, chemical distinct K-rich overgrowth with an apparent age of ~44 Ma. Steps 4 and 6 have similar Ca/K (Fig. 3.5c), but the amount of argon released (~33%) in the fourth heating step is almost three-times as large as that in step 6, and probably reflects the realistic age of 46.55±0.52 Ma. “Forced plateau” age calculation of step 3 to 7 yielded 46.65±0.24 Ma.

Biotite: The last two steps have elevated Ca/K ratios and also higher apparent ages that may be due to the presence of an older, Ca-rich phase, such as plagioclase. Step four has a low Ca/K, contains a high amount of ^{39}Ar and has an apparent age of 22.51±0.42 Ma that might reflect an overgrowth. The plateau age (Fig. 3.5i) is 23.55±0.14 Ma, comprising 60.5% of the ^{39}Ar released with moderate Ca/K ratios. Steps 5 and 8 with similar Ca/K (Table 3.4) have also similar apparent ages (23.76±0.40 Ma and 23.40±0.34 Ma). Their validity is supported by the 23.35±0.40 Ma isotope correlation age, the air-like ^{40}Ar/^{36}Ar intercept ratio of 298±2, and absence of a correlation between apparent age and ^{40}Ar*.

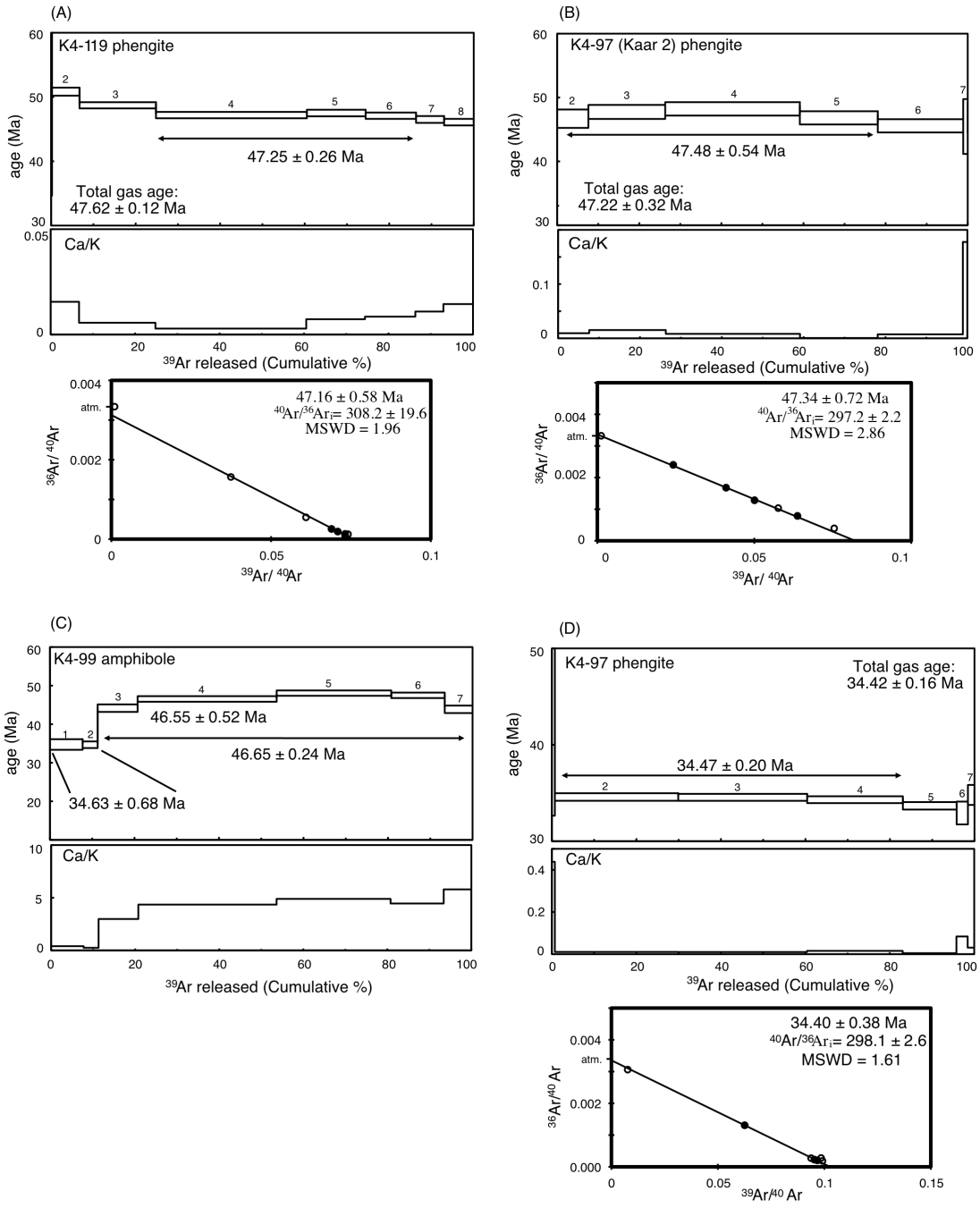
(A)
K4-119 phengite
age (Ma)
47.25 ± 0.26 Ma
Total gas age:
47.62 ± 0.12 Ma
Ca/K
39Ar released (Cumulative %)
47.16 ± 0.58 Ma
40Ar/36Ari= 308.2 ± 19.6
MSWD = 1.96
atm.
36Ar/ 40Ar
39Ar/ 40Ar
(B)
K4-97 (Kaar 2) phengite
47.48 ± 0.54 Ma
Total gas age:
47.22 ± 0.32 Ma
47.34 ± 0.72 Ma
40Ar/36Ari= 297.2 ± 2.2
MSWD = 2.86
(C)
K4-99 amphibole
46.55 ± 0.52 Ma
46.65 ± 0.24 Ma
34.63 ± 0.68 Ma
(D)
K4-97 phengite
Total gas age:
34.42 ± 0.16 Ma
34.47 ± 0.20 Ma
34.40 ± 0.38 Ma
40Ar/36Ari= 298.1 ± 2.6
MSWD = 1.61

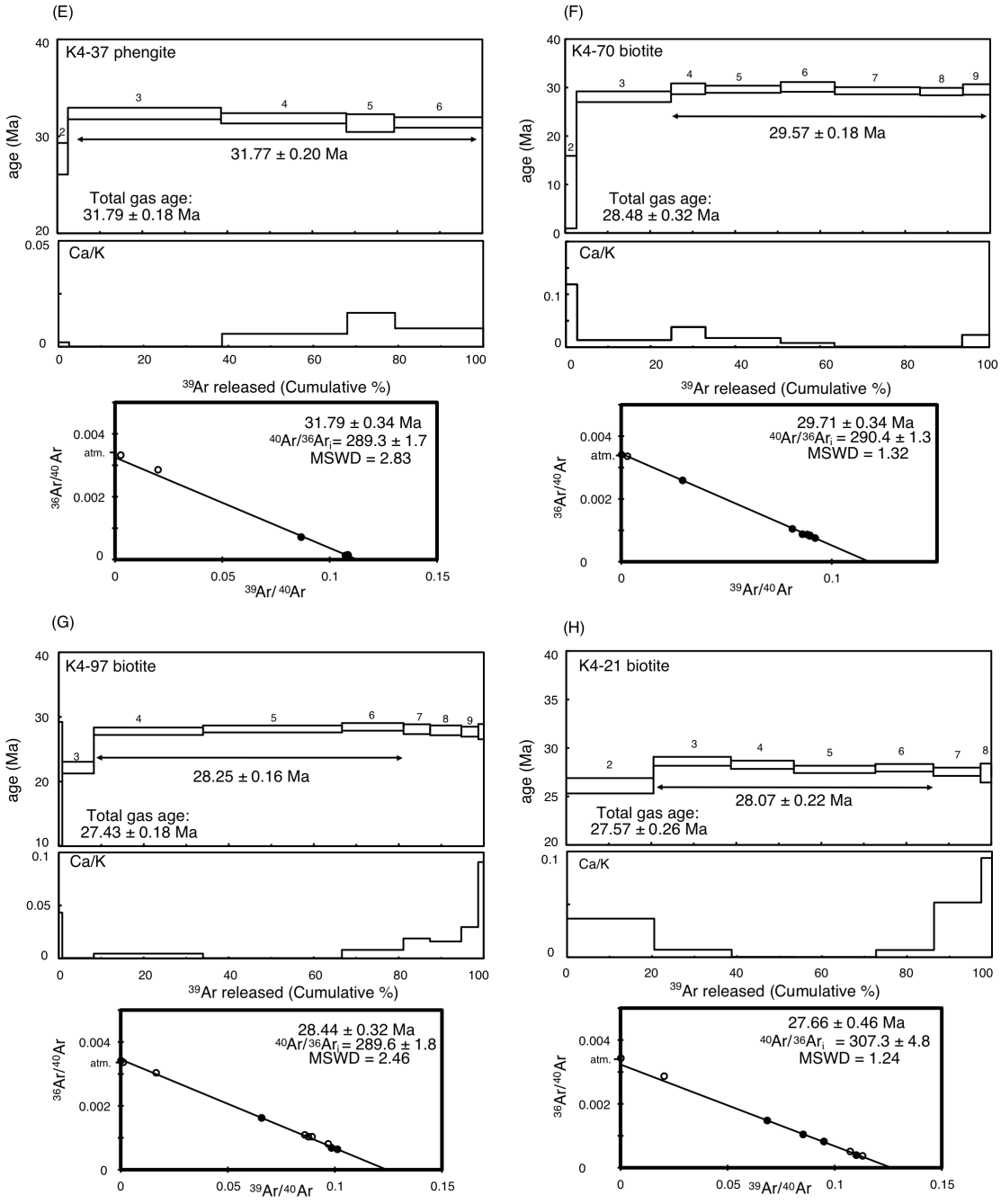
(E)
K4-37 phengite
age (Ma)
31.77 ± 0.20 Ma
Total gas age:
31.79 ± 0.18 Ma
Ca/K
39Ar released (Cumulative %)
31.79 ± 0.34 Ma
40Ar/36Ari= 289.3 ± 1.7
MSWD = 2.83
36Ar/40Ar
39Ar/40Ar
(F)
K4-70 biotite
29.57 ± 0.18 Ma
Total gas age:
28.48 ± 0.32 Ma
29.71 ± 0.34 Ma
40Ar/36Ari = 290.4 ± 1.3
MSWD = 1.32
(G)
K4-97 biotite
28.25 ± 0.16 Ma
Total gas age:
27.43 ± 0.18 Ma
28.44 ± 0.32 Ma
40Ar/36Ari = 289.6 ± 1.8
MSWD = 2.46
(H)
K4-21 biotite
28.07 ± 0.22 Ma
Total gas age:
27.57 ± 0.26 Ma
27.66 ± 0.46 Ma
40Ar/36Ari = 307.3 ± 4.8
MSWD = 1.24

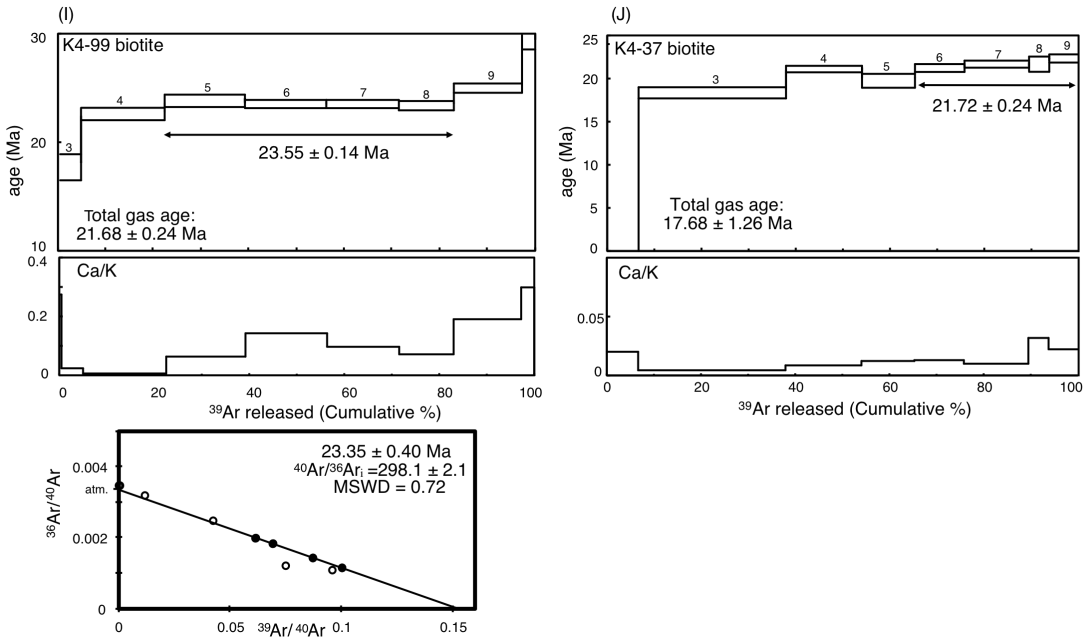

Fig. 3.5. A-J Age [Ma] profile and Ca/K profile vs. ^{39}Ar released [%] for measured micas and amphibole. Errors are 2σ. The number of each heating step (above the steps), total gas age, apparent age or plateau age (extent of plateau indicated by the arrow) is given. Inverse isotope correlation diagrams are shown for plateau ages using plateau steps (black circles). $^{40}Ar/^{36}Ar$ intercept for air (atm.) is inserted as reference.

3.5.2.3. Sample K4-97

Kaar 2 phengite: Steps 2 to 5 comprise 78% of the ^{39}Ar released (Table 3.4; Fig. 3.5b) and define a plateau age at 47.48±0.54 Ma. These steps have similar low Ca/K ratios and define a 47.34±0.72 Ma correlation age that correspond well with the plateau age with an air-like $^{40}Ar/^{36}Ar$ intercept ratio of 297±2.

Phengite: The first step has the highest Ca/K ratios, again shows the effects of minor alteration. Steps 2 to 4 comprise >82% of the ^{39}Ar released and define a plateau age at 34.42±0.16 Ma (Fig. 3.5d). The steps have similar, low Ca/K ratios and define a 34.40±0.38 Ma correlation age that agrees well with the plateau age. The high degree (volumetrically) of breakdown of primary phengite to secondary biotite and plagioclase in this sample strongly suggests that this is not the formation age but a product of partial resetting.

Biotite: Step 3 has a 22.02±0.96 Ma age that overlaps that of step four of biotite sample K4-99 from the same outcrop. This, and the "forced plateaux" age of 21.72±0.24 Ma for

K4-37 biotite suggest an overgrowth event. Steps four to six have similar ages, defining a 28.25±0.16 Ma plateau age (Fig. 3.5g). Steps seven to ten fall in the same age range but are disregarded due to the rapid increase of the Ca/K ratios probably representing plagioclase impurities. The isotope correlation age (28.44±0.32 Ma) overlaps the plateau age. The $^{40}Ar/^{36}Ar$ ratio of 289±2 is not significantly different from the atmospheric value.

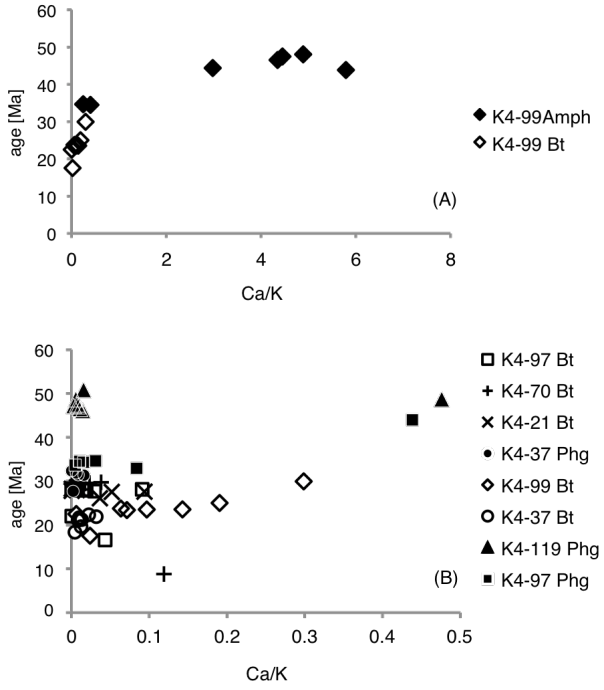

Fig. 3.6. A-B Ca/K ratios vs. age [Ma] correlation diagrams. A High Ca/K ratios diagnostic for amphibole (Amph: black diamonds) in comparison to small ratios for biotite (Bt: white diamonds) from eclogite K4-99. B Compilation of all measured micas (Phengite: Phg). K-depleted alteration rims produce highest Ca/K ratios (e.g. black box and triangle), detectable only in the first heating step.

3.5.2.4. Sample K4-70

Biotite: Ca/K ratios are fairly constant from step 3 onwards (Fig. 3.5f). Apparent ages for steps 4 to 9 vary between 29.74 and 29.60 Ma, resulting in a plateau age of 29.57±0.18 Ma comprising >75% ^{39}Ar released. The validity is supported by the 29.71±0.34 Ma isotope correlation age and the air-like $^{40}Ar/^{36}Ar$ intercept ratio of 290±1.3.

3.5.2.5. Sample K4-37

Phengite: The 31.77±0.20 Ma plateau age starts with step 5 and overlaps the 31.79±0.34 Ma isotope correlation age (Fig. 3.5e). The second step possibly reflects a younger overgrowth at 27.69±1.76 Ma. The Ca/K ratios of all gas fractions are very low.

Biotite: This age spectrum looks similar to that of sample K4-99 biotite, having low amounts of 40Ar*, a poor correlation between Ca/K and apparent ages, and the shape of the spectrum suggesting argon loss (Table 3.2; Fig. 3.5j). All gas fractions have very low Ca/K ratios, but step three has the lowest Ca/K and a high amount of ^{39}Ar (>31%), pointing to a second biotite generation formed at 18.35±0.82 Ma. The "forced plateau" age for steps 6 to 9 (~35% ^{39}Ar released) is 21.72±0.24 Ma.

3.5.2.6. Sample K4-21

Biotite: Steps 3 to 6 define a 28.07±0.22 Ma plateau age (Fig. 3.5h) that comprises >65% of the released ^{39}Ar and have low Ca/K ratios. Steps 2, 7 and 8 have ages that differ only slightly from the plateau age, but were not included into the calculation because of their strongly elevated Ca/K ratios. Late degassing steps 7 and 8 show probably plagioclase impurities whereas slight variations towards the grain rims are confirmed by microprobe analyses (Table 3.2). The isotope correlation age for the plateau-defining steps is 27.66±0.46 Ma, with an air-like ^{40}Ar/^{36}Ar intercept of 307±4.8.

3.6. Exhumation rates and processes

High pressure metamorphism in the Himalaya, first noted in blueschists of the Indus suture zone (Desio, 1977; Honegger et al., 1989) was taken to a new dimension with the finding of eclogite and locally coesite-bearing eclogite in the Kaghan Valley, Pakistan (e.g. Spencer et al., 1991; O'Brien et al., 2001) and in the Tso Morari area, NE India (e.g. Guillot et al., 1995; Sachan et al., 2004): findings requiring subduction of Indian Plate rocks to over 100 km depth as well as their subsequent exhumation. Petrological and petrographical studies (e.g., Guillot et al., 1997; Massonne & O'Brien, 2003; Sachan et al., 2004; Wilke et al., 2009), and radiometric ages (e.g. Tonarini et al., 1993; de Sigoyer et al., 2000; Treloar et al., 2003; Kaneko et al., 2003; Parrish et al., 2006) estimated and revealed many similarities concerning the pressure-temperature-time (PTt) path for both the Kaghan and Tso Morari area. The two stage — fast initially then slower later — exhumation that was first proposed by de Sigoyer et al. (2000) for the Tso Morari was

later also revealed in the Kaghan rocks by Treloar et al. (2003) and Parrish et al. (2006) by U-Pb chronology of accessory phases. In order to consolidate this database, in this study we applied both U-Pb and $^{40}Ar/^{39}Ar$ methods to a range of Kaghan Valley rocks. As the U-Pb methods predominantly date high temperature phases and mica geochronology typically low temperature petrogenetic processes, both techniques were applied and a variety of minerals measured in order to extract the most information about the exhumation and retrogression history of the area.

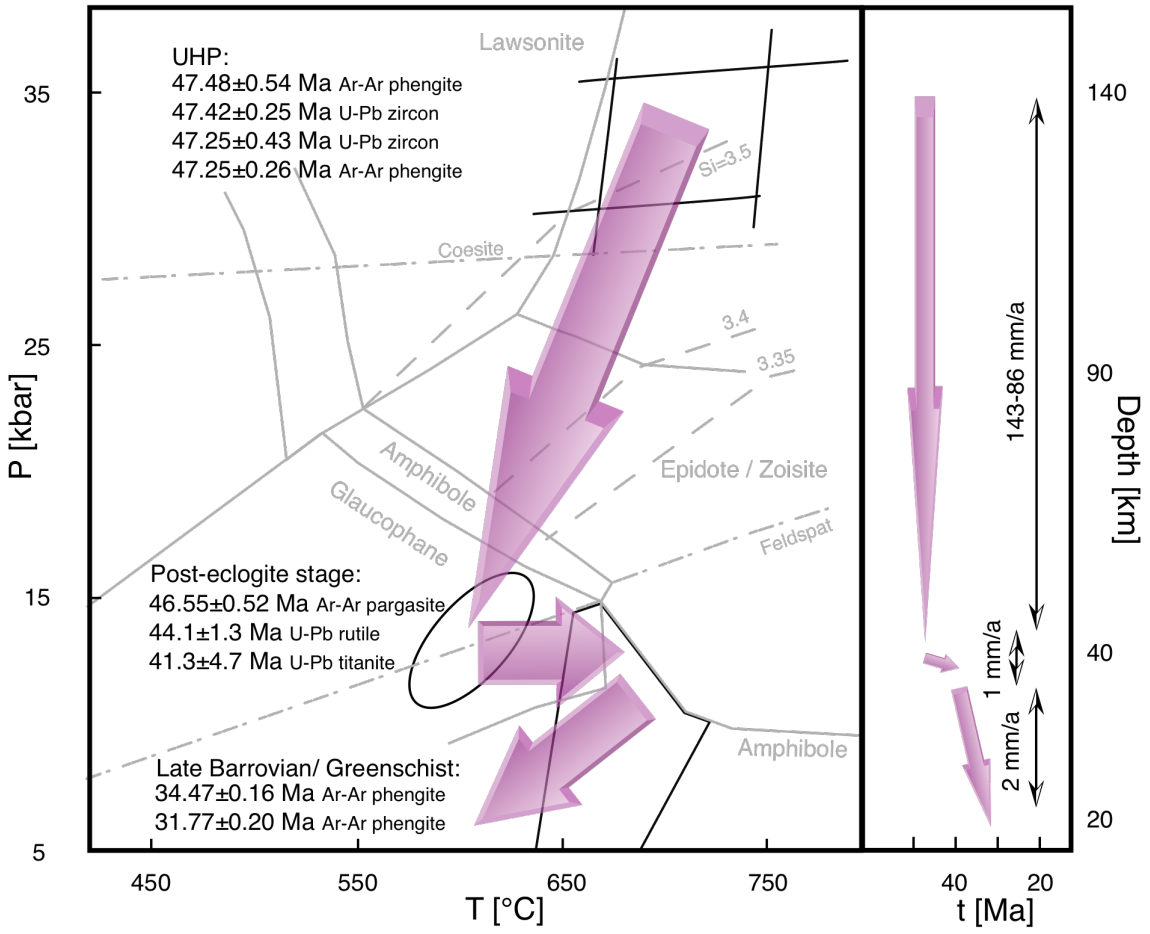

Fig. 3.7. Reduced phase diagram: plotted in grey are Si content in phengite, Coesite-Quartz and Albite=Jadeite+Quartz equilibria. Calculations with Perple_X have been made using garnet-fractionated bulk rock chemistry of the UHP eclogite (for details see Wilke et al., 2009). Black stroked pattern indicating fields of measured or thermo-barometrically calculated PT-conditions. Large arrows show the determined pressure–temperature–time-path. Accompanying ages, method and dated minerals are given left to the appropriate pressure conditions. Inset shows depth-time profile emphasising the contrast in rates between processes at mantle (fast) and crustal (slower) depths. Vertical arrows indicate distances of exhumation steps with derived velocities given for each stage.

U-Pb geochronologies of zircons from orthogneisses (K3-26 & K4-78) reveal core ages of 276+37/-39 Ma and 303±20 Ma representing the Permian magmatic event that produced the protolith. Such ages have been already described for quartzofeldspathic rocks by Noble et al. (2001: 270-268 Ma) in the western Zanskar, by Anczkiewicz et al. 2001 (267+6-3 Ma) for the Swat granite gneiss and by Kaneko et al. (2003: ca. 253 and 170 Ma) for felsic gneisses directly enclosing Kaghan Valley eclogites. These quartzofeldspathic gneisses represent metamorphosed granites and rhyolites produced contemporaneously with the Panjal Trap continental basalts (Papritz & Rey, 1989 and references therein). The zircon rims for both samples, yielding ages of 47.25±0.43 Ma and 47.42±0.25 Ma, reflecting metamorphic conditions as suggested by a low U/Th ratio (<0.2), obvious overgrowth nature (under cathodoluminescence) with an indistinct zoning, and the coincidence to the 46.2±0.7 Ma UHP age derived by Kaneko et al. (2003) from coesite-bearing zircon rims. The lack of coesite inclusions in these zircons avoid a definite pressure estimation therefore the age of the UHP stage is consolidated by a $^{40}Ar/^{39}Ar$ plateau age of 47.25±0.26 Ma for high pressure, Si-rich (>3.4 p.f.u.) phengite, separated from an *in situ* quartz-rich lens enclosed within coesite-bearing eclogite for which formation conditions of 640-790°C/ 30-36 kbar (Wilke et al., 2009) have been deduced. For this sample (Fig. 3.5a), the first two heating steps (disregarded in the plateau age) suggest incomplete Ar retention but the total gas age is only slightly older at 47.62±0.12 Ma. This phengite age, essentially indistinguishable from the zircon age for peak metamorphism despite greater susceptibility to diffusive resetting is backed up by another $^{40}Ar/^{39}Ar$ age of 47.48±0.54 Ma for phengite from a quartz-rutile vein clearly cutting the peak pressure fabric. The up to cm sized phengite books in these samples have the advantage that thermal or fluid-induced resetting is highly unlikely and thus that these are crystallisation ages. These results strongly support the short time period for the high-grade part (>27 kbar) of the metamorphic history as proposed by Massonne & O'Brien (2003), Treloar et al. (2003) and Parrish et al. (2006) for the Kaghan Valley which is also remarkably similar to that suggested for Tso Morari by de Sigoyer et al. (2000) and Massonne & O'Brien (2003).

The post-eclogite facies evolution of the Kaghan Valley rocks is well documented in a series of amphibole-bearing assemblages. Secondary pargasitic amphibole from eclogite K4-99 yielded a $^{40}Ar/^{39}Ar$ age of 46.65±0.24 Ma. No plateau age was obtained for this pargasite. Microprobe analyses and composition maps (Table 3.2, Fig. 3.2) clearly

reveal two amphibole generations that differ in Al, Ti and K contents as well as intergrowth of biotite with amphibole rims. The effect of biotite is recognised in the first two heating steps (Figs. 3.5c, 3.6a) by its lower Ca/K value. Disregarding these two steps results in the presented age of 46.65±0.24 Ma. The volumetrically largest amount of ^{39}Ar (33%) was released in step 4 (yielding 46.55±0.52 Ma) thus not significantly different to the combined age for steps 3 to 7. Existing K-Ar amphibole ages from Treloar & Rex (1990: 48±2; 49±2 Ma) and Ar-Ar hornblende ages from Chamberlain et al. (1991: 42.6±1.4 Ma) are compatible with these new results. Again, as for the white mica, the obvious post-peak metamorphic amphibole cannot be distinguished in age from the peak pressure minerals: a feature directly comparable with the results from Tso Morari (de Sigoyer et al., 2000).

In the Kaghan Valley eclogites no amphibole was stable at peak pressure conditions but different generations of amphibole are clearly linked to distinct stages of the exhumation history. Detailed petrological studies of a suite of eclogite samples revealed the formation of sodic-calcic amphiboles with calcic amphibole (pargasite) rims at 650-720°C and 12 kbar following an initial growth of glaucophane (only locally preserved) at 580-630°C/10-17 kbar (Wilke et al., 2009). The experimental data of Dahl (1996) predict a closure temperature between 500-550°C for pargasitic amphibole (80 μm radius; 10°C/Ma) that have to be extrapolated to ca. 620°C, taking the estimated cooling rate of 100°C/Ma (Treloar et al., 2003) into account. Considering the two to three times larger grain size of the dated pargasites than that of the reference amphiboles used by Dahl (1996) and the reassessment of laboratory determinations of amphibole diffusivity (Villa et al., 1996), the estimated more realistic closure temperature is at least 650°C and thus overlaps the growth conditions. As peak metamorphic conditions at 47.3 Ma are 640-790°C at 30-36 kbar, corresponding to 100-140 km depth, we infer that exhumation must have started very shortly afterwards, with an initial rate of ca. 86-143 mm/a (with respect to the depth uncertainties), in order to allow firstly glaucophane growth and then the formation of the other amphiboles by 46.6 Ma at around 12 kbar (about 40 km; Fig. 3.7). This rate is directly comparable to modern plate velocities, which commonly reach 100 mm/a.

Rutile from eclogite (K4-60) yielded a U-Pb age of 44.1±1.3 Ma thus overlapping the 44.1±1.1 Ma age for a cm-sized rutile from a quartz vein reported by Treloar et al. (2003). Depending on the closure temperature model for Pb diffusion in rutile, this age

can be interpreted as dating rutile growth or post-peak cooling (Treloar et al., 2003). Several studies report different closure temperatures that, depending on grain size and cooling rate, vary between 380 and 530°C (Mezger et al., 1989; 1991: 90-210 µm; 0.5-1°C/Ma), ~550°C (Kotková et al., 2007: 120-200 µm; 40°C/Ma) and 600°C (Cherniak, 2000: 100 µm; 1°C/Ma). Considering the similar grain size but a cooling rate that is several times faster that that in the Cherniak (2000) study, a T_c of ca. 650-700°C (or higher) seems appropriate for our study. Since the temperature conditions for rutile formation (peak conditions) is equivalent or less than the predicted closure temperature for titanite of at least 660-700°C (Scott et al., 1995), the age of 41.3±4.7 Ma for titanite in overprinted eclogite K4-71, although less constrained, dates the petrographically observed titanite growth after rutile. Parrish et al. (2006) dated titanites at 44.0-46.4 Ma from orthogneisses: values that overlap our new U-Pb rutile, titanite and $^{40}Ar/^{39}Ar$ pargasite data and which were interpreted to reflect amphibolite facies conditions (ca. 600°C and 10 kbar) following an initial rapid exhumation. Note that the range of amphibole (46.65±0.24 Ma; Ar-Ar) and titanite (41.3±4.7 Ma; U-Pb) ages, although representing very similar PT-conditions, most probably reflect a much longer duration at amphibolite-greenschist facies conditions (40-35 km depth) compared to that at the eclogite and UHP stages, and thus a slowing of exhumation to more normal (ca. 1 mm/a; Fig. 3.7) rates. This is most likely due to a change in buoyancy forces for the predominantly much less dense crustal rocks of the subducted Indian Plate at >100 km depth in a mantle environment compared to those at typical 35-40 km continental Moho depths. This marked slowing in exhumation might also have initiated the reheating event that is petrologically evident by rims of barroisite and magnesiohornblende surrounding low temperature glaucophane and by growth of ilmenite after rutile.

Further $^{40}Ar/^{39}Ar$ analyses on phengites and biotites from an eclogite, a vein crosscutting an amphibolitised eclogite and various gneisses show the timing and influence of late Barrovian- to greenschist facies conditions. Phengites with silica contents (around 3.25 Si p.f.u.), significantly lower than those in well-preserved UHP rocks, have been dated at 34.47±0.20 (K4-97) and 31.77±0.20 Ma (K4-37). As phengites without wide kelyphitic biotite+plagioclase breakdown coronas from sample K4-97 (Kaar2) yield 47.48±0.54 Ma, and taking into consideration the estimated closure temperature of 550-580°C for phengite (Villa, 1998), these younger ages are interpreted to reflect partial resetting of HP/UHP phengites due to the presence of a fluid phase

during kelyphite growth. Measured biotites cluster at 28-29 Ma and around 22 Ma, which indicate replacement of phengite under greenschist facies conditions. At this stage in the geological evolution of the Kaghan Valley east–west-trending open folds deformed both the south-vergent thrusts and north-vergent extensional shear zones (Treloar et al., 2003). The change from ductile mid-crustal levels to surface related brittle rheological behaviour of the rocks in the Higher Himalayan crystalline during final exhumation gave way to external fluid infiltration, also needed for biotite growth and K transport, that may have opened chemical systems resulting in Ar-loss: a process perhaps explaining the youngest biotites (ca. 22 Ma). A mid-Miocene age (17 Ma) is, so far, only revealed by Fontan et al. (2000) for a phlogopite in marble in the adjacent Neelum valley but was interpreted in the same way. Further studies for the Neelum Valley yielded a number of Oligocene ages around 25-38 Ma for muscovites, interpreted as cooling ages through medium- to low-grade metamorphic conditions (450-500°C/~6 kbar). Another aspect that should not be discarded is the possible younger hydrothermal effects, post-dating regional cooling, e.g. of the rapidly exhuming Nanga Parbat-Haramosh Massif just a few tens of km from the Upper Kaghan Valley: something already mentioned as a possible cause of younger white mica ages by Pêcher et al. (2002). As a comparison, investigations from the Tso Morari area show around 31 Ma for muscovite and 29 Ma for biotite, interpreted as recrystallisation ages (de Sigoyer et al., 2000), which indicate that the final exhumation stage in the NW Himalayan appears contemporaneous. It should be pointed out, however, that zircon fission track ages for Tso Morari crystalline rocks of 35-45 Ma (Schlup et al., 2003) cast doubt on the significance of the young biotite and muscovite ages. The exhumation rate for this third distinguishable stage in the Kaghan rocks is ca. 2 mm/a: comparable with estimations for the same stage in the Tso Morari area (de Sigoyer et al., 2000). If the fission track ages for Tso Morari rocks are to be believed then these rates could have been significantly higher. Nevertheless, a distinct change in exhumation rates for processes occurring at mantle depths compared to those in a normal continental crust environment are clear. Results from recent modelling by Beaumont et al. (2009) show that within the first 10 Ma of continental collision subsequent exhumation of more than 1cm/a will take place if crustal material was buried to more than 100 km depth. The Tso Morari complex, as a natural example, has been incorporated by Beaumont et al. (2009) within general models predicting the exhumation of a dome in the “form of a nappe stack” cored by UHP rocks overlain by lower grade rocks within a subduction channel situated below an accretionary wedge. Pressure-temperature paths from both the Kaghan and Tso Morari

rocks show remarkable similarities (Wilke et al., 2009) indicated by a heating phase (glaucophane growth to calcic amphibole stages) following initial rapid exhumation (itself driven by buoyancy, increasing subduction channel thickness and decreasing viscosity) most likely reflecting stacking of deeply subducted crust at the end of the subduction phase before continent-continent collision and under-thrusting of the Indian Plate below these already exhumed UHP slices occurred (cf. Massonne & O'Brien, 2003). This new modelling by Beaumont et al. (2009) consolidates the results of modelling by (Chemenda et al., 2000) which also proposed rapid exhumation of UHP series back to normal Moho depths at around 40-45 Ma It is noteworthy, that this type of multi-stage exhumation could well be a characteristic feature of preserved UHP terranes elsewhere (Massonne & O'Brien, 2003 suggested this type of scenario for the European Variscides) thus indicating that deformation mechanisms, and rates, at both mantle and crustal conditions need to be understood in order to explain the surface exposure of UHP rocks.

3.7. Acknowledgements

This work was undertaken within the environs of Graduate School 1364, funded by the German Science Foundation (DFG). Christine Fischer prepared excellent thin sections and mineral mounts, CL-images production were carried out by Linda Marko (University of Frankfurt), and Oona Appelt, GFZ Potsdam, supported microprobe analysis.

4. Apatite fission track and (U-Th)/He ages from the Higher Himalayan Crystallines, Kaghan Valley, Pakistan: implications for an Eocene Plateau and Oligocene to Pliocene exhumation

Abstract

Apatite fission track and apatite and zircon (U-Th)/He ages were obtained from high- and ultra high-pressure rocks of the Kaghan Valley, Pakistan. Four samples yielded apatite fission track ages of 24.5±3.8 to 15.6±2.1 Ma and apatite (U-Th)/He ages of 21.0±0.6 to 5.3±0.2 Ma suggesting a moderate Oligocene to Miocene cooling rate, and thus also low exhumation rate, in the high altitude northern parts of the Valley. These data are consistent with extension and back sliding along the reactivated, normal-acting Main Mantle Thrust which induced denudation, exhumation and cooling of the formerly deeply-subducted high-grade metamorphic rocks. An overlap between zircon (10.9±0.4 Ma) and apatite (9.7±0.3 Ma) (U-Th)/He ages is recognised at one location (Besal) due to brittle reactivation of a former thrust fault. A widespread cooling during the Miocene is also evident in adjacent areas to the west (Deosai Plateau, Tso Morari) most likely related to uplift and unroofing linked to continued underplating of the Indian lower crust beneath Ladakh and Kohistan in the late Eocene to Oligocene. In the southern-most part of the study area, near Naran, significantly younger Miocene to Pliocene apatite fission track ages of 7.6±2.1 to 4.0±0.5 Ma suggest a spatial and temporal separation of exhumation processes. These younger ages are best explained by enhanced Late Miocene uplift and erosion driven by thrusting along the Main Boundary Thrust.

4.1. Introduction

The application of low temperature thermochronology in the Himalaya has proven to be a powerful technique to reconstruct the magnitude and timing of exhumation and thus constrain the extent and rates of erosive versus tectonic denudation processes. In particular, several workers have attempted to reconstruct the low temperature history in the north–western Himalaya by apatite and zircon dating (e.g. Zeitler et al., 1982; Zeitler, 1985; Chamberlain et al., 1991; Schlup et al., 2003) in order to constrain the late stages of exhumation of Himalayan crystalline rocks. An understanding of this younger part of the

history helps explain the appearance of once deeply buried rocks at the present-day surface: processes perhaps completely detached from those linked to the stages of the evolution in these rocks that took place at deep crustal or even mantle depths.

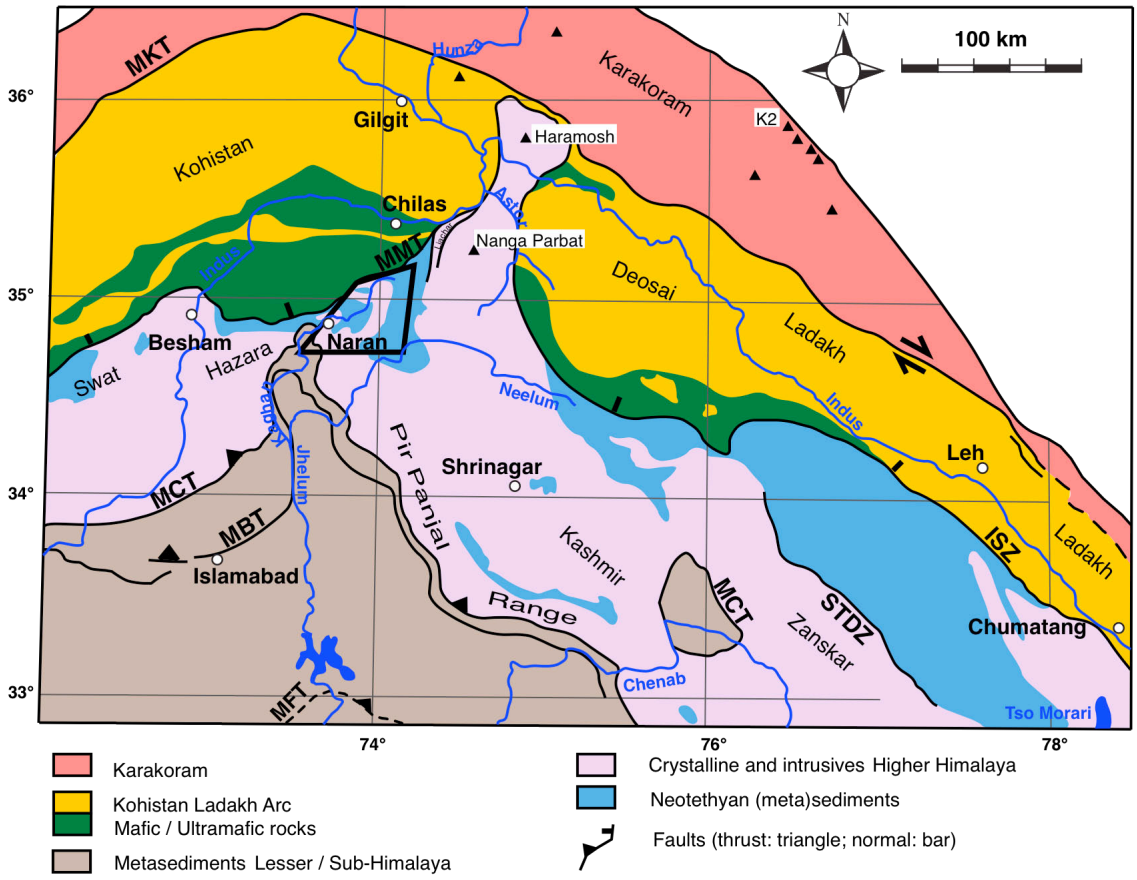

Fig. 4.1. Geological map of the NW Himalaya (simplified from Pêcher et al., 2008 and references therein). MKT: Main Karakoram Thrust; MMT: Main Mantle Thrust (ISZ: Indus Suture Zone); MCT: Main Central Thrust (BT: Batal Thrust); MBT: Main Boundary Thrust. Rectangle showing the location of Fig. 4.2.

Following the closure of Tethys in the area of the northwest Himalaya at around 50 Ma, the Indian Plate collided with the Kohistan-Ladakh oceanic island arc which itself had been accreted to Asia in the Jurassic. Initial deep subduction and subsequent stacking of Indian continental basement and cover sequences beneath the arc induced high grade metamorphism, including an eclogite facies stage, reflected today (Fig. 4.1) in the units mapped as Higher Himalayan Crystalline (HHC). These high-grade rocks are tectonically emplaced along a southward-vergent thrust system onto low-grade to greenschist facies rocks of the Lesser Himalayan (LH) series, and, further south the low-grade series are

emplaced onto early Himalayan erosion products in the so-called Sub-Himalaya. Important to recognise is the southward migration of thrust activity with the Main Boundary Thrust, the boundary between the Lesser- and Sub-Himalayan series, being apart from the Main Frontal Thrust (MFT) the present-day seismically most active thrust fault (e.g. Le Fort, 1975; Kayal, 2001). The original suture zone between India and Asia, the Main Mantle Thrust (MMT: known as the Indus Suture Zone – ISZ – in India), transformed from being a major thrust fault in the Eocene to become a top-to-the-northwest extensional normal fault in the Oligocene: an evolution reflected in the deformation of pervasive greenschist facies assemblages, in overprinted eclogite and amphibolite facies rocks, in the northern-most part of the HHC in the Kaghan Valley, Pakistan (Burg et al., 1996; Treloar et al., 2003; 2007). This extremely rapid exhumation of the crystalline rocks from mantle depths is well documented in the eclogite-bearing HHC series in the Kaghan Valley which were at 140-100 km depth (36-30 kbar at 790-640°C) at 47 Ma (Ar-Ar phengite and U-Pb zircon), cooled during decompression (exhumation) to around 40-35 km depth (17-10 kbar, 630-580°C) before undergoing a phase of reheating to about 720-650°C at roughly the same depth at ca. 46 Ma (Ar-Ar pargasite) and then a greenschist-facies (ca. 34-28 Ma, Ar-Ar phengite and biotite) overprint (Wilke et al. 2010; Wilke et al., in review). A remarkably similar extremely rapid initial Eocene exhumation of subducted Indian Plate rocks from mantle depths is also documented for the Tso Morari crystalline nappes in NW India (de Sigoyer et al., 2000; Guillot et al., 2008).

The spectacular result of the India-Asia collision is not only an impressive mountain chain but also the largest region of high altitude on the present-day planet namely the Tibetan Plateau. The timing of plateau formation is of paramount importance as the high elevation affects atmospheric circulation patterns and is the main cause of the African-Asian monsoon (e.g. Hahn & Manabe, 1975). In addition, the relief contrast off the edge of the plateau is a major driving force for erosion and therefore it is expected that there is a direct relationship between plateau formation, precipitation patterns, erosion rates and thus exhumation ages of crystalline rocks along and across the orogen (e.g. Zeitler et al., 2001). Paleoelevation estimates suggest for central Tibet an elevation of 4 km since the Late Eocene (Rowley & Currie, 2006; Polissar et al., 2009) but indicate for southern Tibet a present-day elevation (around 5000 m) at least by ca. 12 Ma (e.g. Rowley et al., 2001). This is supported by an intensification of the Asian monsoon at around

10 Ma, following a middle Miocene (15-17 Ma) warm phase recorded in global deep-sea oxygen and carbon isotope records (Zachos et al., 2001; and references therein). In addition, stratigraphic records from the deltas of the Indus and Ganges-Brahmaputra river systems, Indus and Bengal fans, respectively, are interpreted to indicate an intensified erosion phase since the Middle Miocene (e.g. Clift et al., 2008; Galy et al., 2010) seemingly supporting the plateau–monsoon–erosion feedback model (Molnar & England, 1990; Burbank, 1992). If these ideas are correct then it should be possible to see evidence of this evolution in the exhumation history, especially from low temperature thermochronology, in rocks exposed in the mountain belt.

Recently, low temperature thermochronological data have been reported for the Deosai region, part of the Kohistan arc in Kashmir and around 150 km NE of the Kaghan Valley, interpreted as evidence for continuous slow denudation rates of 0.25 mm/a since late Eocene times (van der Beek et al., 2009). Based on a comparison of thermochronological data from high-elevation and low-relief regions, such as Kohistan, Ladakh and Deosai to the north and the Tso Morari dome to the south of the MMT, the existence of an extended Tibetan Plateau in this region since Eocene times was proposed. In comparison, for the root zone of the Tso Morari dome close to the MMT, Schlup et al. (2003) suggested a vertical exhumation rate of 2-5 mm/a during the Eocene that slowed down to <0.5 mm/a in the early Miocene but rose again (>0.5 mm/a) towards the present. The relatively low exhumation rates in the Kohistan-Ladakh arc and directly adjoining Higher Himalayan Crystalline are markedly different to the 1-3mm/a extracted from low temperature thermochronology studies from crystalline series, belonging to both High and Low Himalayan series, further away from the MMT (e.g. Thiede et al., 2005; 2009; Grujic et al., 2006; Blythe et al., 2007). As the studied rocks of the Higher Himalayan Crystallines in the Kaghan Valley also terminate against the Kohistan Arc they allow an excellent chance to complement and extend the dataset from these previous studies and at the same time test and refine existing models.

We present new apatite fission track (AFT), apatite (U-Th)/He (AHe), and one zircon (U-Th)/He (ZHe) age from the Kaghan Valley and summarise published Ar-Ar ages from the rocks. The aim is to present a detailed study of the late stage cooling and the complex exhumation history of the Kaghan Valley ultra high-pressure (UHP) rocks as well as accompanying series that experienced significantly lower pressures. This dataset, when combined with that of previous studies from neighbouring areas, is the basis for a

discussion about the driving forces for exhumation in the NW Himalaya and especially relationships to channel flow models mainly proposed for the central parts of the Himalayan chain.

4.2. Geological Setting

In the upper Kaghan Valley, Indian Plate rocks of the Higher Himalayan Crystalline nappes comprise a basement of metagranites and paragneisses overlain by a first, metapelites+greywacke-rich Paleozoic unit and a stratigraphically younger second cover of probably Permo-Mesozoic marble-bearing metasediments (Fig. 4.2). Mafic dykes, sills and lava flows in the sequence, metamorphosed under eclogite- and amphibolite facies conditions, have been attributed to the extensive Permo-Triassic Panjal Trap magmatism by comparison with unmetamorphosed units in Kashmir (Wadia, 1931; Chaudhry & Ghazanfar, 1987; Greco & Spencer, 1993). Structurally, recumbent fold nappes and isoclinal folds pre-date south-southwest–directed thrusting and accompanied nappe stacking within the Indian plate that occurred in the late Eocene to Oligocene (Treloar et al., 1989; Greco & Spencer, 1993). In the northern Kaghan Valley, rocks of the second cover unit protrude through a tectonic window composed of rocks of the basement and first cover units (Besal window; Fig. 4.2). This dome-like structure is caused by WNW-ESE-trending large wavelength, open folds refolded by NE-SW-trending structures (Treloar et al., 1989a).

The dominant metamorphism in the northern Kaghan Valley is of amphibolite facies but abundant eclogites (Massonne & O'Brien, 2003) indicate higher pressures even locally reaching the coesite field (36-30 kbar at 790-640°C: O'Brien et al., 2001: Wilke et al., 2010). The metamorphic history includes an initial cooling during decompression to produce glaucophane but then a reheating at about 10 kbar to give the dominant amphibolite facies assemblages. High temperature geochronology indicates 47 Ma for the UHP coesite eclogite stage (Ar-Ar phengite and U-Pb zircon ages), and ca. 46 Ma (Ar-Ar pargasite) for the subsequent hornblende-producing stage. A greenschist facies overprint (ca. 34-28 Ma, Ar-Ar phengite and biotite) predates unroofing related to reactivation of the MMT as a north-side-down normal fault (Burg et al., 1996; Treloar et al., 2003; Wilke et al., in review).

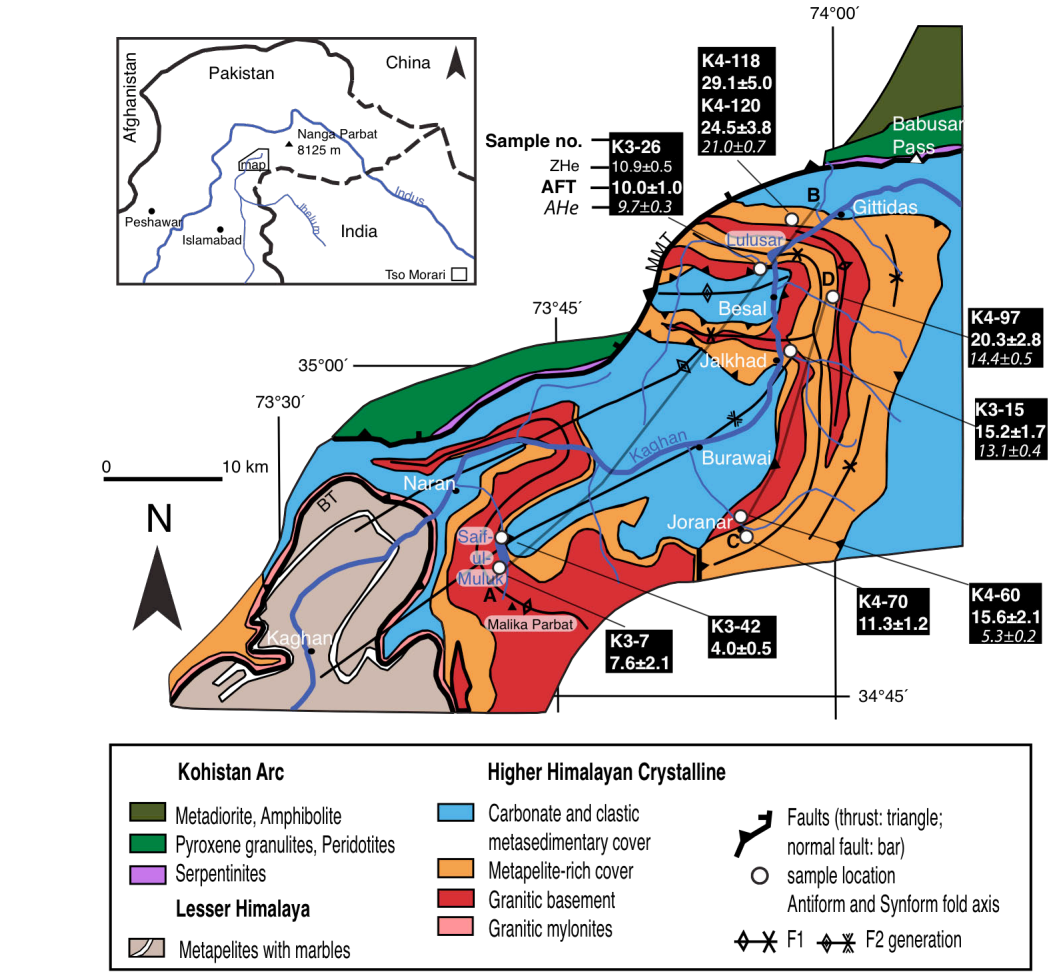

Kohistan Arc

- Metadiorite, Amphibolite
- Pyroxene granulites, Peridotites
- Serpentinites

Lesser Himalaya

- Metapelites with marbles

Higher Himalayan Crystalline

- Carbonate and clastic metasedimentary cover
- Metapelite-rich cover
- Granitic basement
- Granitic mylonites

- Faults (thrust: triangle; normal fault: bar)
- sample location
- Antiform and Synform fold axis
- F1 F2 generation

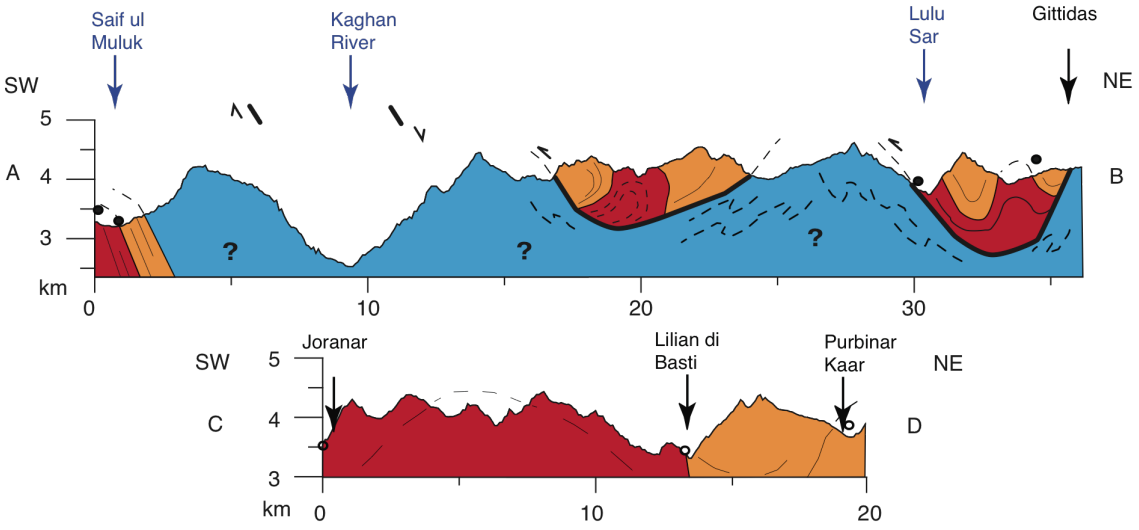

Fig. 4.2. (Top) Simplified geological map of upper Kaghan Valley, north Pakistan (modified from Greco & Spencer, 1993; Lombardo et al., 2000) showing locations of dated samples and of the profiles. Inset map shows the regional location. Abbreviation as in Fig. 4.1, first (F1) and second (F2) generation of folds are shown. (Bottom) Simplified geologic cross sections and distribution of cooling ages along the Kaghan Valley. Dashed lines denote inferred and internal structures. Ages plotted with filled and open symbols refer to cross-section AB and CD, respectively. Time period of the Kohistan back sliding after Zeitler (1985) and Chamberlain et al. (1991). The relief is from the Landsat Image, UTM 43 with one point every 90m.

In the southern part of the Higher Himalayan Crystalline series, a tectonically lower part of the nappe pile, no evidence for an eclogite facies stage is recorded. The studied samples (Fig. 4.2 and Table 4.1) come from: Saleh Gali in the north of the Kaghan Valley close to the MMT; north of Besal; east of Besal; Jalkhad; Joranar (SE of Burawai) and Saif-ul-Muluk (SE Naran).

4.3. AFT and (U-Th)/He Thermochronology

Apatite fission track and (U-Th)/He dating are well-established thermochronometric techniques that are widely employed in geological studies because of their uniquely low closure temperatures (e.g. Stockli et al., 2000; Reiners, 2005). Tectonic and erosional unroofing of sufficient magnitude to exhume samples from below the fission track annealing and the He partial retention zone allow the timing of faulting and crustal exhumation to be obtained (e.g., Stockli, 2005). In general, the partial annealing temperature (PAZ) is constrained to be between ~60 and 120°C (e.g. Ketcham et al., 1999) but depends on the cooling rate and kinematic characteristics of the apatites the latter of which we constrain by measuring etch pit diameters (Dpar; e.g. Donelick et al., 2005). At lower temperatures fission tracks are stable and remain unmodified. (U-Th-[Sm])/He dating is based on the decay of ^{235}U, ^{238}U, ^{232}Th, and ^{147}Sm by alpha (^{4}He nucleus) emission (e.g. Hurley & Goodman, 1941). Alpha particles are emitted with high kinetic energy and travel significant distances of ca. 20μm before coming to rest, leading to α loss from the grain during decay (Farley et al., 1996). Thus, measured (U-Th)/He ages are corrected for this ejection effect, using a statistical approach taking into account mineral density and crystal geometry (Farley et al., 1996; Farley, 2000). The ^{4}He is completely expelled from apatite at temperatures above ~80°C and almost totally retained below ~40°C (e.g., Wolf et al., 1998): a temperature interval defining the He Partial

Retention Zone (HePRZ). Assuming a mean annual surface temperature of 10±5° C and a geothermal gradient of 30±5°C/km, the relevant temperature range is equivalent to depths of ~1 to 3 km. Farley, (2000) obtained a (U-Th)/He closure temperature of 65-70°C for the Durango apatite for a grain of 100 µm radius assuming a 10°C/Ma cooling rate. The (U-Th)/He thermochronometer zircon is characterized by a He closure temperature of about 180°C (e.g., Reiners et al., 2004) and a HePRZ spanning a temperature range from about 120 to 200°C (Reiners & Farley, 2001; Tagami et al., 2003; Stockli, 2005).

4.3.1. Analytical techniques

Eleven samples from metamorphic basement and first cover metapelitic rocks contained sufficient amounts of apatite. Apatite and zircon concentrates were obtained by crushing, sieving, magnetic separation and heavy liquid techniques. For AFT analysis, mounting, polishing and etching were carried out following the procedures outlined in Sobel & Strecker (2003) and Sobel & Seward, 2010; apatites were etched with 5.5mol HNO_3 at 21°C for 20s. Mounts were irradiated with muscovite external detectors and CN5 dosimeter glass at the Oregon State University reactor (U.S.). Micas were afterwards etched with 40%HF at 21°C for 45min. Age determinations are based on the zeta calibration method by Hurford & Green (1983) with a zeta of 377±8 (FW).

After separation, one zircon sample and apatites from five samples were selected for (U-Th)/He dating based on shape, clarity, size (>70 µm) and lack of inclusions. Apatites and zircons were handpicking under a binocular microscope in Potsdam and then sent to the University of Kansas where D. Stockli and T. Glauser performed secondary purification. (U-Th-[Sm])/He age determinations were carried out at the University of Kansas using laboratory procedures described in Stockli et al. (2000) and House et al. (2001). Inclusion-free apatite grains were wrapped in acid-treated Pt foil and heated by laser for 5 minutes at 1070°C and subsequently reheated to ensure complete degassing. Zircons were wrapped in Pt foil, heated for 10 minutes at 1290°C and reheated until >99% of the He was extracted from the crystal. All ages were calculated using standard α-ejection corrections using morphometric analyses (Farley et al., 1996; Farley, 2000). After laser heating, apatites were spiked using an enriched ^{235}U-^{230}Th-^{149}Sm tracer and dissolved in HNO_3. Zircons were unwrapped from the Pt foil and dissolved using HF-HNO3 and HCl pressure vessel digestion procedures. U, Th, and Sm concentrations were determined by isotope dilution ICP-MS analysis. Mean (U-Th-[Sm])/He ages were calculated on the basis of 2-3 inclusion-free apatite and 3 zircon replicate analyses.

Estimated analytical uncertainties are ~6% (2σ) for apatite and ~8% (2σ) for zircon He ages, respectively. Age uncertainties are reported in 1 σ.

4.3.2. Results

All Fission Track analyses passed the χ^2 test (>5%), indicating the absence of non-Poissonian error (e.g. Green, 1985) and thus suggest a single cooling event for each apatite sample. Central and pooled ages are therefore equal and listed with an uncertainty of 1 σ for each sample along with location, elevation, properties and detailed results in Table 4.1. The diameter of the intersect of the c-axis parallel trace of a track with the polished surface (Dpar) were measured in microns [µm] for each sample; this provides information about the annealing kinetics of the apatite crystals (e.g. Donelick et al., 2005; Sobel & Seward, 2010). (U-Th)/He ages have been obtained, each by three aliquots (except for one sample where only two aliquots were used) of ca. 125µm sized apatites. Error is given as 1 σ. Details are given in Table 4.2. The spatial distribution of all samples and their accompanied results are shown in Figs. 4.2 & 4.3, the latter shows the correlation between elevation and age. Using the mineral-pair method, cooling rates have been determined using derived annealing kinetics for AFT ages and retention zone temperatures (ApHePRZ: 68°C; ZrHePRZ: 180°C) with an approximated cooling rate of around 10°C/Ma (Ketcham et al., 1999; Reiners & Brandon, 2006).

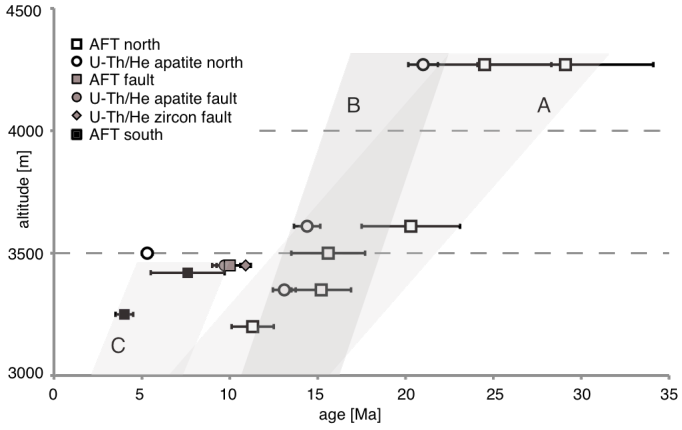

Fig. 4.3. Age–elevation correlation diagram of AFT and (U-Th)/He data. AFT data from the northern Kaghan Valley are in swath A whereas (U-Th)/He data are in swath B and AFT data from the southern-most study area are in swath C: revealing a positive correlation.

Sample	N Latitude [° dec]	E Longitude [° dec]	Elevation [m]	Unit	Rock type	No Xls	NS	Rho-S [x10^{-5}]	NI	Rho-I [x10^{-6}]	ND	Rho-D [x10^{-6}]	P(χ2) [%]	Age [Ma]	error [±1σ]	U [ppm]	Dpar
K4-120a	35.128	73.938	4270	first cover	eclogite	21	49	0.239	417	0.204	4435	1.1110	97	24.5	3.7	2	1.92
K4-118	35.128	73.938	4270	first cover	qz-grt vein in eclogite K4-120a	15	39	0.373	266	0.254	4435	1.0550	96	29.1	5.0	3	2.04
K4-97a	35.046	74.010	3610	first cover	qz-phg vein in amphibolitised eclogite	20	62	0.349	609	0.343	4435	1.0630	95	20.3	2.7	4	1.87
K3-26	35.060	73.934	3450	basement	grt-bearing orthogneiss	19	108	0.732	2157	1.461	4178	1.0623	91	10.0	1.0	17	1.60
K3-15a	35.007	73.963	3350	basement	fine-grained micaschist	20	90	0.471	1129	0.591	4178	1.0170	99	15.2	1.7	7	1.64
K4-60	34.893	73.898	3500	basement	eclogite	20	63	0.340	838	0.453	4435	1.1030	100	15.6	2.1	5	1.67
K4-70a	34.882	73.903	3200	basement	gneiss	18	92	0.687	1654	1.235	4435	1.0790	96	11.3	1.2	14	1.65
K3-7	34.859	73.704	3420	basement	grt-amphibolite	13	14	0.132	358	0.337	4178	1.0300	100	7.6	2.1	4	1.66
K3-42a	34.879	73.698	3250	first cover	grt-bearing orthogneiss	18	65	0.528	3182	2.586	4178	1.0494	76	4.0	0.5	31	1.77

Table 4.1. No Xls: number of grains dated per sample; NS: number of spontaneous tracks counted; Rho-S: spontaneous track density; NI: number of induced tracks counted; Rho-I: induced track density in external detector; ND: number of tracks counted in determining Rho-D; Rho-D: induced track density in external detector adjacent to CN-5 dosimetry glass; P(χ2): chi-square probability; Zeta=376.6±8.0. Dpar have been corrected after linear retrogression equation for Dur and FCT of Donelick et al., 2005. qz: quartz, grt: garnet, phg: phengite

Sample	Age [Ma]	error [±1σ]	U [ppm]	Th [ppm]	Sm [ppm]	Th/U	He [ncc/mg]	mass [mg]	Ft
apatite									
K3-15-1	16.5	0.5	1.4	3.8	7.9	2.7	0.15	3.5	0.71
K3-15-2	9.6	0.3	2.7	6.8	8.5	2.5	0.17	6.5	0.75
K3-15-3	13.3	0.4	0.8	1.3	5.4	1.6	0.06	4.9	0.73
K3-15	**13.1**	**0.4**	**1.6**	**4.0**	**7.2**	**2.3**	**0.1**	**5.0**	**0.7**
K3-26-1	8.1	0.2	8.2	21.5	44.7	2.6	0.37	1.5	0.62
K3-26-2	9.9	0.3	7.8	13.8	30.7	1.8	0.39	1.8	0.64
K3-26-3	11.2	0.3	10.1	20.1	58.6	2.0	0.61	2.3	0.66
K3-26	**9.7**	**0.3**	**8.7**	**18.5**	**44.7**	**2.1**	**0.5**	**1.9**	**0.6**
K4-60-1	4.8	0.1	1.3	1.7	46.7	1.3	0.04	4.9	0.73
K4-60-2	5.9	0.2	0.9	1.3	66.9	1.4	0.04	3.6	0.71
K4-60-3	5.2	0.2	1.3	1.3	56.8	1.0	0.04	6.7	0.76
K4-60	**5.3**	**0.2**	**1.2**	**1.4**	**56.8**	**1.3**	**0.0**	**5.1**	**0.7**
K4-120a-1	10.8	0.3	1.5	0.8	41.9	0.6	0.09	4.4	0.74
K4-120a-2*	674.5	20.2	1.9	1.0	43.6	0.6	6.73	3.4	0.71
K4-120a-3	31.3	0.9	1.9	0.6	30.6	0.3	0.29	4.5	0.74
K4-120 (a)	**21.0**	**0.6**	**1.7**	**0.7**	**36.2**	**0.4**	**0.2**	**4.5**	**0.7**
K4-97-1	12.0	0.4	2.3	4.1	6.7	1.7	0.16	6.5	0.76
K4-97-2	12.0	0.4	2.7	4.2	6.9	1.5	0.19	11.7	0.80
K4-97-3	19.0	0.6	3.0	2.7	9.7	0.9	0.29	6.9	0.77
K4-97	**14.4**	**0.4**	**2.7**	**3.6**	**7.8**	**1.4**	**0.2**	**8.4**	**0.8**
zircon									
ZK3-26-1	10.8	0.4	778.9	34.3	n.d.	<0.1	34.68	4.4	0.75
ZK3-26-2	10.1	0.4	1220.8	55.4	n.d.	<0.1	50.51	4.2	0.75
ZK3-26-3	11.6	0.5	969.1	29.0	n.d.	<0.1	46.18	4.5	0.76
ZK3-26	**10.9**	**0.4**	**989.6**	**39.6**	n.d.	**<0.1**	**43.8**	**4.4**	**0.8**

Table 4.2. Results of apatite and zircon U-Th/He analyses. Ft: fraction of retained α-particles (radius dependent) after Farley et al., 1996. Bold data are the simple mean of the three aliquots.

The samples from close to the MMT, at Saleh Gali in the northernmost part of the Kaghan Valley (Fig. 4.2) yielded surprisingly old AFT ages of 29.1±5.0 Ma (high F/Cl ratio grain) and 24.5±3.8 Ma. The latter sample also gave an AHe age of 21.0±0.6. Further away from the MMT, E of Besal and at Jalkhad, ages are younger: AFT of 20.3±2.8 and 15.2±1.7 Ma, AHe of 14.4±0.5 and 13.1±0.4 Ma, respectively. The youngest AFT ages of 7.6±2.1 and 4.0±0.5 Ma were recorded from samples collected close to the lake Saif-ul-Muluk in the southernmost part of the area. Apatites from the intermediate location, Joranar SE of Burawai, yielded Middle Miocene FT ages of 11.2±1.2 and 15.6±2.1 Ma with the latter sample also showing a He age of 5.3±0.2 Ma. For the other measured sample, K3-26 from N of Besal, the ZHe age of 10.9±0.4 Ma overlaps the AFT age of 10.0±1.0 Ma and the AHe age of 9.7±0.3 Ma.

4.4. Discussion and Implications

The timing of exhumation of crystalline rocks in orogenic belts to the surface (or at least to shallow depths and thus low temperatures) is intimately linked to the tectonic and erosional history. The rates and importance of these process, and possibility of feedback mechanisms between them, are a question of continued debate even in intensively studied mountain chains such as the Himalaya. In the central Himalaya, Tertiary high grade crystalline rocks of the Higher Himalayan Crystalline (HHC) nappes are tectonically bounded in their hanging wall to the Tethyan Sequence by the normal fault (north-side-down) of the South Tibetan Detachment System (STDS) in their footwall to the Lesser Himalaya by the south-vergent Main Central Thrust. Many recent works have proposed that the high-grade Higher Himalayan sequences represent the extruded part of a hot channel, bounded by the STDS above and MCT below, with extrusion aided by accelerated erosion driven by the enhancement of the Indian monsoon along the orogenic front of the Tibetan Plateau (e.g. Beaumont et al., 2001; 2004; Grujic et al., 2002). In the central part of the Himalaya results from low temperature thermochronology are consistent with Late Miocene to Pliocene exhumation of HHC rocks and increased rates of fluvial incision, which have been attributed to this coupled channel flow-enhanced monsoon process (Molnar & England, 1990; Burbank, 1992; Thiede et al., 2005; 2009; Grujic et al., 2006).

The recent study by van der Beek et al. (2009), suggests a much older, Eocene age for the plateau based on AFT and U/Th/He ages and thus casts doubt on the validity of the channel flow model at least for the NW Himalaya. These new results from Deosai, a high-elevation (4000m), low-relief area within the Kohistan-Ladakh arc, suggest only very low erosion rates of 0.25 mm/a for the last 35 Ma and thus that a plateau already existed at this time. The study area of the Upper Kaghan Valley is only about 150 km west of the Deosai area and on the digital elevation map of van der Beek et al. (2009: their Figure 1) is a southwestward extension of the continuous high elevation area forming the Tibetan Plateau. It is therefore no great surprise that our most northerly samples, from a very low relief, ca. 4000m high location very close to the MMT, yield Oligocene ages directly comparable with those from Deosai (Figs. 4.4, 4.5). These Kaghan rocks are undoubtedly Indian Plate rocks metamorphosed in the Eocene (cf. Wilke et al., 2010; Wilke et al., in review) and thus the near-surface exhumation of these rocks, based on the Ar-Ar, AFT and (U-Th)/He results, occurred very soon after the metamorphic peak. The rapid exhumation of high grade Himalayan metamorphic rocks is also recognised in the Tso Morari area of India, 450 km to the SE of the Kaghan Valley (Figs. 4.4, 4.5). Here, very similar coesite-bearing eclogite series yield zircon FT ages of 45 to 34 (Schlup et al., 2003). Thus it is clear that this part of the HHC was exhumed very early in the collision process and, although the tectonic situation (normal fault above, thrust below) is similar to that proposed for the channel flow model for the central Himalaya, there is no evidence for a Tibetan Plateau–monsoon–channel flow feedback mechanism at this stage of the collision.

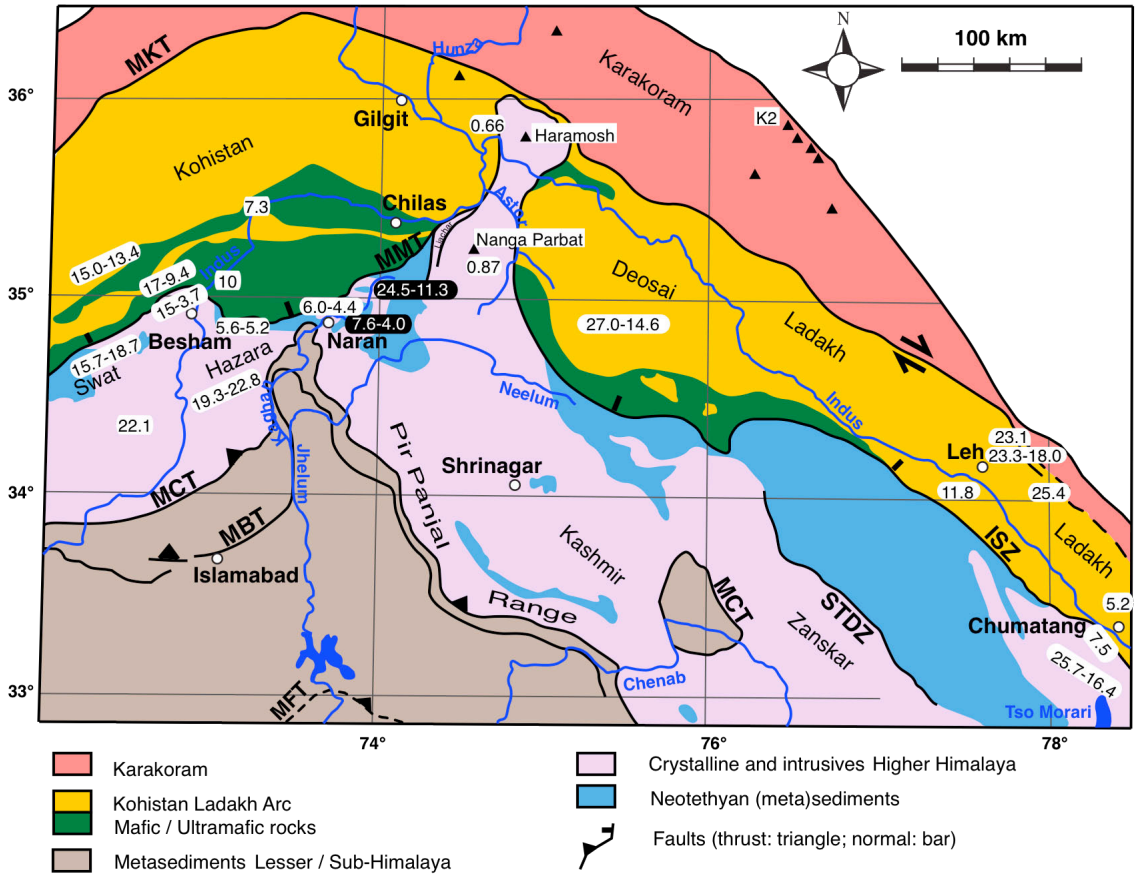

Fig. 4.4. Spatial distribution of apatite fission track ages in the NW Himalaya. Data from Zeitler et al. (1982); Zeitler, (1985); Zeilinger et al. (2007); van der Beek et al. (2009); Kirstein et al. (2006); Kumar et al. (2007); Schlup et al. (2003); Inger (1998). White ages on black background: this paper. Abbreviations as in Fig. 4.1.

In both the Kaghan and Tso Morari areas, HHC rocks are directly adjacent to the Kohistan-Ladakh arc separated only by the MMT (also known as the Indus Suture Zone). In both cases it is the MMT that acted as a top-down-north normal fault driving the late Oligocene post-greenschist exhumation of the crystalline unit from beneath the Asian margin (e.g. Treloar et al., 2003; Schlup et al., 2003). This is a significantly different situation to that of the central Himalaya where the HHC series are exhumed from below the unmetamorphosed to very-low-grade Tethyan sedimentary series in places 200 km south of the actual suture zone. In this situation the top-down-north normal fault is the STDZ where the oldest movement is early Miocene in age (e.g. Searle & Godin, 2003) i.e. much later than the final activity recorded in the eclogite-bearing crystalline units. Although the crystalline rocks of both Upper Kaghan and Tso Morai are generally attributed to the Higher Himalaya it is clear in both cases that the rocks yielding the oldest

FT ages represent the tectonically uppermost units of stacked nappe sequences such that the common map continuity of the HHC along and across the belt is erroneous. In addition, some of the NW Himalayan rocks mapped as belonging to the HHC are lithostratigraphically actually Tethyan Series equivalents (Neotethyan in Fig. 4.1) that have also been subducted to mantle depths: a feature not apparent on maps showing just metamorphic grade.

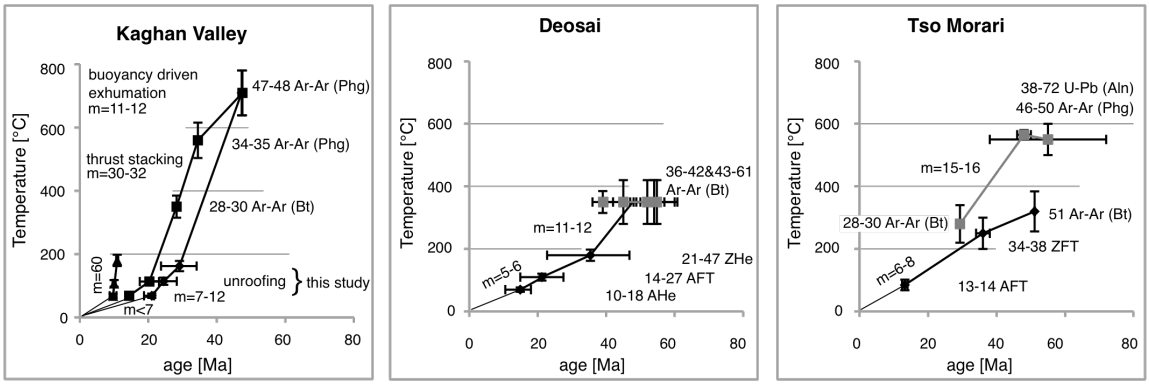

Fig. 4.5. Temperature–time plots for the Kaghan Valley (Pakistan), the Deosai Plateau (Kashmir) and the Tso Morari nappe (Ladakh, India) illustrating the differences between the early Eocene to Paleocene history of the UHP areas in comparison to Deosai as well as the contemporaneous exposure during the early to middle Miocene. Data from Kaghan Valley: triangle: K3-26; box: K4-97, diamond: K4-120a&119&118 (for details see Wilke et al., 2010; Wilke et al., in review). Data Deosai: black diamond (van der Beek et al., 2009); gray box (Bard et al., 1980; Maluski & Schaeffer, 1982). Data from Tso Morari: black diamond (Schlup et al., 2003); grey box (de Sigoyer et al., 2000 and references therein). Biotite Ar-Ar ages have been interpreted to reflect cooling through 300-400°C. Cooling rates (m) in °C/Ma are given for each area and each exhumation stage. Calculation of cooling rates does not take advection into account.

Contrasting results come from sample K3-26 (from N of Besal, Fig. 4.2), which shows overlapping ZHe (10.9±0.4), AFT (10.0±1.0 Ma) and AHe (9.7±0.3 Ma) ages indicating very rapid cooling. This sample comes from close to the boundary of the upper and lower nappe sheets and has most likely been affected by reactivation of this structural boundary related to up-doming of the nearby Nanga Parbat Massif (Schneider et al., 2001; Whittington, 1996).

When the low-temperature thermochronological results from the southern part of the study area are compared with those from the north, it is immediately obvious that the

values do not fit the same pattern. Our new AFT ages of 7.6±2.1 and 4.0±0.5 Ma for a garnet-amphibolite and garnet-bearing granitic gneiss, respectively, are significantly younger than those from the Upper Kaghan Valley. However, these new data correspond perfectly with previous AFT results from Zeitler (1985) from the same area which range between 4.2±0.9 and 6.0±1.2 Ma. When compared with AFT results from elsewhere in the HHC further west in the Hazara, Besham and Swat areas (Fig. 4.4), where values fall mostly in the range 15-22 Ma (Zeitler, 1985; Zeilinger et al., 2007), it is clear that the HHC of the southern Kaghan Valley has been affected by much younger tectonic activity.

The rock units of the Naran–Saif-ul-Muluk area represent the southernmost part of the HHC and in addition belong to a tectonically lower level of the nappe pile (Fig. 4.2): a level that shows no evidence for an eclogite facies stage in metabasites, although a coronitic garnet-bearing stage testifies to at least high pressure amphibolite facies conditions (Wilke et al., 2010). Immediately south of Naran the HHC is terminated by the Batal thrust which has been correlated to the MCT in many previous studies (e.g. Chaudhry & Ghazanfar, 1987) although the rocks south of this boundary also exhibit amphibolite facies assemblages (staurolite in metapelites) rather than the low grade greenschist facies parageneses more typical for Lesser Himalaya elsewhere. More notable for this region, however, is the very close vicinity of the Main Boundary Thrust. The MBT is, apart from the MFT, the seismically most active thrust in the region today (e.g. Kayal, 2001) with the most recent demonstration being the 2005 Magnitude 7.6 Muzaffarabad earthquake (Avouac et al., 2006). Activity on the MBT, based on AFT ages from conglomeritic sediments derived from the HHC, initiated prior to 10 Ma (Meigs et al., 1995) and continues today whereas the MCT is seismically inactive in this region (Hodges et al., 1992; 1996). Connected to this thrust activity along the MBT is clearly also the development of a further topographic barrier reflected in the Pir Panjal range along the southern side of the Kashmir Valley (Burbank & Johnson, 1982). This chain stretches for around 300 km until it ends immediately adjacent to Saif-ul-Muluk at Malika Parbat: at 5290 m the highest peak of the Kaghan Valley. Thus, as topographic relief, rainfall concentration, erosion and exhumation are intimately linked, the young AFT ages of the southern Kaghan HHC can be directly attributed to the development of the more southerly orographic barrier driven by southward propagation of Himalayan thrust activity during the Late Miocene/Pliocene. Further evidence of the effects of this MBT thrust activity can be seen in the increased incision rates of rivers, development of narrow

gorges, and changing sediment accumulation rates which extends across the chain from the NW Himalaya in Pakistan (e.g. Meigs et al., 1995) through India (Thiede et al., 2004) to Nepal (Burbank et al., 2003; Robert et al., 2009).

4.5. Conclusions

Three events in the tectonic evolution of the Kaghan Valley, Pakistan are outlined by low temperature apatite fission track and (U-Th)/He thermochronology.

1) During the early to middle Miocene cooling of Kaghan HHC rocks reflect the period of exhumation from beneath the Kohistan-Ladakh Island Arc driven by the backsliding along the MMT. This early event led to the formation of an early plateau and thus the channel flow mechanism developed for the central Himalaya is not valid for the NW Himalaya.

2) Reactivation of the intra-nappe thrust near Besal as a normal fault, tied to the up-doming of the nearby Nanga Parbat massif, led to local rapid cooling and thus overlapping AFT and (U-Th)/He ages for this location.

3) Late Miocene to Pliocene cooling of HHC rocks from the southern-most part of the study area reflect thrusting along the MBT and development of an additional orogenic barrier (Malika Parbat at Saif-ul-Muluk lies on the extension of the Pir Panjal range) which enhanced erosion and exhumation.

This large variation in low temperature thermochronological ages from the relatively narrow belt of the HHC in the Kaghan Valley, contrasts strongly with the generally more limited range of ages from the HHC in the central part of the belt and thus is further evidence for an extended, multi-stage evolution of the India-Asia collision zone as is becoming increasingly recognised (e.g. O'Brien, 2001a; Massonne & O'Brien, 2003; Beaumont et al., 2009).

4.6. Acknowledgments

We thank Gerold Zeilinger for helpful discussions and ideas. This work was undertaken within the environs of Graduate School 1364, funded by the German Science Foundation (DFG).

5. Results and conclusions

This study discusses and answers questions concerning the conditions and time scale of the formation and exhumation of ultra high-pressure eclogites and their host rocks from the NW Himalaya in Pakistan, combining petrology, petrography, mineral- and geochemistry, geochronology, thermochronology and geodynamics. In general, the new results have important implications for understanding processes occurring at mantle depths, as well as at lower, middle and even shallow crustal levels in this highly dynamic subduction–collision orogen. In addition, I pursue the question of whether or not a positive feedback between monsoon-driven erosion and exhumation is evident in the Kaghan Valley.

In the upper Kaghan Valley the occurrence of eclogites in the north and metadolerites in the south, testifies to a spatial variation in peak-metamorphic pressure conditions over a relatively short distance. Responsible for this is a tectonic stacking of crustal basement–cover units. In order to exclude influences of the whole rock composition on the PT estimates and to constrain protolith character, I analysed major-, trace- and rare earth element (REE) contents of five petrographically distinct eclogite types. Despite the obvious textural differences and variations in the degree of alteration, geochemical compositions suggest that they are all petrogenetically related. All are subalkaline/alkaline metabasalts showing tholeiitic affinity and, apart from two types, exhibit similar REE patterns. Major and trace element trends exclude a subduction-related magmatic origin, whereas chondrite–normalised La/Sm, La/Nb ratios and high Zr amounts are essentially the same as those of rift tholeiites and within-plate volcanic rocks. Furthermore, the eclogites resemble geochemically the non-metamorphic Permo-Triassic Panjal Trap continental flood basalts in Kashmir, which has long been recognised as a non-metamorphosed stratigraphic continuation of the Kaghan area (Wadia, 1931; Chaudry&Ghanzafar, 1987). Minor differences in REE patterns probably reflect different amounts of contamination during the emplacement in the continental crust.

To constrain the PT conditions of the different eclogite types in the Kaghan Valley, I applied a variety of conventional geothermobarometers based on garnet–clinopyroxene–phengite–plagioclase–hornblende equilibria. These methods yielded similar equilibrium conditions within the coesite field at around 30-36 kbar. Coesite

occurs as inclusions in garnet and omphacite in eclogites from the northern-most locations close to the contact with the suture zone, and was indentified petrographically and by *in situ* micro-Raman spectroscopy. The lack of coesite in eclogite samples from further south could merely be a problem of preservation potential. During exhumation, retrogression took place and is obvious as reaction textures comprising newly-formed amphiboles, plagioclase, biotite and titanite. Non-equilibrated secondary glaucophane is rimmed by barroisite and pargasite. This is the first time that glaucophane is recognised in some of the coesite-bearing eclogites of the Kaghan Valley. As glaucophane is not stable in the coesite stability field this indicates relatively low temperatures after peak conditions for this amphibole growth stage. Subsequently, a temperature increase that is also supported by ilmenite overgrowth on rutile, produced the Na-Ca and Ca amphiboles that rim or replace glaucophane. Standard amphibole-plagioclase thermometry and modelled phase diagrams ("pseudosections") for the effective bulk rock compositions of coesite- and glaucophane-bearing eclogites were used to quantitatively constrain this part of the history. The resulting PT-path implies a complex exhumation path that starts at ca. 640-790°C and 100-140 km depth (coesite) and continues with cooling via decompression to 580-630°C at 10-17 kbar (glaucophane), followed by a re-heating event of ca. 650-720°C at 10-12 kbar (pargasite, ilmenite).

Interestingly, the metadolerites from the southern-most part of the study area show no petrographical evidence of the former presence of eclogite facies assemblages, consistent with the calculated metamorphic conditions of ca. 650-750°C and 8-9 kbar, which are comparable to those for the reheating stage of the formerly described eclogites. Thus, peak metamorphic conditions for the metadolerites are similar to the retrograde metamorphism in the eclogite varieties, which indicates tectonic juxtaposition and metamorphic convergence of these units after the eclogite facies stage.

Another petrographic find in some of the eclogites of related interest are quartz-phengite-zoisite and kyanite-bearing leucocratic segregations. These are interpreted as products of metasomatic fluid flow driven by dehydration reactions in the metabasites and their surrounding pelitic gneisses. Due to the complete absence of albite-rich plagioclase the segregations are most likely not derived by partial melting, as also supported by the fact that the PT-path did not cross the wet melting curve.

Now that pressure and temperature conditions have been determined, questions remain as to the timing and duration of each metamorphic and exhumation stage. In order to constrain both high- and low-temperature parts of the history I applied suitable high- and low-closure temperature dating methods namely the U-Pb and Ar-Ar techniques. U-Pb geochronology of zircons from felsic gneisses (metamorphosed granites and rhyolites) enclosing eclogites reveal core ages of around 276+37/-39 and 303±20 Ma, which show that they are contemporaneous (i.e. part of a bimodal sequence) to the eruption of the Permo-Triassic Panjal Trap basalts. The ages support the geochemical findings, which suggest that the Panjal Trap basalts were protoliths of the Kaghan Valley eclogites. The zircon rims for both gneiss samples yield ages of 47.25±0.43 Ma and 47.42±0.25 Ma, reflecting metamorphic conditions as suggested by e.g. low U/Th ratios (<<0.2) and the obvious overgrowth nature as seen by cathodoluminescence microscopy. The lack of coesite inclusions in these zircon rims does not permit a definite pressure estimate. Instead, the age of the UHP stage was consolidated by a $^{40}Ar/^{39}Ar$ plateau age of 47.25±0.26 Ma for high pressure, Si-rich phengites separated from an *in situ* quartz-rich lens enclosed within coesite-bearing eclogite. Secondary pargasitic amphibole, separated from an eclogite, yielded a $^{40}Ar/^{39}Ar$ age of 46.65±0.24 Ma, which infers that exhumation must have started very shortly afterwards, with an initial rate of ca. 86-143 mm/a. Subsequently, the rocks remained at temperatures very similar to that of the pargasite formation stage for a longer time period, as inferred from 44.1±1.3 Ma and 41.3±4.7 Ma U-Pb ages for rutile and titanite from two eclogites. This result clearly indicates a change of the exhumation style as suggested by a slowing of exhumation to more normal (ca. 1 mm/a) rates at about 40-35 km depth causing a longer duration of amphibolite-greenschist facies conditions and the petrologically evident reheating event. Phengites, containing a significantly lower amount of silica (p.f.u.) than those in UHP rocks and that formed at around 20 km depth, have Ar-Ar ages of 34.47±0.20 Ma and 31.77±0.20 Ma. These ages indicate a slightly higher exhumation rate of ca. 2 mm/a under upper greenschist facies conditions. Biotite Ar-Ar ages cluster at 28-29 Ma and around 22 Ma indicating replacement of phengite under greenschist facies conditions. Late biotite growth may be explained by infiltration of external fluids and potassium transport related to the change from ductile mid-crustal levels to surface related brittle rheological behaviour of the rocks in the Higher Himalayan crystalline during final exhumation. This growth stage ties to the late unroofing event well documented in the formation of large

albite porphyroblasts, themselves folded, in the dominant metapelitic and metagranitic series of the northern Kaghan Valley.

Finally, I used fission track and U-Th/He thermochronology for to investigate apatite and a single zircon sample to obtain insight into the ultimate exhumation stages. Interestingly, in the northern and central parts of the study area these ages indicate a moderate cooling rate of about 10°C/Ma for early to mid Miocene times. In the southern-most part of the study area, late Miocene to Pliocene ages point again to a different evolution in this part of the area as already inferred from petrographic and petrologic data. From field observations (P.J. O'Brien pers. comm.) and tectonic reconstructions this southern basement–cover unit underlies the northern one. Therefore, younger ages may reflect a later exhumation of the southern unit due to out of sequence thrusting of the different thrust nappes within the Higher Himalayan Crystalline as in the neighbouring Hazara Crystalline (Treloar, 1989). Beside possible enhanced advection due to the rapid ascent of the once deeply-buried rocks, a resetting of the apatite fission track ages by (hydro-) thermal influence, e.g. by various hot fluids circulating from major faults into nearby rock units or by the rapidly extruding Nanga Parbat doming cannot be discarded.

Significantly, the S-shaped PT-path deduced here for the Kaghan Valley eclogites is remarkably similar to that of the coesite-bearing eclogites in Tso Morari (Ladakh, India). Both PT-paths record exhumation from deep mantle to normal crustal depths under various conditions, thus suggesting changes in exhumation mechanisms: a process that might be valid for ultra high-pressure metamorphic series elsewhere. Geochronological results strongly support the short time period for the ultra high-grade part (>27 kbar) of the metamorphic history and the initial buoyancy-driven rapid exhumation proposed by various authors for the Kaghan Valley, which have been also suggested for Tso Morari. Less pronounced buoyancy forces for the subducted crustal rocks of the Indian Plate at continental Moho depths compared to mantle depths have initiated a remarkable slowdown of the exhumation velocity of these UHP rocks and significant reheating under amphibolite facies conditions. Soon afterwards, stacking of the formerly deeply subducted crust under regional amphibolite–greenschist facies conditions predates the synconvergent extension and back sliding of the Kohistan Island Arc along the MMT that finally exposed the eclogites. Thus, the pronounced similarities between the Kaghan Valley in Pakistan and the Tso Morari in NW India indicate that this type of multi-stage exhumation could well be a characteristic feature of preserved UHP terranes elsewhere.

Important to recognise is that this high- and ultra high-pressure metamorphism reflects the early continental subduction-related stage and significantly predates the collision-related metamorphism widespread in the central part of the Himalaya.

In conclusion, my study has shown that a multidisciplinary approach, combining field geology, isotope geochemistry with petrology and petrography is a prerequisite for geochronological studies of complex metamorphosed rocks. Regarding the question as to the exhumation mechanism of ultra high-pressure rocks in the Himalaya it is noteworthy that not only a single mechanism, such as the proposed channel flow, is capable of exposing rocks that have been buried to mantle depths. A range of processes constrained by their local environment (buoyancy contrast, thermal contrast) is required. Apart from the fact that most of the exhumation of the UHP series had already occurred well before the initiation of the monsoonal system, I have found that two substantial requirements for the establishment of a channel flow mechanism are not evident: 1) a small percentage of in situ partial melt to reduce the viscosity of the flow and 2) the significant recent high erosion rate at the exhumation front. Therefore, a positive feedback mechanism between climate (erosion) and exhumation cannot be postulated for the Kaghan Valley UHP rocks. However, the rapid extrusion of the Nanga Parbat–Haramosh Massif, a relatively young phenomenon, might well be equivalent to the extruding channel proposed for the central Himalaya as e.g., in the Mount Everest region.

6. Bibliography

Anczkiewicz, R., Oberli, F., Burg, J.P., Villa, I.M., Günther, D., Meier, M., 2001. Timing of normal faulting along the Indus Suture in Pakistan Himalaya and a case of major $^{231}Pa/^{235}U$ initial disequilibrium in zircon. Earth and Planetary Science Letters, 191, 101-114.

Argles, T., Foster, G., Whittington, A., Harris, N., George, M., 2003. Isotope studies reveal a complete Himalayan section in the Nanga Parbat syntaxis. Geology, 31, 1109-1112.

Avouac, J.-P., Ayoub, F., Leprince, S., Konca, O., Helmberger, D.V., 2006. The 2005, M_w 7.6 Kashmir earthquake: Sub-pixel correlation of ASTER images and seismic waveforms analysis. Earth and Planetary Science Letters, 249, 514-528.

Bard, J.P., Maluski, H., Proust, F., 1980. The Kohistan Sequence: Crust and Mantle of an obducted Island Arc. Gological Bulletin of the University of Peshawar, Special Issue, 13, 23-29.

Beaumont, C., Jamieson, R.A., Nguyen, M. H., Lee, B., 2001. Himalayan tectonics explained by extrusion of a low-viscosity crustal channel coupled to focused surface denudation. Nature, 414, 738-742.

Beaumont, C., Jamieson, R.A., Nguyen, M.H., Medvedev, S., 2004. Crustal channel flows: 1.Numerical models with application to the tectonics of the Himalayan-Tibetan orogen. Journal of Geophysical Research, 109.

Beaumont, C., Jamieson, R.A., Butler, J.P., Warren, C.J., 2009. Crustal structure: A key constraint on the mechanism of ultra-high-pressure rock exhumation. Earth and Planetary Science Letters, doi: 10.1016/j.epsl.2009.08.001.

Becker, H., Jochum, K.-P., Carlson, R.W., 1999. Constraints from high-pressure veins in eclogites on the composition of hydrous fluids in subduction zones. Chemical Geology, 160, 291-308.

Berman, R. G., 1990. Mixing properties of Ca-Mg-Fe-Mn garnets. American Mineralogist, 75, 328-344.

Bhat, M.I., Zainuddin, S.M., Rais, A., 1981. Panjal Trap chemistry and the birth of Tethys. Geological Magazine, 118, 367-375.

Blankenburg, F.v., Villa, I.M., Baur, H., Morteani, G., Steiger, R.H., 1989. Time calibration of a PT-path from the western Tauern Window, eastern Alps: the problem of closure temperatures. Contribution to Mineralogy and Petrology, 101, 1-11.

Blythe, A.E., Burbank, D.W., Carter, A., Schmidt, K., Putkonen, J., 2007. Plio-Quaternary exhumation history of the central Nepalese Himalaya: 1. Apatite and zircon fission track and apatite (U-Th)/He analyses. Tectonics, 26, TC3002.

Boundy, T.M., Hall, C.M., Li,G., Essene, E.J., Halliday, A.N., 1997. Fine-scale isotopic heterogeneities and fluids in the deep crust: a $^{40}Ar/^{39}Ar$ laser ablation and TEM study of muscovites from a granulite-eclogite transition zone. Earth and Planetary Science Letters, 148, 223-242.

Burbank, D.W., Johnson, G.D., 1982. Intermontane-basin development in the past 4 Myr in the north-west Himalaya. Nature, 298, 432-436.

Burbank, D.W., 1992. Causes of recent Himalayan uplift deduced from deposited patterns in the Ganges basin. Nature, 357, 680-683.

Burbank, D.W., Blythe, A.E., Putkonen, J., Pratt-Sitaula, B., Gabet, E., Oskin, M., Barros, A., Ojha, T.P., 2003. Decoupling of erosion and precipitation in the Himalaya. Nature, 426, 652-655.

Burg, J.-P., Chaudhry, M.N., Ghazanfar, M., Anczkiewicz, R., Spencer, D., 1996. Structural evidence for back sliding of the Kohistan arc in the collisional system of northwest Pakistan. Geology, 24, 739-742.

Carswell, D.A., O´Brien, P.J., Wilson, R.N., Zhai, M., 1997. Thermobarometry of phengite-bearing eclogites in the Dabie Mountains of central China. Journal of Metamorphic Geology, 15, 239-252.

Castelli, D., Rolfo, F., Compagnoni, R., Xu, S., 1998. Metamorphic veins with kyanite, zoisite and quartz in the Zhu-Jia-Chong eclogite, Dabie Shan, China. The Island Arc, 7, 159-173.

Chamberlain, C.P., Zeitler, P.K., Erickson,E., 1991. Constraints on the tectonic evolution of the northwestern Himalaya from geochronologic and petrologic studies of the Babusar Pass, Pakistan. Journal of Geology, 99, 829-849.

Chaudhry, M.N., Ghazanfar, M., 1987. Geology, structure and geomorphology of upper Kaghan Valley, NW Himalaya, Pakistan. Geological Bulletin, Punjab University, 22, 13- 57.

Chauvet, F., Lapierre, H., Bosch, D., Guillot, S., Mascle, G., Vannay, J.-C., Cotton, J., Brunet, P., Keller, F., 2008. Geochemistry of the Panjal Trap basalts (NW Himalaya): record of the Pangea Permian break-up. Bulletin de la Societé Géologique de France, 179, 383-395.

Chemenda, A.I., Burg, J.-P., Mattauer, M., 2000. Evolutionary model of the Himalaya-Tibet system: geopoem based on new modelling, geological and geophysical data. Earth and Planetary Science Letters, 174, 197-409.

Cherniak, D.J., 2000. Pb diffusion in rutile. Contribution to Mineralogy and Petrology, 139, 198-207.

Clift, P., Hodges, K.V., Heslop, D., Hannigan, R., van Long, H, Calves, G., 2008. Correlation of Himalayan exhumation rates and Asian monsoon intensity. Nature geoscience, 11, 875-880.

Dahl, P.S., 1996. The effect of composition on tetentivity of argon and oxygen in hornblende and related amphiboles: A field-tested empirical model. Geochimica et Cosmochimica Acta, 60, 2687-3700.

Dale, J., Powell, R., White, R.W., Elmer, F.L., Holland, T.J.B., 2005. A thermodynamic model for Ca-Na clinoamphiboles in Na_2O-CaO-FeO-MgO-Al_2O_3-SiO_2-H_2O-O for petrological calculations. Journal of metamorphic Geology, 23, 771-791.

DeCelles, P.G., Robinson, D.M., Zandt, G., Implications of shortening in the Himalayan fold-thrust belt for uplift of the Tibetan Plateau, Tectonics, 21, 1062, doi: 10.1029/2001TC001322.

DeCelles, P.G., Quade, J., Kapp, P., Fan, M., Dettman, D.L., Ding, L., 2007. High and dry central Tibet during the Late Oligocene. Earth and Planetary Science Letters, 253, 389-401.

Deniel, C., Vidal, P., Coulon, C., Vellutini, P., Piquet, P., 1994. Temporal evolution of mantle sources during continental rifting: the volcanism of Djibouti (Afar). Journal of Geophysical Research, 99, 2853-2869.

De Sigoyer, J., Guillot, S., Lardeaux, J.-M., Mascle, G., 1997. Glaucophane bearing eclogites in the Tso Morari dome (eastern Ladakh, NW Himalaya). European Journal of Mineralogy, 9, 1073-1083.

De Sigoyer, J., Chavagnac, V., Blichert-Toft, A., Villa, I.M., Luais, B., Guillot, S., Cosca, M., Mascle, G., 2000. Dating the Indian continental subduction and collisional thickening in the northwest Himalaya: Multichronology of the Tso Morari eclogites. Geology, 28, 487-490.

Desio, A., 1977. The occurance of blueschists betwen the middle Indus and Swat valleys as an evidence of subduction in northern Pakistan. Rendiconti Accademia Nazionale dei Lincei, 52, 74-79.

DiPietro, J.A., Lawrence, R.D., 1991. Himalayan structure and metamorphism south of the Main Mantle Thrust, Lower Swat, Pakistan. Journal of metamorphic Geology, 9, 481-495.

DiPietro, J., Pogue, K.R., Lawrence, R.D., Baig, M.S., Hussain, A., Ahmad, I., 1993. Stratigraphy south of the Main Mantle Thrust, Lower Swat, Pakistan. In: Treloar, P.J., Searle, M.P., (eds). Himalayan Tectonics. Geological Society, London, Special Publications, 74, 207-220.

DiVincenzo,G., Carosi, R., Palmeri, R., 2004. The relationship between tectonometamorphic evolution and Argon isotope records in white mica: constrains from in situ ^{40}Ar-^{39}Ar Laser analysis of the Variscan basement of Sardinia. Journal of Petrology, 45, 1013-1043.

Donelick, R.A., O'Sullivan, P.B., Ketcham, R.A., 2005. Apatite fission-track analysis. Reviews in Mineralogy and Geochemistry, 58, 49-94.

Ehlers, T.A., Farley, K.A., 2003. Apatite (U-Th)/He thermochronometry: methods and applications to problems in tectonic and surface processes. Earth and Planetary Science Letters, 206, 1-14.

England, P.C., Holland, T.J.B., 1979. Archimedes and the Tauern eclogites: the role of buoyancy in the preservation of exotic eclogite blocks. Earth and Planetary Science Letters, 44, 287-294.

Ernst, W.G., Maruyama, S., Wallis, S., 1997. Buoyancy-driven, rapid exhumation of ultrahigh-pressure metamorphosed continental crust. Proceedings of the National Academy of Sciences, 94, 9532-9537.

Ernst, W.G., 2001. Subduction, ultrahigh-pressure metamorphism, and regurgitation of buoyant crustal slices – implications for arcs and continental growth. Physics of the Earth and Planetary Interiors, 127, 253-275.

Farley, K.A., Wolf, R.A., Silver, L.T., 1996. The effects of long alpha-stopping distances on (U-Th)/He ages. Geochimica et Cosmochimica Acta, 60, 4223-4229.

Farley, K.A., 2000. Helium diffusion from apatite: General behaviour as illustrated by Durango fluorapatite. Journal of Geophysical Research (Solid Earth), 105, 2903-2914.

Fontan, D., Schouppe, M., Hunziker, C.J., Martinotti, G., Verkaeren, J., 2000. Metamorphic evolution, ^{40}Ar-^{39}Ar chronology and tectonic model for the Neelum valley, Azad Kashmir, NE Pakistan. In: Khan, M.A., Treloar; P.J., Searle, M.P., Jan, M.Q. (eds). Tectonics of the Nanga Parbat Syntaxis and the Western Himalaya. Geological Society, London, Special Publications, 170, 431-453.

Fuhrman, M.L., Lindsley, D.H., 1988. Ternary-feldspar modelling and thermometry. American Mineralogist, 73, 201-215.

Galy, V., France-Lanord, C., Peucker-Ehrenbrink, B., Huyghe, P., 2010. Sr-Nd-Os evidence for a stable erosion regime in the Himalaya during the past 12 Myr. Earth and Planetary Science Letters, doi: 10.1016/j.epsl.2010.01.004.

Gerdes, A., Zeh, A., 2006. Combined U-Pb and Hf isotope LA-(MC-)ICP-MS analyses of detrital zircons: comparison with SHRIMP and new constraints fort he provenance and age of an Amorican metasediment in Cetral Germany. Earth and Planetary Science Letters, 249, 47-61.

Gerdes, A., Zeh, A., 2009. Zircon formation versus zircon alteration – New insights from combined U-Pb and Lu-Hf in-situ LA-ICP-MS analyses, and consequences for the interpretation of Archean zircon from the Central Zone of the Limpopo Belt. Chemical Geology, 261, 230-243.

Greco, A., Martinotti, G., Papritz, K., Ramsay, J.G., Rey, R., 1989. The crystalline rocks of the Kaghan Valley (NE-Pakistan). Eclogae Geologicae Helvetiae, 82, 629-653.

Greco, A., Spencer, D.A., 1993. A section through the Indian Plate, Kaghan Valley, NW Himalaya, Pakistan. In: Treloar, P.J., Searle, M.P., (eds). Himalayan Tectonics. Geological Society, London, Special Publications, 74, 221- 236.

Green, P.F., 1985. Comparison of zeta calibration baselines for fission-track dating of apatite, zircon and sphene. Chemical Geology, 58, 1-22.

Green, T.H., Hellman, P.I., 1982. Fg-Mg partioning between coexisting garnet and phengite at high pressure, and comments on a garnet-phengite geothermometer. Lithos, 15, 253-266.

Grujic, D., Hollister, L.S., Parrish, R.R., 2002. Himalayan metamorphic sequence as an orogenic channel: insights from Bhutan. Earth and Planetary Science Letters, 198, 177-191.

Grujic, D., Coutand, I., Bookhagen, B., Bonnet, S., Blythe, A., Cuncan, C., 2006. Climatic forcing of erosion, landscape, and tectonics in the Bhutan Himalayas. Geology, 34, 801-804.

Guillot, S., Lardeaux, J.M., Mascle, G., Colchen, M., 1995. Un nouveau témoin du métamorphisme de haute-pression dans la chaîne himalayenne: les éclogites rétromophosées du Dôme du Tso Morari, (Est Ladakh, Himalaya). Comptes Rendus de l´Académie des Sciences, Paris, 320, 931-936.

Guillot, S., de Sigoyer, J., Lardeaux, J.M., Mascle, G., 1997. Eclogitic metasediments from the Tso Morari area (Ladakh, Himalaya) evidence for continental subduction during India-Asia convergence. Contribution to Mineralogy and Petrology, 128, 197-212.

Guillot, S., Garzanti, E., Baratoux, D., Marquer, D., Mahéo, G., de Sigoyer, J., 2003. Reconstructing the total shortening history of the NW Himalaya. Geochemistry Geophysics Geosystems, 4, 1064, doi: 10.1029/2002GC000484.

Guillot, S., Mahéo, G., de Sigoyer, J., Hattori, K.H., Pêcher, A., 2008. Tethyan and Indian subduction viewed from the Himalayan high- to ultrahigh-pressure metamorphic rocks. Tectonophysics, 451, 225-241.

Hahn, D.G., Manabe, S., 1975. The role of mountains in the South Asian Monsoon circulation. Journal of the athmospheric sciences, 32, 1515-1541.

Harrison, T.M., Célérier, J., Aikman, A.B., Hermann, J., Heizler, M.T., 2009. Diffusion of ^{40}Ar in muscovite. Geochimica et Cosmochimica Acta, 73, 1093-1051.

Hermann, J., Spandler, C., Hack, A., Korsakov, A.V., 2006. Aqueous fluids and hydrous melts in high-pressure and ultra-high pressure rocks: Implications for element transfer in subduction zones. Lithos, 92, 399-417.

Hess, J. C., Lippolt, H. J., 1994. Compilation of K-Ar measurements on HD-B1 standard biotite, 1994 status report. In: Odin G. S., (eds.). Phanerozoic time scale. Bulletin of Liaison and Informatics. IGCP project 196. Calibration of the Phanerozoic time scale, 12, 19-23.

Hodges, K.V., Parrish, R.R., Housh, T.B., Lux, D.R., Burchfield, B.C., Royden, L.H., Chen, Z., 1992. Simultaneous Miocene extension and shortening in the Himalayan Orogen. Science, 258, 1466-1470.

Hodges, K.V., Parrish, R.R., Searle, M.P., 1996. Tectonic evolution of the central Annapurna Range, Nepalese Himalayas. Tectonics, 15, 1264-1291.

Hofmann, A.W., 1988. Chemical differentiation of the Earth: the relationship between mantle, continental crust, and ocean crust. Earth and Planetary Science Letters, 90, 297-314.

Holland, T., Blundy, J., 1994. Non-ideal interactions in calcic amphiboles and their bearing on amphibole-plagioclase thermometry. Contribution to Mineralogy and Petrology, 116, 433-447.

Holland, T., Powell, R., 1996. Thermodynamics of order-disorder in minerals: II. Symmetric formalism applied to solid solutions. American Mineralogist, 81, 1425-1437.

Holland, T., Powell, R., 1998. An internally consistent thermodynamic data set for phases of petrological interest. Journal of metamorphic Geology, 16, 309-343.

Holland, T., Baker, J., Powell, R., 1998. Mixing properties and activity-composition and relationships of chlorites in the system MgO-FeO-Al_2O_3-SiO_2-H_2O. European Journal of Mineralogy, 10, 395-406.

Honegger, K.V., LeFort, P., Mascle, G., Zimmermann, J.L., 1989. The blueschists along the Indus Suture Zone in Ladakh, NW Himalaya. Journal of Metamorphic Petrology, 7, 57-73.

House, M.A, Farley, K.A., Stockli, D.F., 2001. Helium chronometry of apatite and titanite using Nd-YAG laser heating. Earth and Planetary Science Letters, 183, 365-368.

Hurford, A.J., Green, P.F., 1983. The zeta age calibration of fission-track dating. Chemical Geology, 41, 285-317.

Hurley, P.M., Goodman, C., 1941. Helium retention in common rocks minerals. Geological Society of America Bulletin, 52, 545-560.

Inger, S., 1998. Timing of an extensional detachment during convergent orogeny: New Rb-Sr geochronological data from the Zanskar shear zone, northwestern Himalaya. Geology, 3, 223-226.

Ishizuka, O., 1998. Vertical and horizontal variation of the fast neutron flux in a single irradiation capsule and their significance in the laser-heating 40Ar/39Ar analysis; Case study for the hydraulic rabbit facility of the JMTR reactor, Japan. Geochemical Journal, 32, 243-252.

Ishizuka, O., Yuasa, M., Uto, K., 2002. Evidence of porphyry copper-type hydrothermal activity from a submerged remnant back-arc volcano of the Izu-Bonin arc: Implication for the volcano tectonic history of back-arc seamounts. Earth and Planetary Science Letters, 198, 381-399.

Jackson, S. E., Pearson, N. J., Griffin, W. L., Belousova, E. A., 2005. The application of laser ablation-inductively coupled plasma-mass spectrometry to in situ U–Pb zircon geochronology. Chemical Geology, 211, 47-69.

Kaneko, Y., Katayama, I., Yamamoto, H., Misawa, K., Ishikawa, M., Rehman, H.U., Kausar, A.B., Shiraishi, K., 2003. Timing of Himalayan ultrahigh-pressure metamorphism: sinking rate and subduction angle of the Indian continental crust beneath Asia. Journal of metamorphic Geology, 21, 589-599.

Kayal, J.R., 2001. Microearthquake activity in some parts of the Himalaya and the tectonic model. Tectonophysics, 339, 331-351.

Kazmi, A.H., Jan, M.Q. (eds.) 1997. Geology and Tectonics of Pakistan. Graphic Publishers, Karachi.

Kelley, S., Turner, G., Butterfield, A.W., Shepherd, T.J., 1986. The source and significance of argon isotopes in fluid inclusions from areas of mineralization. Earth and Planetary Science Letters, 79, 303-318.

Kennedy, C.S., Kennedy, G.C., 1976. The equilibrium boundary between graphite and diamond. Journal of Geophysical Research, 81, 2467-2470.

Ketcham, R.A., Donelick, R.A., Carlson, W.D., 1999. Variability of apatite fission-track annealing kinetics: III. Extrapolation to geological time scales. American Mineralogist, 84, 1235-1255.

Khan, M.A., Treloar, P.J., Searle, M.P., Jan, M.Q., 2000. Tectonics of the Nanga Parbat syntaxis and the western Himalaya. Geological Society Special Publication, 170, pp 485.

Kirstein, L.A., Sinclair, H., Stuart, F.M., Dubson, K., 2006. Rapid early Miocene exhumation of the Ladakh batholith, western Himalaya. Geology, 34, 1049-1052.

Konrad-Schmolke, M.,Handy, M.R., Babist, J., O´Brien, P.J., 2005. Thermodynamic modelling of diffusion-controlled garnet growth. Contribution to Mineralogy and Petrology, 16, 181-195.

Konrad-Schmolke, M., O´Brien, P.J., de Capitani, C., Carswell, D.A., 2008. Garnet growth at high- and ultra- high pressure conditions and the effect of element fractionation on mineral modes and composition. Lithos, 103, 309-332.

Kotková, J., Gerdes, A., Parrish, R.R., Novák, M., 2007. Clasts of Variscan high-grade rocks within Upper Viséan conglomerates–constraints on exhumation history from petrology and U-Pb chronology. Journal of metamorphic Geology, 25, 781-801.

Krogh, E.J., 1988. The garnet-clinopyroxene Fe-Mg geothermometer – a reinterpretation of existing experimantal data. Contribution to Mineralogy and Petrology, 99, 44-48.

Kumar, R., Lal, N., Singh, S., Jain, A.K., 2007. Cooling and exhumation of the Trans-Himalayan Ladakh batholith as constrained by fission track apatite and zircon ages. Current Science, 92, 490-496.

Lambert, I. B., Wyllie, P. J., 1972. Melting of gabbro (quartz eclogite) with excess water to 35 kilobars, with geological applications. Journal of Geology, 80, 693–708.

Lanphere, M.A., Dalrymple, G.B., 2000. First-Principles Calibration of ^{38}Ar Tracers: Implications for Ages of ^{40}Ar/^{39}Ar Fluence Monitors: US Geological Survey professional paper, 1621.

Lanphere, M.A., Baadsgaard, H., 2001. Precise K-Ar, ^{40}Ar/^{39}Ar, Rb-Sr and U/Pb mineral ages from the 27.5 Ma Fish Canyon Tuff reference standard. Chemical Geology, 175, 653-671.

Leake, B.E., 1997. Nomenclature of amphiboles. Report of the Subcommittee on Amphiboles of the International Mineralogical Association Commission on new Minerals and Mineral names. European Journal of Mineralogy, 9, 623-651.

Le Fort, P., 1975. Himalayas: the collided range. Present knowledge of the continental arc. American Journal of Science, 275-A, 1-44.

Liebscher, A., Franz, G., Frei, D., Dulski, P., 2007. High-pressure melting of eclogite and the P-T-X history of tonalitic to trondhjemitic zoisite pegmatites, Münchberg Massif, Germany. Journal of Petrology, 48, 1001-1019.

Liou, J.G., Tsujimori, T., Zhang, R.Y., Katayama, I., Maruyama, S., 2004. Global UHP metamorphism and continental subduction/collision: The Himalayan model. International geology review, 46, 1-27.

Lombardo, B., Rolfo, F., Compagnoni, R., 2000. Glaucophane and barroisite eclogites from the Upper Kaghan nappe: implications for the metamorphic history of the NW Himalaya. In: Khan, M.A., Treloar; P.J., Searle, M.P., Jan, M.Q. (eds). Tectonics of the Nanga Parbat Syntaxis and the Western Himalaya. Geological Society, London, Special Publications, 170, 411-430.

Lombardo, B., Rolfo, F., 2000. Two contrasting types in the Himalayas: implications for the Himalaya orogeny. Journal of Geodynamics, 30, 37-60.

Luvizotto, G.L., Zack, T., Meyer, H.P., Ludwig, T., Triebold, S., Kronz, A., Münker, C., Stockli, D.F., Prowatke, S., Klemme, S., Jacob, D.E., von Eynatten, H., 2009. Rutile crystals as potential trace element and isotope mineral standards for microanalysis. Chemical Geology, 261, 346-369.

Maluski, H., Schaeffer, O.A., 1982. ^{39}Ar-^{40}Ar laser probe dating of terrestrial rocks. Earth and Planetary Science Letters, 59, 21-27.

Massonne, H.J., O'Brien, P.J., 2003. The Bohemian Massif and the NW Himalaya. In Carswell, D.A., Compagnoni, R., (Ed.), Ultrahigh pressure metamorphism, 5, 145-187. European Notes in Mineralogy, Eötvös University Press, Budapest.

McDonough, W.F., Sun, S.-s., 1995. The composition of the Earth. Chemical Geology, 120, 223-253.

McDougall, I., Harrison, T.M., 1999. Geochronology and Thermochronology by the ^{40}Ar/^{39}Ar Method. Oxford University Press, New York. 2rd edition.

Meigs, A.J., Burbank, D.W., Beck, R.A., 1995. Middle-late Miocene (>10 Ma) formation of the Main Boundary thrust in the western Himalaya. Geology, 23, 423-426.

Mezger, K., Hanson, G.N., Bohlen, S.R., 1989. High precision U-Pb ages of metamorphic rutile: application to the cooling history of high-grade terranes. Earth and Planetary Science Letters, 96, 106-118.

Mezger, K., Rawnslay, C., Bohlen, S.R., 1991. U–Pb garnet, sphene, monazite and rutile ages: implications for the duration of high grade metamorphism and cooling histories Adirondack Mountains, New York. Journal of Geology, 99, 415-428.

Middlemost, E.A.K., 1975. The basalt clan. Earth Science Reviews, 11,337-364.

Molnar, P., England, P., 1990. Late Cenozoic uplift of mountain ranges and global climate: chicken or egg? Nature, 346, 29-34.

Morimoto, N., 1988. Nomenclature of pyroxenes. Mineralogy and Petrology, 39, 55-76.

Noble, S.R., Searle, M.P., Walker, C.B., 2001. Age and tectonic significance of Permian granites in Western Zanskar, High Himalaya. The Journal of Geology, 109, 127-135.

O'Brien, P.J., Sachan, H.K., 2000. Diffusion modelling in garnet from Tso Morari eclogites and implications for exhumation models. Earth Science Frontiers, 7, 25-27.

O'Brien, P.J., 2001a. Subduction followed by Collision: Alpine and Himalayan examples. In: Rubie, D.C. & van der Hilst, R. (eds.). Processes and Consequences of Deep Subduction, Physics of the Earth and Planetary Interiors, 127, 277-291.

O'Brien, P.J., Zotov, N., Law, R., Ahmed Khan, M., Quasim Jan M., 2001. Coesite in Himalayan eclogite and implications for models of India-Asia collision. Geology, 29, 435-438.

Papritz, K., Rey, R., 1989. Evidence of the occurrence of permian Panjal Trap basalts in the Lesser- and Higher-Himalayas of the Western Syntaxis Area, NE Pakistan. Eclogae Geologicae Helvetiae, 82, 603-627.

Parrish, R.R., Gough, S.J., Searle, M.P., Waters, D.J., 2006. Plate velocity exhumation of ultrahigh-pressure eclogites in the Pakistan Himalaya. Geology, 34, 989-992.

Patriat, P., Achache, J., 1984. India–Eurasia collision chronology has implications for crustal shortening and driving mechanism of plates. Nature, 311, 615-621.

Pearce, J.A., Norry, M.J. 1979. Petrogenetic implications of Ti, Zr, Y and Nb variations in volcanic rocks. Contributions to Mineralogy and Petrology, 69, 33-47.

Pêcher, A., Giuliani, G., Garnier, V., Maluski, H., Kausar, A.B., Malik, R.H., Muntaz, H.R., 2002. Geology, geochemistry and Ar-Ar geochronology of the Nangimali ruby deposit, Nanga Parbat Himalaya (Azad Kashmir, Pakistan). Journal of Asian Earth Sciences, 21, 265-282.

Pêcher, A., Seeber, L., Guillot, S., Jouanne, F., Kausar, A., Latif, M., Majid, A., Mahéo, G., Mugnier, J.L., Rolland, Y., van der Beek, P., Van Melle, J., 2008. Stress field evolution in the Northwest Himalayan syntaxis, Northern Pakistan, Tectonics, 27, TC6005, doi: 10.1029/2007TC002252.

Pognante, U., Spencer, D.A., 1991. First report of eclogites from the Himalayan belt, Kaghan valley (northern Pakistan). European Jounal of Mineralogy, 3, 613-618.

Polissar, P.J., Freeman, K.H., Rowley, D.B., McInerney, F.A., Currie, B.S., 2009. Paleoaltimetry of the Tibetan Plateau from D/H ratios of lipid biomarkers. Earth and Planetary Science Letters, 287, 64-76.

Rehman, H.U., Yamamoto, H., Kaneko, Y., Kausar, A.B., Murata, M., Ozawa, H., 2007. Thermobaric structure of the Himalayan Metamorphic Belt in Kaghan Valley, Pakistan. Journal of Asian Eaerth Sciences, 29, 390-406.

Rehman, H.U., Yamamoto, H., Khalil, M.A.K., Nakamura, E., Zafar, M., Khan, T., 2008. Metamorphic history and tectonic evolution of the Himalayan UHP eclogites in Kaghan Valley, Pakistan. Journal of Mineralogical and Petrological Sciences, 13, 242-254.

Reiners, P.W., Farley, K.A., 2001. Influence of crystal size on apatite (U-Th)/He thermochronology: an example from the Bighorn Mountains, Wyoming. Earth and Planetary Science Letters, 188, 413-420.

Reiners, P.W., Spell, T.L., Nicolescu, S., and Zanetti, K., 2004, Zircon (U-Th)/He thermochronometry: He diffusion and comparisons with $^{40}Ar/^{39}Ar$ dating. Geochimica et Cosmochimica Acta, 68, 1857-1887.

Reiners, P.W., 2005. Zircon (U-Th)/He Thermochronometry. Reviews in Mineralogy & Geochemistry, 58, 151-179.

Reiners, P.W., Brandon, M.T., 2006. Using Thermochronology to understand Orogenic erosion. Annual Reviews in Earth and Planetary Science, 34, 419-466.

Robert, X., van der Beek, P., Braun, J., Perry, C., Dubille, M., Mugnier, J.-L., 2009. Assessing Quaternary reactivation of the Main Central thrust zone (central Nepal Himalaya): New thermochronological data and numerical modelling. Geology, 37, 731-734.

Rowley, D.B., Pierrehumbert, R.T., Currie, B.S., 2001. A new approach to stable isotope-based paleoaltimetry: Implications for paleoaltimetry and paleohypsometry of the High Himalaya since the late Miocene. Earth and Planetary Science Letters, 188, 253-268.

Rowley, D.B., Currie, B.S., 2006. Paleo-altimetry of the late Eocene to Miocene Lunpola basin, central Tibet. Nature, 439, 677-681.

Sachan, H.K., Mukhrjee, B.K., Ogasawara, Y., Maruyama, S., Ishida, H., Muko, A., Yoshioka, N., 2004. Discovery of coesite from the Indus Suture Zone (ISZ), Ladakh, India: Evidence for deep subduction. European Journal of Mineralogy, 16, 235-240.

Schilling, J.G., Zajac, M., Evans, R., Johnston, T., White, W., Devine, J.D., Kingsley, R., 1983. Petrologic and geochemical variations along the Mid-Atlantic Ridge from 27 N to 73 N. American Journal of Science, 283, 510-586.

Schlup, M., Carter, A., Cosca, M., Steck, A., 2003. Exhumation history of eastern Ladakh revealed by $^{40}Ar/^{39}Ar$ and fission-track ages: the Indus River-Tso Morari transect, NW Himalaya. Journal of the Geological Society, London, 160, 385-399.

Schneider, D.A., Zeitler, P.K., Kidd, W.S.F., Edwards, M.A., 2001. Geochronologic constraints on the tectonic evolution of Nanga Parbat, Western Himalaya Syntaxis, Revisted. The Journal of Geology, 109, 563-583.

Scott, D.J., St-Onge, M.R., 1995. Constraints on Pb closure temperature in titanite based on rocks from the Ungava orogen, Canada: Implications for U-Pb geochronology and P-T-t path determinations. Geology, 23, 1123-1126.

Searle, M.P., Godin, L., 2003. The South Tibetan Detachment and the Manasula leucogranite: a structural reinterpretation and restoration of the Annapurna-Manasula Himalaya, Nepal. The Journal of Geology, 111, 505-523.

Sherlock, S., Arnaud, N., 1998. Argon geochronology and phengites: a story of excess argon, diagrams and paradoxes. Goldschmidt Conference Toulouse, Abstract, 1379-1380.

Shervais, J.W., 1982. Ti–V plots and the petrogenesis of modern and ophiolitic lavas. Earth and Planetary Science Letters, 59,101-118.

Sláma, J., Košler, J., Condon, D.J., Crowley, J.L., Gerdes, A., Hanchar, J.M., Horstwood, M.S.A., Morris, G.A., Nasdala, L., Norberg, N., Schaltegger, U., Schoene, B., Tubrett, M.N., Whitehouse, M.J., 2008. Plešovice zircon–A new natural reference material for U–Pb and Hf isotopic microanalysis. Chemical Geology, 249, 1-35.

Smith, H.A., Chamberlain, C.P., Zeitler, P.K., 1994. Timing and duration of Himalayan metamorphism within the Indian plate, northwest Himalaya, Pakistan. The Journal of Geology, 102, 493-508.

Sobel, E.R., Strecker, M.R., 2003. Uplift, exhumation and precipitation: tectonic and climatic control of Late Cenozoic landscape evolution in the northern Sierras Pampeanas, Argentina. Basin Research, 15, 431-451.

Sobel, E.R., Seward, D., 2010. Influence of etching conditions on apatite fission-track etch pit diameter. Chemical Geology, doi: 10.1016/j.chemgeo.2009.12.012

Spandler, C., Hermann, J., 2006. High-pressure veins in eclogite from New Caledonia and their significance for fluid migration in subduction zones. Lithos, 89, 135-153.

Spear, F.S., 1988. Metamorphic fractional crystallization and internal metasomatism by diffusional homogenization of zoned garnets. Contribution to Mineralogy and Petrology, 99, 507-517.

Spencer, D.A., Ramsay, J.G., Pognante, U., Ghazanfar, M., Chaudhry, M., 1991. The significance of eclogites in the Indian plate, NW Himalayas, Geologie Alpine, Memoire HS, 16, 85.

Spencer, D.A., Tonarini, S., Pognante, U., 1995. Geochemical and Sr-Nd isotopic characterisation of Higher Himalayan eclogites (and associated metabasites). European Journal of Mineralogy, 7, 89- 102.

Spencer, D.A., Gebauer, D., 1996 SHRIMP evidence for a permian protolith age and a 44 Ma metamorphic age fort he Himalayan eclogites (Upper Kaghan, Pakistan): implications for the subduction of Tethys and the subdivision terminology of the NW Himalaya. 11th Himalaya-Karakorum-Tibet Workshop, 147.

Stockli, D.F., Farley, K.A., Dumitru, T.A., 2000. Calibration of the apatite (U-Th)/He thermochronometer on an exhumed fault block, White Mountains, California. Geology, 28, 983-986.

Stockli, D.F., 2005, Application of low-temperature thermochronometry to extensional tectonic settings. In: Reiners, P.W., Ehlers, T.A., (eds). Low-temperature thermochronology: Techniques, Interpretations, and Applications: Reviews in Mineralogy and Geochemistry, 58, 411-448.

Sudo, M., Uto, K., Anno, K., Ishizuka, O., Uchiumi, S., 1998. SORI93 biotite: A new mineral standard for K-Ar dating. Geochemical Journal, 32, 49-58.

Sun, S.-s., McDonough, W.F., 1989. Chemistry and isotopic systematic of ocean basalts: implications for mantle composition and processes. In: Saunders, A.D., Norry, M.J., (eds). Magmatism in the Ocean Basin. Geological Society, London, Special Publications, 42, 313-345.

Tagami, T., Farley, K.A., Stockli, D.F., 2003. (U-Th)/He geochronology of single zircon grains of known Tertiary eruption age. Earth and Planetary Science Letters, 207, 57-67.

Thiede, R.C., Bookhagen, B., Arrowsmith, J.R., Sobel, E.R., Strecker, M.R., 2004. Climatic control on rapid exhumation along the Southern Himalayan Front. Earth and Planetary Science Letters, 222, 791-806.

Thiede, R.C., Arrowsmith, J.R., Bookhagen, B., McWilliams, M.O., Sobel, E.R., Strecker, M.R., 2005. From tectonically to erosionally controlled development of the Himalayan orogen. Geology, 33, 689-692.

Thiede, R.C., Ehlers, T.A., Bookhagen, B., Strecker, M.R., 2009. Erosional variability along the northwest Himalaya. Journal of Geophysical Research, 114, F01015, doi: 10.1029/2008JF001010.

Tonarini, S., Villa, I.M., Oberli, F., Meier, M., Spencer, D.A., Pognante, U., Ramsay, J.G., 1993. Eocene age of eclogite metamorphism in Pakistan Himalaya: implications for India-Eurasia collision. Terra Nova, 5, 13-20.

Treloar, P.J., Williams, M.P., Coward, M.P., 1989. Metamorphism and crustal stacking in the North Indian Plate, North Pakistan. Tectonophysics, 165, 167-184.

Treloar, P.J., Broughton, R.D., Williams, M.P., Coward, M.P. Windley, B.F., 1989a. Deformation, metamorphism and imbrication of the Indian plate, south of the Main Mantle Thrust, north Pakistan. Journal of metamorphic Geology, 7, 111-125.

Treloar, P.J., Rex, D.C., 1990. Cooling and uplift of the crystalline thrust stack of the Indian Plate internal zones west of Nanga Parbat, Pakistan Himalaya. Tectonophysics, 180, 323-349.

Treloar, P.J., Coward, M.P., 1991. Indian Plate motion and shape: constrains on the geometry of the Himalayan orogen. Tectonophysics, 191, 189-198.

Treloar, P.J., Searle, M.P., (eds), 1993. Himalayan Tectonics. Geological Society, London, Special Publications, 74.

Treloar, P.J., O'Brien, P.J., Parrish, R.R., Khan, M.A., 2003. Exhumation of early Tertiary, coesite-bearing eclogites from the Pakistan Himalaya. Journal of the Geological Society, London, 160, 367-376.

Treloar, P.J., Vince, K.J., Law, R.D., 2007. Two-phase exhumatin of ultra high-pressure Indian Plate rocks from the Pakistan Himalaya. In: Ries, A.C., Butler, R.W.H., Graham, R.H., (eds). Deformation of the continental crust: The legacy of Mike Coward. Geological Society, London, Special Publications, 272, 155-185.

Uto, K., Ishizuka, O., Matsumoto, A., Kamioka, H., Togashi, S., 1997. Laser-heating $^{40}Ar/^{39}Ar$ dating system of the Geological Survey of Japan: System Outline and Priliminary Results. Bulletin of the Geological Survey of Japan, 48, 23-46.

van der Beek, P., VanMelle, J., Guillot, S., Pêcher, A., Reiners, P.W., Nicolescu, S., Latif, M., 2009. Eocene Tibetan plateau remnants preserved in the northwestern Himalaya. Nature Geoscience, 2, 364-368.

Verma, S.P., 2006. Extension-related origin of magmas from a garnet-bearing source in the Los Tuxtlas volcanic field. International Journal of Earth Science, 95, 871-901.

Villa, I.M., Grobéty, B., Kelley, S.P., Trigila, R., Wieler, R., 1996. Assessing Ar transport and mechanisms in the McClure Mountains hornblende. Contributions to Mineralogy and Petrology, 126, 67-80.

Villa, I.M., Ruggieri, G., Puxeddu, M., 1997. Petrological and geochronological discrimination of two white-mica generations in a granite cored from the Larderello-Tavale geothermal field (Italy). European Journal of Mineralogy, 9, 563-568.

Villa, I.M., 1998. Isotopic closure. Terra Nova, 10, 42-47.

Villa, I.M., Hermann, J., Müntener, O., Trommsdorff, V., 2000. $^{39}Ar/^{40}Ar$ dating of multiply zoned amphibole generations (Malenco, Italian Alps). Contributions to Mineralogy and Petrology, 140, 363-381.

Wadia, D.N., 1931. The syntaxis of the North-West Himalaya: Its rocks, tectonics and orogeny. Records of the Geological Survey of India, 65, 189-220.

Warren, C.J., Beaumont, C., Jamieson, R.A., 2008. Modelling tectonic styles and ultra-high pressure (UHP) rock exhumation during the transition from oceanic subduction to continental collision. Earth and Planetary Science Letters, 267, 129-145.

Whittington, A.G., 1996. Exhumation overrated at Nanga Parbat, northern Pakistan. Tectonophysics, 206, 215-226.

Wilke, F.D.H., O'Brien, P.J., Altenberger, U., Konrad-Schmolke, M., Khan, M.A., 2010. Multi-stage history in different eclogite types from the Pakistan Himalaya and implications for exhumation processes. Lithos, 114, 70-85.

Wilke, F.D.H., O'Brien, P.J., Gerdes, A., Timmerman, M.J., Sudo, M., Khan, M.A. The multistage exhumation history of the Kaghan Valley UHP series, NW Himalaya, Pakistan from U-Pb and $^{40}Ar/^{39}Ar$ ages. European Journal of Mineralogy, in review.

Winchester, J.A., Floyd, P.A., 1977. Geochemical discrimination of different magma series and their differentiation products using immobile elements. Chemical Geology, 20, 325-343.

Wolf, R.A., Farley, K.A., Kass, D.M., 1998. Modelling of the temperature sensitivity of the apatite (U-Th)/He thermochronometer. Chemical Geology, 148, 105-114.

York, D., 1969. Least square fitting of a straight line with correlated errors. Earth and Planetary Science Letters, 5, 320-324.

Zachos, J., Pagani, M., Sloan, L., Thomas, E., Billups, K., 2001. Trends, rhythms, and aberrations in global climate 65 Ma to present. Science, 292, 686-693.

Zeilinger, G., Seward, D., Burg, J.-P., 2007. Exhumation across the Indus Suture Zone: a record of back sliding of the hanging wall. Terra Nova, 19, 425-437.

Zeitler, P.K., Tahirkheli, R.A.K., Naeser, C.W., Johnson, N.M., 1982. Unroofing history of a suture zone in the Himalaya of Pakistan by means of fission track annealing ages. Earth and Planetary Science Letters, 57, 227-240.

Zeitler P.K., 1985. Cooling history of the NW Himalaya, Pakistan. Tectonics, 4, 127-151.

Zeitler, P.K., Meltzer, A.S., Koons, P.O., Craw, D., Hallet, B., Chamberlain, C.P., Kidd, W.S.F., Park, S.K., Seeber, L., Bishop, M., Shroder, J., 2001. Erosion, Himalayan geodynamics, and the geomorphology of metamorphism. Geological Society of America Today, 11, 4-9.

Zuleger, E., Erzinger, J., 1988. Determination of the REE and Y in silicate materials with ICP-AES. Fresenius Zeitschrift für Analytische Chemie, 332,140-43.

Appendix

Table A1. Sample Index with location and applied analyses

Table A2-7. Microprobe analysis

Analyses of minerals of a polished thin section were obtained using a 4 spectrometer Cameca SX100 electron microprobe at the GeoForschungsZentrum (GFZ) Potsdam operating at 15 kV and 20 nA with a 2-10 µm beam. Counting time were 10-30 s on peaks and half this on background. Synthetic and natural standards were used.

Table A8. Whole rock geochemistry

Analyses for major and trace elements were obtained using a Phillips PW-2400 X-ray fluorescence (XRF) spectrometer at the GeoForschungsZentrum Potsdam and the Geochemical Laboratory of the Institute of Geosciences in Mainz using internationally accepted rock standards yielding a determined precision better than 1–3% for major elements (depending on concentrations levels) and 2–3% for trace elements. The H_2O and CO_2 contents were analysed by quantitative high-temperature decomposition with an Elemental CHN analyser. Rare earth elements (REE) were determined by inductively coupled plasma–optical emission spectrometer (ICP-OES, Vista MPX) at the Geochemical Laboratory of the University of Potsdam. Sample preparation involved Na_2O_2 standard fusion and dilution techniques for dissolving rock powders into solution (Zuleger et al. 1988). Analytical precision was checked with international reference standards and found to be better than 12%.

Table A9. Ar-Ar analysis

Samples have been wrapped in aluminium foil, and placed in a sample capsule made of 5N (99.999% pure) aluminium. The sample capsule was wrapped in 0.5 mm thick cadmium foil and irradiated for 96 h in position 6 of the ICI (In Core Irradiation) system in the Geesthacht Neutron Facility (GeNF) at FRG-1, GKSS research centre at Geesthacht (Germany). The neutron flux variation over the length of the sample capsule was monitored by Fish Canyon Tuff Sanidine (FC3 sanidine) provided by the Geological Survey of Japan where an age of 27.5 Ma was determined (Uto et al., 1997, Ishizuka 1998; Ishizuka et al., 2002) that is consistent with that of 27.51 Ma obtained by first-principle measurements of K and radiogenic Ar by Lanphere &

Dalrymple (2000) and Lanphere & Baadsgaard (2001). The uncertainty in the *J* value is estimated at 0.4% based on 4 earlier irradiations. The $^{40}Ar/^{39}Ar$ analyses were performed at the argon geochronology laboratory of the University of Potsdam, which uses a New Wave laser ablation system with a 50 W CO_2 laser (wavelength 10.6 µm) for gas extraction. The gas fractions were extracted by heating the separates for 1 min with a continuous laser beam defocused to a diameter similar to that of the sample. The gas is purified for 10 min in an ultra-high vacuum line using SAES getters and a cold trap kept at ca. -100°C. After purification the argon gas is analysed using a Micromass 5400 noble gas mass spectrometer with a high sensitivity and an ultra-low background. The mass spectrometer is fitted with an electron multiplier pulse counting system suitable for analysing small amounts of argon. Blanks were run at the start of each session and after every three unknowns. For further details see chapter 3.5.

Table A10. Calculation of zeta

Zetas were calculated from three times repeated determinations of three apatite fission track standards of known age (Durango-, Fish Canyon Tuff- and Mount Dromedary Apatite). An overall weighted arithmetic mean with error (±1σ) was calculated that represents the solid horizontal lines in the diagram. Each result was displayed graphically, illustrating a consistent and reproducible fission track counting. The calibration baseline was therefore used to determine unknown ages.

Table A1. Sample Index

	sample	location	GPS	elvation [m]	map	secti	EMPA	WR	Ar-Ar	U-Pb	AFT	He
Field trip 2004 M. Ahmad Khan, Roland Oberhänsli, Robert Schmid, Paddy O'Brien												
K4	4	Saif-ul-Muluk	34°51,824 73°41,740	3186	as K3-3	x			x			
K4	21	N of Naran, W side KunharR	34°56,432 73°42,234		Fig. 3.1.	x	x		x			
K4	37	JakhadNar, Nuritop	34°55,814 74°03,746	3916	Fig. 3.1.	x	x		x			
K4	35	Jalkhadnar	34°59,220 74,01,020	3589	4.6 km ESE JNar2	x	x					
K4	53	Joranar, SE Burawai; all loose samples	34°53,354 73°54,057		as K4-60	x	x					
K4	57	Joranar, SE Burawai; all loose samples	34°53,354 73°54,057		Fig. 2.1.	x	x					
K4	58	Joranar, SE Burawai; all loose samples	34°53,354 73°54,057		Fig. 2.1.	x	x					
K4	60	Joranar, SE Burawai; all loose samples	34°53,354 73°54,057		Fig. 2.1.&3.1.&4.2.	x				x	x	x
K4	61				as K4-60	x			x			
K4	70	Joranar 2 rivers meet	34°52,774 73°55,004	3203	Fig. 3.1.&4.2.	x	x		x		x	
K4	71	Joranar 2 rivers meet	34°52,774 73°55,004	3203	Fig. 3.1.	x				x		
K4	76	Joranar 2 rivers meet	34°52,774 73°55,004	>3500	Fig. 2.1.	x	x					
K4	78	Jalkhad	35°00,134 73°55,872	3267	Fig. 3.1.	x				x		
K4	84	from basement block in Schutt	35°01,323 73°55,268	3810	Fig. 2.1.	x	x					
K4	86		35°01,219 73°56,303	3251	Fig. 2.1.	x						
K4	87	at the sharp bend,road Jalkhad-Besal			Fig. 2.1.	x						
K4	97	Purbinar Kaar	35°02,984 74°00,069	3612	Fig. 3.1.&4.2.	x	x		x		x	x
K4	98	Purbinar Kaar	35°02,984 74°00,069	3612	Fig. 2.1.	x	x					
K4	99	Purbinar Kaar	35°02,984 74°00,069	3612	Fig. 3.1.	x	x		x			
K4	100	Purbinar Kaar	35°02,984 74°00,069	3612	as K4-99			x				
K4	105	Gittidas Nala	35°05,066 73°57,797	3509	Fig. 2.1.	x	x	x				
K4	106	Saleh di Baihk several pieces	35°08,060 73°58,736	3667	Fig. 2.1.	x	x	(x)				
K4	117	Saleh Gali	35°07,508 73°57,145		as K4-120	x	x		x			
K4	118	4 pieces Saleh Gali	35°07,508 73°57,145		Fig. 4.2.	x	x		x		x	
K4	119	Saleh Gali	35°07,508 73°57,145		Fig. 3.1.	x	x		x			
K4	120a	Saleh Gali	35°07,508 73°57,145		Fig. 2.1.&4.2.	x	x				x	x
K4	120b	Saleh Gali	35°07,508 73°57,145		Fig. 2.1.	x	x	x	x			
K4	120c	Saleh Gali	35°07,508 73°57,145		Fig. 2.1.	x	x	x				
K4	120d	Saleh Gali	35°07,508 73°57,145		Fig. 2.1.	x	x		x			
Field trip 09/10 2003 Robert Schmid and Paddy O`Brien												
K3	3	ESE side of Saif ul Muluk, loose boulder at beach			Fig. 2.1.	x		(x)				
K3	7	half way of lake up the hill, in contact w. calcschists			Fig. 4.2.	x					x	
K3	11	road E of Jalkad to Kaschmir, second river from N 80m uphill,close Joranar			Fig. 2.1.	x	x	x				
K3	15	road E of Jalkad to Kaschmir, second river from N 80m uphill, country rock to eclogite			Fig. 4.2.	x					x	x
K3	26	Lake Lulusar			Fig. 3.1.&4.2.	x				x	x	x
K3	42	E-coast of Saif ul Muluk, loose piece			Fig. 4.2.	x					x	
K3	47	SW coast of Saif ul Muluk			Fig. 2.1.	x		(x)				
Field trip Pakistan (Kaghan Valley) samples collected by P.J. O´Brien and P. Treloar												
PK	2–4(a-g)	Gittidas Nala			Fig. 2.1.	x	x					
PKB	3(2x)				Fig. 2.1.	x		x				
PKL	1	Saleh di Baikh (unten)			as K4-106	2x	x	(x)				
PKL	2				as K4-106	2x	x					
PKL	3				as K4-106	2x		(x)				
JNar	2 3/4	Jakhad Nar			Fig. 2.1.	x	x					

(x) analyses made by PD Dr. Uwe Altenberger

Table A2. Microprobe analyses of garnet

Sample [Profile length in μm]	SiO_2	TiO_2	Al_2O_3	Cr_2O_3	FeO	MnO	MgO	CaO	Na_2O	Sum
K3-11,1grtProfil1 [240]	38.61	0.02	21.59	0.00	25.43	0.36	5.90	7.88	0.03	99.81
K3-11,1grtProfil1	38.46	0.09	21.54	0.00	24.69	0.35	5.94	8.53	0.06	99.66
K3-11,1grtProfil1	38.85	0.14	21.44	0.00	24.20	0.31	5.70	9.26	0.05	99.94
K3-11,1grtProfil1	38.81	0.13	21.48	0.00	23.43	0.38	5.25	10.18	0.03	99.69
K3-11,1grtProfil1	39.06	0.16	21.53	0.00	23.80	0.45	5.18	10.58	0.02	100.77
K3-11,1grtProfil1	38.73	0.02	21.38	0.00	25.28	0.46	5.77	8.56	0.00	100.19
K3-11,1grtProfil1	38.68	0.08	21.38	0.02	22.83	0.39	4.99	11.02	0.03	99.43
K3-11,1grtProfil1	38.50	0.06	21.37	0.00	22.60	0.39	4.72	11.97	0.05	99.66
K3-11,1grtProfil1	38.02	0.04	21.55	0.00	22.77	0.42	4.65	11.92	0.03	99.41
K3-11,1grtProfil1	38.73	0.07	21.59	0.05	22.81	0.42	4.66	11.72	0.03	100.07
K3-11,1grtProfil1	38.77	0.12	21.43	0.00	22.99	0.49	4.73	11.19	0.01	99.72
K3-11,1grtProfil1	39.07	0.13	21.30	0.03	22.78	0.55	4.39	11.66	0.02	99.92
K3-11,1grtProfil1	38.73	0.13	21.51	0.00	22.77	0.53	4.39	11.74	0.06	99.85
K3-11,1grtProfil1	38.63	0.06	21.51	0.01	23.35	0.36	5.05	10.47	0.03	99.47
K3-11,1grtProfil1	38.96	0.10	21.48	0.00	23.72	0.46	5.13	10.63	0.05	100.53
K3-11,1grtProfil1	38.68	0.09	21.42	0.00	23.46	0.46	5.17	10.73	0.02	100.02
K3-11,1grtProfil1	38.64	0.08	21.50	0.02	24.37	0.41	5.65	9.43	0.04	100.14
K3-11,1grtProfil1	38.71	0.06	21.50	0.02	24.74	0.41	6.13	8.10	0.02	99.68
K3-11,1grtProfil1	38.59	0.18	21.16	0.15	24.24	0.39	5.46	9.72	0.04	99.93
K3-11,1grtProfil1	38.40	0.27	21.19	0.20	24.05	0.44	5.77	9.11	0.05	99.48
K3-11,1grtProfil1	38.78	0.20	21.22	0.16	24.37	0.42	5.66	9.35	0.06	100.23
K3-11,1grtProfil1	38.90	0.06	21.50	0.04	25.28	0.43	6.09	8.25	0.02	100.56
K3-11,1grtProfil1	38.65	0.04	21.70	0.02	22.93	0.35	5.09	10.84	0.03	99.65
K3-11,1grtProfil2 [120]	38.81	0.04	21.55	0.00	24.83	0.42	5.96	7.80	0.04	99.45
K3-11,1grtProfil2	38.48	0.13	21.32	0.00	24.49	0.43	5.61	9.13	0.01	99.61
K3-11,1grtProfil2	38.66	0.16	21.23	0.01	24.12	0.41	5.40	9.91	0.06	99.97
K3-11,1grtProfil2	38.72	0.10	21.52	0.00	23.79	0.40	5.59	9.24	0.00	99.36
K3-11,1grtProfil2	39.11	0.13	21.23	0.06	21.69	0.37	5.07	11.36	0.22	99.24
K3-11,1grtProfil2	38.91	0.09	21.55	0.02	22.22	0.32	4.90	11.56	0.05	99.61
K3-11,1grtProfil2	38.66	0.12	21.30	0.04	23.65	0.36	5.36	10.05	0.04	99.57
K3-11,1grtProfil2	38.65	0.08	21.26	0.01	22.71	0.40	5.23	10.39	0.03	98.76
K3-11,1grtProfil2	38.51	0.14	21.31	0.06	23.52	0.41	5.25	10.18	0.01	99.38
K3-11,1grtProfil2	38.73	0.06	21.43	0.01	24.56	0.41	5.74	8.74	0.05	99.74
K3-11,1grtProfil2	38.78	0.11	21.22	0.02	23.85	0.40	5.58	9.53	0.01	99.49
K3-11,1grtProfil2	38.85	0.14	21.08	0.05	24.40	0.51	5.80	9.02	0.04	99.89
K3-11,2grtProfil1 [120]	38.64	0.17	21.47	0.00	24.55	0.37	5.44	8.98	0.07	99.71
K3-11,2grtProfil1	38.76	0.17	21.41	0.00	24.39	0.42	5.64	8.86	0.07	99.71
K3-11,2grtProfil1	38.53	0.15	21.39	0.00	24.69	0.40	5.54	8.95	0.05	99.69
K3-11,2grtProfil1	38.74	0.13	21.48	0.00	23.60	0.43	5.30	9.99	0.01	99.69
K3-11,2grtProfil1	38.65	0.13	21.58	0.00	23.81	0.37	5.06	10.34	0.04	99.97
K3-11,2grtProfil1	38.97	0.18	21.28	0.00	24.24	0.42	4.83	11.01	0.04	100.96
K3-11,2grtProfil1	38.83	0.12	21.35	0.01	24.02	0.40	5.02	10.42	0.04	100.21
K3-11,2grtProfil1	38.83	0.15	21.46	0.00	23.83	0.39	4.88	10.70	0.03	100.25
K3-11,2grtProfil1	38.86	0.11	21.51	0.00	23.85	0.34	5.08	10.50	0.06	100.30
K3-11,2grtProfil1	38.79	0.13	21.45	0.00	23.46	0.39	5.09	10.20	0.04	99.53
K3-11,2grtProfil1	38.91	0.06	21.61	0.02	25.16	0.34	5.85	8.49	0.04	100.47
K4-53,1GrtProfil1 [180]	39.17	0.04	21.34	0.02	21.74	0.42	4.86	11.88	0.01	99.46
K4-53,1GrtProfil1	38.96	0.04	21.32	0.04	21.48	0.38	4.96	11.46	0.03	98.66
K4-53,1GrtProfil1	39.11	0.03	21.24	0.02	21.83	0.40	4.91	11.85	0.03	99.40
K4-53,1GrtProfil1	39.25	0.03	21.52	0.05	22.37	0.39	4.97	11.95	0.00	100.51
K4-53,1GrtProfil1	39.01	0.06	21.28	0.01	21.23	0.35	5.02	12.61	0.01	99.56
K4-53,1GrtProfil1	39.07	0.07	21.34	0.02	20.72	0.29	4.92	12.87	0.01	99.31
K4-53,1GrtProfil1	39.10	0.07	21.32	0.05	20.54	0.31	4.83	13.19	0.06	99.46
K4-53,1GrtProfil1	39.23	0.07	21.30	0.00	21.02	0.36	4.74	13.31	0.00	100.02
K4-53,1GrtProfil1	39.26	0.07	21.38	0.01	21.45	0.40	4.79	13.44	0.03	100.81
K4-53,1GrtProfil1	39.30	0.06	21.32	0.01	20.83	0.27	4.81	13.73	0.04	100.37
K4-53,1GrtProfil1	38.95	0.07	21.33	0.00	20.70	0.28	4.76	13.54	0.02	99.65
K4-53,1GrtProfil1	39.14	0.06	21.38	0.02	20.59	0.32	4.76	13.44	0.01	99.73
K4-53,1GrtProfil1	39.05	0.04	21.55	0.03	21.23	0.35	4.83	13.42	0.01	100.50
K4-53,1GrtProfil1	39.14	0.05	21.46	0.00	22.17	0.36	4.94	13.78	0.00	101.89
K4-53,1GrtProfil1	39.08	0.07	21.42	0.00	21.97	0.38	5.05	13.44	0.05	101.46
K4-53,1GrtProfil1	38.91	0.05	21.34	0.01	22.71	0.45	4.52	13.15	0.02	101.15
K4-53,1GrtProfil1	39.03	0.02	21.37	0.09	23.82	0.75	4.15	12.54	0.06	101.82
K4-57,2GrtProfil1 [ca 70]	38.43	0.06	21.31	0.02	24.00	0.33	4.94	10.90	0.01	100.00
K4-57,2GrtProfil1	38.61	0.04	21.37	0.00	23.63	0.30	4.84	11.06	0.02	99.88
K4-57,2GrtProfil1	38.59	0.03	21.45	0.01	22.99	0.33	4.90	11.31	0.03	99.64
K4-57,2GrtProfil1	39.00	0.02	21.37	0.01	23.00	0.31	4.90	11.23	0.03	99.86
K4-57,2GrtProfil1	38.68	0.02	21.46	0.03	23.48	0.34	4.83	11.20	0.02	100.06
K4-57,2GrtProfil1	38.68	0.03	21.39	0.03	23.37	0.35	4.82	11.09	0.00	99.75
K4-57,2GrtProfil1	38.82	0.02	21.27	0.00	23.44	0.32	4.68	11.11	0.00	99.66
K4-57,2GrtInSymp1	38.53	0.03	21.21	0.00	22.25	0.28	4.37	12.36	0.01	99.02
K4-57,2GrtInSymp2	35.71	0.04	19.69	0.02	22.91	0.51	3.82	10.38	0.03	93.09
K4-57,1grtProfil1 [50]	38.78	0.02	21.45	0.01	25.58	0.28	5.52	7.84	0.03	99.51
K4-57,1grtProfil1	38.51	0.05	21.16	0.00	25.48	0.34	5.53	7.40	0.02	98.48

K4-57,1grtProfil1	38.38	0.04	21.12	0.06	26.07	0.26	5.57	7.63	0.00	99.12
K4-57,1grtProfil1	38.23	0.07	21.30	0.03	25.78	0.37	5.49	7.65	0.06	98.97
K4-57,1grtProfil1	38.57	0.06	21.36	0.03	25.81	0.31	5.50	7.65	0.04	99.32
K4-57,1grtProfil1	38.14	0.02	21.36	0.00	25.48	0.28	5.54	7.58	0.00	98.40
K4-57,1grtProfil1	38.83	0.00	21.26	0.00	25.31	0.29	5.52	7.50	0.04	98.74
K4-57,1grtProfil1	38.48	0.03	21.06	0.00	25.13	0.30	5.53	7.47	0.06	98.06
K4-57,1grtProfil1	38.49	0.04	21.12	0.00	25.63	0.29	5.45	7.66	0.03	98.70
K4-57,1grtProfil1	38.45	0.02	21.03	0.00	26.11	0.29	5.43	7.65	0.01	98.99
K4-57,1grtProfil1	38.34	0.01	21.12	0.00	25.68	0.30	5.44	7.70	0.02	98.61
K4-57,1grtProfil1	38.20	0.06	21.30	0.02	25.99	0.28	5.43	7.86	0.03	99.16
K4-57,1grtProfil1	38.12	0.06	21.11	0.00	25.64	0.28	5.47	7.74	0.02	98.44
K4-57,1grtProfil1	38.26	0.05	21.26	0.03	25.31	0.32	5.53	7.56	0.04	98.36
K4-57,1grtProfil1	38.47	0.04	21.14	0.01	25.66	0.30	5.45	7.78	0.00	98.84
K4-57,1grtProfil1	38.48	0.03	20.94	0.02	25.36	0.29	5.32	7.92	0.03	98.38
K4-57,1grtProfil1	38.72	0.04	21.20	0.02	25.89	0.32	5.49	7.53	0.03	99.23
K4-57,1grtProfil1	38.56	0.03	21.20	0.01	25.58	0.27	5.52	7.54	0.04	98.75
K4-57,1grtProfil1	38.70	0.05	21.33	0.02	26.03	0.24	5.48	7.47	0.02	99.35
K4-57,1grtProfil1	38.70	0.03	21.16	0.00	25.28	0.30	5.44	7.47	0.00	98.38
K4-57,1grtProfil1	38.55	0.02	21.41	0.00	25.20	0.26	5.62	7.22	0.03	98.30
K4-57,1grtProfil1	38.29	0.01	21.31	0.01	25.46	0.26	5.45	7.36	0.03	98.17
K4-57,1grtProfil1	38.69	0.02	21.21	0.00	25.53	0.24	5.46	7.59	0.02	98.75
K4-57,1grtProfil1	38.30	0.02	21.11	0.01	25.46	0.30	5.33	7.54	0.03	98.09
K4-57,1grtProfil1	38.42	0.02	21.06	0.00	25.48	0.27	5.36	7.56	0.01	98.16
K4-57,1grtProfil1	38.44	0.05	21.33	0.01	25.20	0.28	5.33	7.71	0.03	98.38
K4-57,1grtProfil1	38.53	0.03	21.16	0.03	25.45	0.28	5.36	7.82	0.01	98.66
K4-57,1grtProfil1	38.43	0.02	21.27	0.01	25.21	0.32	5.30	7.82	0.02	98.42
K4-57,1grtProfil1	38.58	0.04	21.36	0.02	25.00	0.34	5.30	8.10	0.01	98.75
K4-57,1grtProfil1	38.11	0.02	21.39	0.00	25.32	0.31	5.31	8.25	0.00	98.71
K4-57,1grtProfil1	38.18	0.03	21.15	0.00	25.50	0.31	5.18	8.27	0.07	98.68
K4-57,1grtProfil1	38.55	0.05	20.98	0.01	25.16	0.26	5.32	8.31	0.03	98.67
K4-57,1grtProfil1	38.36	0.01	20.93	0.00	24.88	0.25	5.37	8.20	0.03	98.02
K4-57,1grtProfil1	38.65	0.03	20.88	0.00	24.46	0.25	5.26	8.61	0.07	98.20
K4-57,1grtProfil1	38.79	0.04	21.11	0.00	25.06	0.27	5.38	8.52	0.01	99.18
K4-57,1grtProfil1	38.72	0.00	21.16	0.02	24.84	0.30	5.25	8.56	0.03	98.88
K4-57,1grtProfil1	38.25	0.04	21.11	0.00	24.71	0.31	5.03	8.89	0.00	98.34
K4-57,1grtProfil1	38.23	0.01	21.13	0.02	24.68	0.30	4.86	9.44	0.02	98.68
K4-57,1grtProfil1	38.21	0.04	21.26	0.03	24.34	0.26	4.78	9.64	0.00	98.58
K4-57,1grtProfil1	38.15	0.04	21.04	0.02	23.99	0.24	4.79	9.86	0.00	98.12
K4-57,1grtProfil1	38.56	0.02	21.35	0.01	23.98	0.29	4.82	9.85	0.04	98.91
K4-57,1grtProfil1	38.26	0.05	21.01	0.00	24.40	0.27	4.78	9.79	0.02	98.56
K4-57,1grtProfil1	38.40	0.04	21.11	0.00	23.75	0.25	4.86	9.48	0.04	97.92
K4-57,1grtProfil1	38.21	0.04	21.08	0.00	24.14	0.29	4.85	9.44	0.02	98.07
K4-57,1grtProfil1	38.17	0.04	21.41	0.00	24.58	0.25	4.82	9.51	0.04	98.83
K4-57,1grtProfil1	38.36	0.05	21.24	0.01	24.23	0.28	4.82	9.47	0.03	98.49
K4-57,1grtProfil1	38.27	0.06	21.21	0.00	24.25	0.26	4.89	9.54	0.00	98.49
K4-57,1grtProfil1	38.08	0.03	21.34	0.01	24.40	0.28	4.93	9.49	0.04	98.61
K4-57,1grtProfil1	38.38	0.03	21.32	0.00	24.35	0.27	4.86	9.50	0.00	98.71
K4-57,1grtProfil2 [250]	38.52	0.06	21.35	0.03	25.42	0.33	4.51	9.86	0.03	100.10
K4-57,1grtProfil2	38.32	0.10	21.15	0.02	26.02	0.29	5.23	8.34	0.04	99.51
K4-57,1grtProfil2	38.50	0.07	21.21	0.00	26.06	0.26	5.11	8.30	0.03	99.53
K4-57,1grtProfil2	38.82	0.05	21.43	0.02	25.14	0.34	4.95	9.06	0.03	99.84
K4-57,1grtProfil2	38.54	0.03	21.27	0.00	25.92	0.34	4.97	8.36	0.05	99.48
K4-57,1grtProfil2	38.81	0.03	21.24	0.00	22.36	0.24	4.22	12.61	0.00	99.51
K4-57,1grtProfil2	38.76	0.03	21.36	0.01	24.16	0.30	4.50	11.11	0.02	100.25
K4-57,1grtProfil2	38.85	0.03	21.38	0.02	23.10	0.24	4.15	12.44	0.01	100.21
K4-57,1grtProfil2	38.47	0.06	21.45	0.03	23.35	0.25	4.12	12.36	0.00	100.08
K4-57,1grtProfil2	38.66	0.02	21.46	0.00	24.61	0.28	4.47	10.62	0.00	100.13
K4-57,1grtProfil2	38.19	0.04	21.40	0.01	25.03	0.29	4.90	9.20	0.03	99.07
K4-57,1grtProfil2	38.43	0.02	21.39	0.03	25.51	0.34	4.67	9.04	0.00	99.44
K4-58,2Grt1	51.78	0.21	5.93	0.01	10.81	0.05	9.70	17.44	3.91	99.83
K4-58,2grtProfil1 [110]	38.00	0.08	21.06	0.00	27.81	0.44	4.84	6.92	0.02	99.17
K4-58,2grtProfil1	37.90	0.06	21.00	0.01	27.39	0.42	4.80	7.01	0.02	98.59
K4-58,2grtProfil1	37.84	0.07	20.86	0.00	27.62	0.44	4.80	6.91	0.04	98.57
K4-58,2grtProfil1	37.73	0.05	21.08	0.00	27.56	0.48	4.76	7.22	0.00	98.90
K4-58,2grtProfil1	37.88	0.07	20.90	0.01	27.93	0.42	4.81	7.01	0.01	99.04
K4-58,2grtProfil1	37.79	0.04	20.97	0.01	28.20	0.41	4.90	6.77	0.06	99.15
K4-58,2grtProfil1	38.02	0.09	21.08	0.00	28.13	0.40	4.83	6.25	0.03	98.81
K4-58,2grtProfil1	37.80	0.04	21.01	0.00	27.96	0.44	4.67	6.51	0.02	98.45
K4-58,2grtProfil1	52.46	0.14	7.68	0.04	10.69	0.06	8.46	15.25	5.27	100.05
K4-58,2grtProfil1	53.88	0.09	8.12	0.03	9.72	0.04	8.00	13.45	6.40	99.72
K4-58,2grtProfil3 [110]	37.92	0.05	20.92	0.02	27.12	0.41	4.79	7.18	0.01	98.41
K4-58,2grtProfil3	37.90	0.04	20.86	0.00	27.41	0.51	4.82	6.84	0.01	98.39
K4-58,2grtProfil3	37.61	0.06	21.07	0.00	27.75	0.49	4.93	7.03	0.05	98.98
K4-58,2grtProfil3	38.01	0.08	20.79	0.00	27.89	0.47	5.00	6.70	0.03	98.97
K4-58,2grtProfil3	37.87	0.04	21.09	0.00	27.81	0.53	4.74	6.69	0.01	98.77
K4-60grtProfil1 [230]	37.73	0.03	20.66	0.00	28.66	0.66	4.68	6.03	0.02	98.46

K4-60grtProfil1	38.16	0.06	20.82	0.00	29.17	0.70	4.70	6.20	0.01	99.80
K4-60grtProfil1	38.02	0.03	21.05	0.00	29.84	0.64	4.94	5.69	0.02	100.24
K4-60grtProfil1	38.21	0.01	20.97	0.00	29.34	0.60	5.16	4.86	0.03	99.18
K4-60grtProfil1	37.84	0.15	20.21	0.00	27.62	0.49	4.16	7.82	0.07	98.36
K4-60grtProfil1	38.04	0.09	20.54	0.01	28.61	0.59	4.23	7.47	0.03	99.61
K4-60grtProfil1	38.14	0.12	20.44	0.00	28.58	0.53	4.13	7.54	0.02	99.49
K4-60grtProfil1	38.38	0.09	20.33	0.00	27.93	0.50	4.18	7.78	0.07	99.26
K4-60grtProfil1	38.05	0.10	20.44	0.03	28.14	0.54	4.05	7.54	0.02	98.92
K4-60grtProfil1	38.22	0.08	20.80	0.01	29.34	0.56	4.17	7.53	0.00	100.71
K4-60grtProfil1	38.05	0.08	20.35	0.00	29.32	0.58	4.05	7.92	0.04	100.39
K4-60grtProfil1	38.01	0.11	20.56	0.00	28.75	0.52	4.08	7.83	0.06	99.91
K4-60grtProfil1	37.92	0.10	20.38	0.00	27.95	0.48	4.01	7.91	0.02	98.78
K4-60grtProfil1	37.98	0.14	20.46	0.02	27.52	0.42	4.08	7.82	0.05	98.49
K4-60grtProfil1	37.84	0.13	20.46	0.00	28.63	0.59	4.15	7.85	0.01	99.66
K4-60grtProfil1	38.03	0.12	20.46	0.00	29.80	0.63	4.07	7.79	0.04	100.94
K4-60grtProfil1	38.03	0.16	20.31	0.00	28.65	0.53	4.14	8.03	0.01	99.86
K4-60grtProfil1	38.17	0.11	20.40	0.00	27.58	0.54	4.13	7.86	0.02	98.80
K4-60grtProfil1	38.07	0.09	20.41	0.00	27.70	0.46	4.40	7.34	0.02	98.49
K4-60grtProfil1	38.28	0.02	21.00	0.00	28.56	0.61	4.68	6.67	0.01	99.82
K4-60grtProfil1	38.17	0.03	21.01	0.02	29.39	0.60	4.80	6.47	0.04	100.51
K4-60grtProfil1	38.28	0.04	20.94	0.02	29.50	0.72	4.94	5.94	0.02	100.38
K4-60grtProfil2 [130]	38.00	0.06	20.87	0.02	28.34	0.58	4.67	5.96	0.01	98.52
K4-60grtProfil2	38.11	0.00	20.87	0.00	28.67	0.63	4.83	5.87	0.03	99.00
K4-60grtProfil2	38.01	0.13	20.33	0.01	29.28	0.51	4.13	7.92	0.04	100.35
K4-60grtProfil2	38.02	0.14	20.22	0.00	28.83	0.57	4.09	8.05	0.04	99.95
K4-60grtProfil2	38.27	0.10	20.47	0.02	28.53	0.61	4.22	7.78	0.02	100.01
K4-60grtProfil2	38.03	0.11	20.38	0.03	27.81	0.54	4.15	8.04	0.05	99.13
K4-60grtProfil2	38.19	0.11	20.43	0.02	28.99	0.53	4.18	7.82	0.02	100.29
K4-60grtProfil2	38.54	0.10	20.44	0.00	28.21	0.59	4.38	7.79	0.21	100.24
K4-60grtProfil2	38.18	0.14	20.46	0.00	29.33	0.57	4.31	7.85	0.04	100.88
K4-60grtProfil2	37.97	0.13	20.62	0.04	28.51	0.57	4.31	7.55	0.04	99.72
K4-60grtProfil2	38.03	0.10	20.54	0.01	28.71	0.55	4.32	7.59	0.02	99.87
K4-60grtProfil2	38.07	0.12	20.45	0.00	28.39	0.60	4.56	7.45	0.06	99.69
K4-60grtProfil2	38.72	0.10	20.41	0.00	28.46	0.70	4.43	7.73	0.23	100.79
K4-60grt1	38.45	0.07	20.92	0.02	29.28	0.67	4.85	6.79	0.03	101.09
K4-60grt2	38.20	0.10	20.47	0.00	28.28	0.55	4.26	8.59	0.03	100.48
K4-76grtProf1 [180]	38.30	0.06	21.13	0.04	23.81	0.79	5.48	10.20	n.d.	99.83
K4-76grtProf1	37.98	0.28	20.93	0.06	24.34	0.74	5.61	10.24	n.d.	100.17
K4-76grtProf1	38.22	0.14	21.02	0.05	24.42	0.73	5.62	10.00	n.d.	100.19
K4-76grtProf1	38.07	0.03	21.44	0.02	24.43	0.66	6.18	9.02	n.d.	99.84
K4-76grtProf1	38.06	0.06	21.48	0.05	24.47	0.72	6.21	9.34	n.d.	100.37
K4-76grtProf1	38.49	0.04	21.54	0.08	24.16	0.70	6.13	9.29	n.d.	100.41
K4-76grtProf1	38.56	0.02	21.45	0.03	24.35	0.70	6.26	8.92	n.d.	100.29
K4-76grtProf1	38.52	0.01	21.52	0.01	24.47	0.71	6.42	8.44	n.d.	100.10
K4-76grtProf1	38.44	0.03	21.58	0.04	25.02	0.76	6.70	7.56	n.d.	100.12
K4-76grtProf1	38.40	0.04	21.55	0.02	25.34	0.69	6.52	7.97	n.d.	100.52
K4-76grtProf1	38.56	0.04	21.37	0.03	24.58	0.70	6.35	8.65	n.d.	100.26
K4-76grtProf1	38.61	0.02	21.47	0.06	24.46	0.66	6.15	9.08	n.d.	100.50
K4-76grtProf1	38.40	0.02	21.43	0.03	24.84	0.73	6.54	8.18	n.d.	100.16
K4-76grtProf1	38.42	0.02	21.46	0.04	24.71	0.65	6.35	8.47	n.d.	100.13
K4-76grtProf1	38.45	0.06	21.72	0.06	24.11	0.65	6.14	8.92	n.d.	100.11
K4-76grtProf1	37.95	0.05	21.25	0.03	24.54	0.68	6.04	9.33	n.d.	99.88
K4-76grtProf1	38.57	0.10	21.54	0.05	24.54	0.77	6.04	9.40	n.d.	100.99
K4-76grtProf1	38.43	0.08	21.50	0.01	24.35	0.79	5.89	9.27	n.d.	100.31
K4-76grtProf1	38.02	0.05	21.21	0.03	24.86	0.73	5.55	9.37	n.d.	99.83
K4-76,3GrtProf1 [430]	38.10	0.29	20.62	0.02	24.74	0.70	5.19	10.66	n.d.	100.32
K4-76,3GrtProf1	37.87	0.28	20.49	0.05	24.65	0.60	5.12	10.67	n.d.	99.72
K4-76,3GrtProf1	38.33	0.04	21.44	0.03	25.16	0.65	5.78	8.80	n.d.	100.23
K4-76,3GrtProf1	38.51	0.07	21.35	0.04	25.00	0.66	5.78	8.95	n.d.	100.36
K4-76,3GrtProf1	38.08	0.06	21.35	0.02	24.79	0.69	5.80	8.96	n.d.	99.74
K4-76,3GrtProf1	38.31	0.05	21.34	0.03	25.08	0.65	5.81	9.04	n.d.	100.30
K4-76,3GrtProf1	38.20	0.03	21.41	0.03	25.14	0.67	5.81	9.11	n.d.	100.39
K4-76,3GrtProf1	38.48	0.00	21.34	0.03	24.90	0.63	5.93	8.90	n.d.	100.21
K4-76,3GrtProf1	38.34	0.04	21.46	0.02	24.65	0.60	5.75	9.59	n.d.	100.46
K4-76,3GrtProf1	38.57	0.03	21.31	0.02	25.30	0.60	5.78	9.45	n.d.	101.06
K4-76,3GrtProf1	38.48	0.07	21.44	0.00	24.58	0.66	5.92	9.39	n.d.	100.54
K4-76,3GrtProf1	38.34	0.03	21.39	0.04	24.39	0.61	5.86	9.43	n.d.	100.09
K4-76,3GrtProf1	38.20	0.04	21.26	0.02	24.67	0.55	5.95	9.21	n.d.	99.89
K4-76,3GrtProf1	38.34	0.07	21.24	0.04	24.73	0.60	5.90	9.19	n.d.	100.09
K4-76,3GrtProf1	38.39	0.05	21.45	0.02	24.60	0.67	6.01	8.90	n.d.	100.09
K4-76,3GrtProf1	38.36	0.04	21.39	0.02	25.08	0.63	5.87	8.78	n.d.	100.17
K4-76,3GrtProf1	38.03	0.02	21.17	0.01	24.92	0.64	5.80	8.63	n.d.	99.21
K4-76,3GrtProf1	38.13	0.04	21.36	0.00	24.90	0.60	5.74	9.14	n.d.	99.92
K4-76,3GrtProf1	38.19	0.13	21.03	0.03	24.98	0.65	5.38	10.06	n.d.	100.45
K4-76,3GrtProf1	38.05	0.25	20.65	0.05	25.03	0.68	5.24	10.33	n.d.	100.28
K4-76,3GrtProf1	38.05	0.24	20.78	0.05	24.54	0.66	5.24	10.36	n.d.	99.93
K4-76,3GrtProf1	37.95	0.21	20.73	0.03	24.41	0.65	5.21	10.40	n.d.	99.58

K4-76,3GrtProf1	38.17	0.19	20.85	0.03	24.65	0.64	5.30	10.39	n.d.	100.20
K4-76,3GrtProf1	38.25	0.06	21.06	0.10	24.36	0.67	5.16	10.48	n.d.	100.13
K4-76,3GrtProf1	38.01	0.02	21.36	0.00	24.66	0.60	5.50	9.65	n.d.	99.79
K4-76,3GrtProf1	38.32	0.00	21.31	0.01	24.83	0.68	5.57	9.39	n.d.	100.12
K4-76,3GrtProf1	38.26	0.04	21.25	0.04	24.78	0.68	5.45	9.72	n.d.	100.21
K4-76,3GrtProf1	38.49	0.02	21.35	0.02	24.93	0.70	5.60	9.64	n.d.	100.75
K4-76,3GrtProf1	37.96	0.07	20.88	0.03	24.88	0.64	5.29	10.20	n.d.	99.93
K4-76,3GrtProf1	38.28	0.12	20.82	0.01	24.92	0.66	5.24	10.32	n.d.	100.37
K4-76,3GrtProf1	38.08	0.13	20.77	0.00	24.77	0.66	5.30	10.30	n.d.	100.01
K4-76,3GrtProf1	38.15	0.03	20.77	0.03	25.28	0.70	5.39	10.08	n.d.	100.43
K4-76,3GrtProf1	38.06	0.02	21.47	0.02	24.72	0.70	5.66	9.09	n.d.	99.72
K4-76,3GrtProf1	38.17	0.01	21.24	0.00	24.65	0.69	5.70	9.00	n.d.	99.46
K4-76,3GrtProf1	38.23	0.04	21.50	0.02	25.20	0.64	5.84	8.76	n.d.	100.23
K4-76,3GrtProf1	37.88	0.02	21.16	0.06	25.31	0.65	5.71	9.05	n.d.	99.84
K4-76,3GrtProf1	38.04	0.03	21.49	0.03	25.07	0.65	5.73	9.04	n.d.	100.08
K4-76,3GrtProf1	38.20	0.02	21.33	0.05	25.40	0.71	5.79	8.89	n.d.	100.39
K4-76,3GrtProf1	38.12	0.03	21.39	0.04	25.45	0.71	5.76	8.91	n.d.	100.39
K4-76,3GrtProf1	37.77	0.19	20.65	0.00	24.39	0.74	5.18	10.40	n.d.	99.32
K4-76,3GrtProf1	38.16	0.26	20.72	0.03	24.32	0.61	5.22	10.83	n.d.	100.14
K4-76,3GrtProf1	37.91	0.28	20.81	0.06	24.52	0.67	5.18	10.53	n.d.	99.95
K4-76,3GrtProf1	38.17	0.23	20.79	0.03	24.37	0.70	5.16	10.56	n.d.	100.02
K4-84,1Grt1	38.48	0.06	21.50	0.01	23.23	0.57	6.60	9.76	n.d.	100.20
K4-84,1Grt2	38.46	0.08	21.36	0.03	21.63	0.59	5.98	11.69	n.d.	99.82
K4-84,1Grt3	38.49	0.11	21.12	0.00	22.75	0.43	7.13	9.95	n.d.	99.99
K4-84,2GrtProfil [430]	38.87	0.04	21.48	0.02	18.94	0.42	6.57	13.49	n.d.	99.83
K4-84,2GrtProfil	38.70	0.05	21.43	0.02	19.01	0.39	6.38	13.75	n.d.	99.72
K4-84,2GrtProfil	38.61	0.02	21.32	0.00	22.39	0.44	7.43	9.16	n.d.	99.37
K4-84,2GrtProfil	38.52	0.06	21.29	0.03	23.86	0.59	7.57	8.23	n.d.	100.14
K4-84,2GrtProfil	38.54	0.09	21.14	0.00	24.12	0.47	6.86	8.74	n.d.	99.95
K4-84,2GrtProfil	38.53	0.10	21.06	0.02	24.48	0.54	6.20	9.16	n.d.	100.09
K4-84,2GrtProfil	37.95	0.15	20.89	0.00	25.44	0.50	5.31	9.41	n.d.	99.64
K4-84,2GrtProfil	37.84	0.13	20.59	0.00	26.54	0.49	4.74	9.41	n.d.	99.75
K4-84,2GrtProfil	37.80	0.15	20.55	0.00	26.79	0.38	4.36	9.49	n.d.	99.52
K4-84,2GrtProfil	37.40	0.14	20.48	0.03	26.42	0.40	3.94	9.72	n.d.	98.51
K4-84,2GrtProfil	37.50	0.13	20.51	0.00	26.84	0.58	3.70	10.00	n.d.	99.27
K4-84,2GrtProfil	37.49	0.16	20.23	0.00	26.85	0.55	3.45	10.34	n.d.	99.07
K4-84,2GrtProfil	37.67	0.15	20.34	0.01	27.41	0.63	3.26	10.72	n.d.	100.20
K4-84,2GrtProfil	37.65	0.18	20.30	0.01	26.74	0.78	3.20	10.74	n.d.	99.61
K4-84,2GrtProfil	37.31	0.16	20.36	0.04	26.99	0.78	2.99	10.73	n.d.	99.36
K4-84,2GrtProfil	37.73	0.12	20.20	0.03	27.68	0.80	2.78	10.57	n.d.	99.90
K4-84,2GrtProfil	37.40	0.12	20.31	0.02	27.27	0.81	2.88	10.50	n.d.	99.31
K4-84,2GrtProfil	37.43	0.11	20.30	0.02	26.88	0.80	3.41	10.63	n.d.	99.57
K4-84,2GrtProfil	37.87	0.14	20.50	0.03	25.61	0.79	3.99	10.84	n.d.	99.78
K4-84,2GrtProfil	37.42	0.10	20.17	0.02	27.26	0.74	2.81	10.64	n.d.	99.15
K4-84,2GrtProfil	37.30	0.10	20.27	0.02	28.32	0.94	2.19	10.54	n.d.	99.68
K4-84,2GrtProfil	37.34	0.11	20.20	0.04	28.28	0.88	1.95	10.65	n.d.	99.45
K4-84,2GrtProfil	37.08	0.10	20.10	0.01	28.08	0.88	1.90	10.53	n.d.	98.68
K4-84,2GrtProfil	37.14	0.13	20.40	0.02	28.15	0.75	1.99	10.78	n.d.	99.34
K4-84,2GrtProfil	37.25	0.14	20.24	0.04	27.86	0.68	2.21	10.67	n.d.	99.09
K4-84,2GrtProfil	37.30	0.13	20.06	0.03	27.52	0.54	2.49	10.64	n.d.	98.72
K4-84,2GrtProfil	37.40	0.17	20.12	0.03	28.00	0.60	2.69	10.24	n.d.	99.24
K4-84,2GrtProfil	37.42	0.17	20.16	0.02	28.05	0.53	3.00	10.34	n.d.	99.68
K4-84,2GrtProfil	37.42	0.15	20.53	0.04	27.50	0.49	3.23	10.02	n.d.	99.38
K4-84,2GrtProfil	37.48	0.15	20.55	0.03	27.47	0.48	3.57	9.78	n.d.	99.51
K4-84,2GrtProfil	37.98	0.15	20.59	0.03	26.70	0.43	4.38	9.76	n.d.	100.02
K4-84,2GrtProfil	37.90	0.10	20.76	0.01	25.40	0.46	4.97	9.61	n.d.	99.21
K4-84,2GrtProfil	38.31	0.11	20.80	0.01	25.39	0.50	6.36	8.77	n.d.	100.25
K4-84,2GrtProfil	38.48	0.05	20.99	0.00	24.48	0.47	6.31	8.72	n.d.	99.50
K4-84,2GrtProfil	38.36	0.09	21.05	0.02	24.28	0.50	6.63	8.75	n.d.	99.67
K4-84,2GrtProfil	38.78	0.01	21.54	0.05	23.65	0.54	6.58	9.65	n.d.	100.79
K4-84,2GrtProfil	38.79	0.02	21.44	0.03	23.47	0.47	7.05	8.92	n.d.	100.19
K4-84,2GrtProfil	38.69	0.01	21.48	0.00	23.64	0.54	7.29	8.49	n.d.	100.14
K4-84,2GrtProfil	38.57	0.03	21.41	0.00	22.84	0.48	7.04	9.68	n.d.	100.04
K4-84,2GrtProfil	38.71	0.02	21.48	0.04	22.53	0.53	7.34	9.18	n.d.	99.82
K4-84,2GrtProfil	38.67	0.01	21.69	0.03	23.28	0.52	7.17	9.21	n.d.	100.59
K4-84,2GrtProfil	39.09	0.05	21.52	0.05	18.87	0.37	6.58	14.08	n.d.	100.60
K4-982_2,1GrtProfil1 [60]	38.98	0.05	21.79	0.07	21.60	0.35	9.26	7.79	n.d.	99.89
K4-982_2,1GrtProfil1	38.50	0.04	21.93	0.14	22.21	0.36	9.20	7.92	n.d.	100.31
K4-982_2,1GrtProfil1	38.97	0.01	21.61	0.11	21.43	0.40	9.21	8.14	n.d.	99.88
K4-982_2,1GrtProfil1	38.70	0.03	21.95	0.06	21.85	0.35	9.88	7.06	n.d.	99.88
K4-982_2,1GrtProfil1	38.92	0.04	21.85	0.04	21.82	0.38	10.07	7.24	n.d.	100.35
K4-982_2,1GrtProfil1	39.22	0.04	21.79	0.05	21.88	0.39	9.48	7.38	n.d.	100.24
K4-982_2,2GrtProfil1 [60]	39.34	0.03	21.65	0.06	20.62	0.36	9.45	8.37	n.d.	99.89
K4-982_2,2GrtProfil1	39.52	0.05	21.82	0.07	19.18	0.28	10.68	8.40	n.d.	99.99
K4-982_2,2GrtProfil1	39.61	0.05	22.03	0.06	19.32	0.31	11.01	8.22	n.d.	100.61
K4-982_2,2GrtProfil1	39.71	0.06	21.99	0.05	19.39	0.26	10.91	8.30	n.d.	100.67

K4-982_2,2GrtProfil1	39.51	0.03	21.71	0.04	19.99	0.34	10.04	8.52	n.d.	100.18
K4-982_2,2GrtProfil1	39.09	0.03	21.71	0.04	21.23	0.40	9.08	8.27	n.d.	99.84
K4-981_2,1GrtProfil [70]	39.16	0.04	21.62	0.06	21.70	0.37	8.97	8.16	n.d.	100.09
K4-981_2,1GrtProfil	39.00	0.02	21.57	0.05	21.45	0.43	9.34	8.01	n.d.	99.87
K4-981_2,1GrtProfil	39.26	0.04	21.82	0.02	21.39	0.39	9.65	7.97	n.d.	100.54
K4-981_2,1GrtProfil	39.34	0.01	21.78	0.04	20.22	0.33	10.36	7.82	n.d.	99.91
K4-981_2,1GrtProfil	39.40	0.03	21.82	0.05	19.92	0.28	10.82	7.67	n.d.	99.98
K4-981_2,1GrtProfil	39.42	0.04	21.71	0.01	19.58	0.30	10.67	8.29	n.d.	100.02
K4-981_2,1GrtProfil	39.29	0.06	21.74	0.04	20.49	0.31	10.08	8.08	n.d.	100.09
K4-99,1GrtProfil1 [70]	38.03	0.06	20.30	0.03	24.35	0.42	3.85	11.74	n.d.	98.78
K4-99,1GrtProfil1	37.99	0.06	20.89	0.02	25.23	0.44	3.79	11.34	n.d.	99.75
K4-99,1GrtProfil1	38.01	0.13	20.51	0.02	26.03	0.49	3.98	10.86	n.d.	100.04
K4-99,1GrtProfil1	37.83	0.12	20.43	0.05	25.78	0.53	3.99	10.93	n.d.	99.65
K4-99,1GrtProfil1	38.14	0.13	20.46	0.05	25.32	0.49	3.84	11.49	n.d.	99.91
K4-99,1GrtProfil1	37.86	0.15	20.49	0.03	26.09	0.44	4.33	10.33	n.d.	99.71
K4-99/2Grt1	38.46	0.12	21.11	0.00	22.34	0.42	4.26	11.90	0.05	98.67
K4-99/2Grt2	38.56	0.08	21.05	0.00	22.09	0.33	3.82	12.96	0.03	98.92
K4-99/2Grt3	38.64	0.06	21.27	0.01	21.50	0.35	3.45	14.09	0.04	99.41
K4-99/2Grt4	38.58	0.04	21.38	0.01	21.37	0.29	3.48	14.20	0.02	99.37
K4-99/1Grt1	38.53	0.06	21.13	0.00	23.62	0.34	4.38	10.90	0.03	98.99
K4-99/1Grt2	38.17	0.08	20.97	0.00	25.47	0.45	3.92	9.89	0.03	98.98
K4-99/1Grt3	38.43	0.05	21.26	0.03	23.80	0.38	3.62	11.65	0.02	99.24
K4-105_1GrtProfil1 [100]	38.46	0.05	21.32	0.04	22.11	0.52	6.82	10.08	n.d.	99.39
K4-105_1GrtProfil1	38.90	0.02	21.43	0.04	20.75	0.40	7.45	10.40	n.d.	99.37
K4-105_1GrtProfil1	38.84	0.08	21.21	0.02	19.91	0.42	7.59	10.23	n.d.	98.30
K4-105_1GrtProfil1	39.03	0.04	21.38	0.05	20.91	0.44	7.74	9.99	n.d.	99.58
K4-105_1GrtProfil1	38.80	0.03	21.39	0.02	22.32	0.56	7.75	8.68	n.d.	99.55
K4-105_1GrtProfil1	38.49	0.02	21.58	0.04	22.90	0.58	7.69	7.79	n.d.	99.11
K4-105_1GrtProfil1	38.71	0.02	21.34	0.02	23.08	0.68	7.26	8.22	n.d.	99.33
K4-105_1GrtProfil1	38.58	0.07	21.23	0.03	21.63	0.60	6.61	10.54	n.d.	99.28
K4-105_1GrtProfil1	38.49	0.04	21.14	0.03	20.86	0.42	6.72	11.18	n.d.	98.87
K4-105_1GrtProfil1	38.82	0.04	21.45	0.03	23.04	0.52	8.26	7.34	n.d.	99.50
K4-106/1GrtProfil1 [220]	37.72	0.05	21.33	0.03	26.09	0.53	4.80	8.38	0.03	98.96
K4-106/1GrtProfil1	37.68	0.07	21.20	0.00	26.59	0.53	5.15	7.59	0.04	98.84
K4-106/1GrtProfil1	37.89	0.15	20.71	0.00	26.43	0.58	4.97	8.25	0.05	99.03
K4-106/1GrtProfil1	38.16	0.17	20.58	0.03	26.47	0.54	4.95	8.64	0.06	99.60
K4-106/1GrtProfil1	37.98	0.16	20.72	0.00	26.24	0.60	4.86	8.81	0.06	99.42
K4-106/1GrtProfil1	38.12	0.17	20.77	0.00	26.08	0.68	4.89	8.98	0.07	99.75
K4-106/1GrtProfil1	38.27	0.13	21.01	0.00	26.14	0.70	4.84	8.63	0.06	99.76
K4-106/1GrtProfil1	37.89	0.13	20.71	0.00	25.51	0.81	4.55	9.47	0.05	99.13
K4-106/1GrtProfil1	37.57	0.17	20.63	0.00	25.97	0.83	4.50	9.57	0.06	99.30
K4-106/1GrtProfil1	38.26	0.13	20.56	0.01	25.50	0.90	4.37	10.04	0.04	99.80
K4-106/1GrtProfil1	37.96	0.19	20.49	0.00	25.16	0.87	4.20	10.29	0.03	99.19
K4-106/1GrtProfil1	37.64	0.16	20.17	0.05	25.83	1.21	3.71	10.35	0.01	99.12
K4-106/1GrtProfil1	37.42	0.18	20.30	0.00	25.21	1.00	3.94	10.43	0.04	98.51
K4-106/1GrtProfil1	38.10	0.09	21.12	0.03	24.78	0.83	4.26	10.72	0.03	99.97
K4-118/1GrtProfil1 [520]	37.89	0.08	20.46	0.00	26.92	0.33	3.05	9.67	0.03	98.44
K4-118/1GrtProfil1	37.86	0.04	20.35	0.01	27.17	0.42	2.97	9.82	0.04	98.68
K4-118/1GrtProfil1	37.47	0.08	19.98	0.04	28.34	1.09	1.82	9.88	0.02	98.71
K4-118/1GrtProfil1	37.58	0.10	20.24	0.01	27.12	0.41	2.94	10.14	0.03	98.56
K4-118/1GrtProfil1	37.75	0.09	20.16	0.00	27.04	0.41	2.97	9.98	0.06	98.45
K4-118/1GrtProfil1	37.63	0.10	20.25	0.03	27.31	0.35	3.07	9.80	0.05	98.58
K4-118/1GrtProfil1	37.54	0.11	20.18	0.02	27.57	0.62	2.29	10.04	0.03	98.40
K4-118/1GrtProfil1	37.61	0.11	19.95	0.01	26.72	0.45	2.59	10.59	0.02	98.05
K4-118/1GrtProfil1	37.70	0.07	20.20	0.02	25.80	0.32	2.79	11.28	0.02	98.20
K4-118/1GrtProfil1	37.65	0.07	20.33	0.02	25.99	0.35	2.84	11.06	0.06	98.37
K4-118/1GrtProfil1	37.96	0.08	20.50	0.01	26.27	0.33	2.84	10.90	0.03	98.92
K4-118/1GrtProfil1	37.88	0.04	20.57	0.02	26.47	0.40	2.87	10.74	0.02	99.00
K4-118/1GrtProfil1	38.05	0.04	20.67	0.03	27.00	0.39	3.03	10.14	0.03	99.38
K4-118/1GrtProfil1	37.62	0.08	20.48	0.01	28.14	0.43	3.17	8.76	0.06	98.74
K4-118/1GrtProfil1	37.82	0.11	20.21	0.02	28.44	0.34	3.10	9.03	0.05	99.10
K4-118/1GrtProfil1	37.67	0.22	19.87	0.03	27.63	0.32	2.98	9.58	0.03	98.33
K4-118/1GrtProfil1	37.71	0.05	20.31	0.01	27.71	0.46	3.05	9.43	0.02	98.74
K4-118/1GrtProfil1	37.60	0.02	20.38	0.02	28.17	0.46	3.11	8.88	0.03	98.68
K4-118/1GrtProfil1	37.51	0.06	20.34	0.00	27.60	0.56	3.09	9.12	0.03	98.30
K4-118/1GrtProfil1	37.63	0.11	20.37	0.01	29.28	0.69	3.07	7.89	0.01	99.05
K4-118/1GrtProfil1	37.51	0.12	20.37	0.00	28.97	0.61	3.23	7.85	0.07	98.72
K4-118/1GrtProfil1	37.70	0.21	20.46	0.04	28.52	0.60	3.15	8.33	0.04	99.04
K4-118/1GrtProfil1	37.80	0.13	20.49	0.01	28.15	0.64	3.24	8.24	0.02	98.70
K4-118/1GrtProfil1	37.46	0.17	20.54	0.03	28.93	0.58	3.37	7.67	0.04	98.79
K4-118/1GrtProfil1	37.71	0.20	20.40	0.00	28.22	0.55	3.24	8.09	0.04	98.44
K4-118/1GrtProfil1	37.49	0.12	20.40	0.05	28.59	0.59	3.22	7.78	0.05	98.29
K4-118/1GrtProfil1	37.55	0.09	20.18	0.00	28.46	0.59	3.18	8.12	0.04	98.21
K4-118/2GrtProfil1 [400]	37.37	0.09	19.96	0.03	28.69	0.33	3.01	9.08	0.05	98.60

K4-118/2GrtProfil1	37.24	0.10	20.07	0.02	29.33	0.27	2.65	8.81	0.04	98.52
K4-118/2GrtProfil1	37.52	0.12	19.96	0.01	29.24	0.28	2.57	8.96	0.03	98.68
K4-118/2GrtProfil1	37.48	0.07	19.84	0.00	28.98	0.33	2.55	8.95	0.05	98.25
K4-118/2GrtProfil1	37.32	0.07	19.99	0.02	28.73	0.25	2.63	9.13	0.04	98.17
K4-118/2GrtProfil1	37.20	0.09	20.12	0.00	28.42	0.33	2.77	9.39	0.06	98.37
K4-118/2GrtProfil1	37.48	0.03	20.27	0.00	27.52	0.34	2.98	9.85	0.03	98.50
K4-118/2GrtProfil1	37.72	0.07	20.24	0.02	27.30	0.33	2.98	9.87	0.02	98.55
K4-118/2GrtProfil1	37.29	0.02	20.27	0.02	27.12	0.35	2.94	10.21	0.04	98.27
K4-118/2GrtProfil1	38.01	0.02	20.66	0.00	26.35	0.31	2.88	10.83	0.04	99.11
K4-118/2GrtProfil1	37.63	0.04	20.66	0.01	26.18	0.29	2.86	10.84	0.02	98.53
K4-118/2GrtProfil1	37.59	0.05	20.70	0.02	25.96	0.27	2.80	11.17	0.04	98.59
K4-118/2GrtProfil1	37.62	0.06	20.51	0.00	26.22	0.37	2.79	10.85	0.01	98.44
K4-118/2GrtProfil1	37.41	0.07	20.29	0.00	26.65	0.34	2.84	10.63	0.01	98.24
K4-118/2GrtProfil1	37.70	0.06	20.26	0.02	27.03	0.39	2.86	10.45	0.03	98.78
K4-118/2GrtProfil1	37.84	0.05	20.23	0.01	26.97	0.35	2.91	10.31	0.04	98.70
K4-118/2GrtProfil1	37.90	0.04	20.24	0.02	26.27	0.38	2.84	11.06	0.02	98.77
K4-118/2GrtProfil1	38.02	0.04	20.38	0.00	25.91	0.40	2.78	11.39	0.04	98.96
K4-118/2GrtProfil1	37.70	0.07	20.33	0.04	25.73	0.35	2.77	11.34	0.04	98.37
K4-118/2GrtProfil1	37.90	0.05	20.39	0.01	25.98	0.39	2.65	11.25	0.04	98.65
K4-118/2GrtProfil1	38.11	0.06	20.21	0.00	26.53	0.37	2.63	11.35	0.04	99.30
K4-118/2GrtProfil1	37.67	0.06	20.31	0.00	26.63	0.35	2.79	10.96	0.05	98.82
K4-118/2GrtProfil1	37.79	0.07	20.15	0.00	26.48	0.36	2.76	11.04	0.04	98.68
K4-118/2GrtProfil1	38.00	0.06	20.13	0.02	26.89	0.36	2.76	11.01	0.03	99.26
K4-118/2GrtProfil1	37.70	0.06	20.42	0.01	26.44	0.33	2.81	10.91	0.04	98.73
K4-118/2GrtProfil1	37.70	0.04	20.37	0.01	26.63	0.32	2.82	10.80	0.03	98.70
K4-118/2GrtProfil1	37.52	0.06	20.24	0.00	26.89	0.36	2.73	10.64	0.04	98.47
K4-118/2GrtProfil1	37.82	0.06	20.23	0.02	26.95	0.33	2.95	10.31	0.05	98.72
K4-118/2GrtProfil1	38.01	0.05	20.49	0.00	26.78	0.34	2.91	10.31	0.04	98.93
K4-118/2GrtProfil1	38.22	0.04	20.37	0.01	27.74	0.79	1.87	9.66	0.01	98.71
K4-118b2GrtProfil1 [1000]	38.04	0.06	20.32	0.00	26.97	0.54	2.95	9.92	0.04	98.83
K4-118b2GrtProfil1	37.89	0.07	20.35	0.01	26.91	0.55	2.93	10.16	0.03	98.90
K4-118b2GrtProfil1	37.78	0.05	20.40	0.00	26.46	0.58	2.87	10.30	0.03	98.48
K4-118b2GrtProfil1	38.11	0.05	20.27	0.03	26.25	0.53	2.70	11.11	0.01	99.06
K4-118b2GrtProfil1	37.92	0.05	20.33	0.02	26.59	0.50	2.73	11.04	0.05	99.22
K4-118b2GrtProfil1	38.02	0.04	20.70	0.05	26.19	0.53	2.80	11.12	0.02	99.45
K4-118b2GrtProfil1	38.11	0.03	20.99	0.03	25.51	0.37	2.80	11.46	0.02	99.32
K4-118b2GrtProfil1	37.99	0.05	21.02	0.02	26.17	0.52	2.81	10.75	0.01	99.34
K4-118b2GrtProfil1	38.07	0.06	21.09	0.00	26.37	0.46	2.90	10.21	0.04	99.20
K4-118b2GrtProfil1	37.90	0.07	21.07	0.01	27.34	0.61	3.12	9.00	0.05	99.17
K4-118b2GrtProfil1	37.87	0.02	20.88	0.03	27.84	0.51	3.21	8.36	0.02	98.75
K4-118b2GrtProfil1	38.06	0.02	21.07	0.02	28.28	0.63	3.32	7.99	0.02	99.40
K4-118b2GrtProfil1	37.79	0.06	21.11	0.00	28.14	0.50	3.30	8.47	0.02	99.39
K4-118b2GrtProfil1	37.92	0.04	21.14	0.00	28.66	0.54	3.32	8.04	0.04	99.69
K4-118b2GrtProfil1	37.80	0.04	21.00	0.00	27.56	0.46	3.08	9.09	0.04	99.06
K4-118b2GrtProfil1	37.84	0.02	20.91	0.00	27.98	0.47	3.22	8.48	0.03	98.95
K4-118b2GrtProfil1	37.75	0.04	20.90	0.01	28.01	0.50	3.12	8.68	0.05	99.06
K4-118b2GrtProfil1	37.70	0.03	20.91	0.03	27.79	0.53	3.14	8.88	0.04	99.04
K4-118b2GrtProfil1	37.77	0.07	20.78	0.00	27.92	0.45	3.06	8.89	0.05	98.99
K4-118b2GrtProfil1	37.85	0.07	20.85	0.00	28.08	0.56	3.07	9.00	0.03	99.52
K4-118b2GrtProfil1	38.01	0.07	20.68	0.01	27.58	0.47	2.99	9.32	0.05	99.17
K4-118b2GrtProfil1	37.82	0.08	20.57	0.04	27.82	0.48	3.00	9.30	0.05	99.17
K4-118b2GrtProfil1	37.86	0.10	20.57	0.04	27.83	0.53	2.99	9.24	0.05	99.20
K4-118b2GrtProfil1	37.83	0.12	20.46	0.01	27.34	0.42	2.95	9.57	0.02	98.72
K4-118b2GrtProfil1	37.87	0.13	20.33	0.06	28.22	0.51	2.83	9.49	0.06	99.50
K4-118b2GrtProfil1	37.54	0.12	20.14	0.00	28.54	0.46	2.70	9.41	0.07	98.96
K4-118b2GrtProfil1	37.57	0.14	20.01	0.04	28.81	0.42	2.50	9.48	0.05	99.01
K4-118b2GrtProfil1	37.40	0.15	19.92	0.01	28.87	0.42	2.46	9.22	0.04	98.48
K4-118b2GrtProfil1	37.80	0.15	20.05	0.04	28.79	0.37	2.45	9.43	0.05	99.12
K4-118b2GrtProfil1	37.51	0.14	19.92	0.03	28.70	0.36	2.41	9.42	0.03	98.52
K4-118b2GrtProfil1	37.55	0.14	19.92	0.00	29.16	0.33	2.43	9.35	0.02	98.90
K4-118b2GrtProfil1	37.66	0.16	19.97	0.00	29.02	0.40	2.45	9.44	0.07	99.17
K4-118b2GrtProfil1	37.47	0.17	20.02	0.00	28.97	0.36	2.37	9.49	0.06	98.88
K4-118b2GrtProfil1	37.45	0.16	19.92	0.00	28.90	0.38	2.38	9.68	0.08	98.95
K4-118b2GrtProfil1	37.53	0.17	19.80	0.00	28.85	0.40	2.41	9.75	0.04	98.94
K4-118b2GrtProfil1	37.51	0.20	19.93	0.00	28.88	0.39	2.38	9.60	0.07	98.96
K4-118b2GrtProfil1	37.54	0.23	19.30	0.02	29.09	0.33	2.37	9.88	0.07	98.83
K4-118b2GrtProfil1	37.79	0.22	19.76	0.02	28.00	0.48	2.62	9.97	0.08	98.95
K4-118b2GrtProfil1	37.52	0.18	19.65	0.01	27.85	0.35	2.66	10.45	0.07	98.76
K4-118b2GrtProfil1	37.58	0.17	19.68	0.00	27.82	0.44	2.64	10.39	0.07	98.79
K4-118b2GrtProfil1	37.67	0.22	19.57	0.00	27.64	0.48	2.82	10.43	0.06	98.89
K4-118b2GrtProfil1	38.02	0.21	19.77	0.00	27.54	0.53	2.75	10.36	0.07	99.24
K4-118b2GrtProfil1	37.94	0.19	19.74	0.02	27.60	0.49	2.83	10.42	0.06	99.28
K4-118b2GrtProfil1	37.95	0.18	19.60	0.00	27.97	0.49	2.90	10.08	0.10	99.26
K4-118b2GrtProfil1	37.67	0.18	19.74	0.01	28.05	0.43	2.80	10.31	0.06	99.24
K4-118b2GrtProfil1	37.95	0.10	20.27	0.03	27.31	0.46	2.91	10.14	0.06	99.22
K4-118b2GrtProfil1	37.95	0.05	20.58	0.01	27.21	0.51	2.69	10.25	0.03	99.29
K4-118b2GrtProfil1	37.79	0.19	19.47	0.03	27.15	0.44	2.67	10.75	0.04	98.53
K4-118b2GrtProfil1	38.27	0.01	20.93	0.02	26.02	0.49	2.84	10.94	0.03	99.55

K4-118b2GrtProfil1	38.00	0.04	20.82	0.01	27.35	0.52	2.43	10.37	0.03	99.58
K4-118b2GrtProfil2 [100]	38.08	0.12	20.29	0.00	25.79	0.42	2.33	11.96	0.03	99.03
K4-118b2GrtProfil2	37.91	0.10	20.22	0.00	25.83	0.42	2.22	12.28	0.08	99.05
K4-118b2GrtProfil2	38.13	0.09	20.19	0.04	25.59	0.42	2.17	12.26	0.02	98.90
K4-118b2GrtProfil2	38.19	0.06	20.32	0.03	25.76	0.42	2.33	12.32	0.04	99.47
K4-118b2GrtProfil2	38.01	0.03	20.35	0.01	25.81	0.48	2.58	11.48	0.07	98.81
K4-118b2GrtProfil2	37.96	0.03	21.15	0.01	26.50	0.44	2.84	10.45	0.02	99.39
K4-118b2GrtProfil2	37.97	0.16	19.85	0.02	27.95	0.41	2.75	9.53	0.08	98.72
K4-118b2GrtProfil2	37.78	0.18	20.06	0.01	28.41	0.41	2.70	9.67	0.07	99.28
K4-118b2GrtProfil2	37.78	0.17	19.71	0.02	28.44	0.48	2.68	9.86	0.08	99.21
K4-118b2GrtProfil2	37.58	0.19	19.75	0.00	27.70	0.40	2.69	10.27	0.05	98.63
K4-120a3GrtProfil1 [120]	37.80	0.08	20.71	0.03	24.20	0.42	3.01	12.46	n.d.	98.70
K4-120a3GrtProfil1	38.28	0.08	20.69	0.04	24.15	0.38	2.96	12.65	n.d.	99.22
K4-120a3GrtProfil1	37.57	0.05	20.05	0.00	25.83	0.36	2.36	12.52	n.d.	98.73
K4-120a3GrtProfil1	37.41	0.06	20.08	0.00	25.94	0.29	2.27	12.38	n.d.	98.42
K4-120a3GrtProfil1	37.60	0.04	19.84	0.01	25.71	0.51	1.93	12.84	n.d.	98.47
K4-120a3GrtProfil1	37.84	0.07	20.73	0.01	23.42	0.49	2.43	13.77	n.d.	98.76
K4-120a3GrtProfil1	37.91	0.08	20.60	0.00	24.15	0.40	3.03	12.39	n.d.	98.58
K4-120a3GrtProfil1	37.88	0.05	20.66	0.02	24.84	0.48	3.31	11.64	n.d.	98.89
K4-120a3GrtProfil1	37.79	0.05	20.77	0.02	24.94	0.52	3.08	11.81	n.d.	98.98
K4-120a3GrtProfil1	37.89	0.09	20.61	0.01	24.35	0.48	3.17	12.27	n.d.	98.85
K4-120a3GrtProfil1	37.94	0.08	20.76	0.03	24.73	0.44	3.14	11.96	n.d.	99.06
K4-120a3GrtProfil1	37.90	0.08	20.62	0.02	23.95	0.36	3.14	12.15	n.d.	98.21
K4-120a3GrtProfil2 [190]	37.96	0.07	20.66	0.04	24.42	0.35	2.94	12.48	n.d.	98.90
K4-120a3GrtProfil2	37.86	0.07	20.44	0.01	24.63	0.42	3.09	11.93	n.d.	98.44
K4-120a3GrtProfil2	37.88	0.09	20.70	0.02	24.86	0.49	3.39	11.40	n.d.	98.83
K4-120a3GrtProfil2	37.86	0.06	20.79	0.00	24.50	0.51	3.21	11.80	n.d.	98.74
K4-120a3GrtProfil2	37.97	0.06	20.70	0.00	24.35	0.46	3.22	12.19	n.d.	98.96
K4-120a3GrtProfil2	37.76	0.05	20.66	0.00	24.44	0.45	3.16	12.01	n.d.	98.55
K4-120a3GrtProfil2	37.96	0.09	20.62	0.04	24.69	0.37	3.17	11.77	n.d.	98.71
K4-120a3GrtProfil2	37.83	0.07	20.77	0.00	24.57	0.47	3.17	11.75	n.d.	98.64
K4-120a3GrtProfil2	37.85	0.10	20.60	0.01	24.86	0.43	3.15	11.92	n.d.	98.92
K4-120a3GrtProfil2	37.87	0.07	20.81	0.00	24.62	0.47	3.14	11.67	n.d.	98.67
K4-120a3GrtProfil2	37.91	0.07	20.69	0.00	24.77	0.39	3.19	11.87	n.d.	98.89
K4-120a3GrtProfil2	37.60	0.10	20.79	0.00	24.75	0.44	3.30	11.65	n.d.	98.62
K4-120a3GrtProfil2	37.91	0.08	20.53	0.03	24.78	0.41	3.24	11.74	n.d.	98.72
K4-120a3GrtProfil2	38.00	0.08	20.59	0.01	24.80	0.42	3.16	11.70	n.d.	98.76
K4-120a3GrtProfil2	37.76	0.07	20.63	0.00	24.52	0.45	3.20	11.79	n.d.	98.41
K4-120a3GrtProfil2	38.15	0.08	20.73	0.00	24.96	0.50	3.24	11.75	n.d.	99.40
K4-120a3GrtProfil2	37.84	0.07	20.72	0.04	24.39	0.41	3.24	11.76	n.d.	98.47
K4-120a3GrtProfil2	37.81	0.07	20.74	0.01	24.87	0.40	3.26	11.71	n.d.	98.87
K4-120a1GrtProfil1 [80]	38.01	0.07	20.68	0.03	25.01	0.49	2.93	12.20	n.d.	99.41
K4-120a1GrtProfil1	38.15	0.07	20.81	0.02	23.96	0.49	3.14	12.19	n.d.	98.83
K4-120a1GrtProfil1	38.03	0.08	20.73	0.00	25.16	0.46	3.11	11.68	n.d.	99.26
K4-120a1GrtProfil1	37.72	0.05	20.72	0.01	24.60	0.48	3.15	11.62	n.d.	98.35
K4-120a1GrtProfil1	37.93	0.09	20.99	0.02	24.45	0.46	3.23	11.93	n.d.	99.10
K4-120a1GrtProfil1	37.99	0.07	20.78	0.00	24.92	0.46	3.22	11.38	n.d.	98.82
K4-120a1GrtProfil1	37.91	0.07	20.79	0.00	24.52	0.48	3.26	11.60	n.d.	98.64
K4-120a1GrtProfil2	37.94	0.07	20.91	0.02	22.79	0.34	2.66	14.17	n.d.	98.89
K4-120a1GrtProfil2 [70]	37.96	0.09	20.67	0.02	24.38	0.35	2.92	12.52	n.d.	98.90
K4-120a1GrtProfil2	38.06	0.06	20.86	0.02	24.13	0.42	3.10	11.90	n.d.	98.53
K4-120a1GrtProfil2	37.95	0.07	20.86	0.03	24.34	0.48	3.30	11.66	n.d.	98.69
K4-120a1GrtProfil2	37.94	0.08	20.59	0.00	24.70	0.49	3.15	11.86	n.d.	98.80
K4-120a1GrtProfil2	37.83	0.09	20.59	0.00	24.24	0.42	3.10	12.01	n.d.	98.27
K4-120a1GrtProfil2	37.79	0.12	20.62	0.02	24.69	0.41	3.11	11.90	n.d.	98.67
K4-120a2GrtZonedProfil1 [220]	37.81	0.13	19.73	0.01	24.86	0.46	2.59	12.90	n.d.	98.47
K4-120a2GrtZonedProfil1	37.65	0.14	19.52	0.01	24.56	0.57	2.64	13.24	n.d.	98.32
K4-120a2GrtZonedProfil1	38.42	0.17	21.97	0.00	23.04	0.38	2.89	11.33	n.d.	98.19
K4-120a2GrtZonedProfil1	37.89	0.09	20.10	0.00	24.22	0.40	2.68	13.61	n.d.	99.00
K4-120a2GrtZonedProfil1	37.52	0.05	19.71	0.03	24.44	0.57	2.63	13.51	n.d.	98.45
K4-120a2GrtZonedProfil1	37.52	0.10	19.50	0.00	24.33	0.47	2.48	13.89	n.d.	98.29
K4-120a2GrtZonedProfil1	37.73	0.13	20.49	0.01	24.32	0.43	2.99	12.53	n.d.	98.62
K4-120a2GrtZonedProfil1	37.80	0.13	20.54	0.02	24.22	0.51	2.87	12.46	n.d.	98.55
K4-120a2GrtZonedProfil1	37.93	0.06	20.63	0.03	24.49	0.45	2.94	12.22	n.d.	98.75
K4-120a2GrtZonedProfil1	37.86	0.07	20.50	0.02	24.39	0.43	3.07	12.12	n.d.	98.45
K4-120a2GrtZonedProfil1	37.71	0.08	20.64	0.00	24.51	0.44	3.15	12.07	n.d.	98.61
K4-120a2GrtZonedProfil1	37.90	0.08	20.71	0.01	24.40	0.40	3.06	12.23	n.d.	98.79
K4-120a2GrtZonedProfil1	37.90	0.06	20.67	0.00	24.24	0.48	3.17	12.15	n.d.	98.67
K4-120a2GrtZonedProfil1	37.88	0.08	20.66	0.01	24.10	0.42	3.16	11.93	n.d.	98.25
K4-120a2GrtZonedProfil1	37.79	0.06	20.65	0.01	24.04	0.43	2.79	12.48	n.d.	98.24
K4-120a2GrtZonedProfil1	37.69	0.08	20.56	0.00	24.26	0.42	3.10	12.17	n.d.	98.29
K4-120a2GrtZonedProfil1	37.75	0.08	20.71	0.00	24.33	0.42	3.17	12.09	n.d.	98.56
K4-120a2GrtZonedProfil1	37.84	0.09	20.69	0.01	24.03	0.43	3.07	12.58	n.d.	98.74
K4-120a2GrtZonedProfil1	37.69	0.08	20.76	0.05	25.03	0.43	2.96	11.82	n.d.	98.82
K4-120b1GrtProfil1 [ca. 500]	38.52	0.06	21.61	0.03	22.39	0.43	4.30	12.42	0.01	99.75
K4-120b1GrtProfil1	38.68	0.06	20.91	0.01	23.28	0.40	3.62	12.97	0.04	99.97
K4-120b1GrtProfil1	38.53	0.05	21.15	0.01	23.98	0.38	4.05	11.96	0.02	100.13

K4-120b1GrtProfil1	38.58	0.05	21.44	0.03	24.21	0.53	4.38	10.75	0.01	99.98
K4-120b1GrtProfil1	38.61	0.04	21.32	0.01	25.43	0.52	4.87	9.56	0.00	100.35
K4-120b1GrtProfil1	38.61	0.09	21.16	0.00	25.66	0.60	5.21	8.83	0.05	100.21
K4-120b1GrtProfil1	38.61	0.07	20.96	0.00	25.52	0.55	5.18	8.63	0.03	99.55
K4-120b1GrtProfil1	38.60	0.09	21.05	0.01	25.79	0.55	5.01	8.81	0.04	99.94
K4-120b1GrtProfil1	38.49	0.11	20.77	0.00	25.53	0.53	4.74	9.66	0.05	99.90
K4-120b1GrtProfil1	38.52	0.11	20.91	0.02	25.22	0.57	4.63	10.15	0.00	100.13
K4-120b1GrtProfil1	38.68	0.13	20.56	0.02	24.62	0.52	4.41	11.25	0.05	100.23
K4-120b1GrtProfil1	38.58	0.11	20.72	0.01	24.28	0.52	4.33	11.74	0.04	100.32
K4-120b1GrtProfil1	38.53	0.07	20.23	0.02	23.78	0.48	3.76	12.78	0.04	99.69
K4-120b1GrtProfil1	38.32	0.07	20.12	0.02	23.86	0.58	3.77	12.81	0.03	99.57
K4-120b1GrtProfil1	38.74	0.06	21.37	0.00	23.60	0.50	3.95	12.19	0.04	100.44
K4-120b1GrtProfil1	38.17	0.08	19.86	0.00	23.47	0.43	3.64	13.68	0.05	99.37
K4-120b1GrtProfil1	38.25	0.04	19.61	0.02	23.09	0.50	3.60	14.32	0.02	99.43
K4-120b1GrtProfil1	38.27	0.08	19.91	0.00	23.65	0.45	3.59	13.56	0.02	99.52
K4-120b1GrtProfil1	38.58	0.08	21.05	0.00	23.75	0.48	3.87	12.07	0.03	99.90
K4-120b2GrtProfil1 [ca 300]	38.73	0.04	21.51	0.01	22.78	0.43	4.70	11.69	0.04	99.93
K4-120b2GrtProfil1	38.71	0.07	21.44	0.02	23.41	0.48	4.53	11.70	0.05	100.41
K4-120b2GrtProfil1	39.00	0.08	21.30	0.04	22.96	0.48	4.45	11.83	0.04	100.15
K4-120b2GrtProfil1	38.85	0.07	21.28	0.02	23.19	0.47	4.59	11.54	0.03	100.04
K4-120b2GrtProfil1	38.73	0.07	21.39	0.02	23.62	0.48	4.43	11.16	0.03	99.92
K4-120b2GrtProfil1	38.83	0.09	21.25	0.00	24.68	0.45	4.42	10.91	0.02	100.65
K4-120b2GrtProfil1	38.42	0.13	20.65	0.02	24.39	0.51	4.28	11.37	0.03	99.80
K4-120b2GrtProfil1	38.77	0.14	20.17	0.00	24.59	0.49	4.26	11.57	0.04	100.03
K4-120b2GrtProfil1	38.35	0.05	20.23	0.02	23.96	0.49	4.05	12.47	0.02	99.64
K4-120b2GrtProfil1	38.13	0.10	19.66	0.02	23.98	0.42	3.76	13.19	0.03	99.30
K4-120b2GrtProfil1	38.49	0.11	20.16	0.02	24.12	0.39	3.78	12.83	0.03	99.92
K4-120b2GrtProfil1	38.49	0.10	20.31	0.00	24.18	0.48	3.86	12.46	0.04	99.91
K4-120b2GrtProfil1	37.83	0.15	19.45	0.00	24.00	0.41	3.82	13.31	0.02	99.00
K4-120b2GrtProfil1	38.31	0.17	19.99	0.00	23.89	0.49	4.07	12.47	0.04	99.42
K4-120b2GrtProfil1	38.19	0.15	20.30	0.01	24.20	0.49	3.75	12.38	0.02	99.48
K4-120b5Grt1	38.58	0.11	19.82	0.00	23.90	0.55	3.82	12.83	0.01	99.63
K4-120b5Grt2	38.59	0.07	21.00	0.00	24.35	0.48	4.35	11.08	0.04	99.96
K4-120b5Grt3	38.92	0.08	21.32	0.02	22.62	0.51	4.27	11.97	0.04	99.77
K4-120c2GrtProf1 [ca 50]	38.55	0.15	20.31	0.00	22.99	0.66	5.87	12.24	n.d.	100.77
K4-120c2GrtProf1	38.49	0.02	21.09	0.00	22.80	0.68	6.32	11.20	n.d.	100.59
K4-120c2GrtProf1	38.77	0.01	21.42	0.02	23.81	0.62	7.09	8.90	n.d.	100.64
K4-120c2GrtProf1	38.72	0.04	21.34	0.03	24.36	0.69	6.31	9.35	n.d.	100.84
K4-120c2GrtProf1	38.88	0.04	20.75	0.02	22.63	0.64	6.15	11.82	n.d.	100.92
K4-120d1GrtProfil1 [ca 1000]	38.31	0.02	21.15	0.02	25.74	0.65	3.15	10.64	0.02	99.69
K4-120d1GrtProfil1	38.82	0.05	21.28	0.02	23.33	0.44	4.34	11.50	0.03	99.82
K4-120d1GrtProfil1	38.69	0.06	21.34	0.04	23.20	0.49	4.38	11.61	0.05	99.84
K4-120d1GrtProfil1	38.90	0.06	21.45	0.03	23.21	0.46	4.39	11.85	0.03	100.38
K4-120d1GrtProfil1	38.80	0.09	21.35	0.01	22.65	0.47	4.45	12.10	0.05	99.98
K4-120d1GrtProfil1	38.91	0.08	21.33	0.01	22.67	0.48	4.44	12.17	0.04	100.12
K4-120d1GrtProfil1	38.85	0.09	21.38	0.01	22.59	0.44	4.40	12.39	0.01	100.14
K4-120d1GrtProfil1	38.74	0.04	21.42	0.01	23.26	0.41	4.34	11.86	0.03	100.09
K4-120d1GrtProfil1	38.63	0.04	21.31	0.01	24.27	0.43	4.76	10.45	0.05	99.95
K4-120d1GrtProfil1	38.66	0.10	21.40	0.02	24.50	0.43	4.76	10.09	0.08	100.04
K4-120d1GrtProfil1	38.74	0.07	21.27	0.02	24.46	0.57	4.68	10.35	0.03	100.19
K4-120d1GrtProfil1	38.71	0.07	21.31	0.01	24.20	0.49	4.46	10.59	0.04	99.88
K4-120d1GrtProfil1	38.88	0.05	21.23	0.00	24.39	0.50	4.71	10.18	0.01	99.96
K4-120d1GrtProfil1	38.76	0.08	21.13	0.00	24.35	0.49	4.72	10.47	0.04	100.03
K4-120d1GrtProfil1	38.66	0.05	21.18	0.02	24.30	0.51	4.57	10.60	0.03	99.92
K4-120d1GrtProfil1	38.70	0.03	21.43	0.01	23.88	0.56	4.42	11.06	0.04	100.13
K4-120d1GrtProfil1	38.77	0.06	21.22	0.00	24.21	0.55	4.72	10.00	0.05	99.58
K4-120d1GrtProfil1	38.53	0.06	21.44	0.01	24.74	0.52	4.90	9.65	0.03	99.86
K4-120d1GrtProfil1	37.81	0.04	21.25	0.01	24.80	0.53	4.88	9.59	0.03	98.94
K4-120d1GrtProfil1	38.62	0.11	20.50	0.02	24.54	0.48	4.49	10.86	0.03	99.65
K4-120d1GrtProfil1	38.67	0.06	21.32	0.01	23.80	0.48	4.42	11.34	0.05	100.14
K4-120d1GrtProfil1	38.93	0.04	21.23	0.00	24.15	0.54	4.68	10.62	0.04	100.24
K4-120d1GrtProfil1	38.87	0.09	20.78	0.00	24.79	0.55	4.49	10.81	0.06	100.43
K4-120d1GrtProfil1	38.92	0.10	20.35	0.02	24.39	0.54	4.15	11.58	0.04	100.10
K4-120d1GrtProfil1	38.59	0.06	20.80	0.00	24.13	0.51	4.43	11.26	0.03	99.81
K4-120d1GrtProfil1	38.61	0.08	20.36	0.02	24.51	0.56	4.30	11.44	0.03	99.90
K4-120d1GrtProfil1	38.32	0.07	20.29	0.00	24.87	0.53	4.33	11.56	0.02	99.99
K4-120d1GrtProfil1	38.46	0.09	20.36	0.01	24.39	0.48	4.19	11.94	0.04	99.95
K4-120d1GrtProfil1	38.62	0.09	20.39	0.00	23.91	0.47	4.01	12.07	0.04	99.59
K4-120d1GrtProfil1	38.59	0.09	20.38	0.02	24.01	0.51	3.91	12.36	0.03	99.89
K4-120d1GrtProfil1	38.52	0.14	20.12	0.01	23.89	0.47	3.79	12.83	0.07	99.83
K4-120d1GrtProfil1	38.33	0.09	19.69	0.01	24.19	0.44	3.79	13.11	0.03	99.67
K4-120d1GrtProfil1	38.62	0.13	20.07	0.02	24.19	0.57	3.87	12.77	0.05	100.28
K4-120d1GrtProfil1	38.52	0.07	20.05	0.00	24.41	0.48	4.11	12.20	0.03	99.88
K4-120d1GrtProfil1	38.54	0.11	20.54	0.00	24.00	0.52	3.98	12.37	0.04	100.10
K4-120d1GrtProfil1	38.66	0.11	20.07	0.02	24.37	0.50	4.05	12.14	0.04	99.95
K4-120d1GrtProfil1	38.51	0.09	19.96	0.00	24.00	0.52	3.82	12.31	0.07	99.30
K4-120d1GrtProfil1	38.64	0.05	21.11	0.01	23.72	0.48	4.28	11.79	0.03	100.10
K4-120d1GrtProfil1	38.55	0.09	21.27	0.01	21.93	0.55	3.95	13.72	0.04	100.11

K4-120d1GrtProfil1	38.76	0.09	21.19	0.00	21.64	0.52	3.70	13.97	0.04	99.91
K4-120d1GrtProfil1	38.81	0.04	21.31	0.00	21.87	0.45	3.80	13.49	0.00	99.78
K4-120d1GrtProfil1	38.61	0.06	21.37	0.02	23.98	0.50	4.28	11.14	0.03	100.00
K4-120d1GrtProfil1	38.47	0.09	20.52	0.01	24.46	0.49	4.11	11.58	0.04	99.75
K4-120d1GrtProfil1	38.46	0.06	20.75	0.01	24.60	0.53	4.30	11.14	0.04	99.89
K4-120d1GrtProfil1	38.49	0.09	20.70	0.00	24.55	0.49	4.17	11.57	0.02	100.08
K4-120d1GrtProfil1	38.40	0.08	20.58	0.03	24.89	0.53	4.31	11.12	0.03	99.96
K4-120d1GrtProfil1	38.53	0.07	20.71	0.00	24.27	0.55	4.22	11.36	0.02	99.72
K4-120d1GrtProfil2 [ca 300]	38.89	0.06	21.21	0.00	21.73	0.66	3.75	13.68	0.03	100.01
K4-120d1GrtProfil2	38.67	0.07	21.06	0.00	22.20	0.53	3.86	13.26	0.05	99.69
K4-120d1GrtProfil2	38.56	0.10	21.22	0.00	22.13	0.67	3.65	13.47	0.06	99.85
K4-120d1GrtProfil2	38.66	0.07	21.15	0.02	22.65	0.77	3.69	13.15	0.03	100.18
K4-120d1GrtProfil2	38.70	0.06	21.19	0.02	22.52	0.69	3.76	13.29	0.04	100.27
K4-120d1GrtProfil2	38.65	0.02	21.24	0.03	21.81	0.62	3.85	13.72	0.04	99.98
K4-120d1GrtProfil2	38.72	0.12	21.28	0.00	21.78	0.55	3.95	13.68	0.04	100.12
K4-120d1GrtProfil2	38.79	0.03	21.37	0.03	22.74	0.53	4.31	12.13	0.02	99.96
K4-120d1GrtProfil2	38.60	0.04	21.26	0.02	23.96	0.52	4.38	11.18	0.03	99.99
K4-120d1GrtProfil2	38.71	0.07	21.13	0.01	24.89	0.61	4.84	9.73	0.03	100.01
K4-120d1GrtProfil2	38.59	0.05	21.28	0.01	25.08	0.67	4.94	9.44	0.05	100.10
K4-120d1GrtProfil2	38.58	0.03	21.30	0.02	24.42	0.62	4.53	10.42	0.03	99.95
K4-120d1GrtProfil2	38.61	0.08	21.14	0.00	24.32	0.68	3.78	11.13	0.03	99.77
K4-120d1GrtProfil2	38.10	0.03	21.23	0.05	26.87	2.34	1.96	9.88	0.03	100.47
K4-120d1GrtProfil2	38.53	0.07	21.16	0.00	24.03	0.53	4.55	10.63	0.01	99.51
K4-120d1GrtProfil2	38.71	0.07	21.12	0.01	24.93	0.49	4.95	9.56	0.04	99.86
K4-120d1GrtProfil3 [ca 50]	38.66	0.09	21.13	0.00	25.78	0.62	4.34	9.90	0.05	100.58
K4-120d1GrtProfil3	38.49	0.08	21.12	0.00	25.99	0.62	4.15	9.72	0.01	100.18
K4-120d1GrtProfil3	38.29	0.06	20.96	0.00	25.88	0.56	4.05	9.74	0.02	99.57
K4-120d1GrtProfil3	38.44	0.14	20.98	0.02	26.20	0.84	3.52	9.77	0.01	99.93
K4-120d3GrtProfil1 [380]	38.68	0.10	20.92	0.01	24.39	0.52	4.36	11.00	0.05	100.01
K4-120d3GrtProfil1	38.14	0.08	21.10	0.01	25.06	0.52	4.56	10.38	0.02	99.88
K4-120d3GrtProfil1	38.64	0.08	21.26	0.00	24.25	0.53	4.42	10.63	0.05	99.86
K4-120d3GrtProfil1	38.42	0.13	20.95	0.02	24.30	0.52	4.34	11.27	0.04	99.98
K4-120d3GrtProfil1	38.30	0.19	20.41	0.00	25.00	0.54	4.38	10.81	0.04	99.66
K4-120d3GrtProfil1	38.36	0.12	20.70	0.00	25.01	0.54	4.47	10.59	0.04	99.82
K4-120d3GrtProfil1	38.30	0.08	20.46	0.00	25.19	0.56	4.55	10.53	0.02	99.70
K4-120d3GrtProfil1	38.49	0.12	20.92	0.03	24.65	0.56	4.44	10.86	0.06	100.14
K4-120d3GrtProfil1	38.36	0.08	20.95	0.00	23.97	0.50	4.19	11.57	0.04	99.65
K4-120d3GrtProfil1	38.89	0.10	20.75	0.02	24.61	0.49	4.21	11.50	0.04	100.60
K4-120d3GrtProfil1	38.49	0.06	20.82	0.00	24.68	0.56	4.33	11.14	0.03	100.09
K4-120d3GrtProfil1	38.55	0.01	20.32	0.00	25.23	0.57	4.38	10.94	0.02	100.02
K4-120d3GrtProfil1	38.65	0.03	20.24	0.00	25.39	0.58	4.35	10.94	0.04	100.23
K4-120d3GrtProfil1	38.58	0.01	20.44	0.00	25.46	0.50	4.53	10.42	0.04	99.98
K4-120d3GrtProfil1	38.49	0.01	20.34	0.02	25.34	0.56	4.46	10.71	0.03	99.96
K4-120d3GrtProfil1	38.68	0.06	20.54	0.03	24.44	0.52	4.22	11.71	0.02	100.21
K4-120d3GrtProfil1	38.36	0.02	19.87	0.01	25.29	0.56	4.25	11.45	0.04	99.85
K4-120d3GrtProfil1	38.04	0.07	19.92	0.00	25.20	0.56	4.13	11.80	0.03	99.74
K4-120d3GrtProfil1	38.49	0.05	20.20	0.01	25.53	0.53	4.38	10.94	0.04	100.17
K4-120d3GrtProfil1	38.21	0.06	20.36	0.02	24.70	0.52	4.31	11.43	0.03	99.64
K4-120d3GrtProfil1	38.71	0.05	20.26	0.01	25.01	0.52	4.27	11.23	0.03	100.09
K4-120d3GrtProfil1	38.40	0.00	19.91	0.04	25.77	0.58	4.40	11.02	0.05	100.16
K4-120d3GrtProfil1	38.21	0.03	20.20	0.01	25.50	0.51	4.35	10.89	0.03	99.71
K4-120d3GrtProfil1	38.60	0.03	20.38	0.00	25.36	0.57	4.36	11.07	0.03	100.39
K4-120d3GrtProfil1	38.65	0.11	20.78	0.04	24.49	0.49	4.34	11.50	0.06	100.44
K4-120d3GrtProfil1	38.63	0.09	20.92	0.00	24.46	0.52	4.42	10.99	0.05	100.09
K4-120d3GrtProfil1	38.55	0.13	20.80	0.01	24.21	0.55	4.27	11.45	0.06	100.03
K4-120d3GrtProfil1	38.61	0.08	20.75	0.03	24.19	0.51	4.28	11.31	0.03	99.79
K4-120d3GrtProfil1	38.54	0.08	21.11	0.00	23.75	0.48	4.17	11.79	0.03	99.94
K4-120d3GrtProfil1	38.77	0.12	20.87	0.01	24.00	0.52	4.28	11.72	0.06	100.35
K4-120d3GrtProfil1	38.50	0.12	20.82	0.00	24.01	0.53	4.30	11.46	0.04	99.78
K4-120d3GrtProfil1	38.44	0.16	20.58	0.00	24.05	0.53	4.13	11.95	0.07	99.91
K4-120d3GrtProfil1	38.63	0.12	21.01	0.00	24.26	0.50	4.22	11.51	0.10	100.34
K4-120d3GrtProfil1	38.22	0.05	20.11	0.00	24.63	0.58	4.00	12.06	0.03	99.67
K4-120d3GrtProfil1	38.27	0.04	20.19	0.05	24.73	0.51	4.19	11.64	0.05	99.64
K4-120d3GrtProfil1	38.63	0.04	21.14	0.04	23.86	0.54	4.07	11.91	0.05	100.27
K4-120d3GrtProfil1	38.35	0.05	20.20	0.00	24.50	0.49	3.97	11.73	0.03	99.33
JNar2,1grtR1	38.71	0.12	21.88	0.04	21.22	0.46	4.45	12.59	0.03	99.49
JNar2,1grtC1	38.59	0.11	21.48	0.00	24.99	0.56	5.23	9.92	0.01	100.90
JNar2,1grtR2	38.89	0.10	21.71	0.04	22.96	0.49	4.52	12.54	0.02	101.26
JNar2,1grtR2	38.90	0.07	21.58	0.02	22.46	0.45	4.71	12.49	0.07	100.76
JNar2,1grtC2	38.47	0.10	21.52	0.00	24.69	0.53	5.18	9.93	0.05	100.47
JNar2,1grtR3	38.59	0.06	21.74	0.02	21.99	0.42	4.26	13.42	0.00	100.50
JNar2,1grtC3	38.77	0.23	21.57	0.00	20.87	0.38	4.84	13.42	0.01	100.10
JNar2,1grtR4	38.75	0.05	21.82	0.03	21.80	0.40	4.47	13.14	0.01	100.45
JNar2,1grtc4	38.64	0.05	21.63	0.02	22.15	0.45	4.34	12.19	0.00	99.46
JNar2,1grtR5	39.32	0.06	21.74	0.00	20.54	0.41	5.09	13.45	0.03	100.63
JNar2,1grtC5	38.90	0.09	21.45	0.01	23.57	0.54	4.69	11.41	0.00	100.66
JNar2,1grtR6	38.68	0.03	21.66	0.04	21.65	0.41	4.83	13.06	0.01	100.37

JNar2,1grtC6	38.58	0.04	21.55	0.03	21.88	0.44	4.55	12.72	0.04	99.83
JNar2,1grtR7	38.76	0.08	21.36	0.01	23.72	0.61	4.60	11.36	0.09	100.58
JNar2,1grtC7	38.48	0.00	21.68	0.03	23.81	0.46	4.85	10.81	0.01	100.13
JNar2,2grtProfil1 [130]	38.86	0.06	21.60	0.01	22.35	0.32	4.49	12.59	0.01	100.28
JNar2,2grtProfil1	39.05	0.08	21.40	0.01	22.97	0.39	4.58	11.99	0.02	100.50
JNar2,2grtProfil1	38.75	0.01	21.58	0.00	24.03	0.40	5.03	10.29	0.04	100.14
JNar2,2grtProfil1	38.70	0.05	21.39	0.01	24.49	0.44	4.62	10.86	0.02	100.58
JNar2,2grtProfil1	38.61	0.06	21.52	0.01	24.63	0.44	4.90	10.81	0.02	101.00
JNar2,2grtProfil1	38.86	0.02	21.60	0.00	24.09	0.41	4.64	11.21	0.02	100.83
JNar2,2grtProfil1	39.00	0.08	21.49	0.03	22.60	0.42	4.75	12.54	0.00	100.89
JNar2,2grtProfil1	39.19	0.09	21.52	0.03	21.59	0.39	4.70	13.27	0.04	100.82
JNar2,2grtProfil1	38.89	0.05	21.65	0.03	22.85	0.38	4.81	12.25	0.00	100.91
JNar2,2grtProfil1	39.09	0.10	21.59	0.04	22.15	0.41	4.89	12.66	0.01	100.94
JNar2,2grtProfil1	38.80	0.05	21.39	0.02	22.34	0.40	4.20	13.17	0.00	100.38
JNar2,2grtProfil2 [130]	38.70	0.05	21.40	0.00	24.02	0.33	4.69	11.09	0.04	100.31
JNar2,2grtProfil2	38.79	0.07	21.52	0.00	23.81	0.43	4.86	10.82	0.00	100.30
JNar2,2grtProfil2	38.71	0.21	21.22	0.00	24.53	0.43	4.69	10.82	0.04	100.65
JNar2,2grtProfil2	38.70	0.09	21.44	0.03	23.68	0.36	4.72	11.25	0.02	100.29
JNar2,2grtProfil2	38.73	0.06	21.38	0.02	24.82	0.43	4.92	10.02	0.00	100.38
JNar2,2grtProfil2	38.76	0.10	21.45	0.03	24.76	0.46	4.89	10.19	0.03	100.67
JNar2,2grtProfil2	38.64	0.05	21.42	0.00	23.52	0.37	4.67	11.44	0.02	100.12
JNar2,2grtProfil2	38.83	0.06	21.35	0.00	22.60	0.33	4.53	12.28	0.02	100.00
JNar2,2grtProfil2	38.67	0.08	21.40	0.03	23.25	0.39	4.89	11.26	0.04	100.01
JNar2,2grtProfil2	38.61	0.03	23.00	0.03	20.00	0.57	2.64	13.97	0.05	98.91
PK2-4cGrtProfil1 [130]	39.22	0.05	21.99	0.02	23.00	0.39	8.42	7.01	0.04	100.13
PK2-4cGrtProfil1	39.27	0.04	21.75	0.06	22.31	0.38	8.58	7.49	0.04	99.91
PK2-4cGrtProfil1	39.80	0.10	21.78	0.00	22.65	0.38	8.41	7.99	0.00	101.12
PK2-4cGrtProfil1	39.45	0.06	21.70	0.00	22.15	0.35	8.20	8.69	0.06	100.65
PK2-4cGrtProfil1	39.56	0.06	21.73	0.00	22.24	0.37	8.30	8.53	0.00	100.81
PK2-4cGrtProfil1	39.34	0.09	21.50	0.00	21.98	0.34	7.97	8.96	0.05	100.22
PK2-4cGrtProfil1	39.15	0.08	21.64	0.00	22.50	0.41	8.36	8.04	0.03	100.23
PK2-4cGrtProfil1	39.60	0.03	21.87	0.02	21.75	0.40	7.79	8.94	0.03	100.44
PK2-4cGrtProfil1	39.37	0.05	21.66	0.02	23.50	0.56	7.05	8.26	0.01	100.46
PK2-4cGrtProfil1	38.68	0.06	21.41	0.08	23.61	0.52	6.45	9.12	0.03	99.95
PK2-4cGrtProfil2 [90]	39.57	0.03	21.70	0.07	21.90	0.32	8.03	9.00	0.01	100.63
PK2-4cGrtProfil2	39.87	0.02	21.80	0.04	20.63	0.32	8.42	9.25	0.03	100.37
PK2-4cGrtProfil2	40.15	0.02	21.78	0.02	20.71	0.32	8.47	9.27	0.01	100.76
PK2-4cGrtProfil2	39.75	0.01	21.95	0.01	20.89	0.38	8.31	9.52	0.02	100.83
PK2-4cGrtProfil2	39.51	0.01	21.88	0.03	20.87	0.35	7.98	9.89	0.00	100.53
PK2-4cGrtProfil2	39.67	0.03	21.89	0.04	21.00	0.35	8.28	9.30	0.04	100.59
PK2-4cGrtProfil2	39.55	0.05	21.82	0.03	21.58	0.38	8.35	9.02	0.04	100.81
PK2-4cGrtProfil2	39.08	0.05	21.66	0.05	22.70	0.47	7.25	8.83	0.00	100.09
PKB3,2GrtProfil1 [180]	38.05	0.04	20.25	0.00	25.86	0.40	4.06	10.04	0.04	98.75
PKB3,2GrtProfil1	38.31	0.06	20.97	0.02	25.11	0.30	3.92	10.37	0.04	99.10
PKB3,2GrtProfil1	38.21	0.07	20.83	0.00	25.37	0.34	3.96	10.26	0.00	99.03
PKB3,2GrtProfil1	38.37	0.13	20.33	0.03	25.34	0.29	3.94	10.30	0.00	98.70
PKB3,2GrtProfil1	38.26	0.03	21.18	0.00	23.92	0.33	3.85	11.05	0.00	98.61
PKB3,2GrtProfil1	38.37	0.05	21.09	0.00	25.05	0.35	3.73	11.02	0.01	99.66
PKB3,2GrtProfil1	38.39	0.06	20.93	0.00	24.97	0.34	3.89	10.89	0.02	99.48
PKB3,2GrtProfil1	38.60	0.05	20.95	0.00	26.02	0.40	4.07	9.78	0.01	99.87
PKB3,2GrtProfil1	38.34	0.07	20.98	0.00	25.05	0.38	3.88	10.39	0.00	99.08
PKB3,2GrtProfil1	38.49	0.03	20.91	0.04	24.95	0.32	4.18	9.58	0.00	98.50
PKB3,2GrtProfil1	38.44	0.03	20.88	0.00	25.63	0.35	4.43	8.43	0.01	98.20
PKB3,2GrtProfil1	38.20	0.06	20.86	0.01	25.42	0.38	4.15	9.67	0.00	98.75
PKB3,2GrtProfil1	38.25	0.06	21.08	0.02	25.67	0.36	4.13	9.85	0.01	99.42
PKB3,1GrtProfil1 [220]	38.49	0.03	20.95	0.01	25.77	0.38	4.21	9.12	0.03	98.98
PKB3,1GrtProfil1	38.38	0.00	20.99	0.04	24.81	0.34	4.04	9.42	0.00	98.01
PKB3,1GrtProfil1	38.64	0.05	21.16	0.01	24.89	0.31	3.87	10.46	0.02	99.41
PKB3,1GrtProfil1	38.48	0.04	21.13	0.02	26.10	0.39	4.11	9.57	0.01	99.83
PKB3,1GrtProfil1	38.31	0.08	21.07	0.02	24.37	0.32	3.76	11.00	0.03	98.95
PKB3,1GrtProfil1	38.36	0.05	20.87	0.03	25.29	0.31	3.95	10.09	0.00	98.96
PKL2grtProfil1 [120]	45.18	0.03	17.13	0.00	25.53	1.77	2.24	7.52	0.04	99.44
PKL2grtProfil1	38.21	0.04	20.58	0.00	26.27	0.67	3.60	8.72	0.03	98.11
PKL2grtProfil1	38.27	0.05	20.74	0.00	22.73	0.42	5.25	10.86	0.03	98.33
PKL2grtProfil1	38.23	0.06	20.66	0.00	23.14	0.47	5.10	10.80	0.03	98.49
PKL2grtProfil1	37.87	0.08	20.57	0.00	23.68	0.44	5.01	10.84	0.02	98.50
PKL2grtProfil1	38.17	0.03	20.68	0.00	25.33	0.52	4.92	9.91	0.03	99.59
PKL2grtProfil1	38.05	0.09	20.62	0.00	25.38	0.48	5.15	9.66	0.05	99.48
PKL2grtProfil1	38.30	0.09	20.75	0.00	24.65	0.46	4.89	10.05	0.07	99.26
PKL2grtProfil1	38.02	0.11	20.50	0.00	24.15	0.40	5.49	9.48	0.06	98.20
PKL2grtProfil1	38.43	0.06	20.78	0.00	23.59	0.42	5.19	10.71	0.03	99.21
PKL2grtProfil2 [ca 30]	38.64	0.07	21.04	0.00	23.35	0.38	5.19	11.08	0.03	99.77
PKL2grtProfil2	38.50	0.12	20.67	0.00	24.23	0.52	4.63	10.44	0.02	99.13
PKL2grtProfil2	38.30	0.14	20.63	0.00	24.24	0.44	5.33	10.40	0.05	99.54

Table A3. Microprobe analyses of pyroxene

Sample [Profile length in μm]	SiO_2	TiO_2	Al_2O_3	Cr_2O_3	FeO	MnO	MgO	CaO	Na_2O	Sum
K3-11,1pyroProfil1 [360]	56.58	0.08	10.76	0.02	2.53	0.00	9.53	14.75	6.59	100.85
K3-11,1pyroProfil1	56.73	0.04	10.82	0.05	2.61	0.00	9.23	14.78	6.57	100.82
K3-11,1pyroProfil1	56.51	0.04	10.97	0.04	2.65	0.01	9.27	14.40	6.66	100.55
K3-11,1pyroProfil1	56.63	0.05	10.59	0.03	2.67	0.00	9.47	14.74	6.55	100.73
K3-11,1pyroProfil1	56.56	0.04	10.66	0.05	2.59	0.04	9.40	14.84	6.67	100.85
K3-11,1pyroProfil1	56.43	0.05	10.60	0.03	2.67	0.00	9.44	14.69	6.51	100.41
K3-11,1pyroProfil1	56.10	0.05	10.62	0.01	2.81	0.00	9.23	14.77	6.60	100.20
K3-11,1pyroProfil1	56.77	0.04	10.73	0.00	2.94	0.02	9.18	14.78	6.70	101.17
K3-11,1pyroProfil1	56.76	0.08	10.49	0.03	3.09	0.02	9.38	14.77	6.55	101.17
K3-11,1pyroProfil1	56.29	0.07	9.58	0.05	2.87	0.00	10.11	15.68	5.93	100.58
K3-11,1pyroProfil1	56.15	0.09	10.71	0.02	3.55	0.00	9.16	14.66	6.52	100.85
K3-11,1pyroProfil1	56.05	0.08	10.89	0.02	3.21	0.03	9.19	14.63	6.75	100.84
K3-11,1pyroProfil1	56.17	0.13	10.60	0.02	3.37	0.00	9.32	14.80	6.34	100.76
K3-11,1pyroProfil1	56.09	0.09	11.09	0.00	3.27	0.04	9.07	14.36	6.68	100.68
K3-11,1pyroProfil1	56.57	0.08	10.34	0.02	3.45	0.00	9.38	15.06	6.43	101.31
K3-11,1pyroProfil1	56.18	0.12	10.93	0.01	3.30	0.00	9.03	14.55	6.52	100.65
K3-11,1pyroProfil1	56.77	0.07	10.99	0.01	2.67	0.05	9.12	14.35	6.75	100.76
K3-11,1pyroProfil1	56.27	0.09	10.76	0.04	3.21	0.00	9.25	14.84	6.46	100.91
K3-11,1pyroProfil1	55.52	0.05	9.97	0.03	2.86	0.00	9.41	15.15	6.11	99.09
K3-11,1pyroProfil1	56.19	0.05	9.14	0.03	3.63	0.01	9.76	15.03	6.25	100.08
K3-11,1pyroProfil1	55.99	0.05	9.50	0.01	3.62	0.06	9.66	15.69	5.99	100.57
K3-11,1pyroProfil1	56.83	0.06	11.19	0.02	3.04	0.00	8.82	14.34	6.77	101.06
K3-11,1pyroProfil1	56.04	0.08	11.05	0.01	3.03	0.00	9.23	14.70	6.58	100.71
K3-11,1pyroProfil1	56.22	0.10	10.77	0.03	3.13	0.03	9.26	14.52	6.46	100.52
K3-11,1pyroProfil1	55.76	0.10	10.54	0.03	3.27	0.00	9.30	14.69	6.52	100.21
K3-11,1pyroProfil1	55.99	0.10	10.60	0.04	3.19	0.01	9.24	14.71	6.45	100.31
K3-11,1pyroProfil1	56.00	0.08	11.14	0.03	3.07	0.00	9.07	14.35	6.72	100.47
K3-11,1pyroProfil1	56.12	0.07	10.04	0.07	3.91	0.00	9.29	15.28	6.30	101.09
K3-11,1pyroProfil1	55.70	0.10	10.59	0.04	3.49	0.01	9.21	14.76	6.45	100.34
K3-11,1pyroProfil1	56.05	0.12	10.48	0.00	3.18	0.03	9.32	14.96	6.32	100.46
K3-11,1pyroProfil1	56.25	0.10	10.51	0.03	3.35	0.05	9.15	14.79	6.47	100.70
K3-11,1pyroProfil1	56.79	0.09	11.84	0.03	2.53	0.01	8.83	13.55	7.31	100.99
K3-11,1pyroProfil1	56.36	0.07	11.17	0.05	2.81	0.02	9.04	14.31	6.77	100.60
K3-11,1pyroProfil1	56.45	0.07	11.17	0.03	2.64	0.02	9.21	14.28	6.78	100.65
K3-11,1pyroProfil1	56.01	0.07	10.62	0.03	3.12	0.04	9.27	14.64	6.51	100.32
K3-11,1pyroProfil1	55.98	0.09	10.65	0.03	3.46	0.01	9.32	14.52	6.49	100.56
K3-11,1pyroProfil2 [90]	56.41	0.09	11.16	0.01	2.91	0.05	9.10	14.22	6.75	100.69
K3-11,1pyroProfil2	56.25	0.09	11.30	0.04	2.75	0.05	8.97	14.13	6.79	100.37
K3-11,1pyroProfil2	56.29	0.09	10.76	0.03	3.20	0.00	9.28	14.75	6.45	100.85
K3-11,1pyroProfil2	58.61	0.10	12.62	0.05	2.74	0.01	7.81	11.78	7.02	100.76
K3-11,1pyroProfil2	56.86	0.06	11.52	0.05	2.46	0.00	8.85	13.92	7.15	100.87
K3-11,1pyroProfil2	56.39	0.05	11.12	0.00	2.79	0.02	9.03	14.18	6.81	100.37
K3-11,1pyroProfil2	56.46	0.09	12.49	0.03	2.45	0.00	8.47	13.20	7.62	100.80
K3-11,1pyroProfil2	56.13	0.12	11.21	0.04	3.05	0.00	8.74	13.92	6.84	100.05
K3-11,1pyroProfil2	56.35	0.08	11.35	0.03	3.16	0.00	8.98	14.14	6.84	100.91
K3-11,1pyroProfil3 [80]	55.45	0.13	10.91	0.04	3.37	0.00	9.08	15.07	6.24	100.28
K3-11,1pyroProfil3	56.03	0.12	10.53	0.04	3.18	0.00	9.35	14.87	6.28	100.39
K3-11,1pyroProfil3	56.02	0.11	10.50	0.06	3.22	0.03	9.37	14.73	6.31	100.35
K3-11,1pyroProfil3	56.39	0.09	10.94	0.03	3.21	0.02	9.19	14.74	6.67	101.28
K3-11,1pyroProfil3	56.26	0.13	10.79	0.02	3.20	0.01	9.21	14.56	6.59	100.77
K3-11,1pyroProfil3	56.56	0.08	10.69	0.01	3.06	0.08	9.15	14.61	6.49	100.72
K3-11,1pyroProfil3	56.58	0.13	11.08	0.03	3.07	0.03	9.09	14.46	6.63	101.09
K3-11,1pyroProfil3	56.10	0.09	10.78	0.01	3.29	0.04	9.07	14.37	6.57	100.32
K4-53,1CpxMatrix2	52.32	0.23	6.00	0.06	8.57	0.06	10.81	19.16	3.04	100.24
K4-53,1CpxMatrix3	52.20	0.24	6.06	0.05	8.78	0.10	10.87	19.57	2.89	100.76
K4-53,3CpxInEp1	52.32	0.34	8.20	0.00	7.93	0.03	9.72	18.42	3.80	100.75
K4-53,3CpxInEp2	53.17	0.18	8.13	0.01	7.62	0.04	9.51	17.24	4.40	100.29
K4-53,3CpxMatrix2	62.87	0.00	22.21	0.01	0.17	0.00	0.00	3.44	9.94	98.64
K4-53,1CpxProfil1 [70]	52.66	0.25	6.56	0.02	8.67	0.07	10.45	19.08	3.44	101.20
K4-53,1CpxProfil1	52.31	0.32	6.75	0.02	8.77	0.10	10.41	19.23	3.34	101.25
K4-53,1CpxProfil1	52.59	0.31	7.06	0.04	8.40	0.08	10.16	18.86	3.65	101.15
K4-53,1CpxProfil1	52.58	0.35	7.17	0.02	8.76	0.06	10.01	18.79	3.42	101.17
K4-53,1CpxProfil1	52.37	0.32	7.35	0.07	8.65	0.10	10.09	18.52	3.67	101.13
K4-53,1CpxProfil1	52.73	0.33	7.65	0.01	8.26	0.10	9.90	18.41	3.89	101.28
K4-53,1CpxProfil2 [70]	54.33	0.11	7.73	0.05	7.34	0.01	9.67	16.56	4.91	100.71
K4-53,1CpxProfil2	53.43	0.20	7.93	0.03	7.90	0.02	9.58	17.26	4.62	100.97
K4-53,1CpxProfil2	53.73	0.22	8.01	0.04	7.84	0.03	9.63	17.20	4.73	101.43
K4-53,1CpxProfil2	54.44	0.11	8.05	0.03	7.63	0.09	9.43	16.43	5.16	101.37
K4-53,1CpxProfil2	54.37	0.15	8.10	0.06	7.57	0.06	9.50	16.57	5.09	101.48
K4-53,1CpxProfil2	53.84	0.15	8.29	0.04	7.38	0.01	9.38	16.40	5.01	100.49
K4-53,1CpxProfil2	54.40	0.18	8.66	0.05	7.47	0.03	9.22	16.33	5.26	101.59
K4-57,1cpxProfil1	53.47	0.20	7.47	0.01	8.83	0.01	9.47	16.15	4.57	100.17
K4-57,1cpxProfil2 [90]	53.25	0.13	7.81	0.01	9.45	0.00	9.07	15.72	4.67	100.11
K4-57,1cpxProfil2	52.71	0.17	7.70	0.00	9.74	0.00	9.07	16.09	4.35	99.83

K4-57,1cpxProfil2	53.48	0.15	8.12	0.01	9.23	0.00	8.83	15.14	4.96	99.91
K4-57,1cpxProfil2	52.82	0.12	8.51	0.03	8.82	0.07	8.54	14.62	5.56	99.09
K4-57,1cpxProfil2	53.75	0.15	8.78	0.03	8.72	0.02	8.63	14.45	5.48	100.01
K4-57,1cpxProfil2	53.81	0.17	8.90	0.01	8.83	0.02	8.48	14.29	5.83	100.33
K4-57,1cpxProfil2	53.95	0.12	8.20	0.00	8.67	0.05	8.94	14.44	5.65	100.01
K4-57,1cpxProfil2	53.82	0.07	8.24	0.00	8.38	0.01	8.91	14.31	5.79	99.51
K4-57,1cpxProfil2	53.13	0.21	8.81	0.00	9.04	0.01	8.56	14.59	5.56	99.92
K4-57,1cpxProfil3 [100]	52.53	0.12	7.11	0.02	9.84	0.07	9.59	17.56	4.04	100.88
K4-57,1cpxProfil3	53.73	0.07	7.71	0.02	9.06	0.08	8.99	16.07	5.06	100.78
K4-57,1cpxProfil3	52.90	0.10	7.89	0.03	9.45	0.07	9.03	16.47	4.81	100.75
K4-57,1cpxProfil3	52.56	0.10	7.71	0.00	10.45	0.03	9.21	17.00	4.20	101.27
K4-57,1cpxProfil3	52.87	0.12	8.03	0.00	9.87	0.00	8.95	16.43	4.71	100.99
K4-57,1cpxProfil3	52.58	0.12	8.62	0.02	9.06	0.01	8.82	16.10	5.04	100.36
K4-57,1cpxProfil3	52.64	0.10	8.41	0.01	9.54	0.01	8.78	16.25	5.03	100.75
K4-57,1cpxProfil3	52.44	0.09	8.35	0.03	9.82	0.00	8.70	16.29	4.92	100.64
K4-58,2cpxProfil1 [100]	51.80	0.21	7.23	0.03	11.32	0.00	8.55	16.47	4.60	100.22
K4-58,2cpxProfil1	52.35	0.18	7.81	0.01	11.02	0.07	7.95	15.29	5.19	99.86
K4-58,2cpxProfil1	52.36	0.18	7.91	0.03	11.19	0.06	7.86	15.09	5.45	100.11
K4-58,2cpxProfil1	51.56	0.22	7.54	0.00	11.58	0.03	8.27	15.80	4.73	99.73
K4-58,2cpxProfil1	50.72	0.20	5.89	0.03	11.02	0.03	9.45	17.74	3.58	98.65
K4-58,2cpxProfil1	50.86	0.16	6.05	0.02	12.60	0.07	10.40	17.51	2.38	100.04
K4-58,2cpxProfil1	53.00	0.19	6.70	0.01	11.51	0.04	9.05	15.25	4.79	100.54
K4-58,2cpxProfil2 [110]	52.47	0.10	7.44	0.04	11.49	0.03	8.29	14.43	5.30	99.56
K4-58,2cpxProfil2	52.94	0.08	7.59	0.02	11.00	0.05	8.02	15.05	5.39	100.13
K4-58,2cpxProfil2	53.93	0.08	8.10	0.03	10.17	0.02	7.57	13.50	6.51	99.91
K4-58,2cpxProfil2	53.50	0.06	8.19	0.04	10.24	0.03	7.79	13.68	6.52	100.04
K4-58,2cpxProfil2	52.98	0.14	7.60	0.03	10.90	0.00	8.23	14.22	5.39	99.48
K4-58,2cpxProfil2	52.60	0.13	8.15	0.03	10.70	0.03	7.73	14.70	5.64	99.69
K4-58,2cpxProfil2	51.49	0.14	7.56	0.02	11.41	0.03	8.24	15.85	4.81	99.54
K4-58,2cpxProfil2	52.89	0.12	8.33	0.01	10.69	0.10	7.94	14.72	5.76	100.58
K4-58,2cpxProfil2	52.67	0.12	8.57	0.02	10.75	0.03	7.72	14.38	5.77	100.03
K4-58,2cpxProfil2	51.81	0.11	5.63	0.02	11.78	0.05	9.69	17.87	3.36	100.31
K4-60pyroProfil1 [880]	54.37	0.11	5.97	0.02	9.77	0.02	8.24	14.20	6.27	98.96
K4-60pyroProfil1	54.39	0.11	6.12	0.02	9.89	0.06	7.92	13.94	6.18	98.62
K4-60pyroProfil1	54.68	0.05	6.28	0.01	10.00	0.00	8.09	13.67	6.43	99.22
K4-60pyroProfil1	54.73	0.05	5.90	0.01	10.35	0.01	8.45	14.14	6.29	99.93
K4-60pyroProfil1	55.21	0.04	6.53	0.05	9.30	0.03	8.20	13.67	6.64	99.68
K4-60pyroProfil1	55.02	0.04	5.65	0.04	9.61	0.03	8.52	14.21	6.30	99.41
K4-60pyroProfil1	54.98	0.07	5.73	0.01	9.29	0.02	8.57	14.18	6.32	99.16
K4-60pyroProfil1	54.67	0.08	5.71	0.04	9.79	0.03	8.42	13.98	6.35	99.07
K4-60pyroProfil1	55.09	0.07	5.92	0.03	9.74	0.07	8.47	13.96	6.46	99.80
K4-60pyroProfil1	55.05	0.03	6.03	0.02	9.06	0.00	8.29	13.93	6.55	98.95
K4-60pyroProfil1	54.64	0.06	6.11	0.03	9.44	0.05	8.24	13.90	6.32	98.79
K4-60pyro1sympl	53.10	0.16	4.79	0.02	11.54	0.06	9.19	16.47	4.44	99.75
K4-60pyro2sympl	53.10	0.09	5.35	0.03	10.87	0.08	9.13	16.82	4.62	100.08
K4-60pyro3sympl	52.55	0.17	6.54	0.02	11.68	0.05	7.87	15.10	5.50	99.48
K4-60pyro4sympl	54.77	0.05	5.93	0.00	10.20	0.02	8.44	14.05	6.39	99.84
K4-60symplPyro1	52.76	0.09	3.60	0.03	11.44	0.10	10.09	18.11	3.35	99.57
K4-60symplPyro2	52.79	0.07	3.48	0.01	11.78	0.06	9.76	17.24	3.83	99.03
K4-60symplPyroMix2	43.94	0.17	10.98	0.02	17.94	0.08	10.85	11.24	2.60	97.80
K4-76,2CpxProf1 [80]	48.89	0.48	7.18	0.02	11.61	0.07	11.16	16.39	2.66	98.46
K4-76,2CpxProf1	51.81	0.27	6.62	0.02	9.41	0.06	9.53	17.92	3.68	99.33
K4-76,2CpxProf1	51.84	0.26	7.20	0.02	9.81	0.04	8.96	16.86	4.33	99.31
K4-76,2CpxProf1	52.13	0.25	7.16	0.03	9.50	0.05	9.06	16.87	4.19	99.24
K4-76,2CpxProf1	51.71	0.28	7.05	0.02	9.51	0.09	9.11	16.93	4.09	98.79
K4-76,2CpxProf1	51.66	0.26	7.03	0.03	9.57	0.07	9.22	17.13	4.10	99.07
K4-76,2CpxProf1	51.84	0.29	6.95	0.03	9.44	0.09	9.25	17.38	4.02	99.26
K4-76,2CpxProf1	51.79	0.26	6.98	0.04	9.53	0.04	9.24	17.30	4.15	99.31
K4-76,2CpxProf2 [60]	52.67	0.18	8.77	0.02	8.22	0.05	8.29	15.45	5.30	98.94
K4-76,2CpxProf2	52.45	0.17	8.81	0.05	8.43	0.01	8.24	15.43	5.27	98.86
K4-76,2CpxProf2	52.67	0.26	8.89	0.05	8.58	0.06	8.15	15.28	5.34	99.28
K4-76,2CpxProf2	52.34	0.24	8.94	0.05	8.56	0.06	8.12	15.33	5.40	99.03
K4-76,2CpxProf2	52.43	0.26	8.79	0.05	8.49	0.05	8.17	15.38	5.44	99.06
K4-76,2CpxProf2	52.47	0.28	8.49	0.05	8.65	0.06	8.36	15.84	5.05	99.25
K4-84,3symplcpx1	52.75	0.11	7.97	0.05	8.57	0.04	9.27	16.31	4.88	99.95
K4-84,3symplcpx2	52.90	0.10	7.89	0.03	9.45	0.07	9.03	16.47	4.81	100.75
K4-982_2,2OmpProfil1 [90]	54.54	0.14	8.22	0.09	5.32	0.03	10.09	16.02	5.04	99.50
K4-982_2,2OmpProfil1	54.74	0.11	7.97	0.07	5.09	0.00	10.26	16.04	4.89	99.17
K4-982_2,2OmpProfil1	54.67	0.13	8.17	0.08	5.24	0.03	10.26	15.87	5.03	99.47
K4-982_2,2OmpProfil1	54.44	0.11	8.19	0.08	5.32	0.02	10.21	16.06	5.19	99.61
K4-982_2,2OmpProfil1	54.56	0.15	7.96	0.09	5.34	0.10	10.29	16.20	5.01	99.69
K4-982_2,2OmpProfil1	54.61	0.12	7.90	0.12	5.13	0.05	10.15	16.05	5.07	99.18
K4-982_2,2OmpProfil1	54.95	0.07	7.88	0.09	4.98	0.02	10.31	16.19	4.85	99.33

K4-982_2,2OmpProfil1	54.93	0.10	7.83	0.08	5.38	0.05	10.46	15.98	4.87	99.68
K4-982_2,2OmpProfil1	54.65	0.11	7.95	0.06	5.12	0.02	10.23	16.02	5.02	99.18
K4-981_2,1OmpProfil1 [60]	54.83	0.17	8.92	0.03	5.04	0.02	9.63	15.42	5.43	99.48
K4-981_2,1OmpProfil1	55.12	0.15	8.91	0.05	5.04	0.01	9.69	15.40	5.48	99.85
K4-981_2,1OmpProfil1	55.01	0.16	8.99	0.03	5.21	0.01	9.52	15.38	5.30	99.60
K4-981_2,1OmpProfil1	55.07	0.14	9.01	0.04	4.64	0.03	9.60	15.56	5.38	99.48
K4-981_2,1OmpProfil1	54.84	0.14	9.08	0.02	4.92	0.02	9.62	15.53	5.50	99.67
K4-981_2,1OmpProfil1	54.94	0.17	9.36	0.03	4.74	0.01	9.54	15.34	5.59	99.72
K4-981_2,1OmpProfil2 [100]	54.91	0.15	8.92	0.08	5.12	0.01	9.71	15.62	5.40	99.90
K4-981_2,1OmpProfil2	54.74	0.14	8.49	0.04	5.44	0.05	9.57	15.51	5.47	99.44
K4-981_2,1OmpProfil2	54.67	0.16	8.37	0.02	5.47	0.02	9.74	15.62	5.25	99.31
K4-981_2,1OmpProfil2	54.62	0.14	8.19	0.05	5.56	0.03	9.80	15.82	5.13	99.33
K4-981_2,1OmpProfil2	54.51	0.16	8.12	0.04	5.63	0.02	9.93	15.95	5.08	99.44
K4-981_2,1OmpProfil2	54.62	0.16	8.06	0.04	5.42	0.02	9.97	16.10	5.04	99.40
K4-981_2,1OmpProfil2	54.62	0.15	8.15	0.03	5.33	0.00	9.92	16.00	5.10	99.29
K4-99,1OmpProfil1 [80]	54.89	0.15	10.54	0.04	7.18	0.04	7.10	12.90	7.07	99.90
K4-99,1OmpProfil1	54.87	0.18	10.92	0.01	7.09	0.00	6.86	13.04	7.07	100.02
K4-99,1OmpProfil1	54.75	0.19	11.07	0.02	7.11	0.00	6.96	12.91	7.00	100.02
K4-99,1OmpProfil1	54.64	0.18	10.83	0.01	7.15	0.00	7.02	12.98	6.97	99.77
K4-99,1OmpProfil1	54.94	0.17	10.73	0.03	7.03	0.04	6.96	13.09	7.06	100.03
K4-99,1OmpProfil1	54.89	0.20	10.98	0.03	6.83	0.05	6.89	12.81	7.21	99.88
K4-99,1OmpProfil1	54.91	0.15	10.74	0.04	6.87	0.04	6.97	12.88	7.16	99.76
K4-99,1OmpProfil1	54.61	0.17	10.65	0.03	7.04	0.01	7.18	13.03	7.27	100.00
K4-99/2Cpx1	54.96	0.02	10.88	0.14	7.36	0.01	6.97	12.71	7.45	100.51
K4-99/1Cpx1	54.77	0.00	9.00	0.17	8.01	0.01	7.75	13.80	6.96	100.47
K4-99/1Cpx2	54.77	0.03	8.93	0.17	8.20	0.02	7.93	13.87	6.67	100.60
K4-99/1Cpx3	54.51	0.00	8.14	0.18	8.08	0.04	8.26	14.48	6.33	100.00
K4-99/1Cpx4	54.36	0.00	8.22	0.17	8.20	0.00	8.34	14.44	6.51	100.24
K4-99/1Cpx5	54.49	0.00	8.24	0.34	8.03	0.06	8.25	14.32	6.48	100.22
K4-99/1Cpx6	54.44	0.01	8.09	0.14	8.15	0.00	8.37	14.29	6.38	99.87
K4-105_1CpxProfil2 [90]	54.20	0.15	9.45	0.08	6.47	0.05	8.69	14.87	5.86	99.83
K4-105_1CpxProfil2	54.42	0.12	9.39	0.03	7.20	0.00	8.15	13.83	6.37	99.50
K4-105_1CpxProfil2	54.74	0.12	9.22	0.04	7.21	0.02	8.25	13.97	6.10	99.67
K4-105_1CpxProfil2	54.62	0.11	9.28	0.02	7.24	0.00	8.29	13.80	6.40	99.76
K4-105_1CpxProfil2	54.62	0.13	9.34	0.04	7.17	0.03	8.14	13.90	6.41	99.79
K4-105_1CpxProfil2	54.52	0.17	9.39	0.04	7.27	0.01	8.17	13.96	6.17	99.71
K4-105_1CpxProfil2	54.46	0.15	9.35	0.04	7.37	0.00	8.26	14.11	6.18	99.91
K4-105_1CpxProfil2	54.24	0.13	9.21	0.04	7.17	0.01	8.29	14.13	6.17	99.39
K4-105_1CpxProfil2	54.79	0.13	9.19	0.05	7.23	0.07	8.43	14.01	6.49	100.39
K4-105_2CpxProfil2	55.86	0.04	23.62	0.03	1.20	0.01	0.02	8.31	6.74	95.84
K4-106/2SymplAnCpx1	54.79	0.11	7.33	0.10	7.43	0.02	9.47	15.44	5.63	100.31
K4-106/2Cpx1	55.65	0.19	7.65	0.07	6.96	0.05	9.31	15.29	5.83	101.00
K4-106/2Cpx2	55.57	0.11	7.53	0.13	7.34	0.02	9.38	15.41	5.57	101.05
K4-106/2Cpx5	63.65	0.02	20.03	0.13	1.56	0.01	1.98	3.28	9.81	100.46
K4-106/2Cpx3	55.62	0.04	7.69	0.06	6.92	0.06	9.40	15.02	6.00	100.80
K4-106/2Cpx4	55.67	0.06	7.96	0.04	6.07	0.02	9.76	15.30	6.02	100.89
K4-106/1Cpx2	55.45	0.02	7.78	0.10	7.20	0.05	9.22	15.12	6.01	100.95
K4-106/1Cpx3	55.14	0.01	7.59	0.11	7.48	0.05	9.43	15.47	5.66	100.94
K4-120a3OmpInGrtProfil1 [50]	54.44	0.12	8.51	0.01	13.25	0.07	5.27	10.20	8.06	99.94
K4-120a3OmpInGrtProfil1	54.39	0.10	7.51	0.01	13.78	0.08	5.14	10.60	8.17	99.77
K4-120a3OmpInGrtProfil1	55.35	0.08	8.82	0.00	10.06	0.01	6.52	11.87	7.71	100.41
K4-120a3OmpInGrtProfil1	55.17	0.07	9.02	0.03	11.09	0.09	5.76	10.84	8.04	100.10
K4-120a3OmpInGrtProfil1	55.13	0.06	8.55	0.00	11.29	0.05	5.86	10.94	8.10	99.98
K4-120b1CpxRand1	55.16	0.05	9.61	0.12	7.44	0.02	7.94	13.64	6.88	100.85
K4-120b1CpxRand2	55.48	0.02	9.45	0.13	7.60	0.02	7.77	13.65	6.92	101.04
K4-120b2CpxAnCoe1	55.27	0.00	9.44	0.12	7.49	0.01	7.90	13.62	6.89	100.74
K4-120b2CpxAnCoe3	55.01	0.00	9.17	0.10	7.56	0.01	7.94	13.54	7.08	100.40
K4-120b3Cpx1	55.53	0.02	9.31	0.12	7.68	0.06	7.90	13.82	6.80	101.24
K4-120b3Cpx2	55.34	0.04	9.26	0.10	8.04	0.00	7.97	13.78	6.96	101.48
K4-120b3Cpx3	55.72	0.02	9.36	0.09	7.81	0.03	7.94	13.71	6.95	101.63
K4-120b3Cpx4	55.37	0.04	9.27	0.15	7.74	0.05	7.87	13.68	6.82	100.98
K4-120c1cpxProf1 [260]	52.83	0.12	6.49	0.04	10.53	0.07	8.37	14.80	5.94	99.18
K4-120c1cpxProf1	52.62	0.09	6.40	0.03	10.43	0.03	8.34	14.85	5.88	98.66
K4-120c1cpxProf1	52.37	0.10	6.60	0.00	10.84	0.04	8.50	14.60	5.71	98.76
K4-120c1cpxProf1	52.78	0.13	6.50	0.02	10.42	0.06	8.48	14.77	5.66	98.81
K4-120c1cpxProf1	52.63	0.11	6.45	0.02	10.66	0.04	8.39	14.96	5.80	99.04
K4-120c1cpxProf1	53.07	0.09	6.31	0.02	10.53	0.02	8.27	14.77	5.76	98.85
K4-120c1cpxProf1	52.97	0.09	6.35	0.02	10.18	0.00	8.33	14.61	5.79	98.34
K4-120c1cpxProf1	53.04	0.09	6.38	0.03	10.56	0.02	8.36	14.82	5.70	99.01
K4-120c1cpxProf1	52.91	0.11	6.43	0.03	10.79	0.03	8.38	14.87	5.69	99.23
K4-120c1cpxProf1	53.22	0.09	6.28	0.00	10.48	0.06	8.33	14.75	5.75	98.97
K4-120c1cpxProf1	52.39	0.09	6.54	0.01	10.75	0.03	8.65	14.72	5.59	98.77
K4-120c1cpxProf1	53.06	0.07	6.29	0.02	10.36	0.03	8.31	14.78	5.80	98.72
K4-120c1cpxProf1	53.61	0.09	6.37	0.01	10.53	0.04	8.43	15.09	5.84	100.00

K4-120c1cpxProf1	53.42	0.07	6.40	0.02	10.49	0.08	8.49	14.79	5.91	99.66
K4-120c1cpxProf1	53.12	0.12	6.39	0.02	10.87	0.00	8.72	14.79	5.92	99.94
K4-120d1Omp1Profil1 [ca 300]	55.07	0.03	9.20	0.12	7.57	0.03	7.75	13.68	6.83	100.27
K4-120d1Omp1Profil1	55.09	0.02	9.44	0.10	7.78	0.00	7.88	13.77	6.75	100.82
K4-120d1Omp1Profil1	55.27	0.03	9.42	0.10	7.70	0.05	7.99	13.77	6.62	100.94
K4-120d1Omp1Profil1	55.26	0.02	9.35	0.14	7.74	0.00	7.96	13.72	6.62	100.80
K4-120d1Omp1Profil1	55.03	0.06	9.33	0.12	7.61	0.02	7.83	13.65	6.72	100.36
K4-120d1Omp1Profil1	55.31	0.05	9.30	0.13	7.44	0.05	7.91	13.70	6.77	100.66
K4-120d1Omp1Profil1	55.33	0.04	9.51	0.12	7.69	0.03	7.85	13.59	6.80	100.94
K4-120d1Omp1Profil1	55.23	0.04	9.39	0.12	7.66	0.00	7.78	13.78	6.73	100.74
K4-120d1Omp1Profil1	55.13	0.04	9.39	0.10	7.81	0.00	7.97	13.85	6.71	101.00
K4-120d1Omp1Profil1	55.21	0.01	9.54	0.08	7.89	0.00	8.04	13.70	6.72	101.19
K4-120d1Omp1Profil1	55.41	0.03	9.40	0.13	7.62	0.05	7.91	13.71	6.76	101.01
K4-120d1Omp1Profil1	55.11	0.03	9.36	0.15	7.62	0.00	7.83	13.66	6.72	100.48
K4-120d1Omp1Profil1	54.29	0.04	9.31	0.12	7.95	0.04	8.22	13.28	6.35	99.60
K4-120d1Omp1Profil1	55.04	0.02	9.47	0.13	7.80	0.05	7.91	13.80	6.73	100.95
JNar2,2CpxInCzoProfil1 [90]	53.26	0.16	5.90	0.04	5.69	0.05	11.76	20.60	2.64	100.09
JNar2,2CpxInCzoProfil1	56.65	0.05	10.90	0.00	4.68	0.03	8.32	13.33	7.35	101.29
JNar2,2CpxInCzoProfil1	56.69	0.06	10.78	0.00	4.71	0.03	8.34	13.42	7.39	101.41
JNar2,2CpxInCzoProfil1	56.51	0.06	10.87	0.00	4.72	0.05	8.32	13.41	7.42	101.36
JNar2,2CpxInCzoProfil1	56.58	0.03	10.43	0.03	4.55	0.00	8.60	13.69	7.25	101.15
JNar2,2CpxInCzoProfil1	56.72	0.07	10.23	0.04	4.38	0.00	8.82	13.89	7.03	101.17
JNar2,2CpxInCzoProfil1	52.73	0.15	12.27	0.03	6.11	0.00	9.39	13.53	5.37	99.56
JNar2,2CpxInCzoProfil2 [80]	56.58	0.05	11.36	0.01	4.16	0.01	8.10	13.10	7.48	100.85
JNar2,2CpxInCzoProfil2	56.27	0.03	10.85	0.03	4.58	0.03	8.34	13.37	7.40	100.90
JNar2,2CpxInCzoProfil2	56.13	0.05	10.48	0.00	4.67	0.01	8.55	13.96	6.95	100.80
JNar2,2CpxInCzoProfil2	55.86	0.07	10.05	0.04	4.95	0.03	8.83	14.50	6.47	100.79
JNar2,2CpxInCzoProfil2	53.18	0.08	12.88	0.02	4.45	0.01	7.38	15.33	5.79	99.11
JNar2,2CpxInCzoProfil3	50.36	0.57	12.40	0.05	7.50	0.04	9.73	12.98	4.65	98.28
PKB3,2CpxProfil1 [150]	52.54	0.21	5.12	0.00	9.53	0.02	9.82	18.49	3.28	99.01
PKB3,2CpxProfil1	52.61	0.16	5.13	0.02	9.73	0.04	9.74	18.22	3.29	98.95
PKB3,2CpxProfil1	52.58	0.20	5.27	0.01	9.78	0.02	9.88	18.51	3.29	99.54
PKB3,2CpxProfil1	52.16	0.19	5.24	0.04	9.60	0.03	9.92	19.28	2.93	99.38
PKB3,2CpxProfil1	51.68	0.16	5.45	0.01	9.70	0.03	9.92	19.48	2.73	99.15
PKB3,2CpxProfil1	51.70	0.12	4.66	0.01	9.79	0.03	10.30	19.98	2.30	98.89
PKB3,2CpxProfil1	59.25	0.01	24.00	0.00	0.94	0.01	0.05	5.97	8.30	98.53
PKB3,2CpxProfil1	61.99	0.04	24.06	0.00	0.32	0.00	0.00	4.97	9.30	100.69
PKB3,2CpxProfil1	57.14	0.03	26.74	0.00	0.64	0.00	0.03	9.02	6.93	100.53
PKB3,1CpxProfil1 [150]	53.12	0.09	5.28	0.01	9.14	0.03	10.06	18.30	3.63	99.67
PKB3,1CpxProfil1	52.91	0.10	5.19	0.01	9.26	0.07	10.10	18.32	3.52	99.46
PKB3,1CpxProfil1	52.68	0.09	5.27	0.03	9.22	0.05	10.12	18.43	3.42	99.32
PKB3,1CpxProfil1	52.75	0.07	5.27	0.02	9.11	0.00	10.07	18.35	3.41	99.03
PKB3,1CpxProfil1	52.93	0.09	5.10	0.03	9.03	0.00	10.19	18.61	3.40	99.38
PKB3,1CpxProfil1	52.67	0.08	5.09	0.03	9.08	0.05	10.03	18.35	3.27	98.66
PKB3,1CpxProfil1	52.52	0.08	5.08	0.01	9.05	0.01	10.23	18.64	3.33	98.95
PKB3,1CpxProfil1	52.70	0.09	5.04	0.04	9.51	0.02	10.39	18.73	3.23	99.75
PKB3,1CpxProfil1	52.75	0.10	5.23	0.02	9.21	0.02	10.19	18.40	3.37	99.28
PKB3,1CpxProfil1	52.97	0.08	5.06	0.01	9.20	0.01	10.12	18.68	3.21	99.34
PKB3,1CpxProfil1	53.11	0.08	5.19	0.00	9.07	0.02	10.12	18.39	3.41	99.39
PKB3,1CpxProfil1	52.83	0.07	5.18	0.04	8.89	0.04	10.20	18.59	3.22	99.06
PKB3,1CpxProfil1	52.72	0.08	5.14	0.00	8.92	0.00	10.14	18.59	3.30	98.89
PKB3,1CpxProfil1	53.02	0.11	5.17	0.02	9.13	0.07	10.17	18.35	3.49	99.53
PKL1,2Cpx1	52.72	0.11	7.41	0.06	10.83	0.02	7.75	12.84	6.89	98.63
PKL1,2Cpx2	52.82	0.12	7.88	0.01	11.31	0.03	7.46	12.87	6.94	99.43
PKL1,2Cpx3	52.70	0.13	7.92	0.00	11.27	0.03	7.46	12.92	6.74	99.16
PKL1,2Cpx4	51.19	0.06	2.03	0.01	12.92	0.17	10.10	19.35	3.15	98.97
PK2-4cCpxProfil2	52.87	0.11	7.98	0.05	7.57	0.04	10.17	16.21	4.87	99.87

Table A4. Microprobe analyses of amphibole

Sample [Profile length in μm]	SiO_2	TiO_2	Al_2O_3	Cr_2O_3	FeO	MnO	MgO	CaO	Na_2O	K_2O	Sum	Cl	F
K3-11,1amp1	47.21	0.44	13.32	0.03	9.21	0.03	13.18	9.33	4.02	0.28	97.06	0.01	0.00
K3-11,1amp2	47.87	0.32	12.51	0.03	8.98	0.00	13.56	9.23	4.05	0.25	96.80	0.01	0.00
K3-11,1amp3	48.36	0.33	12.29	0.03	9.01	0.00	13.86	9.15	3.97	0.26	97.25	0.00	0.00
K3-11,1amp5	48.54	0.31	12.39	0.05	9.46	0.04	13.51	9.15	3.84	0.24	97.52	0.02	0.00
K3-11,2amp1	47.84	0.36	12.55	0.05	9.00	0.07	13.92	8.89	4.09	0.36	97.11	0.01	0.00
K3-11,2amp2	48.31	0.38	12.35	0.02	8.95	0.00	13.92	9.01	4.05	0.40	97.38	0.00	0.00
K3-11,2amp3	48.30	0.37	12.20	0.02	9.46	0.03	13.88	8.90	4.05	0.31	97.53	0.01	0.00
K3-11,2amp4	48.55	0.34	12.08	0.01	9.41	0.01	14.25	8.84	3.98	0.40	97.86	0.00	0.00
K3-11,2amp5	48.33	0.34	12.22	0.00	9.14	0.04	14.56	9.05	4.00	0.34	98.01	0.00	0.00
K3-11,2amp6	47.88	0.33	12.34	0.02	8.84	0.01	14.26	9.12	3.74	0.34	96.88	0.01	0.00
K3-11,2amp7	47.38	0.46	12.32	0.03	9.76	0.05	13.97	8.91	4.08	0.31	97.26	0.01	0.00
K3-11,2amp8	47.54	0.35	12.47	0.04	9.72	0.01	14.14	9.00	4.02	0.34	97.61	0.01	0.00
K3-11,2amp9	46.97	0.65	10.60	0.03	10.61	0.07	14.42	11.10	3.01	0.11	97.57	0.01	0.00
K4-35,1AmpProfil1 [90]	50.05	0.15	10.14	0.02	10.61	0.08	16.12	9.35	1.33	0.38	98.22	0.00	0.00
K4-35,1AmpProfil1	51.01	0.11	8.72	0.02	10.07	0.06	16.70	9.86	1.12	0.31	97.95	0.00	0.00
K4-35,1AmpProfil1	50.16	0.12	9.42	0.00	9.29	0.05	16.20	11.49	1.22	0.36	98.30	0.01	0.00
K4-35,1AmpProfil1	52.40	0.09	7.58	0.00	10.02	0.11	17.20	10.20	0.96	0.27	98.81	0.01	0.00
K4-35,1AmpProfil1	51.40	0.09	8.23	0.03	9.98	0.07	17.01	10.84	0.98	0.28	98.92	0.01	0.00
K4-35,1AmpProfil1	50.72	0.09	8.58	0.01	9.43	0.06	16.52	11.08	0.99	0.30	97.78	0.01	0.00
K4-35,1AmpProfil1	48.31	0.11	11.55	0.00	10.66	0.08	14.59	11.31	1.44	0.52	98.58	0.00	0.00
K4-35,1AmpProfil1	46.44	0.13	13.13	0.02	10.76	0.09	13.52	11.66	1.44	0.67	97.85	0.01	0.00
K4-53,1amp1	42.16	1.28	14.81	0.06	14.57	0.05	10.53	10.75	2.81	1.64	98.66	0.00	0.00
K4-53,1amp2	42.14	1.35	14.80	0.06	14.47	0.10	10.54	10.68	2.95	1.60	98.67	0.00	0.00
K4-53,1amp3	42.01	1.24	14.27	0.04	14.53	0.09	10.40	10.85	2.74	1.54	97.70	0.00	0.00
K4-53,1AmphMatrix2	42.20	1.30	14.29	0.06	15.46	0.04	10.74	10.90	2.81	1.45	99.25	0.00	0.00
K4-53,1AmphMatrix3	43.08	1.02	13.42	0.04	14.87	0.04	11.56	10.99	2.80	1.17	98.99	0.00	0.00
K4-53,1AmphMatrix4	43.16	0.89	13.63	0.01	15.33	0.08	11.46	10.36	3.23	1.13	99.27	0.01	0.00
K4-57,2AmpProfil1 [40]	42.04	0.50	14.04	0.04	16.00	0.04	10.32	11.57	2.21	1.32	98.06	0.00	0.00
K4-57,2AmpProfil1	41.88	0.52	14.26	0.07	16.38	0.05	10.49	11.23	2.39	1.45	98.70	0.00	0.00
K4-57,2AmpProfil1	41.65	0.51	14.42	0.02	16.24	0.03	10.38	11.25	2.26	1.42	98.17	0.01	0.00
K4-57,2AmpProfil1	42.07	0.57	14.02	0.02	16.90	0.04	10.53	11.35	2.23	1.60	99.33	0.01	0.00
K4-57,2amp2	47.83	0.63	18.39	0.04	10.13	0.00	5.72	9.61	4.79	1.14	98.27	0.01	0.00
K4-57,1ampProfil1 [190]	43.18	0.34	13.66	0.00	15.76	0.05	10.41	10.23	2.10	1.04	96.75	0.02	0.00
K4-57,1ampProfil1	44.86	0.37	11.44	0.00	15.96	0.03	12.07	11.02	2.26	0.94	98.93	0.01	0.00
K4-57,1ampProfil1	46.20	0.28	10.49	0.03	15.77	0.05	12.56	10.77	2.23	0.82	99.19	0.01	0.00
K4-57,1ampProfil1	45.53	0.26	11.09	0.05	15.59	0.04	12.42	10.95	2.25	0.95	99.12	0.00	0.00
K4-57,1ampProfil1	49.48	0.26	10.19	0.04	15.04	0.06	11.40	10.24	2.01	0.89	99.60	0.00	0.01
K4-57,1ampProfil1	45.01	0.36	10.99	0.00	15.62	0.03	12.28	11.04	2.22	1.04	98.59	0.00	0.00
K4-57,1ampProfil1	47.35	0.27	9.65	0.00	15.69	0.01	13.24	10.37	2.10	0.78	99.46	0.01	0.00
K4-57,1ampProfil1	46.99	0.30	9.97	0.00	15.86	0.04	12.79	9.93	1.89	0.84	98.61	0.00	0.00
K4-57,1ampProfil2 [70]	43.54	1.43	13.20	0.03	15.37	0.02	10.96	11.11	2.39	1.27	99.31	0.01	0.00
K4-57,1ampProfil2	43.80	1.34	12.85	0.01	15.16	0.02	11.34	11.23	2.46	1.18	99.39	0.00	0.00
K4-57,1ampProfil2	44.48	1.38	12.16	0.03	14.81	0.02	11.61	10.83	2.42	1.16	98.90	0.00	0.00
K4-57,1ampProfil2	44.67	1.47	12.14	0.03	14.24	0.05	11.92	10.96	2.31	1.11	98.91	0.00	0.00
K4-57,1ampProfil2	44.03	1.63	12.24	0.01	13.94	0.01	11.96	10.96	2.48	1.11	98.37	0.00	0.00
K4-57,1ampProfil2	44.28	1.60	12.13	0.06	13.96	0.04	12.13	11.02	2.55	1.20	98.97	0.00	0.00
K4-57,1ampProfil2	44.34	1.70	12.36	0.08	13.89	0.02	12.11	11.19	2.52	1.26	99.47	0.01	0.00
K4-58,1AmpProfil1 [180]	42.49	0.93	12.70	0.04	18.28	0.00	9.81	10.38	2.73	1.35	98.70	0.00	0.08
K4-58,1AmpProfil1	40.31	0.48	17.22	0.02	25.23	0.33	6.77	8.14	1.54	0.70	100.72	0.01	0.00
K4-58,1AmpProfil1	42.23	0.86	13.44	0.00	18.58	0.08	9.77	9.80	2.75	1.46	98.96	0.01	0.04
K4-58,1AmpProfil1	41.83	0.86	13.44	0.04	19.04	0.04	9.50	9.66	2.84	1.43	98.68	0.01	0.03
K4-58,1AmpProfil1	41.80	0.86	13.68	0.01	18.58	0.06	9.41	9.65	2.93	1.45	98.43	0.01	0.02
K4-58,1AmpProfil1	41.95	0.88	13.47	0.00	18.82	0.06	9.47	9.78	2.74	1.52	98.68	0.01	0.06
K4-58,1AmpProfil1	42.34	0.94	13.18	0.05	18.33	0.05	9.77	9.63	2.87	1.49	98.64	0.00	0.06
K4-58,1AmpProfil1	42.14	1.09	12.82	0.01	18.63	0.08	9.82	10.09	2.83	1.47	98.98	0.00	0.07
K4-58,1AmpProfil1	42.52	1.28	12.55	0.06	16.90	0.05	9.85	10.68	2.73	1.17	97.79	0.00	0.00
K4-58,1AmpProfil1	62.76	0.05	21.51	0.00	0.60	0.00	0.13	3.46	9.68	0.35	98.53	0.02	0.00
K4-58,2ampProfil1 [250]	42.80	0.80	11.90	0.01	18.80	0.04	9.92	9.87	2.60	1.21	97.96	0.01	0.06
K4-58,2ampProfil1	42.83	0.83	12.28	0.00	18.37	0.03	9.89	10.01	2.64	1.16	98.04	0.01	0.05
K4-58,2ampProfil1	43.22	0.76	11.97	0.03	18.92	0.02	9.93	9.73	2.62	1.28	98.47	0.01	0.03
K4-58,2ampProfil1	42.89	0.73	12.06	0.02	19.14	0.06	9.94	9.62	2.63	1.30	98.38	0.01	0.02
K4-58,2ampProfil1	43.14	0.76	11.96	0.01	18.75	0.04	9.88	9.64	2.74	1.28	98.20	0.01	0.06
K4-58,2ampProfil1	43.80	0.77	11.53	0.02	19.13	0.06	10.42	10.11	2.42	1.20	99.46	0.00	0.04
K4-58,2ampProfil1	43.54	0.77	11.88	0.03	18.70	0.05	10.29	10.13	2.49	1.13	99.01	0.00	0.00
K4-58,2ampProfil1	43.09	0.74	11.85	0.00	17.42	0.01	10.24	10.05	2.48	1.13	97.01	0.03	0.06
K4-58,2ampProfil1	43.37	0.71	12.01	0.04	18.04	0.08	10.15	10.47	2.50	1.19	98.55	0.00	0.02
K4-58,2ampProfil1	44.46	0.66	10.36	0.00	17.82	0.03	11.19	9.22	2.15	1.03	96.90	0.02	0.02
K4-58,2ampProfil1	43.80	0.71	11.39	0.00	17.77	0.09	10.56	10.35	2.49	1.00	98.16	0.00	0.05
K4-58,2ampProfil1	43.11	0.77	11.72	0.07	18.17	0.07	10.06	10.62	2.45	1.21	98.24	0.00	0.00
K4-58,2ampProfil1	42.92	0.64	12.02	0.02	18.40	0.05	9.60	10.72	2.52	1.12	98.02	0.01	0.06
K4-60ampProfil1 [490]	45.00	0.57	10.16	0.01	16.38	0.10	11.98	8.95	2.78	0.44	96.37	0.00	0.05
K4-60ampProfil1	44.71	0.59	10.50	0.01	16.57	0.12	11.82	8.85	3.03	0.47	96.66	0.01	0.09

K4-60ampProfil1	44.94	0.53	10.62	0.00	17.04	0.06	11.98	8.70	3.01	0.46	97.33	0.01	0.05
K4-60ampProfil1	44.63	0.54	11.06	0.00	16.31	0.09	11.70	9.26	3.27	0.35	97.20	0.01	0.04
K4-60ampProfil1	45.20	0.56	10.59	0.01	16.39	0.17	11.83	8.80	2.87	0.36	96.78	0.01	0.05
K4-60ampProfil1	45.35	0.55	10.55	0.03	16.57	0.08	11.90	8.69	3.19	0.42	97.34	0.01	0.13
K4-60ampProfil1	45.25	0.51	10.45	0.02	16.77	0.09	12.00	8.55	3.05	0.49	97.16	0.01	0.10
K4-60ampProfil1	45.01	0.56	10.50	0.00	17.35	0.11	11.59	8.96	3.08	0.44	97.60	0.01	0.06
K4-60ampProfil1	44.65	0.52	10.44	0.01	15.77	0.08	11.46	9.47	3.18	0.44	96.01	0.01	0.03
K4-60ampProfil1	44.17	0.69	10.83	0.02	16.26	0.08	11.53	9.82	3.14	0.41	96.95	0.02	0.08
K4-76,2AmpProf1 [220]	43.16	1.17	12.85	n.d.	15.66	0.06	11.32	11.58	2.46	0.80	99.06	0.01	0.00
K4-76,2AmpProf1	42.19	1.21	13.43	n.d.	16.16	0.04	11.03	11.48	2.56	0.86	98.95	0.00	0.00
K4-76,2AmpProf1	42.06	1.25	13.39	n.d.	16.45	0.02	11.09	11.35	2.68	0.90	99.21	0.02	0.00
K4-76,2AmpProf1	42.14	1.29	13.39	n.d.	16.04	0.07	10.93	11.32	2.64	0.96	98.77	0.00	0.00
K4-76,2AmpProf1	42.32	1.35	13.74	n.d.	16.22	0.05	10.97	11.04	2.76	1.02	99.48	0.01	0.00
K4-76,2AmpProf1	42.21	1.32	13.83	n.d.	16.39	0.05	10.94	11.03	2.65	1.08	99.49	0.02	0.00
K4-76,2AmpProf1	42.16	1.40	13.94	n.d.	15.97	0.09	10.88	10.95	2.68	1.06	99.13	0.02	0.00
K4-76,2AmpProf1	42.24	1.38	14.14	n.d.	16.19	0.06	10.71	10.91	2.82	1.12	99.55	0.02	0.00
K4-76,2AmpProf1	42.31	1.37	14.17	n.d.	16.27	0.05	10.79	10.72	2.80	1.16	99.64	0.01	0.00
K4-76,2AmpProf1	42.15	1.30	14.29	n.d.	16.46	0.09	10.80	10.79	2.68	1.17	99.72	0.02	0.00
K4-76,2AmpProf1	41.69	1.40	14.34	n.d.	16.31	0.10	10.70	10.58	2.72	1.19	99.03	0.01	0.00
K4-76,2AmpProf1	42.03	1.35	14.37	n.d.	16.62	0.13	10.56	10.55	2.86	1.24	99.69	0.00	0.00
K4-76,2AmpProf1	42.29	1.38	14.44	n.d.	16.28	0.10	10.65	10.38	2.79	1.26	99.57	0.01	0.00
K4-76,2AmpProf1	39.13	1.25	13.39	n.d.	15.86	0.07	9.78	9.39	2.42	1.16	92.45	0.04	0.00
K4-76,2AmpProf1	40.17	1.27	13.68	n.d.	15.76	0.13	9.87	9.58	2.44	1.25	94.14	0.06	0.00
K4-76,2AmpProf1	42.17	1.36	14.68	n.d.	16.01	0.05	10.62	10.57	2.74	1.30	99.51	0.00	0.00
K4-76,2AmpProf1	41.96	1.38	14.68	n.d.	16.18	0.06	10.32	10.44	2.86	1.31	99.19	0.01	0.00
K4-76,2AmpProf1	42.08	1.37	14.65	n.d.	16.62	0.05	10.51	10.49	2.77	1.34	99.88	0.01	0.00
K4-76,2AmpProf1	41.65	1.43	14.67	n.d.	16.11	0.13	10.37	10.41	2.75	1.31	98.83	0.01	0.00
K4-76,2AmpProf1	41.99	1.39	14.86	n.d.	16.14	0.07	10.49	10.50	2.62	1.28	99.33	0.01	0.00
K4-76,2AmpProf1	42.26	1.30	15.22	n.d.	16.00	0.07	10.99	10.79	2.78	0.99	100.40	0.01	0.00
K4-84,1AmpProfil1 [230]	40.42	0.19	19.75	n.d.	12.83	0.08	9.48	11.23	2.15	1.37	97.49	0.00	0.00
K4-84,1AmpProfil1	43.75	0.18	15.92	n.d.	11.82	0.03	11.54	11.24	2.06	0.79	97.32	0.00	0.00
K4-84,1AmpProfil1	49.12	0.13	10.88	n.d.	10.36	0.09	14.43	10.92	1.66	0.38	97.96	0.01	0.00
K4-84,1AmpProfil1	50.84	0.12	8.84	n.d.	10.27	0.12	15.66	10.06	1.33	0.31	97.56	0.00	0.00
K4-84,1AmpProfil1	51.40	0.15	7.96	n.d.	10.52	0.09	16.02	9.57	1.25	0.27	97.21	0.00	0.00
K4-84,1AmpProfil1	51.53	0.16	8.23	n.d.	9.88	0.03	15.87	9.46	1.41	0.33	96.90	0.01	0.00
K4-84,1AmpProfil1	51.45	0.15	8.28	n.d.	9.91	0.03	15.98	9.50	1.43	0.36	97.09	0.01	0.00
K4-84,1AmpProfil1	52.04	0.16	8.61	n.d.	9.10	0.06	16.20	9.94	1.48	0.34	97.92	0.00	0.00
K4-84,1AmpProfil1	51.19	0.17	8.65	n.d.	8.81	0.05	16.28	9.87	1.59	0.34	96.95	0.00	0.00
K4-84,1AmpProfil1	51.75	0.15	8.38	n.d.	8.82	0.02	16.44	9.92	1.45	0.36	97.28	0.01	0.00
K4-84,1AmpProfil1	52.18	0.17	8.25	n.d.	8.25	0.01	16.74	10.34	1.54	0.37	97.84	0.01	0.00
K4-84,1AmpProfil1	51.71	0.16	8.16	n.d.	8.26	0.00	16.81	10.02	1.50	0.36	96.98	0.00	0.00
K4-84,1AmpProfil1	51.90	0.15	8.15	n.d.	8.29	0.00	16.90	9.99	1.49	0.36	97.23	0.00	0.00
K4-84,1AmpProfil1	52.29	0.17	8.17	n.d.	7.81	0.00	16.87	10.14	1.63	0.34	97.43	0.00	0.00
K4-84,1AmpProfil1	51.77	0.18	7.74	n.d.	8.39	0.00	17.21	10.18	1.36	0.34	97.17	0.00	0.00
K4-84,1AmpProfil1	51.39	0.19	8.31	n.d.	7.80	0.03	16.95	10.93	1.57	0.28	97.45	0.01	0.00
K4-84,1AmpProfil1	51.38	0.18	8.66	n.d.	7.87	0.01	17.03	10.44	1.52	0.32	97.40	0.00	0.00
K4-84,1AmpProfil1	51.72	0.19	8.42	n.d.	7.88	0.07	16.86	10.12	1.40	0.32	96.99	0.00	0.00
K4-84,1AmpProfil1	52.02	0.15	8.23	n.d.	8.17	0.02	16.77	9.88	1.53	0.32	97.09	0.00	0.00
K4-84,1AmpProfil1	51.90	0.16	8.17	n.d.	8.20	0.04	16.99	9.99	1.56	0.31	97.33	0.00	0.00
K4-84,1AmpProfil1	51.74	0.16	8.32	n.d.	8.11	0.03	16.85	10.24	1.47	0.31	97.21	0.01	0.00
K4-84,1AmpProfil1	51.92	0.17	8.31	n.d.	8.34	0.01	16.70	10.01	1.57	0.36	97.37	0.01	0.00
K4-84,1Amp1	40.72	1.38	16.64	n.d.	13.42	0.04	12.03	7.78	1.09	2.90	95.99	0.01	0.00
K4-84,1Amp2	50.46	0.36	7.86	n.d.	10.21	0.10	15.19	11.12	1.34	0.33	96.95	0.01	0.00
K4-84,1Amp3	42.91	0.86	14.08	n.d.	13.41	0.08	11.11	11.78	1.84	1.20	97.27	0.02	0.00
K4-84,1AmpSympl1	42.33	0.48	15.39	n.d.	12.86	0.04	11.11	11.86	2.00	1.23	97.30	0.00	0.00
K4-84,1AmpSympl2	59.76	0.01	25.24	n.d.	0.22	0.01	0.00	6.74	8.04	0.14	100.15	0.01	0.00
K4-84,1Amp4	51.27	0.17	7.75	n.d.	10.07	0.12	16.15	10.53	1.27	0.32	97.65	0.00	0.00
K4-84,4Amp1	51.74	0.21	6.13	n.d.	16.02	0.29	12.07	12.00	0.64	0.15	99.25	0.02	0.00
K4-84,4Amp2	50.30	0.25	5.72	n.d.	17.01	0.29	11.30	12.19	0.44	0.16	97.65	0.00	0.00
K4-84,4Amp3	50.73	0.23	5.75	n.d.	16.19	0.27	11.74	12.18	0.52	0.12	97.72	0.00	0.00
K4-84,4Amp4	50.17	0.31	6.15	n.d.	16.85	0.32	11.57	12.08	0.52	0.15	98.11	0.01	0.00
K4-84,4Amp5	50.75	0.30	5.13	n.d.	16.60	0.37	11.50	12.17	0.39	0.15	97.33	0.01	0.00
K4-84,4Amp9	50.90	0.21	4.78	n.d.	17.43	0.27	11.46	12.18	0.49	0.12	97.84	0.00	0.00
K4-982_2,1Amp1	47.78	0.33	8.20	n.d.	14.20	0.14	13.45	10.75	2.27	0.02	97.13	0.01	0.00
K4-982_2,1Amp3	47.49	0.30	8.25	n.d.	13.93	0.15	13.98	11.05	2.29	0.02	97.45	0.01	0.00
K4-982_2,1Amp4	40.28	0.40	16.16	n.d.	15.47	0.15	10.32	10.28	3.79	0.05	96.88	0.01	0.00
K4-982_2,1Amp5	44.85	0.42	11.78	n.d.	14.31	0.11	12.08	11.18	2.68	0.07	97.48	0.00	0.00
K4-982_2,1Amp6	46.90	0.32	13.41	n.d.	10.81	0.11	12.92	9.75	3.18	0.20	97.60	0.01	0.00
K4-982_2,1Amp7	45.26	0.24	14.57	n.d.	12.52	0.17	11.90	9.93	3.33	0.15	98.07	0.03	0.00
K4-982_2,1Amp8	46.80	0.36	13.52	n.d.	9.71	0.05	13.83	9.91	3.37	0.17	97.72	0.03	0.00
K4-982_2,1Amp9	47.94	0.44	12.42	n.d.	8.76	0.01	14.56	9.78	3.02	0.20	97.13	0.04	0.00
K4-982_2,1Amp10	47.90	0.90	12.59	n.d.	9.14	0.00	13.98	9.82	3.25	0.21	97.78	0.04	0.00
K4-982_2,1Amp11	48.67	0.28	12.01	n.d.	9.09	0.05	14.65	9.59	3.18	0.17	97.66	0.02	0.00
K4-982_2,1Amp13	46.89	0.45	13.35	n.d.	8.76	0.01	14.05	10.72	3.21	0.25	97.68	0.01	0.00
K4-982_2,1Amp12	48.51	0.27	12.51	n.d.	8.94	0.00	14.47	9.54	3.08	0.19	97.51	0.02	0.00

K4-982_2,2Amp1	54.87	0.34	8.50	n.d.	5.29	0.03	9.98	16.04	5.16	0.00	100.21	0.01	0.00
K4-982_2,2Amp2	54.83	0.18	9.53	n.d.	4.58	0.03	9.71	16.01	5.53	0.00	100.40	0.00	0.00
K4-981_2,1AmpAnRtProf1 [200]	43.29	1.54	16.26	n.d.	9.88	0.00	12.21	10.56	3.52	0.39	97.67	0.03	0.00
K4-981_2,1AmpAnRtProf1	43.13	1.27	16.26	n.d.	10.06	0.01	11.88	10.50	3.38	0.44	96.93	0.02	0.00
K4-981_2,1AmpAnRtProf1	45.73	0.96	14.19	n.d.	9.36	0.03	13.20	10.26	3.37	0.32	97.42	0.02	0.00
K4-981_2,1AmpAnRtProf1	45.91	0.89	14.09	n.d.	9.24	0.00	13.33	10.24	3.48	0.31	97.51	0.01	0.00
K4-981_2,1AmpAnRtProf1	46.36	0.69	13.76	n.d.	9.20	0.04	13.56	10.04	3.22	0.29	97.17	0.02	0.00
K4-981_2,1AmpAnRtProf1	47.09	0.47	12.93	n.d.	9.19	0.04	14.00	9.87	3.13	0.32	97.04	0.01	0.00
K4-981_2,1AmpAnRtProf1	48.26	0.40	12.16	n.d.	9.25	0.06	14.18	9.58	3.13	0.35	97.36	0.01	0.00
K4-981_2,1AmpAnRtProf1	47.91	0.38	11.92	n.d.	9.45	0.02	14.40	9.75	3.01	0.31	97.15	0.02	0.00
K4-981_2,1AmpAnRtProf1	47.94	0.36	12.04	n.d.	9.02	0.02	14.41	9.82	3.04	0.35	97.00	0.04	0.00
K4-981_2,1AmpAnRtProf1	47.51	0.38	12.81	n.d.	8.86	0.03	14.14	9.77	3.29	0.33	97.12	0.03	0.00
K4-981_2,1AmpAnRtProf1	46.59	0.40	13.52	n.d.	9.48	0.04	13.90	9.98	3.27	0.28	97.47	0.02	0.00
K4-981_2,1AmpAnRtProf1	47.04	0.36	13.09	n.d.	9.10	0.00	14.11	10.03	3.13	0.30	97.16	0.01	0.00
K4-981_2,1AmpAnRtProf1	46.57	0.34	13.77	n.d.	9.38	0.03	13.89	9.98	3.28	0.29	97.53	0.02	0.00
K4-981_2,1AmpAnRtProf1	46.83	0.36	13.52	n.d.	9.29	0.02	13.71	9.92	3.44	0.26	97.35	0.02	0.00
K4-981_2,1AmpAnRtProf1	47.41	0.31	13.21	n.d.	9.12	0.05	14.03	9.88	3.39	0.27	97.68	0.02	0.00
K4-981_2,1AmpAnRtProf1	47.33	0.34	13.16	n.d.	8.91	0.07	14.01	9.80	3.23	0.25	97.09	0.02	0.00
K4-981_2,1AmpAnRtProf1	47.50	0.33	13.23	n.d.	9.05	0.00	14.07	9.88	3.26	0.27	97.58	0.04	0.00
K4-981_2,1AmpAnRtProf1	47.69	0.36	13.03	n.d.	8.96	0.04	14.19	9.70	3.30	0.30	97.56	0.02	0.00
K4-981_2,1AmpAnRtProf1	46.91	0.35	13.71	n.d.	9.20	0.03	13.75	9.64	3.32	0.29	97.19	0.02	0.00
K4-981_2,1AmpAnRtProf2 [300]	43.96	2.88	13.98	n.d.	9.31	0.06	12.70	10.55	3.35	0.45	97.25	0.03	0.00
K4-981_2,1AmpAnRtProf2	46.37	1.64	13.12	n.d.	8.93	0.02	13.47	9.68	3.45	0.34	97.02	0.02	0.00
K4-981_2,1AmpAnRtProf2	47.15	1.17	12.96	n.d.	8.99	0.02	13.79	9.85	3.38	0.36	97.68	0.02	0.00
K4-981_2,1AmpAnRtProf2	47.40	0.97	13.02	n.d.	8.53	0.06	13.68	9.69	3.30	0.30	96.95	0.02	0.00
K4-981_2,1AmpAnRtProf2	47.55	0.84	12.96	n.d.	8.81	0.04	13.91	9.71	3.35	0.33	97.50	0.01	0.00
K4-981_2,1AmpAnRtProf2	47.62	0.74	12.82	n.d.	8.86	0.07	13.87	9.57	3.34	0.37	97.25	0.01	0.00
K4-981_2,1AmpAnRtProf2	47.80	0.70	12.81	n.d.	8.82	0.00	13.93	9.63	3.33	0.40	97.41	0.02	0.00
K4-981_2,1AmpAnRtProf2	47.70	0.61	12.56	n.d.	8.81	0.05	13.93	9.61	3.20	0.38	96.84	0.02	0.00
K4-981_2,1AmpAnRtProf2	47.95	0.54	12.62	n.d.	8.74	0.00	14.10	9.62	3.16	0.43	97.16	0.01	0.00
K4-981_2,1AmpAnRtProf2	47.84	0.46	12.58	n.d.	8.77	0.07	14.18	9.53	3.05	0.42	96.88	0.02	0.00
K4-981_2,1AmpAnRtProf2	47.99	0.45	12.53	n.d.	8.64	0.02	14.07	9.52	3.13	0.47	96.81	0.00	0.00
K4-981_2,1AmpAnRtProf2	48.12	0.47	12.45	n.d.	8.82	0.05	14.17	9.58	3.21	0.43	97.29	0.02	0.00
K4-981_2,1AmpAnRtProf2	48.36	0.44	12.24	n.d.	8.73	0.03	14.14	9.49	3.18	0.45	97.06	0.02	0.00
K4-981_2,1AmpAnRtProf2	47.98	0.42	12.25	n.d.	8.88	0.03	14.23	9.54	2.99	0.48	96.80	0.01	0.00
K4-981_2,1AmpAnRtProf2	48.31	0.40	12.36	n.d.	8.85	0.00	14.31	9.71	3.12	0.48	97.53	0.01	0.00
K4-981_2,1AmpAnRtProf2	47.83	0.39	12.55	n.d.	8.97	0.03	14.13	9.58	3.25	0.36	97.08	0.01	0.00
K4-981_2,1AmpAnRtProf2	47.82	0.37	12.43	n.d.	8.70	0.02	14.22	9.74	3.19	0.34	96.84	0.02	0.00
K4-981_2,1AmpAnRtProf2	48.07	0.36	12.33	n.d.	8.84	0.02	14.31	9.65	3.15	0.37	97.09	0.02	0.00
K4-981_2,1AmpAnRtProf2	48.17	0.37	12.35	n.d.	8.81	0.00	14.31	9.56	3.13	0.38	97.08	0.01	0.00
K4-981_2,1AmpAnRtProf2	47.25	0.39	12.20	n.d.	8.78	0.03	13.87	9.57	3.13	0.34	95.54	0.01	0.00
K4-981_2,1AmpAnRtProf2	47.70	0.43	12.26	n.d.	8.95	0.00	14.25	9.62	3.16	0.31	96.67	0.02	0.00
K4-981_2,1AmpAnRtProf2	45.64	0.44	14.48	n.d.	9.56	0.00	13.57	9.55	3.51	0.42	97.16	0.03	0.00
K4-981_2,1AmpAnRtProf2	47.26	0.39	12.68	n.d.	8.85	0.04	14.15	9.79	3.10	0.31	96.56	0.02	0.00
K4-981_2,1AmpAnRtProf2	48.00	0.38	12.50	n.d.	9.10	0.00	14.25	9.68	3.18	0.30	97.37	0.02	0.00
K4-981_2,1AmpAnRtProf2	48.16	0.40	12.65	n.d.	8.71	0.05	14.20	9.50	3.21	0.32	97.21	0.00	0.00
K4-981_2,1AmpAnRtProf2	47.95	0.38	12.60	n.d.	8.69	0.02	14.21	9.67	3.29	0.31	97.12	0.01	0.00
K4-981_2,1AmpAnRtProf2	47.67	0.37	12.61	n.d.	8.99	0.04	14.18	9.68	3.31	0.34	97.18	0.02	0.00
K4-981_2,1AmpAnRtProf2	47.99	0.37	12.49	n.d.	8.96	0.03	14.35	9.94	3.14	0.32	97.58	0.02	0.00
K4-981_2,1AmpAnRtProf2	48.07	0.35	12.35	n.d.	8.59	0.02	14.47	9.85	2.98	0.31	96.98	0.01	0.00
K4-981_2,1AmpAnRtProf2	47.91	0.35	12.38	n.d.	8.73	0.06	14.46	9.80	3.09	0.29	97.06	0.02	0.00
K4-981_2,1AmpAnRtProf2	46.75	0.39	13.82	n.d.	9.26	0.00	13.63	9.95	3.30	0.33	97.43	0.03	0.00
K4-981_2,1TiInAmp1	47.36	0.85	12.78	n.d.	8.78	0.03	14.00	9.72	3.26	0.33	97.11	0.02	0.00
K4-99/2GruenA1	41.46	0.51	14.33	0.00	18.95	0.16	8.85	10.24	3.20	0.87	98.58	0.01	0.00
K4-99/2GruenA2	41.00	0.45	14.83	0.01	18.81	0.13	8.76	10.59	3.21	0.91	98.70	0.02	0.00
K4-99/2GruenA3	40.42	0.96	14.12	0.04	18.68	0.11	9.24	11.40	2.99	0.87	98.82	0.02	0.00
K4-99/2GruenA4	39.87	0.63	17.05	0.02	18.12	0.04	8.00	10.37	3.61	0.84	98.55	0.02	0.00
K4-99/2GruenA5	39.62	0.75	17.92	0.02	16.87	0.07	8.28	10.75	3.26	1.02	98.54	0.04	0.00
K4-99/2GruenA6	41.35	2.38	16.16	0.01	13.02	0.07	10.45	11.29	3.18	1.12	99.02	0.02	0.00
K4-99/1GruenAInSympl1	41.56	0.80	12.40	0.02	20.03	0.08	8.85	11.24	2.99	0.58	98.56	0.01	0.00
K4-99/1GruenAInSympl2	42.06	0.71	13.04	0.00	19.70	0.08	8.63	10.82	3.10	0.72	98.84	0.00	0.00
K4-99/1GruenAInSympl3	41.58	0.54	13.41	0.02	20.18	0.05	8.35	10.97	3.08	0.64	98.81	0.02	0.00
K4-99/1GruenAInSympl4	40.33	0.57	14.63	0.03	20.13	0.09	7.99	11.12	3.13	0.68	98.68	0.01	0.00
K4-99,1Amp1	42.98	1.82	15.35	n.d.	10.19	0.03	12.52	11.07	3.20	0.71	97.88	0.00	0.00
K4-99,1Amp2	43.15	1.73	14.64	n.d.	10.33	0.05	12.43	11.22	3.34	0.63	97.52	0.01	0.00
K4-99,1Amp3	41.88	1.95	15.81	n.d.	10.93	0.05	11.84	11.17	3.28	0.80	97.71	0.01	0.00
K4-99,1Amp4	42.23	1.92	14.73	n.d.	11.62	0.07	11.60	11.16	3.09	0.65	97.05	0.01	0.00
K4-99,1Amp5	41.70	1.33	13.31	n.d.	15.19	0.03	10.43	11.46	2.98	0.42	96.84	0.00	0.00
K4-99,1Amp7	39.39	1.73	18.95	n.d.	12.04	0.10	9.93	10.72	3.62	0.59	97.06	0.01	0.00
K4-99,1Amp9	39.77	0.31	15.13	n.d.	19.89	0.04	7.53	11.33	3.01	0.39	97.38	0.01	0.00
K4-105_1AmpMitRtProfI1 [100]	43.51	1.70	14.04	n.d.	11.67	0.03	12.69	10.15	3.37	0.37	97.52	0.01	0.00
K4-105_1AmpMitRtProfI1	45.86	1.14	12.00	n.d.	11.60	0.05	13.98	9.67	2.92	0.37	97.57	0.00	0.00
K4-105_1AmpMitRtProfI1	46.32	0.94	11.85	n.d.	10.96	0.06	14.00	9.86	2.98	0.37	97.34	0.00	0.00
K4-105_1AmpMitRtProfI1	46.34	0.87	12.27	n.d.	10.92	0.05	13.79	9.67	2.96	0.36	97.21	0.00	0.00
K4-105_1AmpMitRtProfI1	46.16	0.89	12.46	n.d.	11.03	0.07	13.62	9.54	3.11	0.34	97.20	0.00	0.00
K4-105_1AmpMitRtProfI1	46.35	0.96	12.28	n.d.	11.24	0.11	13.68	9.82	3.16	0.35	97.96	0.00	0.00

K4-105_1AmpMitRtProfl1	46.51	1.10	12.15	n.d.	10.62	0.02	13.67	9.80	3.04	0.35	97.25	0.00	0.00
K4-105_1AmpMitRtProfl1	46.10	1.26	12.32	n.d.	10.89	0.03	13.64	10.35	2.98	0.35	97.93	0.00	0.00
K4-105_1AmpMitRtProfl1	43.41	1.56	15.26	n.d.	10.37	0.00	12.63	10.80	3.13	0.34	97.49	0.00	0.00
K4-105_1AmpMitRtProfl2 [140]	45.16	1.84	12.23	n.d.	10.31	0.01	14.14	10.08	3.14	0.37	97.28	0.00	0.00
K4-105_1AmpMitRtProfl2	44.18	1.77	13.31	n.d.	10.53	0.05	13.60	10.56	3.20	0.43	97.63	0.02	0.00
K4-105_1AmpMitRtProfl2	44.06	1.55	13.53	n.d.	11.19	0.07	13.24	10.26	3.24	0.39	97.53	0.00	0.00
K4-105_1AmpMitRtProfl2	43.92	1.36	13.41	n.d.	11.30	0.04	13.38	10.45	3.20	0.42	97.47	0.01	0.00
K4-105_1AmpMitRtProfl2	45.34	1.09	12.43	n.d.	11.15	0.11	13.93	9.88	3.27	0.38	97.57	0.00	0.00
K4-105_1AmpMitRtProfl2	45.89	0.73	12.11	n.d.	11.61	0.08	14.01	9.52	3.11	0.34	97.39	0.00	0.00
K4-105_1AmpMitRtProfl2	45.45	0.53	12.87	n.d.	11.74	0.06	13.88	9.55	3.17	0.35	97.59	0.01	0.00
K4-105_1AmpMitRtProfl2	45.40	0.40	13.52	n.d.	11.38	0.07	13.65	9.29	3.14	0.35	97.19	0.00	0.00
K4-105_1AmpMitRtProfl2	45.92	0.41	12.79	n.d.	12.02	0.08	13.78	9.27	3.30	0.32	97.88	0.00	0.00
K4-105_1AmpMitRtProfl2	45.86	0.43	12.94	n.d.	11.99	0.06	13.48	9.12	3.28	0.36	97.53	0.01	0.00
K4-105_1AmpMitRtProfl2	46.23	0.45	12.68	n.d.	11.49	0.03	13.71	9.03	3.09	0.36	97.06	0.00	0.00
K4-105_1AmpMitRtProfl2	46.34	0.44	12.38	n.d.	11.85	0.10	13.79	9.03	3.13	0.40	97.45	0.00	0.00
K4-105_1AmpMitRtProfl2	44.34	0.56	14.09	n.d.	11.84	0.06	13.11	9.69	3.28	0.38	97.33	0.00	0.00
K4-105_2Amp2	38.66	11.13	11.06	n.d.	13.34	0.12	10.42	10.63	1.71	1.07	98.13	0.02	0.00
K4-105_2Amp3	43.02	1.33	12.13	n.d.	15.07	0.10	11.11	11.58	2.03	1.25	97.64	0.00	0.00
K4-105_2Amp4	43.67	1.21	11.64	n.d.	14.50	0.12	11.56	11.57	1.74	1.13	97.14	0.00	0.00
K4-105_2Amp5	42.95	1.16	12.16	n.d.	14.86	0.14	11.33	11.66	1.82	1.24	97.31	0.01	0.00
K4-105_2AmpeProfil1 [90]	39.32	0.07	21.70	n.d.	21.88	0.62	6.82	9.64	0.04	0.00	100.08	0.00	0.00
K4-105_2AmpeProfil1	39.00	0.07	21.50	n.d.	23.80	0.97	5.67	9.55	0.01	0.00	100.57	0.02	0.00
K4-105_2AmpeProfil1	40.63	0.92	15.11	n.d.	15.12	0.25	9.37	11.33	1.82	1.19	95.74	0.01	0.00
K4-105_2AmpeProfil1	41.81	1.10	14.19	n.d.	14.74	0.12	10.43	11.36	2.03	1.38	97.17	0.01	0.00
K4-105_2AmpeProfil1	41.91	1.12	14.13	n.d.	14.77	0.11	10.43	11.27	2.00	1.34	97.08	0.01	0.00
K4-105_2AmpeProfil1	42.12	1.08	13.85	n.d.	14.74	0.10	10.48	11.44	2.03	1.26	97.10	0.01	0.00
K4-105_2AmpeProfil1	41.10	1.12	14.35	n.d.	14.92	0.16	9.99	11.39	1.92	1.27	96.22	0.02	0.00
K4-105_2AmpeProfil1	43.55	1.11	12.69	n.d.	14.21	0.08	11.21	11.11	2.06	1.16	97.18	0.00	0.00
K4-105_2AmpeProfil1	45.07	0.96	11.32	n.d.	13.59	0.11	12.10	11.19	1.97	1.02	97.31	0.00	0.00
K4-105_2Amp8	42.08	1.88	13.27	n.d.	14.23	0.14	10.47	11.55	2.05	1.30	96.97	0.00	0.00
K4-106/1GruenAProfil1 [250]	50.24	0.20	9.99	0.07	12.91	0.04	12.66	8.43	3.66	0.22	98.42	0.01	0.00
K4-106/1GruenAProfil1	50.63	0.19	9.81	0.03	13.08	0.01	12.79	8.53	3.70	0.23	99.00	0.01	0.00
K4-106/1GruenAProfil1	50.76	0.18	9.53	0.07	12.92	0.05	12.82	8.52	3.78	0.21	98.82	0.00	0.00
K4-106/1GruenAProfil1	51.40	0.17	9.02	0.04	12.77	0.01	13.12	8.59	3.69	0.21	99.01	0.01	0.00
K4-106/1GruenAProfil1	51.03	0.19	9.13	0.04	12.93	0.04	13.13	8.67	3.60	0.23	98.98	0.00	0.00
K4-106/1GruenAProfil1	51.03	0.17	9.03	0.06	12.94	0.03	13.30	8.63	3.56	0.23	98.98	0.00	0.01
K4-106/1GruenAProfil1	50.49	0.23	9.48	0.04	13.51	0.03	12.87	8.60	3.81	0.25	99.31	0.00	0.00
K4-106/1GruenAProfil1	50.62	0.19	10.00	0.04	13.47	0.12	12.57	8.50	3.73	0.24	99.47	0.01	0.00
K4-106/1GruenAProfil1	50.22	0.25	10.16	0.04	13.50	0.02	12.36	8.31	3.85	0.25	98.95	0.00	0.00
K4-106/1GruenAProfil1	50.34	0.22	10.15	0.06	13.42	0.03	12.42	8.41	3.88	0.25	99.18	0.00	0.00
K4-106/1GruenAProfil1	50.24	0.20	10.22	0.04	13.24	0.06	12.41	8.46	3.76	0.27	98.88	0.01	0.00
K4-106/1GruenAProfil1	50.27	0.23	10.31	0.02	13.60	0.02	12.36	8.63	3.94	0.26	99.64	0.00	0.00
K4-106/1GruenAProfil1	49.93	0.21	11.03	0.07	13.52	0.01	12.01	8.23	3.91	0.27	99.18	0.00	0.00
K4-106/1GruenAProfil1	49.57	0.23	11.12	0.06	13.24	0.04	11.91	8.36	3.88	0.29	98.70	0.00	0.00
K4-106/1GruenAProfil1	48.58	0.30	12.21	0.03	13.69	0.05	11.38	8.43	4.11	0.34	99.11	0.00	0.00
K4-106/1GruenAProfil1	47.66	0.28	13.23	0.04	14.22	0.05	10.96	8.53	4.11	0.39	99.46	0.01	0.00
K4-106/1LilaA2	53.63	0.10	9.85	0.04	7.82	0.05	8.37	14.69	5.18	0.05	99.78	0.03	0.00
K4-118b1BlauerA5	42.27	0.21	15.95	0.04	20.43	0.16	6.09	10.90	1.73	0.73	98.50	0.01	0.06
K4-120a3Amp1	41.61	0.38	12.81	n.d.	20.39	0.12	8.01	10.60	2.50	0.89	97.31	0.05	0.00
K4-120a3Amp2	41.28	0.54	12.86	n.d.	20.60	0.16	8.24	10.88	2.57	0.94	98.07	0.06	0.00
K4-120a3Amp3	41.95	0.74	12.07	n.d.	20.20	0.18	8.64	11.17	2.45	0.86	98.26	0.05	0.00
K4-120a3Amp4	43.70	0.74	9.98	n.d.	18.38	0.11	10.22	11.27	2.06	0.89	97.33	0.07	0.00
K4-120a1AmpBlauProfil1 [190]	46.14	0.18	8.53	n.d.	18.17	0.13	11.00	11.00	1.91	0.52	97.57	0.03	0.00
K4-120a1AmpBlauProfil1	45.70	0.21	9.18	n.d.	19.00	0.13	10.54	10.64	2.31	0.52	98.23	0.03	0.00
K4-120a1AmpBlauProfil1	45.87	0.21	9.82	n.d.	19.29	0.15	9.68	8.94	3.02	0.47	97.44	0.02	0.00
K4-120a1AmpBlauProfil1	46.89	0.15	8.94	n.d.	20.44	0.19	9.91	6.22	3.16	0.40	96.27	0.01	0.00
K4-120a1AmpBlauProfil1	46.68	0.19	9.85	n.d.	20.42	0.18	9.38	6.55	3.81	0.41	97.46	0.01	0.00
K4-120a1AmpBlauProfil1	47.90	0.19	9.63	n.d.	19.28	0.20	9.65	6.71	3.91	0.36	97.81	0.01	0.00
K4-120a1AmpBlauProfil1	48.15	0.19	9.17	n.d.	18.68	0.15	10.01	7.03	3.60	0.35	97.32	0.01	0.00
K4-120a1AmpBlauProfil1	47.79	0.18	9.37	n.d.	17.95	0.16	9.98	7.57	3.55	0.36	96.91	0.01	0.00
K4-120a1AmpBlauProfil1	48.33	0.15	9.02	n.d.	18.59	0.21	10.04	6.96	3.68	0.33	97.30	0.03	0.00
K4-120a1AmpBlauProfil1	48.05	0.17	9.35	n.d.	18.57	0.24	9.82	6.84	3.76	0.35	97.13	0.02	0.00
K4-120a1AmpBlauProfil1	48.29	0.18	9.33	n.d.	18.45	0.23	9.88	6.63	3.76	0.33	97.07	0.01	0.00
K4-120a1AmpBlauProfil1	48.84	0.17	9.34	n.d.	18.70	0.20	10.20	6.29	3.99	0.30	98.02	0.01	0.00
K4-120a1AmpBlauProfil1	47.13	0.18	9.48	n.d.	17.98	0.14	10.32	8.78	3.26	0.41	97.67	0.01	0.00
K4-120a1AmpBlauProfil1	46.13	0.17	8.67	n.d.	17.81	0.16	10.99	10.92	1.96	0.50	97.30	0.02	0.00
K4-120a1AmpBlauProfil1	46.60	0.16	8.19	n.d.	17.59	0.16	11.22	11.13	2.00	0.46	97.52	0.01	0.00
K4-120a1AmpBlauProfil1	47.14	0.18	7.78	n.d.	16.76	0.12	11.82	11.24	1.77	0.41	97.22	0.03	0.00
K4-120a1AmpBlauProfil1	46.24	0.24	7.95	n.d.	17.55	0.10	11.44	11.32	1.72	0.53	97.09	0.03	0.00
K4-120a1AmpBlauProfil1	45.11	0.28	9.23	n.d.	18.31	0.13	10.73	11.40	1.96	0.63	97.78	0.03	0.00
K4-120a1AmpBlau1	40.25	0.17	14.68	n.d.	21.71	0.21	6.51	9.77	3.00	0.73	97.02	0.03	0.00
K4-120a1AmpBlau2	45.46	0.13	10.90	n.d.	20.51	0.18	8.44	8.79	2.96	0.39	97.76	0.01	0.00
K4-120a1AmpBlau5	47.68	0.10	8.22	n.d.	16.32	0.15	11.50	10.68	1.98	0.31	96.92	0.00	0.00
K4-120a1AmpBlau6	44.55	0.22	10.07	n.d.	19.30	0.13	9.51	9.69	2.97	0.49	96.92	0.03	0.00
K4-120a1AmpBlau7	43.50	0.52	10.05	n.d.	19.50	0.04	9.34	10.99	2.28	0.85	97.05	0.02	0.00

K4-120a2AmpAnGrt1	40.53	0.16	15.38	n.d.	22.92	0.10	5.05	9.10	3.37	0.81	97.42	0.05	0.00
K4-120a2AmpAnGrt2	42.70	0.24	14.05	n.d.	19.95	0.06	6.96	10.79	2.46	0.69	97.89	0.07	0.00
K4-120a2AmpAnGrt3	41.64	0.43	13.00	n.d.	20.10	0.14	8.08	9.84	3.04	0.95	97.21	0.05	0.00
K4-120a2AmpAnGrt4	43.76	0.27	13.22	n.d.	20.83	0.19	6.95	8.47	3.68	0.51	97.88	0.03	0.00
K4-120b1LilaAProfil1 [ca 190]	52.05	0.09	10.64	0.04	14.67	0.07	10.20	7.36	4.45	0.23	99.80	0.01	0.00
K4-120b1LilaAProfil1	55.06	0.08	10.45	0.03	14.03	0.01	10.48	3.21	6.52	0.09	99.95	0.02	0.00
K4-120b1LilaAProfil1	54.88	0.06	10.31	0.03	14.05	0.08	10.39	3.17	6.61	0.07	99.65	0.00	0.16
K4-120b1LilaAProfil1	54.82	0.10	10.26	0.00	14.13	0.07	10.15	2.86	6.71	0.06	99.15	0.00	0.00
K4-120b1LilaAProfil1	51.50	0.14	9.67	0.04	15.77	0.08	10.90	5.92	5.11	0.20	99.34	0.01	0.03
K4-120b1LilaAProfil1	55.50	0.07	10.30	0.00	14.17	0.03	10.08	2.45	6.87	0.05	99.53	0.00	0.00
K4-120b1LilaAProfil1	56.06	0.05	10.51	0.04	13.78	0.05	9.89	2.09	7.19	0.05	99.71	0.01	0.00
K4-120b1LilaAProfil1	56.01	0.04	10.24	0.02	13.35	0.05	9.96	1.89	7.01	0.02	98.58	0.01	0.00
K4-120b1LilaAProfil1	55.96	0.06	10.22	0.00	13.71	0.04	10.17	2.46	6.99	0.07	99.67	0.00	0.00
K4-120b1LilaAProfil1	52.07	0.16	9.71	0.01	14.87	0.05	11.11	5.78	5.49	0.15	99.38	0.01	0.08
K4-120b1LilaAProfil1	51.47	0.18	9.21	0.00	14.99	0.07	11.97	6.92	4.78	0.23	99.81	0.00	0.09
K4-120b1LilaAProfil1	51.23	0.13	9.00	0.01	14.82	0.10	12.10	7.18	4.61	0.26	99.45	0.01	0.07
K4-120b1LilaAProfil1	51.24	0.19	9.11	0.02	14.39	0.08	11.99	7.06	4.57	0.27	98.91	0.00	0.02
K4-120b1LilaAProfil1	51.34	0.12	9.14	0.03	15.35	0.10	11.87	7.10	4.71	0.31	100.06	0.00	0.00
K4-120b1LilaAProfil1	50.91	0.16	9.36	0.07	15.36	0.09	11.52	7.32	4.44	0.29	99.52	0.01	0.08
K4-120b2lilaA1,1	46.57	0.12	14.18	0.03	16.46	0.07	9.45	8.24	4.38	0.49	99.98	0.04	0.08
K4-120b2lilaA1,2	46.83	0.17	13.74	0.03	16.41	0.10	9.30	8.97	4.04	0.61	100.18	0.01	0.05
K4-120b2lilaA2,1	44.81	0.35	15.35	0.02	17.16	0.06	8.62	7.79	4.80	0.47	99.42	0.01	0.03
K4-120b2lilaA2,2	45.68	0.39	14.57	0.06	16.60	0.11	8.60	7.43	5.10	0.45	98.99	0.02	0.07
K4-120b3lilaA1	56.97	0.03	10.61	0.03	12.13	0.01	10.86	1.93	7.33	0.04	99.92	0.02	0.00
K4-120b3lilaA2	55.93	0.08	10.41	0.02	12.64	0.03	10.96	2.90	6.59	0.08	99.63	0.00	0.00
K4-120b3lilaA3	54.91	0.05	10.36	0.04	13.28	0.07	11.07	3.52	6.28	0.13	99.70	0.02	0.01
K4-120b3lilaA4	50.50	0.15	10.10	0.02	14.91	0.05	11.89	7.31	4.62	0.28	99.83	0.00	0.10
K4-120b3lilaA5	51.13	0.11	9.39	0.00	14.75	0.07	12.21	7.55	4.48	0.31	100.00	0.01	0.12
K4-120b3lilaA6	47.50	0.16	10.75	0.02	15.48	0.05	11.80	9.70	3.46	0.40	99.32	0.01	0.17
K4-120b3lilaA7	50.89	0.19	8.81	0.02	14.54	0.07	12.91	7.59	4.37	0.29	99.68	0.00	0.10
K4-120b3lilaA8	50.67	0.21	9.51	0.02	16.16	0.07	11.15	7.48	4.26	0.29	99.80	0.00	0.05
K4-120b3lilaA9	45.93	0.09	14.18	0.00	17.60	0.05	8.67	8.28	4.34	0.48	99.63	0.02	0.02
K4-120b3lilaA10	51.01	0.10	9.75	0.06	15.32	0.06	11.71	7.66	4.15	0.32	100.15	0.00	0.02
K4-120b3lilaAProfil1 [70]	48.98	0.13	11.70	0.01	16.75	0.07	10.27	6.76	5.00	0.40	100.07	0.01	0.04
K4-120b3lilaAProfil1	52.96	0.05	10.31	0.04	15.48	0.11	10.47	4.26	5.91	0.23	99.81	0.00	0.02
K4-120b3lilaAProfil1	49.38	0.13	10.89	0.00	15.97	0.13	10.83	6.66	4.77	0.50	99.25	0.00	0.08
K4-120b3lilaAProfil1	49.14	0.09	11.06	0.05	16.62	0.06	10.74	6.57	5.00	0.49	99.82	0.01	0.10
K4-120b3lilaAProfil1	48.19	0.17	11.45	0.02	16.63	0.02	10.65	7.27	4.75	0.54	99.68	0.01	0.11
K4-120b3lilaAProfil1	47.38	0.18	11.95	0.04	16.89	0.10	10.33	7.45	4.70	0.62	99.63	0.03	0.06
K4-120b3lilaAProfil1	48.50	0.22	11.63	0.03	15.96	0.09	10.44	7.05	4.91	0.45	99.27	0.00	0.11
K4-120b3lilaA11	46.00	0.31	13.48	0.03	16.77	0.04	9.56	8.13	4.48	0.59	99.40	0.02	0.11
K4-120b4lilaAProfil1 [90]	44.01	0.23	15.07	0.01	19.19	0.09	8.17	8.16	4.34	0.69	99.95	0.02	0.09
K4-120b4lilaAProfil1	48.54	0.19	10.75	0.05	17.92	0.12	10.06	6.88	4.73	0.37	99.61	0.01	0.10
K4-120b4lilaAProfil1	49.29	0.22	10.10	0.05	17.68	0.15	10.43	6.48	4.83	0.32	99.55	0.00	0.08
K4-120b4lilaAProfil1	50.03	0.16	10.21	0.03	17.46	0.09	10.40	6.10	5.03	0.31	99.84	0.01	0.09
K4-120b4lilaAProfil1	49.39	0.17	10.45	0.02	17.49	0.12	10.33	6.30	4.94	0.37	99.57	0.00	0.11
K4-120b4lilaAProfil1	48.36	0.23	10.98	0.02	16.99	0.14	10.21	7.49	4.41	0.46	99.27	0.00	0.06
K4-120b4lilaAProfil1	48.42	0.26	11.82	0.04	16.96	0.14	9.69	7.30	4.72	0.35	99.69	0.01	0.02
K4-120b4lilaAProfil1	38.89	0.12	21.14	0.04	22.56	0.43	4.22	13.40	0.65	0.22	101.66	0.00	0.00
K4-120b5BlauerAProfil1 [250]	42.84	0.91	15.52	0.05	16.92	0.12	8.37	8.82	4.41	0.84	98.80	0.01	0.08
K4-120b5BlauerAProfil1	44.86	0.63	14.30	0.03	16.65	0.08	9.21	8.53	4.55	0.73	99.56	0.01	0.07
K4-120b5BlauerAProfil1	46.97	0.39	12.79	0.03	16.06	0.15	10.35	8.13	4.50	0.63	99.99	0.01	0.10
K4-120b5BlauerAProfil1	50.41	0.17	10.03	0.03	15.01	0.06	11.62	7.33	4.68	0.34	99.67	0.01	0.10
K4-120b5BlauerAProfil1	50.60	0.16	9.33	0.01	14.57	0.05	12.34	7.94	4.27	0.33	99.61	0.00	0.09
K4-120b5BlauerAProfil1	50.68	0.15	9.20	0.02	14.46	0.11	12.74	7.93	4.25	0.34	99.87	0.00	0.09
K4-120b5BlauerAProfil1	51.00	0.18	9.28	0.03	14.10	0.06	12.59	7.92	4.31	0.36	99.82	0.02	0.09
K4-120b5BlauerAProfil1	50.91	0.19	9.25	0.02	14.12	0.08	12.71	8.00	4.31	0.35	99.94	0.00	0.12
K4-120b5BlauerAProfil1	51.37	0.18	9.22	0.01	13.51	0.06	12.89	7.84	4.35	0.34	99.77	0.00	0.17
K4-120b5BlauerAProfil1	50.99	0.20	9.41	0.05	13.44	0.07	12.98	7.80	4.47	0.37	99.78	0.01	0.15
K4-120b5BlauerAProfil1	51.23	0.16	9.25	0.04	13.29	0.02	13.20	7.90	4.43	0.33	99.84	0.01	0.13
K4-120b5BlauerAProfil1	51.53	0.19	9.13	0.05	13.21	0.07	13.45	7.93	4.41	0.33	100.30	0.00	0.13
K4-120b5BlauerAProfil1	51.42	0.17	9.21	0.07	13.09	0.08	13.46	8.07	4.30	0.34	100.20	0.00	0.14
K4-120b5BlauerAProfil1	51.36	0.17	8.98	0.05	12.95	0.08	13.49	8.09	4.38	0.34	99.90	0.00	0.13
K4-120b5BlauerAProfil1	51.23	0.18	8.90	0.06	13.19	0.10	13.64	8.11	4.18	0.34	99.92	0.01	0.19
K4-120b5BlauerAProfil1	50.68	0.17	9.07	0.02	13.54	0.07	13.26	8.07	4.36	0.38	99.61	0.01	0.17
K4-120b5BlauerAProfil1	50.81	0.15	9.27	0.06	13.37	0.04	12.94	7.95	4.39	0.34	99.31	0.00	0.11
K4-120b5BlauerAProfil1	50.74	0.19	9.11	0.08	13.86	0.03	12.69	8.58	4.41	0.33	100.01	0.01	0.14
K4-120b5BlauerAProfil2 [100]	51.49	0.14	8.94	0.00	13.40	0.05	13.25	7.59	4.47	0.31	99.63	0.00	0.14
K4-120b5BlauerAProfil2	50.87	0.12	8.82	0.02	13.47	0.04	13.22	7.80	4.47	0.32	99.14	0.01	0.16
K4-120b5BlauerAProfil2	51.13	0.17	8.72	0.00	13.99	0.04	12.92	7.60	4.39	0.30	99.26	0.01	0.11
K4-120b5BlauerAProfil2	50.73	0.16	8.84	0.05	14.31	0.06	12.85	7.58	4.26	0.30	99.14	0.01	0.15
K4-120b5BlauerAProfil2	50.49	0.15	9.06	0.00	14.11	0.03	12.75	7.88	4.34	0.34	99.14	0.01	0.08
K4-120b5BlauerAProfil2	50.78	0.18	8.96	0.02	14.05	0.00	12.85	7.88	4.19	0.31	99.21	0.01	0.10
K4-120b5BlauerAProfil2	51.05	0.17	9.26	0.02	14.07	0.07	12.59	7.64	4.49	0.32	99.68	0.00	0.10
K4-120b5BlauerAProfil2	51.23	0.22	9.22	0.02	14.45	0.04	12.33	7.41	4.66	0.29	99.85	0.00	0.11
K4-120b5BlauerAProfil2	50.95	0.20	9.30	0.03	14.93	0.08	12.11	7.37	4.67	0.28	99.90	0.01	0.04
K4-120b5BlauerAProfil2	50.59	0.19	9.04	0.05	15.19	0.14	11.69	6.98	4.61	0.28	98.77	0.01	0.12

K4-120b5BlauerAProfil2	50.67	0.21	9.34	0.05	15.29	0.07	11.68	6.87	4.86	0.27	99.31	0.00	0.09
K4-120b5BlauerAProfil2	48.75	0.22	10.56	0.00	16.61	0.12	10.89	7.18	4.79	0.41	99.54	0.00	0.12
K4-120b5BlauerAProfil2	48.15	0.27	10.75	0.01	16.85	0.13	10.61	7.50	4.73	0.45	99.46	0.01	0.15
K4-120b5BlauerAProfil2	47.69	0.25	11.29	0.03	17.00	0.10	10.38	7.72	4.75	0.49	99.70	0.00	0.17
K4-120b5BlauerAProfil2	46.49	0.36	12.15	0.06	17.38	0.09	10.10	8.02	4.74	0.57	99.97	0.01	0.12
K4-120b5BlauerAProfil2	45.82	0.32	12.38	0.05	17.50	0.10	10.03	8.19	4.64	0.55	99.57	0.00	0.14
K4-120b5BlauerAProfilEnd	43.97	0.46	14.34	0.01	17.03	0.11	9.50	8.85	4.42	0.73	99.41	0.01	0.07
K4-120b1amp1	50.98	0.17	11.45	n.d.	14.46	0.10	10.15	4.97	5.67	0.26	98.19	0.00	0.07
K4-120b1amp2	52.55	0.09	11.23	n.d.	13.95	0.08	9.77	3.35	6.36	0.14	97.51	0.03	0.00
K4-120b1amp3	53.09	0.10	11.38	n.d.	13.63	0.06	9.62	2.61	6.53	0.12	97.13	0.01	0.00
K4-120b1amp4	54.48	0.05	11.38	n.d.	13.60	0.08	9.67	2.55	6.79	0.08	98.70	0.02	0.00
K4-120b1amp5	54.46	0.07	11.45	n.d.	13.62	0.05	9.65	2.56	6.66	0.07	98.61	0.01	0.00
K4-120b1amp6	50.65	0.18	11.10	n.d.	14.62	0.05	10.71	5.24	5.42	0.25	98.21	0.00	0.03
K4-120b1amp7	51.21	0.14	11.03	n.d.	13.79	0.08	10.21	4.33	5.81	0.17	96.77	0.02	0.00
K4-120b1amp8	50.23	0.21	11.00	n.d.	15.26	0.05	10.55	5.97	5.19	0.21	98.67	0.01	0.04
K4-120b1amp9	54.51	0.07	11.28	n.d.	13.90	0.04	9.58	2.41	6.66	0.10	98.54	0.01	0.00
K4-120b1amp10	49.69	0.12	12.39	n.d.	14.91	0.09	9.70	5.73	5.34	0.27	98.25	0.00	0.03
K4-120b1amp11	47.71	0.29	12.05	n.d.	15.01	0.12	10.17	6.50	4.91	0.40	97.16	0.01	0.07
K4-120b1amp12	48.81	0.23	11.38	n.d.	14.81	0.13	10.33	5.80	4.99	0.26	96.73	0.01	0.04
K4-120b1amp13	48.58	0.20	11.28	n.d.	16.05	0.14	10.55	6.63	4.94	0.38	98.75	0.01	0.14
K4-120b1amp14	47.68	0.21	11.32	n.d.	16.04	0.11	10.38	6.71	4.84	0.41	97.70	0.02	0.10
K4-120b1amp15	46.72	0.38	12.27	n.d.	15.42	0.10	10.35	7.55	4.53	0.42	97.74	0.02	0.10
K4-120b2ampProf1 [50]	54.20	0.07	10.85	n.d.	13.25	0.05	10.52	3.42	6.18	0.09	98.64	0.00	0.00
K4-120b2ampProf1	54.54	0.05	10.81	n.d.	13.34	0.11	10.43	3.01	6.32	0.05	98.66	0.01	0.00
K4-120b2ampProf1	54.08	0.07	10.97	n.d.	13.23	0.07	10.38	3.05	6.32	0.07	98.23	0.00	0.00
K4-120b2ampProf1	54.38	0.07	11.02	n.d.	13.32	0.07	10.17	2.74	6.28	0.05	98.09	0.01	0.00
K4-120b2ampProf1	54.23	0.07	11.09	n.d.	13.46	0.04	10.12	2.81	6.30	0.06	98.16	0.01	0.00
K4-120b2ampProf1	54.14	0.06	11.29	n.d.	13.56	0.05	10.09	2.91	6.44	0.06	98.60	0.02	0.00
K4-120b2ampProf1	54.37	0.06	11.11	n.d.	13.40	0.06	10.12	2.88	6.49	0.06	98.56	0.00	0.00
K4-120b2ampProf1	53.87	0.09	11.20	n.d.	13.72	0.05	9.96	2.95	6.29	0.07	98.19	0.00	0.00
K4-120b2ampProf1	54.21	0.10	11.13	n.d.	13.62	0.05	10.03	3.02	6.48	0.07	98.71	0.00	0.00
K4-120b2ampProf1	54.11	0.10	11.24	n.d.	13.65	0.04	10.23	3.09	6.24	0.06	98.75	0.00	0.00
K4-120b2ampProf2 [20]	53.63	0.11	11.31	n.d.	13.56	0.07	10.09	3.25	6.28	0.07	98.35	0.00	0.00
K4-120b2ampProf2	53.47	0.14	10.92	n.d.	13.94	0.06	10.31	3.67	6.06	0.07	98.63	0.01	0.00
K4-120b2ampProf2	51.37	0.20	10.85	n.d.	14.09	0.10	10.80	5.81	4.97	0.14	98.33	0.00	0.00
K4-120b2ampProf2	52.05	0.15	9.85	n.d.	13.61	0.05	11.30	6.08	4.67	0.12	97.87	0.00	0.00
K4-120b2ampProf3 [20]	53.19	0.12	9.52	n.d.	13.38	0.02	11.33	5.37	4.97	0.08	97.98	0.00	0.00
K4-120b2ampProf3	52.79	0.18	10.69	n.d.	13.65	0.06	10.47	4.93	5.32	0.10	98.18	0.01	0.00
K4-120b2ampProf3	53.43	0.30	10.77	n.d.	13.61	0.05	10.46	4.00	5.87	0.06	98.53	0.00	0.00
K4-120b2ampProf3	49.73	0.73	10.98	n.d.	14.05	0.08	11.23	7.56	4.15	0.18	98.68	0.00	0.01
K4-120b2ampProf4 [50]	53.96	0.08	10.94	n.d.	13.34	0.03	10.26	3.07	6.61	0.05	98.34	0.00	0.00
K4-120b2ampProf4	54.00	0.08	10.99	n.d.	13.61	0.04	10.29	3.09	6.28	0.06	98.43	0.01	0.00
K4-120b2ampProf4	54.59	0.07	11.02	n.d.	13.41	0.04	10.15	2.77	6.33	0.06	98.44	0.00	0.00
K4-120b2ampProf4	54.55	0.05	10.88	n.d.	13.27	0.05	10.04	2.62	6.52	0.06	98.04	0.02	0.00
K4-120b2ampProf4	54.30	0.10	11.00	n.d.	13.82	0.06	10.28	2.67	6.17	0.09	98.49	0.00	0.00
K4-120b2ampProf4	53.94	0.07	10.99	n.d.	13.71	0.08	10.28	2.69	6.53	0.06	98.34	0.00	0.00
K4-120b2ampProf4	53.92	0.09	11.05	n.d.	13.60	0.07	10.08	2.79	6.38	0.06	98.03	0.00	0.00
K4-120b2ampProf4	54.01	0.09	11.10	n.d.	13.52	0.05	10.12	2.89	6.14	0.06	97.99	0.01	0.00
K4-120b2ampProf4	54.07	0.10	11.01	n.d.	13.74	0.03	9.98	3.07	6.30	0.05	98.34	0.02	0.00
K4-120b2ampProf4	53.51	0.11	11.22	n.d.	13.56	0.02	10.22	3.30	6.19	0.07	98.20	0.00	0.00
K4-120b2ampProf5 [30]	53.26	0.17	11.01	n.d.	13.79	0.00	10.31	3.68	6.11	0.08	98.41	0.00	0.00
K4-120b2ampProf5	52.53	0.25	10.36	n.d.	13.54	0.11	10.89	4.81	5.26	0.09	97.84	0.00	0.00
K4-120b2ampProf5	42.27	8.77	10.98	n.d.	12.42	0.05	7.93	13.16	2.85	0.24	98.66	0.00	0.11
K4-120b2ampProf5	48.65	0.48	11.48	n.d.	14.76	0.06	10.79	7.40	4.24	0.21	98.06	0.00	0.00
K4-120b2ampProf5	50.21	0.45	11.04	n.d.	14.37	0.05	10.80	6.63	4.62	0.16	98.33	0.01	0.01
K4-120b2ampProf5	51.10	0.46	10.43	n.d.	13.94	0.08	11.03	5.99	4.78	0.12	97.92	0.00	0.02
K4-120b2ampProf6 [20]	55.39	0.04	11.14	n.d.	12.97	0.04	9.94	1.85	7.15	0.04	98.56	0.00	0.00
K4-120b2ampProf6	55.54	0.04	11.15	n.d.	13.07	0.06	9.87	1.65	7.18	0.03	98.61	0.01	0.00
K4-120b2ampProf6	55.34	0.08	11.16	n.d.	12.91	0.03	10.07	1.99	6.83	0.05	98.45	0.00	0.00
K4-120b2ampProf6	54.30	0.13	11.18	n.d.	13.28	0.07	10.25	3.02	6.28	0.06	98.57	0.01	0.00
K4-120b3ampProf1 [10]	48.78	0.23	10.49	n.d.	15.58	0.09	10.97	7.80	4.25	0.21	98.40	0.01	0.00
K4-120b3ampProf1	50.85	0.19	10.18	n.d.	14.73	0.08	11.28	6.43	4.71	0.17	98.61	0.00	0.00
K4-120b3ampProf2 [10]	49.07	0.19	10.24	n.d.	14.34	0.05	11.72	8.22	3.90	0.20	97.93	0.01	0.00
K4-120b3ampProf2	46.89	0.15	11.67	n.d.	15.12	0.09	11.25	9.52	3.39	0.30	98.37	0.01	0.03
K4-120b3amp1	47.73	0.17	11.13	n.d.	15.19	0.04	10.87	8.12	3.84	0.25	97.33	0.01	0.00
K4-120b5ampProf1 [40]	53.98	0.10	10.90	n.d.	13.96	0.05	10.09	3.08	6.32	0.05	98.53	0.00	0.00
K4-120b5ampProf1	55.05	0.07	11.23	n.d.	13.30	0.06	10.09	2.40	6.55	0.03	98.78	0.01	0.00
K4-120b5ampProf1	54.35	0.07	11.03	n.d.	13.63	0.03	10.24	3.06	6.15	0.05	98.59	0.00	0.00
K4-120b5ampProf1	53.93	0.04	10.81	n.d.	13.35	0.01	10.56	3.62	6.01	0.07	98.40	0.01	0.00
K4-120b5ampProf2 [40]	54.51	0.05	11.07	n.d.	13.69	0.07	10.00	2.73	6.51	0.06	98.68	0.01	0.00
K4-120b5ampProf2	55.74	0.09	10.93	n.d.	12.84	0.02	9.61	3.15	5.95	0.06	98.39	0.00	0.00
K4-120b5ampProf2	57.89	0.07	10.42	n.d.	12.50	0.05	9.07	4.22	4.81	0.10	99.13	0.02	0.00
K4-120b5ampProf2	54.52	0.07	11.15	n.d.	13.65	0.01	10.38	3.37	6.26	0.05	99.46	0.01	0.00
K4-120b5ampProf2	53.68	0.11	10.65	n.d.	13.75	0.07	10.58	4.08	5.85	0.06	98.81	0.00	0.00
K4-120b5ampProf2	52.83	0.11	10.98	n.d.	13.76	0.06	10.74	4.51	5.55	0.09	98.62	0.00	0.00
K4-120b5ampProf2	53.16	0.10	10.59	n.d.	13.71	0.02	11.01	4.58	5.51	0.08	98.76	0.00	0.00
K4-120b5ampProf2	49.05	0.24	12.24	n.d.	14.64	0.02	10.36	8.57	3.54	0.25	98.90	0.00	0.00
K4-120b5ampProf3 [30]	46.11	0.34	13.45	n.d.	15.67	0.07	10.30	8.98	3.66	0.30	98.87	0.01	0.02

K4-120b5ampProf3	49.34	0.19	12.52	n.d.	14.78	0.02	10.41	6.77	4.67	0.21	98.91	0.01	0.02
K4-120b5ampProf3	51.36	0.20	11.74	n.d.	14.42	0.07	9.79	7.75	3.57	0.19	99.08	0.01	0.00
K4-120b5ampProf3	52.43	0.10	11.06	n.d.	13.95	0.04	10.72	4.96	5.42	0.10	98.77	0.00	0.00
K4-120b5ampProf3	53.84	0.07	11.35	n.d.	13.72	0.06	10.32	3.41	6.05	0.07	98.87	0.00	0.00
K4-120b5amp1	56.00	0.50	12.36	n.d.	12.69	0.00	7.19	7.55	3.16	0.32	99.76	0.01	0.00
K4-120b6ampProfil1 [30]	48.97	0.10	11.27	n.d.	14.54	0.11	11.15	8.17	4.05	0.27	98.64	0.00	0.09
K4-120b6ampProfil1	48.32	0.16	11.36	n.d.	15.07	0.00	10.79	7.95	4.13	0.31	98.09	0.01	0.04
K4-120b6ampProfil1	47.76	0.16	11.64	n.d.	15.36	0.08	10.69	7.77	3.98	0.29	97.73	0.01	0.08
K4-120b6ampProfil1	46.74	0.15	12.26	n.d.	15.57	0.08	10.51	7.97	4.07	0.40	97.74	0.01	0.06
K4-120b6ampProfil1	48.34	0.17	11.54	n.d.	14.99	0.05	10.51	7.91	4.48	0.32	98.29	0.01	0.04
K4-120b6ampProfil1	51.04	0.09	10.85	n.d.	14.29	0.06	10.06	6.91	5.41	0.19	98.91	0.00	0.01
K4-120b6ampProfil2 [30]	50.31	0.11	10.66	n.d.	14.61	0.09	10.83	6.21	4.98	0.20	97.99	0.01	0.00
K4-120b6ampProfil2	50.89	0.10	10.79	n.d.	14.52	0.08	10.54	6.03	5.23	0.20	98.39	0.00	0.00
K4-120b6ampProfil2	50.95	0.12	10.87	n.d.	14.88	0.07	10.52	5.27	5.35	0.19	98.21	0.01	0.06
K4-120b6ampProfil2	49.98	0.17	11.37	n.d.	14.96	0.11	10.42	5.94	5.15	0.21	98.31	0.00	0.00
K4-120b6ampProfil2	51.71	0.11	10.55	n.d.	14.32	0.08	10.65	4.91	5.56	0.14	98.03	0.00	0.00
K4-120b6ampProfil2	50.80	0.12	11.12	n.d.	14.24	0.07	10.89	6.21	4.90	0.18	98.53	0.00	0.00
K4-120b6ampProfil3 [50]	51.30	0.08	10.93	n.d.	14.27	0.07	10.82	5.60	5.20	0.17	98.44	0.00	0.03
K4-120b6ampProfil3	52.87	0.09	10.95	n.d.	14.13	0.14	10.23	3.92	6.05	0.13	98.50	0.00	0.00
K4-120b6ampProfil3	51.11	0.14	11.01	n.d.	14.58	0.01	10.59	5.32	5.33	0.20	98.28	0.02	0.02
K4-120b6ampProfil3	49.64	0.14	10.97	n.d.	15.19	0.05	10.57	6.11	5.03	0.22	97.92	0.00	0.02
K4-120b6ampProfil3	49.49	0.17	11.09	n.d.	15.10	0.06	10.52	6.57	4.70	0.25	97.95	0.00	0.05
K4-120b6ampProfil3	48.92	0.17	11.77	n.d.	15.39	0.05	10.48	6.77	4.95	0.27	98.76	0.01	0.07
K4-120b6ampProfil3	50.11	0.13	11.43	n.d.	14.83	0.08	10.41	5.78	5.23	0.24	98.24	0.00	0.00
K4-120b6ampProfil3	50.53	0.07	11.15	n.d.	15.07	0.04	10.58	5.90	5.15	0.20	98.69	0.00	0.04
K4-120b6ampProfil3	49.04	0.15	11.33	n.d.	15.27	0.09	10.76	7.39	4.42	0.25	98.70	0.01	0.07
K4-120b6ampProfil3	46.08	0.20	12.87	n.d.	15.63	0.07	10.21	9.00	3.66	0.44	98.15	0.01	0.07
K4-120b6amp1	46.96	0.20	12.21	n.d.	15.64	0.07	10.49	8.43	4.03	0.38	98.40	0.02	0.09
K4-120b7ampProfil1 [40]	54.62	0.09	11.12	n.d.	12.05	0.05	10.91	2.74	6.58	0.09	98.24	0.02	0.00
K4-120b7ampProfil1	53.59	0.09	11.26	n.d.	13.08	0.05	11.00	3.41	6.48	0.12	99.08	0.00	0.00
K4-120b7ampProfil1	54.24	0.11	11.29	n.d.	12.52	0.05	10.71	3.03	6.61	0.07	98.65	0.00	0.00
K4-120b7ampProfil1	53.77	0.08	11.34	n.d.	12.37	0.04	11.02	3.29	6.26	0.12	98.29	0.00	0.00
K4-120b7ampProfil1	52.51	0.15	11.24	n.d.	12.81	0.07	11.07	4.33	5.79	0.15	98.11	0.00	0.02
K4-120b7ampProfil1	52.56	0.16	11.14	n.d.	12.97	0.08	11.03	4.19	6.03	0.15	98.30	0.01	0.00
K4-120b7ampProfil1	51.68	0.15	11.12	n.d.	13.20	0.05	11.24	4.62	5.73	0.18	97.95	0.01	0.03
K4-120b7ampProfil2 [60]	52.14	0.07	11.95	n.d.	12.51	0.04	11.25	4.78	5.63	0.22	98.57	0.03	0.01
K4-120b7ampProfil2	53.63	0.11	11.62	n.d.	12.40	0.06	11.10	3.43	6.36	0.11	98.82	0.00	0.00
K4-120b7ampProfil2	55.60	0.09	11.06	n.d.	12.17	0.06	10.45	2.14	7.00	0.05	98.62	0.00	0.00
K4-120b7ampProfil2	54.24	0.08	11.26	n.d.	12.38	0.05	10.78	2.71	6.69	0.08	98.27	0.00	0.00
K4-120b7ampProfil2	54.10	0.11	11.11	n.d.	12.26	0.07	10.76	2.56	6.65	0.10	97.71	0.01	0.00
K4-120b7ampProfil2	53.40	0.10	11.20	n.d.	13.09	0.05	10.88	3.31	6.30	0.11	98.42	0.00	0.00
K4-120b7ampProfil2	53.60	0.15	11.22	n.d.	13.02	0.08	10.99	3.23	6.35	0.11	98.75	0.02	0.00
K4-120b7ampProfil2	54.39	0.12	11.30	n.d.	12.44	0.05	10.88	2.25	6.69	0.09	98.21	0.00	0.00
K4-120b7ampProfil2	55.59	0.11	11.24	n.d.	12.05	0.03	10.50	1.93	7.08	0.06	98.58	0.01	0.00
K4-120b7ampProfil2	55.52	0.12	11.07	n.d.	12.55	0.05	10.53	2.05	7.00	0.05	98.94	0.00	0.00
K4-120b7ampProfil2	54.82	0.14	11.12	n.d.	12.02	0.04	10.62	2.22	6.77	0.07	97.82	0.01	0.00
K4-120b7ampProfil2	54.67	0.14	11.03	n.d.	12.02	0.01	10.63	2.39	6.78	0.07	97.75	0.01	0.00
K4-120b7ampProfil2	53.96	0.16	10.98	n.d.	12.34	0.07	10.89	2.78	6.59	0.07	97.83	0.01	0.00
K4-120b7ampProfil3 [40]	53.46	0.09	11.40	n.d.	12.32	0.06	11.28	3.79	6.17	0.16	98.73	0.00	0.00
K4-120b7ampProfil3	53.83	0.09	11.42	n.d.	12.07	0.01	10.74	3.25	6.27	0.12	97.80	0.01	0.00
K4-120b7ampProfil3	53.78	0.10	11.38	n.d.	11.97	0.06	10.47	2.57	6.26	0.08	96.67	0.02	0.00
K4-120b7ampProfil3	54.28	0.11	11.16	n.d.	11.89	0.03	10.76	2.27	6.68	0.06	97.25	0.01	0.00
K4-120b7ampProfil3	54.36	0.14	11.32	n.d.	12.04	0.03	10.73	2.60	6.62	0.07	97.91	0.00	0.00
K4-120b7ampProfil3	54.47	0.19	11.20	n.d.	12.14	0.02	10.80	2.54	6.58	0.08	98.01	0.00	0.00
K4-120b7ampProfil3	55.43	0.20	11.10	n.d.	12.05	0.04	10.73	2.42	6.78	0.08	98.83	0.00	0.00
K4-120b7ampProfil3	55.07	0.25	11.30	n.d.	11.76	0.03	10.59	2.12	6.97	0.08	98.17	0.01	0.00
K4-120b7ampProfil3	52.03	0.38	10.81	n.d.	13.19	0.09	11.48	4.80	5.57	0.22	98.58	0.00	0.00
K4-120c2ampProf1 [30]	50.74	0.15	8.35	n.d.	17.20	0.21	11.33	7.00	3.85	0.24	99.07	0.01	0.00
K4-120c2ampProf1	50.18	0.20	8.84	n.d.	16.93	0.15	11.25	7.50	3.64	0.26	98.95	0.01	0.00
K4-120c2ampProf1	49.77	0.20	9.21	n.d.	17.47	0.20	11.00	7.57	3.81	0.24	99.46	0.00	0.00
K4-120c2ampProf1	50.01	0.14	9.07	n.d.	17.05	0.16	11.20	7.62	3.63	0.17	99.04	0.01	0.00
K4-120c2ampProf1	50.27	0.16	8.88	n.d.	17.29	0.16	11.14	7.20	3.92	0.20	99.23	0.00	0.00
K4-120c2ampProf1	50.24	0.17	9.04	n.d.	17.27	0.14	11.03	7.32	3.76	0.22	99.20	0.00	0.00
K4-120c2ampProf2 [100]	50.44	0.18	9.26	n.d.	17.21	0.18	10.81	6.80	4.01	0.25	99.14	0.01	0.00
K4-120c2ampProf2	51.04	0.16	8.70	n.d.	16.90	0.18	11.24	7.28	3.81	0.18	99.48	0.02	0.00
K4-120c2ampProf2	46.02	0.22	10.62	n.d.	18.37	0.15	10.60	11.25	2.42	0.16	99.81	0.01	0.00
K4-120c2ampProf2	48.96	0.14	9.44	n.d.	16.84	0.09	11.11	10.73	2.13	0.15	99.60	0.00	0.00
K4-120c2ampProf2	48.80	0.15	8.27	n.d.	16.53	0.15	12.03	10.90	2.23	0.13	99.19	0.01	0.00
K4-120c2ampProf2	54.00	0.20	9.28	n.d.	15.13	0.14	9.80	9.77	1.89	0.13	100.32	0.01	0.00
K4-120c2ampProf2	48.53	0.12	8.64	n.d.	16.82	0.14	11.81	10.39	2.35	0.17	98.96	0.00	0.00
K4-120c2ampProf2	47.44	0.18	9.74	n.d.	17.18	0.15	11.35	10.87	2.39	0.15	99.45	0.01	0.00
K4-120c2ampProf2	50.26	0.15	8.63	n.d.	16.73	0.19	11.46	8.00	3.39	0.20	99.02	0.00	0.00
K4-120c2ampProf2	50.55	0.16	8.64	n.d.	17.01	0.16	11.42	8.08	3.33	0.22	99.57	0.00	0.00
K4-120c3amp7	46.19	0.22	10.70	n.d.	17.34	0.13	10.77	10.84	2.31	0.13	98.62	0.01	0.00
K4-120c3amp8	48.86	0.21	8.22	n.d.	16.34	0.16	12.28	10.23	2.46	0.15	98.91	0.01	0.00
K4-120c3amp9	47.11	0.56	10.01	n.d.	15.64	0.16	11.96	10.44	2.66	0.18	98.72	0.02	0.00
K4-120c1ampProf1 [100]	51.24	0.17	8.25	n.d.	16.38	0.16	11.85	6.76	4.22	0.24	99.26	0.00	0.00

K4-120c1ampProf1	51.05	0.20	8.49	n.d.	16.40	0.10	11.55	6.81	4.18	0.22	99.00	0.01	0.00
K4-120c1ampProf1	50.75	0.18	8.98	n.d.	16.45	0.14	11.44	6.91	4.12	0.24	99.21	0.01	0.00
K4-120c1ampProf1	50.80	0.15	8.86	n.d.	16.39	0.08	11.46	6.74	4.23	0.21	98.91	0.00	0.00
K4-120c1ampProf1	50.60	0.17	8.66	n.d.	16.44	0.11	11.44	6.71	4.26	0.23	98.59	0.01	0.00
K4-120c1ampProf1	50.49	0.17	9.00	n.d.	16.61	0.10	11.46	6.65	4.15	0.22	98.85	0.00	0.00
K4-120c1ampProf1	50.43	0.15	9.10	n.d.	16.47	0.16	11.09	6.75	4.26	0.21	98.64	0.01	0.00
K4-120c1ampProf1	50.17	0.19	8.99	n.d.	16.65	0.10	11.41	6.92	4.29	0.22	98.94	0.00	0.00
K4-120c1ampProf1	49.95	0.18	9.07	n.d.	16.95	0.11	11.53	7.45	3.85	0.20	99.30	0.00	0.00
K4-120c1ampProf1	50.00	0.16	9.14	n.d.	16.77	0.07	11.49	7.42	3.84	0.21	99.08	0.01	0.00
K4-120c1ampProf2 [50]	51.24	0.14	8.03	n.d.	16.50	0.14	11.85	6.68	4.10	0.22	98.88	0.00	0.00
K4-120c1ampProf2	51.76	0.14	7.89	n.d.	16.37	0.08	12.26	6.91	3.94	0.17	99.52	0.00	0.00
K4-120c1ampProf2	50.99	0.14	7.83	n.d.	16.31	0.13	12.13	7.11	3.86	0.17	98.67	0.01	0.00
K4-120c1ampProf2	50.75	0.16	8.16	n.d.	16.16	0.15	11.79	7.32	3.82	0.16	98.46	0.01	0.00
K4-120c1ampProf2	49.73	0.15	8.76	n.d.	16.40	0.11	11.82	8.71	3.40	0.15	99.21	0.01	0.00
K4-120d1BlauAGross1	49.53	0.46	11.50	0.04	15.59	0.06	10.54	6.76	4.97	0.13	99.58	0.01	0.00
K4-120d1BlauAGross2	54.83	0.08	10.90	0.03	13.75	0.03	10.29	2.96	6.53	0.07	99.47	0.01	0.00
K4-120d1BlauAGross3	54.10	0.09	10.75	0.03	14.76	0.08	10.46	3.62	6.15	0.07	100.11	0.02	0.00
K4-120d1BlauAGross4	52.16	0.12	10.40	0.03	15.77	0.06	10.40	4.87	5.62	0.09	99.52	0.01	0.00
K4-120d1BlauAGross5	50.41	0.20	10.84	0.04	15.19	0.06	10.89	6.93	4.63	0.12	99.31	0.02	0.03
K4-120d1BlauAGross6	55.77	0.07	10.59	0.04	13.82	0.08	10.39	2.71	6.65	0.05	100.16	0.01	0.00
K4-120d1BlauAGross8	48.30	0.47	12.68	0.03	14.79	0.03	10.83	8.96	3.74	0.13	99.94	0.01	0.00
K4-120d1BlauAGross9	55.06	0.09	10.95	0.03	14.49	0.06	9.80	2.99	6.50	0.05	100.01	0.01	0.00
K4-120d1BlauAGross10	54.17	0.09	11.00	0.02	14.62	0.08	10.14	3.45	6.36	0.07	100.00	0.00	0.00
K4-120d1BlauAGross11	51.36	0.17	9.84	0.04	15.94	0.04	11.12	6.37	4.79	0.18	99.85	0.01	0.00
K4-120d1BlauAGross12	54.72	0.10	10.38	0.03	13.63	0.08	11.00	3.71	6.10	0.05	99.78	0.01	0.00
K4-120d1BlauAMittel3	57.35	0.12	10.65	0.02	12.53	0.02	8.07	7.80	3.17	0.17	99.93	0.02	0.00
K4-120d2BlauAKlein1	48.10	0.13	9.76	0.00	17.67	0.14	10.95	7.24	4.96	0.59	99.53	0.01	0.20
K4-120d2BlauAKlein2	48.40	0.14	10.38	0.00	16.67	0.11	10.90	6.79	5.04	0.55	98.98	0.00	0.13
K4-120d2BlauAKlein3	47.95	0.18	10.18	0.01	15.92	0.15	11.54	8.63	4.14	0.64	99.33	0.01	0.17
K4-120d2BlauAKlein4	49.70	0.19	9.79	0.04	16.37	0.13	10.93	6.26	5.23	0.43	99.07	0.01	0.16
K4-120d2BlauAMittel1	47.87	0.16	9.51	0.04	16.10	0.11	11.66	9.67	3.28	0.69	99.12	0.01	0.10
K4-120d2BlauAMittel2	49.59	0.14	10.03	0.02	15.94	0.09	11.10	7.10	4.77	0.59	99.36	0.00	0.11
K4-120d2BlauAMittel3	50.90	0.13	9.13	0.00	15.07	0.12	11.74	7.20	4.69	0.32	99.30	0.00	0.18
K4-120d2BlauAMittel4	50.66	0.18	8.86	0.00	14.99	0.07	12.37	7.55	4.60	0.33	99.60	0.00	0.08
K4-120d2BlauAMittel5	50.68	0.16	10.12	0.01	14.68	0.08	11.44	6.98	4.85	0.29	99.28	0.00	0.14
K4-120d2BlauAMittel6	50.41	0.21	10.25	0.04	14.90	0.12	11.59	6.93	4.72	0.29	99.45	0.01	0.15
K4-120d2BlauAMittel7	51.26	0.11	8.46	0.02	14.03	0.08	12.69	7.88	4.12	0.32	98.97	0.00	0.06
K4-120d2BlauAMittel8	53.42	0.08	10.22	0.02	14.24	0.16	10.66	4.52	5.93	0.26	99.50	0.00	0.05
K4-120d2BlauAMittel9	49.43	0.17	9.74	0.01	15.55	0.12	11.55	7.82	4.41	0.54	99.34	0.00	0.17
K4-120d2BlauAGross1	51.04	0.16	8.78	0.00	15.00	0.12	12.26	7.64	4.22	0.32	99.54	0.00	0.15
K4-120d2BlauAGross2	50.74	0.17	8.84	0.00	14.02	0.09	13.00	7.98	4.08	0.33	99.26	0.00	0.14
K4-120d2BlauAGross3	50.72	0.20	8.77	0.02	13.53	0.05	13.00	8.23	3.94	0.36	98.82	0.01	0.14
K4-120d2BlauAGross4	50.60	0.18	8.29	0.04	14.43	0.10	12.95	7.83	4.27	0.32	99.01	0.00	0.18
K4-120d2BlauAGross5	51.33	0.17	8.78	0.05	14.25	0.04	12.77	7.99	4.12	0.36	99.84	0.01	0.13
K4-120d2BlauAGross6	51.03	0.12	8.69	0.02	15.03	0.11	12.33	7.38	4.35	0.27	99.33	0.00	0.15
K4-120d2BlauAGross7	50.53	0.12	8.81	0.01	16.16	0.09	11.77	7.33	4.45	0.31	99.57	0.00	0.13
K4-120d3BlauerAGross1	47.73	0.24	11.41	0.03	16.39	0.08	10.64	7.91	4.58	0.43	99.42	0.01	0.12
K4-120d3BlauerAGross2	50.11	0.16	9.78	0.04	15.64	0.09	11.64	6.68	4.99	0.36	99.49	0.01	0.19
K4-120d3BlauerAGross3	51.18	0.13	9.97	0.05	14.79	0.11	11.32	6.32	5.18	0.38	99.42	0.00	0.10
K4-120d3BlauerAGross4	50.48	0.11	8.85	0.01	14.33	0.11	12.77	8.21	4.10	0.40	99.36	0.01	0.18
K4-120d3BlauerAKlProfil1 [160]	46.56	0.23	9.85	0.00	17.02	0.09	11.77	10.29	3.18	0.66	99.65	0.02	0.19
K4-120d3BlauerAKlProfil1	48.21	0.14	9.80	0.02	16.06	0.04	11.85	9.03	3.82	0.51	99.49	0.02	0.13
K4-120d3BlauerAKlProfil1	48.53	0.15	10.11	0.03	15.92	0.08	11.45	8.21	4.33	0.45	99.27	0.00	0.16
K4-120d3BlauerAKlProfil1	48.87	0.18	10.37	0.02	15.79	0.10	11.25	7.70	4.54	0.40	99.23	0.01	0.15
K4-120d3BlauerAKlProfil1	48.16	0.21	10.30	0.01	16.20	0.08	11.25	8.02	4.44	0.47	99.14	0.02	0.15
K4-120d3BlauerAKlProfil1	49.15	0.18	10.04	0.00	15.77	0.11	11.36	7.62	4.60	0.41	99.24	0.00	0.10
K4-120d3BlauerAKlProfil1	48.84	0.19	10.57	0.01	16.09	0.09	11.08	7.39	4.67	0.45	99.39	0.02	0.16
K4-120d3BlauerAKlProfil1	49.46	0.18	10.29	0.00	15.64	0.06	11.37	6.96	4.85	0.37	99.18	0.00	0.09
K4-120d3BlauerAKlProfil1	49.61	0.21	10.29	0.03	15.82	0.09	11.37	6.75	4.97	0.36	99.50	0.00	0.14
K4-120d3BlauerAKlProfil1	50.10	0.14	10.22	0.02	15.84	0.10	11.28	6.47	5.26	0.35	99.77	0.02	0.14
K4-120d3BlauerAKlProfil1	50.54	0.17	10.06	0.02	15.36	0.08	11.28	6.30	5.30	0.30	99.39	0.00	0.14
K4-120d3BlauerAKlProfil1	50.72	0.15	10.15	0.01	15.33	0.07	11.21	6.18	5.34	0.26	99.41	0.01	0.12
K4-120d3BlauerAKlProfil1	50.53	0.22	9.95	0.05	15.03	0.12	11.34	6.20	5.29	0.27	98.99	0.00	0.12
JNar2,2AmpInCzo1	46.80	0.32	11.16	0.02	11.85	0.08	13.45	11.61	2.09	0.78	98.14	0.00	0.15
JNar2,2AmpInCzo2	48.00	0.32	11.81	0.04	10.31	0.06	11.35	13.33	2.90	0.59	98.70	0.00	0.01
JNar2,1amp1	44.70	0.26	12.91	0.01	13.95	0.06	11.51	11.02	2.44	0.87	97.73	0.00	0.09
JNar2,1amp2	45.85	0.35	11.52	0.00	13.33	0.09	12.16	11.22	2.22	0.77	97.50	0.00	0.09
JNar2,1amp3	43.28	0.70	13.28	0.03	13.40	0.00	10.96	11.85	1.97	1.45	96.93	0.00	0.11
JNar2,1amp4	45.76	0.80	11.46	0.02	13.30	0.08	12.20	11.10	2.36	0.88	97.94	0.01	0.04
PKB3,2ampProfil1 [80]	44.21	1.66	11.84	0.05	14.09	0.10	11.39	10.48	2.68	0.55	97.02	0.02	0.00
PKB3,2ampProfil1	44.22	1.59	11.93	0.02	14.21	0.03	11.35	10.29	2.81	0.56	97.00	0.00	0.00
PKB3,2ampProfil1	44.58	1.56	12.16	0.02	14.46	0.02	11.36	10.25	2.88	0.60	97.90	0.00	0.00
PKB3,2ampProfil1	43.65	1.62	11.89	0.01	13.92	0.08	11.17	10.46	2.55	0.61	95.95	0.01	0.00
PKB3,2ampProfil1	44.19	1.82	11.64	0.00	14.19	0.06	11.26	10.70	2.50	0.55	96.90	0.00	0.00
PKB3,2ampProfil2 [50]	43.02	1.29	12.86	0.02	15.97	0.03	10.36	11.01	2.62	0.50	97.66	0.04	0.00

PKB3,2ampProfil2	42.93	1.22	13.18	0.05	15.60	0.05	10.08	10.80	2.58	0.46	96.96	0.01	0.00
PKB3,2ampProfil2	43.19	1.10	13.57	0.01	15.44	0.09	10.04	10.90	2.64	0.47	97.44	0.02	0.00
PKB3,2ampProfil2	42.87	0.91	13.80	0.01	15.21	0.02	9.99	10.73	2.58	0.39	96.49	0.00	0.00
PKB3,1ampProfil1 [50]	42.50	0.73	12.25	0.03	16.28	0.07	10.18	10.88	2.55	0.36	95.81	0.01	0.00
PKB3,1ampProfil1	42.50	0.68	12.25	0.02	16.21	0.05	9.92	11.05	2.44	0.36	95.48	0.02	0.00
PKB3,1ampProfil1	42.64	0.70	12.52	0.04	15.28	0.06	9.77	10.96	2.45	0.39	94.80	0.01	0.00
PKB3,1ampProfil1	41.63	0.75	13.47	0.00	16.31	0.07	9.32	11.24	2.34	0.40	95.53	0.02	0.00
PKB3,1ampProfil2 [160]	41.17	0.59	10.95	0.02	15.75	0.07	9.57	9.74	2.10	0.49	90.45	0.04	0.00
PKB3,1ampProfil2	44.67	0.65	11.79	0.02	15.90	0.10	10.47	10.11	2.50	0.47	96.67	0.01	0.00
PKB3,1ampProfil2	38.32	0.63	11.87	0.03	12.46	0.34	8.42	8.63	1.57	0.47	82.73	0.05	0.00
PKB3,1ampProfil2	44.27	0.68	12.57	0.05	15.49	0.04	10.83	10.50	2.66	0.56	97.64	0.01	0.00
PKB3,1ampProfil2	43.91	0.64	11.86	0.04	16.29	0.02	10.62	10.38	2.56	0.51	96.83	0.01	0.00
PKB3,1ampProfil2	44.15	0.62	11.54	0.02	15.52	0.03	10.69	10.35	2.54	0.53	95.99	0.01	0.00
PKB3,1ampProfil2	43.73	0.61	11.34	0.04	15.54	0.08	10.33	10.50	2.32	0.45	94.93	0.01	0.00
PKB3,1ampProfil2	44.13	0.68	11.48	0.02	15.32	0.05	10.86	10.81	2.51	0.38	96.24	0.02	0.00
PKL1,2Amp1	51.10	0.11	6.91	0.00	16.74	0.18	12.51	7.02	3.69	0.25	98.53	0.00	0.00
PKL1,2Amp2	50.33	0.10	7.43	0.00	16.43	0.10	12.52	7.03	3.71	0.29	97.95	0.00	0.00
PKL1,2Amp3	45.03	0.32	8.41	0.04	20.56	0.13	10.30	10.90	2.30	0.19	98.18	0.03	0.00
PKL1,2Amp4	50.71	0.12	6.89	0.01	15.90	0.18	13.20	7.11	3.85	0.27	98.25	0.00	0.00
PKL2ampProfil1 [80]	42.01	0.49	15.55	0.00	18.72	0.13	7.61	11.00	2.31	0.67	98.50	0.02	0.00
PKL2ampProfil1	41.95	0.36	15.28	0.01	19.36	0.18	7.89	10.84	2.38	0.40	98.64	0.02	0.00
PKL2ampProfil1	46.31	0.16	11.91	0.01	17.30	0.23	9.71	10.02	2.42	0.24	98.31	0.01	0.00
PKL2ampProfil1	45.98	0.22	11.94	0.00	18.52	0.20	9.36	9.50	2.60	0.33	98.64	0.03	0.00
PKL2ampProfil1	46.51	0.22	11.71	0.00	19.55	0.26	9.54	8.43	2.69	0.30	99.20	0.01	0.00
PKL2ampProfil1	47.66	0.22	11.20	0.01	18.26	0.24	9.76	8.44	2.72	0.24	98.73	0.02	0.00
PKL2ampProfil1	48.08	0.19	10.44	0.00	17.83	0.22	10.14	8.73	2.61	0.17	98.41	0.00	0.00
PK2-4g,2Ampsympl1	45.56	0.75	12.40	0.04	12.52	0.02	13.08	11.65	2.13	0.67	98.82	0.02	0.00
PK2-4g,2Ampsympl2	43.55	0.96	14.23	0.06	12.62	0.03	12.34	11.60	2.24	0.69	98.32	0.01	0.00
PK2-4g,1Amphsympl1	44.88	0.57	12.02	0.05	13.41	0.08	12.81	11.69	1.84	0.93	98.28	0.01	0.00
PK2-4cAmpProfil1 [50]	46.15	0.36	12.42	0.07	12.66	0.07	13.08	10.87	2.44	0.51	98.64	0.01	0.00
PK2-4cAmpProfil1	45.47	0.33	12.92	0.06	12.97	0.03	13.04	11.10	2.50	0.47	98.89	0.00	0.00
PK2-4cAmpProfil1	44.66	0.44	13.55	0.04	13.43	0.05	12.67	11.46	2.62	0.54	99.45	0.00	0.00
PK2-4cAmpProfil1	44.64	0.47	13.79	0.01	13.33	0.04	12.47	11.52	2.63	0.58	99.46	0.00	0.00
PK2-4cAmpProfil1	43.01	0.59	15.12	0.02	14.17	0.07	11.55	11.67	2.69	0.65	99.54	0.02	0.00
PK2-4cAmpProfil2 [50]	41.64	1.59	15.49	0.13	13.35	0.05	11.17	11.41	2.74	0.66	98.23	0.02	0.00
PK2-4cAmpProfil2	42.80	1.76	15.13	0.13	13.10	0.03	11.69	11.73	2.89	0.67	99.93	0.01	0.00
PK2-4cAmpProfil2	42.72	1.60	14.59	0.11	13.53	0.06	11.96	11.55	2.76	0.61	99.49	0.00	0.00
PK2-4cAmpProfil2	44.26	1.18	13.51	0.05	12.87	0.06	12.59	11.54	2.64	0.52	99.21	0.00	0.00

Table A5. Microprobe analyses of mica

Sample [Profile length in μm]	SiO_2	TiO_2	Al_2O_3	FeO	MnO	MgO	CaO	BaO	Na_2O	K_2O	Sum	Cl	F
K4-4PhgProfil1 [480]	46.71	0.61	33.51	2.67	0.00	0.93	0.01	0.17	0.45	10.39	95.45	0.00	0.00
K4-4PhgProfil1	47.02	0.61	33.36	2.62	0.00	0.97	0.02	0.00	0.41	10.54	95.54	0.00	0.00
K4-4PhgProfil1	47.23	0.65	33.51	2.70	0.02	0.94	0.01	0.06	0.41	10.50	96.03	0.00	0.00
K4-4PhgProfil1	43.91	0.54	31.70	2.42	0.00	0.88	0.06	0.00	0.32	9.62	89.45	0.04	0.00
K4-4PhgProfil1	46.64	0.63	33.66	2.66	0.05	0.97	0.05	0.03	0.44	10.36	95.47	0.00	0.00
K4-4PhgProfil1	46.98	0.63	33.57	2.57	0.00	0.90	0.03	0.01	0.42	10.21	95.32	0.00	0.00
K4-4PhgProfil1	46.67	0.65	33.45	2.56	0.05	0.89	0.04	0.02	0.45	10.47	95.24	0.00	0.00
K4-4PhgProfil1	47.05	0.65	33.64	2.47	0.01	0.95	0.03	0.00	0.46	10.39	95.64	0.01	0.00
K4-4PhgProfil1	47.02	0.68	33.71	2.54	0.00	0.94	0.04	0.10	0.46	10.24	95.71	0.02	0.00
K4-4PhgProfil1	46.65	0.63	33.91	2.61	0.04	0.90	0.02	0.06	0.42	10.10	95.36	0.00	0.00
K4-4PhgProfil1	46.79	0.63	34.15	2.47	0.00	0.88	0.01	0.08	0.50	10.30	95.81	0.00	0.00
K4-4PhgProfil1	46.63	0.70	33.61	2.67	0.00	0.90	0.04	0.03	0.49	10.31	95.38	0.00	0.00
K4-4PhgProfil1	46.56	0.64	33.88	2.49	0.00	0.87	0.03	0.08	0.50	10.33	95.38	0.00	0.00
K4-4PhgProfil1	46.80	0.62	33.91	2.48	0.04	0.88	0.07	0.00	0.49	10.12	95.42	0.01	0.00
K4-4PhgProfil1	46.81	0.62	33.77	2.53	0.00	0.86	0.00	0.00	0.48	10.24	95.31	0.02	0.00
K4-4PhgProfil1	46.68	0.70	34.16	2.44	0.03	0.86	0.00	0.06	0.53	10.20	95.67	0.00	0.00
K4-4PhgProfil1	47.05	0.68	34.06	2.52	0.00	0.86	0.01	0.05	0.58	10.24	96.04	0.00	0.00
K4-4PhgProfil1	46.85	0.64	33.99	2.58	0.02	0.86	0.00	0.00	0.49	10.38	95.80	0.00	0.00
K4-4PhgProfil1	46.92	0.63	33.87	2.53	0.00	0.84	0.01	0.00	0.47	10.38	95.64	0.01	0.00
K4-4PhgProfil1	46.82	0.66	34.16	2.47	0.00	0.89	0.04	0.05	0.47	10.18	95.73	0.01	0.00
K4-4PhgProfil1	46.97	0.65	33.91	2.38	0.04	0.88	0.01	0.01	0.47	10.23	95.56	0.00	0.00
K4-4PhgProfil1	47.20	0.65	33.88	2.57	0.03	0.92	0.00	0.06	0.49	10.34	96.13	0.01	0.00
K4-4PhgProfil1	47.06	0.61	33.62	2.61	0.00	0.92	0.03	0.01	0.43	10.37	95.66	0.00	0.00
K4-4PhgProfil1	46.82	0.64	33.43	2.50	0.02	0.96	0.05	0.00	0.41	10.43	95.24	0.01	0.00
K4-4PhgProfil1	46.70	0.65	33.79	2.52	0.02	0.89	0.00	0.02	0.48	10.22	95.30	0.01	0.00
K4-4PhgProfil1	46.93	0.66	33.94	2.57	0.01	0.89	0.07	0.14	0.51	10.27	95.98	0.01	0.00
K4-4PhgProfil1	46.63	0.64	33.74	2.38	0.00	0.85	0.05	0.00	0.54	10.26	95.10	0.01	0.00
K4-4PhgProfil1	46.85	0.66	34.15	2.58	0.02	0.83	0.02	0.12	0.54	10.22	95.99	0.01	0.00
K4-4PhgProfil1	46.80	0.66	34.01	2.58	0.00	0.87	0.03	0.00	0.51	10.23	95.68	0.02	0.00
K4-4PhgProfil1	46.84	0.66	34.07	2.61	0.00	0.84	0.05	0.00	0.50	10.33	95.89	0.00	0.00
K4-4PhgProfil1	46.74	0.67	34.11	2.59	0.00	0.86	0.01	0.00	0.52	10.36	95.87	0.01	0.00
K4-4PhgProfil1	46.69	0.64	34.22	2.48	0.02	0.90	0.03	0.08	0.59	10.35	96.00	0.00	0.00
K4-4PhgProfil1	46.63	0.66	34.35	2.55	0.00	0.81	0.01	0.00	0.54	10.35	95.91	0.00	0.00
K4-4PhgProfil1	46.72	0.65	34.35	2.49	0.01	0.80	0.01	0.01	0.55	10.24	95.82	0.01	0.00
K4-4PhgProfil1	46.57	0.67	34.24	2.50	0.00	0.75	0.02	0.05	0.53	10.16	95.48	0.01	0.00
K4-4PhgProfil1	46.93	0.67	33.85	2.56	0.01	0.85	0.00	0.01	0.40	10.33	95.60	0.00	0.00
K4-4PhgProfil1	46.73	0.64	33.59	2.61	0.01	0.90	0.03	0.00	0.50	10.30	95.29	0.00	0.00
K4-4PhgProfil1	47.06	0.64	34.07	2.40	0.00	0.87	0.09	0.00	0.50	10.14	95.78	0.00	0.00
K4-4PhgProfil1	46.83	0.65	34.36	2.47	0.02	0.81	0.00	0.00	0.51	10.19	95.84	0.00	0.00
K4-4PhgProfil1	46.77	0.65	34.29	2.40	0.06	0.83	0.01	0.00	0.58	10.16	95.74	0.01	0.00
K4-4PhgProfil1	47.14	0.60	34.31	2.58	0.00	0.87	0.04	0.04	0.52	10.29	96.38	0.00	0.00
K4-4PhgProfil1	46.92	0.66	34.11	2.72	0.01	0.84	0.02	0.00	0.56	10.26	96.11	0.01	0.00
K4-4PhgProfil1	46.53	0.62	33.80	2.62	0.02	0.86	0.00	0.00	0.46	10.28	95.19	0.01	0.00
K4-4PhgProfil1	46.49	0.70	34.11	2.45	0.00	0.88	0.05	0.10	0.59	10.24	95.62	0.01	0.00
K4-4PhgProfil1	46.75	0.63	33.87	2.45	0.03	0.83	0.03	0.00	0.52	10.30	95.40	0.00	0.00
K4-4PhgProfil1	46.84	0.67	34.25	2.40	0.05	0.81	0.01	0.08	0.55	10.39	96.05	0.00	0.00
K4-4PhgProfil1	46.36	0.61	34.01	2.55	0.00	0.80	0.06	0.01	0.51	10.45	95.36	0.02	0.00
K4-4PhgProfil1	47.14	0.65	33.84	2.56	0.04	0.87	0.05	0.00	0.46	10.48	96.09	0.01	0.00
K4-4PhgProfil1	47.04	0.57	33.26	2.83	0.01	0.96	0.02	0.03	0.41	10.45	95.58	0.00	0.00
K4-4PhgProfil2 [440]	46.93	0.58	33.45	2.56	0.03	0.90	0.01	0.04	0.41	10.44	95.36	0.00	0.00
K4-4PhgProfil2	47.18	0.62	33.62	2.30	0.00	0.96	0.01	0.06	0.32	10.49	95.56	0.00	0.00
K4-4PhgProfil2	47.09	0.60	33.77	2.46	0.00	0.89	0.00	0.05	0.50	10.36	95.71	0.00	0.00
K4-4PhgProfil2	46.72	0.56	34.12	2.44	0.01	0.77	0.04	0.00	0.54	10.29	95.49	0.00	0.00
K4-4PhgProfil2	46.42	0.62	33.98	2.48	0.00	0.84	0.05	0.01	0.53	10.20	95.12	0.00	0.00
K4-4PhgProfil2	46.96	0.59	33.82	2.53	0.03	0.93	0.00	0.15	0.42	10.48	95.91	0.01	0.00
K4-4PhgProfil2	41.92	0.60	31.57	2.30	0.00	0.78	0.01	0.08	0.41	8.88	86.54	0.11	0.00
K4-4PhgProfil2	46.69	0.63	34.55	2.35	0.02	0.80	0.00	0.00	0.52	10.34	95.89	0.00	0.00
K4-4PhgProfil2	46.67	0.58	34.14	2.45	0.02	0.82	0.00	0.04	0.49	10.35	95.56	0.01	0.00
K4-4PhgProfil2	46.30	0.59	34.50	2.46	0.00	0.79	0.01	0.00	0.54	10.28	95.46	0.00	0.00
K4-4PhgProfil2	46.44	0.55	34.40	2.53	0.03	0.75	0.00	0.02	0.57	10.33	95.61	0.00	0.00
K4-4PhgProfil2	46.57	0.56	34.03	2.49	0.00	0.86	0.06	0.03	0.57	10.16	95.32	0.01	0.00
K4-4PhgProfil2	47.14	0.61	34.21	2.51	0.00	0.80	0.03	0.00	0.49	10.26	96.04	0.01	0.00
K4-4PhgProfil2	46.66	0.62	34.24	2.43	0.01	0.80	0.00	0.01	0.54	10.34	95.65	0.00	0.00
K4-4PhgProfil2	46.70	0.59	34.05	2.53	0.00	0.81	0.03	0.01	0.49	10.23	95.43	0.00	0.00
K4-4PhgProfil2	46.92	0.64	34.29	2.38	0.00	0.75	0.00	0.00	0.49	10.39	95.87	0.01	0.00
K4-4PhgProfil2	46.73	0.61	34.15	2.45	0.00	0.82	0.01	0.04	0.54	10.18	95.51	0.01	0.00
K4-4PhgProfil2	47.06	0.60	33.86	2.50	0.03	0.83	0.03	0.00	0.49	10.27	95.66	0.01	0.00
K4-4PhgProfil2	46.72	0.61	33.99	2.49	0.00	0.79	0.03	0.09	0.54	10.30	95.56	0.00	0.00
K4-4PhgProfil2	46.71	0.66	34.09	2.37	0.00	0.85	0.01	0.01	0.55	10.41	95.67	0.02	0.00
K4-4PhgProfil2	46.36	0.59	33.89	2.48	0.01	0.78	0.01	0.00	0.43	10.29	94.85	0.01	0.00
K4-4PhgProfil2	47.11	0.63	34.35	2.43	0.00	0.82	0.01	0.14	0.50	10.32	96.30	0.00	0.00
K4-4PhgProfil2	46.96	0.65	34.38	2.43	0.07	0.81	0.00	0.00	0.56	10.36	96.22	0.00	0.00
K4-4PhgProfil2	47.07	0.60	34.54	2.44	0.00	0.81	0.01	0.00	0.50	10.30	96.27	0.01	0.00
K4-4PhgProfil2	44.94	0.56	33.28	2.35	0.04	0.80	0.01	0.03	0.46	9.64	92.12	0.03	0.00
K4-4PhgProfil2	46.55	0.58	34.35	2.43	0.06	0.79	0.01	0.00	0.53	10.39	95.68	0.00	0.00

K4-4PhgProfil2	46.43	0.63	34.21	2.36	0.00	0.83	0.01	0.19	0.51	10.42	95.58	0.02	0.00
K4-4PhgProfil2	46.79	0.58	34.36	2.50	0.01	0.81	0.00	0.05	0.48	10.30	95.89	0.01	0.00
K4-4PhgProfil2	46.52	0.59	34.07	2.31	0.00	0.84	0.02	0.00	0.54	10.38	95.28	0.01	0.00
K4-4PhgProfil2	46.74	0.58	33.89	2.57	0.06	0.79	0.01	0.08	0.51	10.49	95.72	0.01	0.00
K4-21,1BtProfil1 [110]	39.18	2.23	17.56	13.86	0.00	14.50	0.03	0.13	0.19	8.43	96.10	0.00	0.00
K4-21,1BtProfil1	38.97	2.09	17.20	13.88	0.02	14.80	0.02	0.14	0.21	8.42	95.74	0.01	0.00
K4-21,1BtProfil1	39.06	1.98	17.64	13.60	0.02	15.11	0.02	0.05	0.21	8.30	95.96	0.00	0.00
K4-21,1BtProfil1	39.08	2.05	17.56	13.94	0.02	14.95	0.03	0.10	0.20	8.44	96.36	0.00	0.00
K4-21,1BtProfil1	38.37	2.88	16.64	13.91	0.00	14.09	0.00	0.18	0.18	8.39	94.62	0.01	0.00
K4-21,1BtProfil1	38.62	3.03	16.45	14.46	0.02	14.37	0.00	0.12	0.21	8.57	95.85	0.00	0.00
K4-21,1BtProfil1	38.80	3.11	16.45	14.53	0.00	14.28	0.02	0.13	0.22	8.53	96.07	0.00	0.00
K4-21,1BtProfil1	39.21	3.28	16.65	14.55	0.00	14.29	0.00	0.14	0.20	8.68	97.00	0.00	0.00
K4-21,1BtProfil1	38.88	3.30	16.27	14.66	0.02	14.24	0.00	0.21	0.20	8.52	96.29	0.00	0.00
K4-21,1BtProfil1	38.82	3.32	16.55	14.78	0.01	14.17	0.01	0.16	0.26	8.55	96.63	0.00	0.00
K4-21,1BtProfil1	39.00	3.27	16.37	14.30	0.00	14.06	0.01	0.14	0.23	8.62	95.99	0.00	0.00
K4-21,1BtProfil1	38.44	3.26	16.64	14.66	0.00	14.20	0.00	0.16	0.20	8.64	96.19	0.00	0.00
K4-21,1BtProfil1	38.88	2.75	16.44	14.43	0.00	14.45	0.04	0.10	0.19	8.44	95.72	0.01	0.00
K4-21,1BtProfil1	38.55	3.13	16.46	14.50	0.02	14.43	0.00	0.13	0.22	8.67	96.10	0.00	0.00
K4-21,1BtProfil1	38.68	2.61	17.00	14.29	0.05	14.42	0.00	0.10	0.22	8.56	95.94	0.00	0.00
K4-21,1BtProfil1	34.89	2.48	15.30	12.67	0.00	13.05	0.07	0.16	0.18	7.49	86.27	0.05	0.00
K4-21,1BtProfil1	38.51	2.63	16.60	14.29	0.00	14.55	0.03	0.06	0.22	8.46	95.33	0.00	0.00
K4-21,1BtProfil1	39.01	2.78	16.76	14.31	0.03	14.03	0.01	0.15	0.19	8.60	95.86	0.01	0.00
K4-21,1BtProfil1	38.44	2.97	16.51	14.25	0.00	14.25	0.00	0.12	0.23	8.49	95.28	0.00	0.00
K4-21,1BtProfil1	38.81	3.17	16.35	14.70	0.00	14.04	0.00	0.12	0.18	8.68	96.05	0.00	0.00
K4-21,1BtProfil1	38.82	3.30	16.31	14.71	0.00	13.88	0.00	0.09	0.23	8.65	96.00	0.01	0.00
K4-21,1BtProfil1	38.89	3.07	16.34	14.29	0.02	14.28	0.01	0.09	0.19	8.59	95.78	0.01	0.00
K4-21,1BtProfil1	39.10	3.02	16.30	14.50	0.04	14.36	0.00	0.01	0.21	8.39	95.93	0.02	0.00
K4-21,1BtProfil2 [80]	37.01	1.93	16.94	15.87	0.02	14.67	0.27	0.02	0.15	6.02	92.90	0.00	0.00
K4-21,1BtProfil2	39.01	2.42	16.72	13.97	0.00	15.06	0.03	0.01	0.19	8.41	95.82	0.00	0.00
K4-21,1BtProfil2	38.42	2.49	16.54	14.00	0.00	14.78	0.06	0.14	0.19	8.26	94.87	0.00	0.00
K4-21,1BtProfil2	38.77	3.00	16.10	14.56	0.00	14.61	0.02	0.15	0.20	8.54	95.94	0.02	0.00
K4-21,1BtProfil2	38.81	3.11	16.42	14.39	0.00	14.70	0.05	0.15	0.18	8.60	96.40	0.00	0.00
K4-21,1BtProfil2	38.84	2.99	16.22	14.44	0.03	14.59	0.14	0.21	0.18	7.82	95.46	0.00	0.00
K4-21,1BtProfil2	37.06	3.04	15.23	14.51	0.00	14.01	0.03	0.17	0.19	8.45	92.69	0.00	0.00
K4-21,1BtProfil2	39.10	3.11	16.01	14.34	0.00	14.73	0.02	0.20	0.20	8.55	96.27	0.00	0.00
K4-21,1BtProfil2	39.00	2.88	16.75	14.43	0.00	14.24	0.05	0.09	0.22	8.54	96.20	0.00	0.00
K4-21Bt1 [10]	39.07	3.20	18.76	14.35	0.03	13.01	0.01	0.11	0.19	8.82	97.54	0.01	n.d.
K4-21Bt1	39.05	3.27	18.77	14.59	0.00	13.03	0.00	0.17	0.17	8.50	97.54	0.00	n.d.
K4-21Bt1	38.85	3.46	18.42	14.52	0.00	13.01	0.02	0.09	0.16	8.60	97.12	0.01	n.d.
K4-21Bt2 [50]	38.65	2.17	18.89	14.55	0.02	13.55	0.09	0.05	0.14	8.01	96.12	0.01	n.d.
K4-21Bt2	38.47	3.35	18.33	14.95	0.04	12.92	0.01	0.00	0.19	8.75	97.00	0.01	n.d.
K4-21Bt2	38.39	3.49	18.14	14.94	0.04	12.80	0.03	0.06	0.20	8.55	96.65	0.01	n.d.
K4-21Bt2	39.12	3.45	18.39	14.81	0.00	12.99	0.00	0.15	0.22	8.69	97.81	0.00	n.d.
K4-21Bt2	38.95	3.40	18.22	15.00	0.03	13.17	0.00	0.17	0.24	8.71	97.89	0.00	n.d.
K4-21Bt2	38.80	3.43	18.17	15.08	0.02	13.03	0.00	0.20	0.22	8.71	97.65	0.01	n.d.
K4-21Bt2	38.69	3.57	18.15	15.01	0.02	13.03	0.01	0.20	0.21	8.66	97.55	0.00	n.d.
K4-21Bt2	38.89	3.57	17.99	15.08	0.00	13.08	0.03	0.17	0.22	8.60	97.63	0.00	n.d.
K4-21Bt2	39.08	3.42	18.13	15.01	0.06	13.06	0.03	0.28	0.14	8.61	97.83	0.00	n.d.
K4-21Bt2	38.58	3.02	18.68	15.19	0.00	12.92	0.10	0.09	0.16	8.28	97.01	0.02	n.d.
K4-21Bt3Rand	36.68	4.00	18.04	13.92	0.03	12.44	0.02	0.07	0.13	8.59	93.92	0.01	n.d.
K4-21Bt3Rand	36.51	3.69	17.55	13.47	0.04	12.32	0.02	0.11	0.13	8.44	92.27	0.02	n.d.
K4-21Bt4 [20]	38.13	3.16	18.14	13.72	0.03	14.40	0.13	0.00	0.15	7.82	95.67	0.00	n.d.
K4-21Bt4	37.60	3.36	17.84	13.82	0.00	14.00	0.27	0.19	0.15	7.52	94.75	0.00	n.d.
K4-21Bt4	38.28	3.47	17.88	14.19	0.01	13.91	0.21	0.14	0.16	7.67	95.91	0.03	n.d.
K4-21Bt4	38.18	3.59	17.88	13.78	0.00	13.76	0.05	0.15	0.20	8.48	96.07	0.02	n.d.
K4-35,1Bt1	38.87	1.66	16.62	13.35	0.00	15.59	0.05	n.d.	0.12	9.08	95.33	0.01	0.00
K4-35,1Bt2	38.37	1.65	17.23	14.54	0.04	15.02	0.11	n.d.	0.06	9.35	96.37	0.01	0.00
K4-37Gl1-l1 embedded [ca 50]	49.46	0.57	30.03	3.64	0.02	1.53	0.00	0.14	0.34	10.62	96.34	0.01	n.d.
K4-37Gl1-l1	50.85	0.49	28.27	3.89	0.03	1.83	0.00	0.26	0.26	10.08	95.97	0.02	n.d.
K4-37Gl1-l1	50.57	0.57	29.16	3.76	0.04	1.69	0.00	0.09	0.32	10.25	96.45	0.00	n.d.
K4-37Gl1-l1	49.36	0.63	30.89	3.18	0.00	1.39	0.05	0.07	0.35	10.29	96.21	0.00	n.d.
K4-37Gl1-l1	47.71	0.91	32.85	2.95	0.00	0.98	0.01	0.22	0.50	10.14	96.27	0.00	n.d.
K4-37Gl1-l2 embedded [ca 80]	50.34	0.28	29.32	3.89	0.04	1.78	0.00	0.05	0.31	10.20	96.22	0.00	n.d.
K4-37Gl1-l2	50.36	0.20	29.09	3.66	0.00	1.76	0.02	0.09	0.33	10.15	95.65	0.00	n.d.
K4-37Gl1-l2	51.48	0.31	29.40	3.95	0.03	1.86	0.00	0.00	0.21	9.04	96.28	0.00	n.d.
K4-37Gl1-l2	50.95	0.37	28.85	3.95	0.05	1.76	0.01	0.19	0.31	9.98	96.42	0.00	n.d.
K4-37Gl1-l2	50.67	0.31	29.06	3.86	0.01	1.71	0.00	0.06	0.37	10.07	96.11	0.00	n.d.
K4-37Gl1-l2	50.49	0.48	29.30	3.67	0.04	1.63	0.02	0.10	0.39	10.06	96.18	0.01	n.d.
K4-37Gl1-l2	49.76	0.64	29.40	3.60	0.03	1.69	0.01	0.12	0.38	10.39	96.01	0.00	n.d.
K4-37Gl1-l2	47.71	0.77	31.81	2.96	0.01	1.14	0.01	0.15	0.51	10.32	95.38	0.01	n.d.
K4-37Gl2-l1 embedded [ca 110]	48.60	0.94	30.65	2.99	0.06	1.35	0.02	0.11	0.42	9.69	94.81	0.00	n.d.
K4-37Gl2-l1	48.52	0.95	30.85	3.01	0.04	1.56	0.00	0.15	0.39	10.32	95.78	0.01	n.d.
K4-37Gl2-l1	49.14	0.94	30.53	3.15	0.01	1.62	0.01	0.09	0.37	10.23	96.07	0.00	n.d.
K4-37Gl2-l1	49.06	0.83	30.52	3.31	0.00	1.65	0.01	0.10	0.40	10.18	96.07	0.00	n.d.

K4-37Gl2-l1	48.96	0.90	30.60	3.17	0.00	1.64	0.00	0.12	0.36	10.15	95.90	0.00	n.d.
K4-37Gl2-l1	48.97	0.96	30.54	3.22	0.04	1.61	0.00	0.12	0.42	10.26	96.14	0.00	n.d.
K4-37Gl2-l1	48.78	0.93	30.56	3.07	0.00	1.60	0.00	0.33	0.36	10.33	95.95	0.00	n.d.
K4-37Gl2-l1	48.20	0.98	30.39	2.98	0.02	1.58	0.01	0.11	0.45	10.28	94.98	0.00	n.d.
K4-37Gl2-l1	49.00	0.91	30.59	3.15	0.00	1.58	0.00	0.14	0.40	10.32	96.09	0.00	n.d.
K4-37Gl3-l1 embedded [ca 100]	49.18	0.75	30.65	3.21	0.00	1.54	0.00	0.09	0.34	10.44	96.21	0.02	n.d.
K4-37Gl3-l1	49.28	0.68	30.43	3.17	0.00	1.56	0.00	0.16	0.39	10.18	95.85	0.00	n.d.
K4-37Gl3-l1	49.06	0.67	30.51	3.11	0.04	1.55	0.02	0.16	0.38	10.15	95.63	0.00	n.d.
K4-37Gl3-l1	49.35	0.74	30.79	3.10	0.05	1.53	0.02	0.11	0.38	10.36	96.42	0.02	n.d.
K4-37Gl3-l1	49.00	0.76	31.24	3.17	0.02	1.44	0.02	0.19	0.42	10.42	96.67	0.00	n.d.
K4-37Gl3-l1	48.56	0.74	31.29	3.14	0.00	1.44	0.04	0.22	0.39	10.49	96.30	0.00	n.d.
K4-37Gl3-l1	48.67	0.74	31.17	2.98	0.03	1.39	0.02	0.00	0.41	10.55	95.95	0.00	n.d.
K4-37Gl3-l1	48.61	0.74	31.73	3.17	0.04	1.28	0.01	0.22	0.43	10.28	96.49	0.00	n.d.
K4-37Gl3-l1	48.35	0.77	32.39	2.97	0.02	1.16	0.00	0.23	0.43	10.26	96.57	0.01	n.d.
K4-37Gl3-l1	48.00	0.69	32.65	2.89	0.01	1.17	0.00	0.20	0.47	10.39	96.46	0.01	n.d.
K4-37(6)Bt1 embedded [ca 70]	34.66	2.78	17.75	27.62	0.08	3.98	0.05	0.02	0.08	8.63	95.64	0.01	n.d.
K4-37(6)Bt1	34.70	2.83	17.50	27.87	0.10	4.05	0.03	0.07	0.12	8.63	95.89	0.00	n.d.
K4-37(6)Bt1	35.26	2.81	17.51	27.69	0.11	4.03	0.00	0.07	0.10	8.97	96.56	0.00	n.d.
K4-37(6)Bt1	33.17	2.74	16.83	25.55	0.07	3.87	0.04	0.20	0.11	7.89	90.45	0.00	n.d.
K4-37(6)Bt1	34.83	2.73	17.68	27.50	0.14	4.12	0.00	0.11	0.10	9.13	96.34	0.01	n.d.
K4-37(6)Bt1	34.97	2.70	17.76	28.04	0.04	4.10	0.01	0.08	0.06	8.75	96.51	0.01	n.d.
K4-37(6)Bt1	35.06	2.74	17.97	27.51	0.06	4.17	0.01	0.07	0.08	8.82	96.49	0.01	n.d.
K4-37(6)Bt1	34.55	2.76	17.73	27.47	0.12	3.86	0.01	0.20	0.10	8.72	95.50	0.00	n.d.
K4-37(6)Bt1	34.69	2.76	17.58	27.81	0.15	3.95	0.02	0.00	0.09	8.83	95.88	0.00	n.d.
K4-37(6)Bt1	35.12	2.73	18.36	26.99	0.14	3.98	0.03	0.17	0.12	8.94	96.58	0.00	n.d.
K4-37(6)Bt2 embedded [ca 90]	34.87	1.09	18.50	26.75	0.14	5.07	0.01	0.00	0.11	8.99	95.52	0.00	n.d.
K4-37(6)Bt2	34.82	1.71	18.44	26.99	0.14	4.87	0.04	0.00	0.06	9.01	96.09	0.00	n.d.
K4-37(6)Bt2	35.28	2.51	17.44	27.34	0.18	4.85	0.08	0.06	0.06	8.47	96.27	0.01	n.d.
K4-37(6)Bt2	35.12	2.58	17.87	27.13	0.15	4.61	0.00	0.12	0.11	8.93	96.61	0.01	n.d.
K4-37(6)Bt2	32.75	2.43	16.73	25.89	0.19	4.22	0.01	0.00	0.08	8.24	90.54	0.02	n.d.
K4-37(6)Bt2	34.84	2.64	18.10	26.95	0.17	4.42	0.01	0.09	0.05	9.08	96.35	0.02	n.d.
K4-37(6)Bt2	34.96	2.65	17.98	27.11	0.17	4.49	0.01	0.10	0.06	9.17	96.71	0.00	n.d.
K4-37(6)Bt2	35.10	2.59	18.13	26.77	0.22	4.41	0.00	0.04	0.11	9.11	96.49	0.01	n.d.
K4-37(6)Bt2	35.02	2.59	18.00	27.08	0.15	4.34	0.03	0.12	0.05	9.05	96.43	0.01	n.d.
K4-37(6)Bt2	35.22	2.73	17.95	26.86	0.12	4.36	0.00	0.00	0.13	9.05	96.42	0.00	n.d.
K4-37(6)Bt3 embedded [ca 70]	35.39	2.37	17.63	25.38	0.15	5.67	0.00	0.00	0.08	9.09	95.76	0.00	n.d.
K4-37(6)Bt3	35.63	2.30	17.49	25.51	0.11	5.75	0.01	0.01	0.09	9.19	96.08	0.00	n.d.
K4-37(6)Bt3	25.74	1.69	13.06	18.39	0.05	4.26	0.03	0.04	0.06	6.36	69.67	0.07	n.d.
K4-37(6)Bt3	35.73	2.27	17.82	24.71	0.11	5.76	0.00	0.08	0.09	9.02	95.61	0.01	n.d.
K4-37(6)Bt3	35.22	2.09	17.57	25.38	0.13	5.69	0.00	0.24	0.07	9.12	95.52	0.00	n.d.
K4-37(6)Bt3	35.74	2.29	17.75	25.47	0.13	5.79	0.00	0.13	0.08	9.26	96.64	0.01	n.d.
K4-37(6)Bt3	35.68	2.30	17.84	25.40	0.11	5.65	0.01	0.24	0.08	9.18	96.50	0.01	n.d.
K4-37(6)Bt3	36.02	2.28	17.79	25.07	0.09	5.73	0.00	0.18	0.06	9.15	96.37	0.01	n.d.
K4-37(6)Bt3	35.89	2.27	17.87	25.22	0.14	5.79	0.00	0.08	0.04	9.19	96.48	0.00	n.d.
K4-37(6)Bt3	35.60	2.20	17.96	25.11	0.11	5.81	0.02	0.05	0.06	9.23	96.14	0.00	n.d.
K4-37(6)Bt4 embedded [ca 50]	35.80	2.81	18.13	25.46	0.10	4.88	0.00	0.14	0.13	9.31	96.76	0.00	n.d.
K4-37(6)Bt4	35.33	2.81	18.43	25.47	0.07	4.84	0.00	0.16	0.11	8.90	96.11	0.00	n.d.
K4-37(6)Bt4	35.34	2.81	18.24	25.67	0.11	4.89	0.00	0.00	0.16	9.01	96.22	0.00	n.d.
K4-37(6)Bt4	35.21	2.82	18.03	26.05	0.07	5.01	0.01	0.12	0.07	9.28	96.65	0.00	n.d.
K4-37(6)Bt4	35.22	2.78	18.06	25.23	0.10	5.01	0.00	0.21	0.12	8.99	95.71	0.00	n.d.
K4-37(6)Bt4	34.25	2.79	17.79	24.93	0.11	4.81	0.00	0.02	0.14	8.85	93.69	0.00	n.d.
K4-37(6)Bt5 embedded [ca 70]	45.46	1.19	28.29	9.43	0.15	2.11	0.03	0.18	0.28	9.69	96.80	0.00	n.d.
K4-37(6)Bt5	49.59	0.63	30.58	3.60	0.00	1.57	0.01	0.20	0.35	10.31	96.83	0.00	n.d.
K4-37(6)Bt5	50.18	0.63	29.89	3.52	0.06	1.76	0.00	0.26	0.37	10.24	96.91	0.00	n.d.
K4-37(6)Bt5	49.42	0.72	30.77	3.26	0.05	1.50	0.02	0.13	0.32	10.30	96.48	0.00	n.d.
K4-37(6)Bt5	49.42	0.72	30.63	3.35	0.00	1.56	0.00	0.02	0.37	10.38	96.43	0.01	n.d.
K4-37(6)Bt5	48.99	0.55	31.56	3.41	0.02	1.42	0.00	0.15	0.37	10.38	96.84	0.00	n.d.
K4-37(6)Bt5	40.09	1.50	23.98	16.00	0.52	2.83	0.08	0.54	0.17	9.06	94.77	0.02	n.d.
K4-53,1BtProfil1 [100]	36.88	4.31	15.13	14.82	0.06	13.39	0.01	n.d.	0.11	9.57	94.28	0.00	0.00
K4-53,1BtProfil1	37.01	4.28	14.86	14.57	0.02	13.48	0.00	n.d.	0.12	9.51	93.85	0.00	0.00
K4-53,1BtProfil1	37.20	4.36	14.96	13.74	0.01	13.42	0.01	n.d.	0.12	9.52	93.32	0.02	0.00
K4-53,1BtProfil1	37.15	4.37	14.85	14.66	0.03	13.37	0.02	n.d.	0.13	9.59	94.16	0.00	0.00
K4-53,1BtProfil1	36.77	4.34	15.23	14.70	0.04	13.19	0.03	n.d.	0.13	9.43	93.85	0.01	0.00
K4-53,1BtProfil2 [ca 20]	36.79	4.24	15.17	15.15	0.02	13.21	0.02	n.d.	0.11	9.62	94.33	0.01	0.00
K4-53,1BtProfil2	36.88	4.22	15.04	15.21	0.00	13.09	0.02	n.d.	0.14	9.61	94.21	0.00	0.00
K4-57,2Bt1	37.06	3.18	16.15	16.55	0.03	14.12	0.02	n.d.	0.09	9.86	97.07	0.01	0.00
K4-57,2Bt2	36.82	2.93	16.57	16.18	0.06	14.17	0.04	n.d.	0.10	9.74	96.60	0.01	0.00
K4-57,2Bt3	36.88	3.77	15.74	15.67	0.00	13.84	0.04	n.d.	0.09	9.56	95.58	0.01	0.00
K4-57,2Bt4	37.33	3.86	15.54	15.50	0.01	14.10	0.06	n.d.	0.13	9.54	96.07	0.01	0.00
K4-57,2Bt5	36.35	3.52	16.18	15.88	0.02	13.39	0.03	n.d.	0.08	9.71	95.15	0.00	0.00
K4-57,2Bt6	36.09	3.45	15.99	16.74	0.02	13.17	0.08	n.d.	0.09	9.20	94.84	0.00	0.00
K4-58,1bt4	37.22	3.32	14.79	18.93	0.03	12.92	0.01	n.d.	0.05	9.65	96.93	0.00	0.16
K4-70Bt1 [90]	36.29	2.99	18.24	22.67	0.39	7.91	0.05	0.03	0.10	9.28	97.94	0.01	n.d.
K4-70Bt1	36.16	2.99	18.19	22.62	0.36	7.85	0.03	0.28	0.06	9.16	97.69	0.00	n.d.

K4-70Bt1	35.94	3.09	18.19	22.65	0.35	7.88	0.07	0.29	0.07	9.26	97.78	0.00	n.d.
K4-70Bt1	35.82	3.19	18.40	21.81	0.40	7.81	0.03	0.18	0.07	9.17	96.89	0.01	n.d.
K4-70Bt1	36.24	3.13	18.26	22.24	0.47	7.84	0.07	0.34	0.06	9.09	97.73	0.02	n.d.
K4-70Bt1	34.13	3.03	18.30	21.77	0.35	7.37	0.32	0.09	0.12	8.49	93.97	0.04	n.d.
K4-70Bt1,2 [190]	36.39	2.91	18.84	22.05	0.41	8.01	0.10	0.13	0.07	9.02	97.92	0.02	n.d.
K4-70Bt1,2	36.20	3.03	18.78	21.94	0.33	7.89	0.03	0.29	0.09	9.53	98.11	0.00	n.d.
K4-70Bt1,2	36.10	2.91	18.78	21.61	0.43	7.90	0.01	0.13	0.08	9.38	97.32	0.01	n.d.
K4-70Bt1,2	36.02	3.06	18.36	22.43	0.39	7.78	0.02	0.34	0.07	9.39	97.86	0.02	n.d.
K4-70Bt1,2	35.80	2.91	18.23	21.96	0.40	7.74	0.04	0.24	0.08	9.22	96.62	0.01	n.d.
K4-70Bt1,2	35.06	2.91	17.97	21.90	0.39	7.67	0.18	0.09	0.19	9.08	95.45	0.05	n.d.
K4-70Bt2 [160]	36.15	3.21	18.02	21.84	0.30	8.44	0.06	0.28	0.02	9.01	97.33	0.00	n.d.
K4-70Bt2	36.09	3.20	18.03	22.03	0.36	8.32	0.05	0.29	0.09	9.00	97.47	0.02	n.d.
K4-70Bt2	35.42	3.27	17.88	21.64	0.33	8.20	0.05	0.29	0.06	9.03	96.15	0.02	n.d.
K4-70Bt2	35.74	3.27	18.29	21.36	0.31	8.21	0.02	0.09	0.08	9.13	96.49	0.00	n.d.
K4-76Bt1	36.16	4.05	15.53	16.50	0.02	13.41	0.02	0.18	0.08	9.16	95.12	0.00	0.00
K4-76Bt2	36.18	3.92	15.36	16.53	0.03	13.29	0.04	0.23	0.06	8.79	94.44	0.00	0.00
K4-76Bt3	36.37	3.85	16.07	16.14	0.03	13.36	0.11	0.28	0.13	8.59	94.92	0.00	0.00
K4-84,1Bt1	37.34	3.66	15.56	14.52	0.02	14.19	0.03	0.12	0.06	9.56	95.06	0.00	0.00
K4-84,1Bt2	37.57	3.61	15.53	14.58	0.05	14.23	0.10	0.19	0.09	9.54	95.49	0.01	0.00
K4-84,1Bt3	37.37	3.70	15.77	14.56	0.04	14.09	0.04	0.21	0.08	9.57	95.40	0.00	0.00
K4-97-Gl1 embedded [ca 20]	48.35	0.97	29.14	4.96	0.00	1.83	0.02	0.23	0.32	10.28	96.08	0.00	n.d.
K4-97-Gl1	46.16	0.99	28.19	4.34	0.02	1.84	0.04	0.27	0.35	9.68	91.87	0.01	n.d.
K4-97-Gl2 embedded [ca 20]	47.64	1.06	29.81	4.60	0.00	1.70	0.00	0.12	0.32	10.66	95.90	0.00	n.d.
K4-97-Gl2	48.14	1.05	29.67	4.54	0.02	1.66	0.00	0.15	0.31	10.56	96.10	0.00	n.d.
K4-97-Gl3 embedded [ca 40]	47.36	0.76	28.86	5.64	0.06	1.75	0.01	0.06	0.31	10.31	95.13	0.00	n.d.
K4-97-Gl3	47.41	0.76	29.18	5.88	0.04	1.71	0.02	0.33	0.37	10.65	96.36	0.00	n.d.
K4-97-Gl3	47.37	0.80	29.16	6.00	0.00	1.69	0.03	0.14	0.42	10.33	95.93	0.00	n.d.
K4-97-Gl3	47.36	0.80	29.06	5.50	0.04	1.70	0.02	0.19	0.34	10.46	95.46	0.00	n.d.
K4-97-Gl4 embedded [ca 60]	47.98	1.00	29.40	4.23	0.00	1.68	0.00	0.13	0.26	10.53	95.22	0.00	n.d.
K4-97-Gl4	48.69	1.04	29.42	4.39	0.06	1.80	0.00	0.17	0.27	10.58	96.41	0.00	n.d.
K4-97-Gl4	48.35	1.10	28.94	4.38	0.00	1.85	0.00	0.20	0.28	10.51	95.60	0.00	n.d.
K4-97-Gl4	48.37	1.07	29.09	4.64	0.01	1.81	0.00	0.28	0.33	10.34	95.94	0.02	n.d.
K4-97-Gl4	48.28	1.15	29.31	4.48	0.00	1.80	0.03	0.15	0.33	10.59	96.12	0.00	n.d.
K4-97-Gl5 embedded [ca 60]	47.41	1.03	29.01	4.34	0.00	1.85	0.00	0.41	0.28	10.34	94.67	0.01	n.d.
K4-97-Gl5	48.44	1.00	29.07	4.65	0.01	1.86	0.00	0.29	0.31	10.47	96.10	0.00	n.d.
K4-97-Gl5	48.71	1.04	29.37	4.55	0.00	1.85	0.00	0.13	0.29	10.49	96.43	0.01	n.d.
K4-97-Gl5	48.76	1.01	29.06	4.70	0.00	1.84	0.01	0.16	0.30	10.59	96.44	0.01	n.d.
K4-97-Gl5	48.66	0.95	29.14	4.45	0.05	1.84	0.01	0.20	0.30	10.53	96.12	0.00	n.d.
K4-97-Gl6 embedded [ca 50]	47.90	1.03	29.36	5.23	0.00	1.63	0.00	0.10	0.31	10.49	96.04	0.00	n.d.
K4-97-Gl6	47.77	1.10	29.37	5.19	0.00	1.66	0.00	0.24	0.30	10.56	96.19	0.00	n.d.
K4-97-Gl6	47.88	0.96	29.30	5.04	0.00	1.63	0.00	0.26	0.29	10.71	96.06	0.01	n.d.
K4-97-Gl6	47.73	1.00	29.84	4.99	0.09	1.54	0.03	0.35	0.25	10.46	96.27	0.00	n.d.
K4-97-Gl7 embedded [ca 80]	45.33	0.97	28.13	4.30	0.00	1.63	0.00	0.30	0.30	9.79	90.74	0.03	n.d.
K4-97-Gl7	48.13	0.92	29.95	4.53	0.02	1.65	0.00	0.18	0.31	10.63	96.30	0.01	n.d.
K4-97-Gl7	48.53	0.95	29.72	4.49	0.03	1.64	0.00	0.16	0.30	10.62	96.43	0.00	n.d.
K4-97-Gl7	47.62	0.97	29.72	4.60	0.00	1.68	0.00	0.39	0.33	10.45	95.75	0.01	n.d.
K4-97-Gl7	48.13	1.00	30.08	4.66	0.02	1.71	0.03	0.38	0.27	10.43	96.71	0.00	n.d.
K4-97-Gl8 embedded [ca 60]	48.00	0.97	29.74	4.47	0.00	1.74	0.00	0.10	0.31	10.36	95.69	0.01	n.d.
K4-97-Gl8	48.63	0.92	30.04	4.27	0.01	1.76	0.00	0.28	0.31	10.43	96.64	0.00	n.d.
K4-97-Gl8	48.66	0.96	29.64	4.51	0.01	1.77	0.00	0.16	0.30	10.82	96.83	0.01	n.d.
K4-97-Gl8	48.27	0.93	29.87	4.23	0.04	1.74	0.02	0.26	0.28	10.47	96.10	0.01	n.d.
K4-97-Gl8	46.75	0.90	31.80	4.12	0.00	1.23	0.00	0.38	0.38	10.49	96.06	0.00	n.d.
K4-97-Gl8	47.03	0.96	31.77	4.16	0.03	1.20	0.00	0.34	0.42	10.60	96.51	0.00	n.d.
K4-97Bt1 embedded [110]	36.92	3.00	17.68	22.08	0.22	8.06	0.01	0.22	0.08	8.83	97.10	0.02	n.d.
K4-97Bt1	36.85	3.04	18.27	21.78	0.17	8.14	0.07	0.18	0.06	8.54	97.10	0.01	n.d.
K4-97Bt1	36.85	3.06	17.84	22.24	0.29	8.01	0.02	0.23	0.12	9.27	97.92	0.01	n.d.
K4-97Bt1	36.41	2.95	18.16	22.09	0.19	8.00	0.00	0.23	0.08	9.25	97.35	0.02	n.d.
K4-97Bt1	36.43	2.93	17.98	22.47	0.21	7.93	0.01	0.28	0.09	9.45	97.78	0.02	n.d.
K4-97Bt1	36.38	3.09	18.21	22.60	0.21	8.00	0.00	0.06	0.11	9.36	98.01	0.00	n.d.
K4-97Bt1	36.56	2.95	18.12	22.29	0.18	8.01	0.00	0.29	0.10	9.34	97.84	0.02	n.d.
K4-97Bt1	36.02	2.97	18.05	22.33	0.21	7.97	0.01	0.23	0.11	9.22	97.12	0.03	n.d.
K4-97Bt1	37.00	3.03	17.75	22.25	0.19	8.05	0.00	0.11	0.06	9.27	97.70	0.01	n.d.
K4-97Bt1	36.72	3.09	17.72	22.05	0.21	8.11	0.05	0.07	0.08	9.04	97.14	0.00	n.d.
K4-97Bt1	37.07	3.06	17.86	22.13	0.23	8.09	0.02	0.15	0.10	9.23	97.93	0.02	n.d.
K4-97Bt1	36.51	3.09	18.00	22.75	0.19	7.97	0.00	0.09	0.11	9.59	98.30	0.01	n.d.
K4-97Bt1	36.38	2.97	17.91	22.73	0.22	8.04	0.00	0.18	0.11	9.32	97.84	0.03	n.d.
K4-97Bt1	36.53	2.97	17.82	22.15	0.23	7.94	0.00	0.15	0.09	9.35	97.23	0.02	n.d.
K4-97Bt1	36.75	3.12	18.01	22.50	0.18	8.01	0.00	0.21	0.09	9.48	98.34	0.03	n.d.
K4-97Bt1	36.92	3.04	17.82	22.34	0.18	8.09	0.01	0.29	0.07	9.34	98.10	0.01	n.d.
K4-97Bt1	37.02	3.08	17.66	22.09	0.24	8.15	0.03	0.20	0.13	9.12	97.71	0.01	n.d.
K4-97Bt1	36.60	3.07	17.78	22.22	0.22	8.04	0.02	0.30	0.07	9.35	97.67	0.01	n.d.
K4-97Bt1	37.33	3.06	17.60	21.79	0.18	8.07	0.11	0.25	0.08	8.50	96.96	0.02	n.d.
K4-97Bt1	37.00	3.04	18.06	22.60	0.24	8.14	0.00	0.21	0.07	9.36	98.72	0.01	n.d.
K4-97Bt1	36.73	3.08	17.88	22.21	0.17	7.86	0.06	0.11	0.12	9.12	97.33	0.01	n.d.
K4-97Bt1	36.56	3.07	18.23	22.53	0.22	7.97	0.00	0.27	0.10	9.26	98.22	0.01	n.d.

K4-97Bt2Rand	35.93	2.88	18.51	21.99	0.18	8.12	0.03	0.20	0.08	9.40	97.31	0.01	n.d.
K4-97Bt2Rand	35.29	2.93	18.04	20.96	0.15	7.79	0.03	0.26	0.10	8.97	94.52	0.03	n.d.
K4-97Bt2Rand	36.05	2.91	18.39	21.43	0.18	8.08	0.06	0.13	0.08	9.07	96.37	0.02	n.d.
K4-99Bt1 embedded [ca 20]	34.31	3.01	19.35	18.24	0.08	10.06	0.05	0.23	0.06	9.10	94.48	0.04	n.d.
K4-99Bt1	34.78	3.24	19.49	18.43	0.11	10.24	0.04	0.14	0.07	9.26	95.81	0.01	n.d.
K4-99Bt1	35.12	3.33	18.51	18.78	0.06	10.30	0.04	0.28	0.07	9.00	95.48	0.02	n.d.
K4-99Bt1	34.07	3.34	18.40	19.09	0.03	9.96	0.06	0.37	0.10	8.81	94.22	0.03	n.d.
K4-99Bt1	35.47	3.25	18.96	18.05	0.07	10.26	0.07	0.15	0.08	9.10	95.46	0.00	n.d.
K4-99Bt2 embedded [100]	36.36	1.40	24.10	17.38	0.08	8.38	0.50	0.28	0.30	9.34	98.11	0.02	n.d.
K4-99Bt2	33.11	1.23	22.14	15.11	5.07	8.19	0.34	0.99	0.88	8.01	95.06	0.02	n.d.
K4-99Bt2	34.79	1.56	23.13	17.72	0.22	9.44	0.03	0.28	0.09	9.50	96.76	0.00	n.d.
K4-99Bt2	34.62	1.53	23.34	18.61	0.14	9.43	0.00	0.21	0.11	9.53	97.51	0.00	n.d.
K4-99Bt2	35.04	1.53	23.18	18.03	0.10	9.62	0.01	0.25	0.11	9.40	97.27	0.01	n.d.
K4-99Bt2	35.35	1.60	22.95	17.78	0.17	9.55	0.01	0.22	0.14	9.59	97.35	0.00	n.d.
K4-99Bt2	34.24	1.62	21.94	17.37	0.10	9.19	0.00	0.33	0.13	9.07	93.97	0.00	n.d.
K4-99Bt2	35.60	1.64	22.62	18.18	0.10	9.59	0.01	0.15	0.15	9.53	97.56	0.02	n.d.
K4-99Bt2	34.80	1.60	23.14	18.16	0.06	9.52	0.01	0.21	0.11	9.79	97.40	0.00	n.d.
K4-99Bt2	35.27	1.58	23.13	18.10	0.11	9.59	0.00	0.35	0.10	9.73	97.96	0.01	n.d.
K4-99Bt2	35.19	1.62	23.04	18.06	0.11	9.56	0.01	0.12	0.11	9.56	97.36	0.02	n.d.
K4-99Bt2	35.10	1.51	23.33	17.94	0.10	9.60	0.00	0.26	0.16	9.82	97.81	0.01	n.d.
K4-99Bt2	35.06	1.61	22.50	17.71	0.06	9.55	0.00	0.12	0.12	9.56	96.29	0.02	n.d.
K4-99Bt2	35.52	1.63	22.76	17.67	0.11	9.61	0.01	0.22	0.12	9.76	97.41	0.01	n.d.
K4-99Bt2	36.26	1.79	21.69	17.18	0.15	9.38	0.00	0.11	0.12	9.40	96.07	0.00	n.d.
K4-99Bt2,1	33.81	1.53	21.33	16.50	0.09	9.25	0.03	0.33	0.12	9.17	92.16	0.03	n.d.
K4-99Bt2,1	35.28	1.59	22.89	17.54	0.12	9.56	0.01	0.15	0.12	9.56	96.82	0.00	n.d.
K4-99Bt2,1	32.74	1.33	22.29	16.42	0.17	9.21	0.05	0.10	0.15	8.85	91.30	0.02	n.d.
K4-99Bt3 embedded [ca 100]	36.03	3.39	18.34	18.78	0.13	11.32	0.01	0.14	0.06	9.64	97.85	0.02	n.d.
K4-99Bt3	35.93	3.39	18.40	18.69	0.00	11.23	0.00	0.17	0.10	9.46	97.37	0.01	n.d.
K4-99Bt3	35.82	3.37	17.96	18.31	0.10	11.34	0.02	0.38	0.05	9.50	96.87	0.02	n.d.
K4-99Bt3	35.34	3.35	18.09	18.32	0.10	11.04	0.02	0.27	0.10	9.34	95.97	0.03	n.d.
K4-99Bt3	35.66	3.36	17.89	18.53	0.09	11.06	0.00	0.09	0.11	9.29	96.09	0.00	n.d.
K4-99Bt3	33.08	3.20	16.37	16.96	0.06	10.46	0.04	0.15	0.09	8.65	89.06	0.03	n.d.
K4-99Bt3	36.01	3.48	18.22	18.65	0.08	11.32	0.03	0.14	0.10	9.34	97.35	0.00	n.d.
K4-99Bt3	36.07	3.31	18.17	18.49	0.05	11.48	0.04	0.13	0.09	9.35	97.18	0.00	n.d.
K4-99Bt3	35.57	3.36	17.89	18.29	0.06	11.26	0.00	0.20	0.09	9.45	96.16	0.02	n.d.
K4-99Bt3	36.20	3.36	17.88	18.47	0.03	11.22	0.03	0.21	0.10	9.68	97.17	0.02	n.d.
K4-99Bt3	35.81	3.29	18.15	18.43	0.14	11.25	0.00	0.11	0.08	9.67	96.92	0.00	n.d.
K4-99Bt3	35.97	3.35	17.81	18.09	0.09	11.30	0.00	0.00	0.06	9.65	96.32	0.03	n.d.
K4-99Bt3	35.35	3.38	17.37	17.69	0.07	11.07	0.05	0.16	0.17	9.13	94.42	0.02	n.d.
K4-99Bt4 embedded [40]	35.49	3.29	19.85	19.12	0.08	10.29	0.01	0.25	0.12	9.58	98.08	0.01	n.d.
K4-99Bt4	35.20	3.24	19.60	18.59	0.07	10.14	0.09	0.20	0.08	8.62	95.81	0.04	n.d.
K4-99Bt4	35.56	3.09	19.80	17.92	0.10	10.19	0.09	0.09	0.02	8.49	95.36	0.06	n.d.
K4-99Bt4	34.95	3.12	19.83	17.96	0.12	10.21	0.02	0.24	0.06	9.35	95.87	0.02	n.d.
K4-99Bt4	35.44	3.34	19.92	18.66	0.07	10.30	0.01	0.25	0.05	9.74	97.78	0.00	n.d.
K4-99Bt4	35.57	3.31	19.77	18.94	0.10	10.20	0.02	0.12	0.09	9.62	97.74	0.02	n.d.
K4-99Bt4	35.23	3.31	19.47	18.85	0.13	10.21	0.02	0.38	0.08	9.28	96.98	0.00	n.d.
K4-99,3BtProfil1 [ca 130]	35.59	1.53	18.99	19.65	0.09	12.66	0.07	0.40	0.21	7.89	97.05	0.00	0.00
K4-99,3BtProfil1	36.21	1.72	18.35	18.30	0.04	12.63	0.04	0.29	0.17	8.94	96.68	0.01	0.00
K4-99,3BtProfil1	36.73	1.72	18.09	18.08	0.08	12.72	0.06	0.14	0.09	8.60	96.29	0.00	0.00
K4-99,3BtProfil1	35.61	1.54	18.76	18.41	0.03	12.43	0.07	0.24	0.15	8.05	95.28	0.02	0.00
K4-99,3BtProfil1	35.19	1.57	18.76	18.20	0.07	12.45	0.07	0.29	0.17	8.65	95.42	0.01	0.00
K4-99,3BtProfil1	35.28	1.54	18.91	18.65	0.04	12.41	0.01	0.32	0.22	9.19	96.55	0.01	0.00
K4-99,3BtProfil1	35.31	1.56	18.89	18.66	0.00	12.35	0.02	0.33	0.19	9.16	96.46	0.01	0.00
K4-99,3BtProfil1	35.53	1.68	18.31	17.90	0.06	12.33	0.03	0.23	0.17	9.22	95.46	0.00	0.00
K4-99,3BtProfil1	35.64	1.65	18.63	18.15	0.04	12.47	0.02	0.28	0.14	9.12	96.13	0.01	0.00
K4-99,3BtProfil1	34.79	1.68	18.62	18.50	0.07	12.39	0.02	0.24	0.18	9.14	95.63	0.02	0.00
K4-99,3BtProfil1	35.36	1.85	18.49	18.11	0.04	12.55	0.02	0.26	0.17	9.15	95.99	0.02	0.00
K4-99,3BtProfil1	35.35	1.94	18.08	17.94	0.07	12.25	0.04	0.37	0.14	9.43	95.60	0.01	0.00
K4-99,3BtProfil1	34.25	1.86	18.48	18.49	0.04	11.99	0.04	0.35	0.18	9.06	94.75	0.01	0.00
K4-99,3BtProfil2 [ca 30]	34.45	2.17	18.34	18.52	0.06	12.12	0.04	0.37	0.15	9.59	95.80	0.00	0.00
K4-99,3BtProfil2	34.14	2.05	18.37	18.77	0.09	11.91	0.03	0.46	0.09	9.63	95.53	0.00	0.00
K4-99,3BtProfil2	34.05	1.95	18.44	18.96	0.02	11.98	0.02	0.46	0.14	9.59	95.60	0.02	0.00
K4-99,3BtProfil2	34.65	1.95	18.45	18.96	0.07	11.87	0.04	0.40	0.13	9.51	96.03	0.01	0.00
K4-99,2BtProfil1[ca 120]	35.95	3.85	18.15	12.43	0.00	14.99	0.03	0.19	0.16	9.41	95.15	0.01	0.00
K4-99,2BtProfil1	36.16	4.03	17.84	12.48	0.03	15.32	0.02	0.40	0.19	9.45	95.90	0.00	0.00
K4-99,2BtProfil1	36.41	4.11	17.76	12.80	0.01	15.12	0.01	0.24	0.22	9.35	96.01	0.01	0.00
K4-99,2BtProfil1	36.39	4.10	17.65	12.56	0.03	15.39	0.02	0.22	0.22	9.39	95.94	0.00	0.00
K4-99,2BtProfil1	36.40	4.13	17.36	12.59	0.02	15.25	0.00	0.24	0.22	9.45	95.66	0.00	0.00
K4-99,2BtProfil1	36.48	3.50	17.77	13.31	0.04	15.05	0.09	0.28	0.24	8.79	95.54	0.01	0.00
K4-99,2BtProfil1	36.27	3.86	17.96	12.93	0.06	15.45	0.05	0.24	0.19	9.16	96.16	0.02	0.00
K4-99,2BtProfil1	35.20	3.62	18.65	12.57	0.04	15.16	0.01	0.49	0.21	9.47	95.42	0.01	0.00
K4-99,2BtProfil1	35.25	3.59	18.86	12.48	0.02	15.39	0.00	0.35	0.22	9.40	95.55	0.00	0.00
K4-99,2BtProfil1	35.63	3.77	18.23	12.22	0.00	15.20	0.01	0.44	0.22	9.44	95.15	0.01	0.00
K4-99,2BtProfil1	35.86	3.86	18.01	12.52	0.01	15.22	0.00	0.47	0.23	9.32	95.49	0.00	0.00
K4-99,2BtProfil1	34.67	3.54	18.51	13.69	0.04	14.73	0.05	0.35	0.26	9.39	95.24	0.00	0.00
K4-99,2BtProfil2 [50]	29.97	38.94	1.57	0.46	0.02	0.00	28.66	0.12	0.02	0.17	99.92	0.00	0.00
K4-99,2BtProfil2	35.80	3.43	18.82	12.16	0.06	15.60	0.06	0.38	0.24	9.40	95.93	0.01	0.00

K4-99,2BtProfil2	35.16	3.35	19.09	12.70	0.03	15.25	0.01	0.61	0.27	9.45	95.92	0.00	0.00
K4-99,2BtProfil2	35.15	3.70	18.00	12.68	0.02	15.49	0.02	0.27	0.24	9.37	94.95	0.01	0.00
K4-99,2BtProfil2	35.01	3.64	17.96	12.52	0.00	15.30	0.01	0.38	0.24	9.45	94.51	0.01	0.00
K4-99,1BtProfil1 [ca 130]	35.30	3.42	16.98	14.44	0.06	14.83	0.04	0.22	0.14	9.69	95.12	0.04	0.00
K4-99,1BtProfil1	35.52	3.56	18.32	14.25	0.05	15.06	0.09	0.16	0.22	9.46	96.69	0.01	0.00
K4-99,1BtProfil1	34.75	3.50	17.55	14.43	0.08	14.67	0.02	0.25	0.16	9.57	94.97	0.02	0.00
K4-99,1BtProfil1	34.17	3.48	17.72	14.41	0.05	14.36	0.02	0.27	0.19	9.46	94.12	0.01	0.00
K4-99,1BtProfil1	35.05	3.54	17.91	13.86	0.00	15.05	0.02	0.24	0.20	9.60	95.45	0.01	0.00
K4-99,1BtProfil1	34.98	3.42	18.29	13.53	0.06	15.02	0.01	0.16	0.20	9.61	95.28	0.02	0.00
K4-99,1BtProfil1	34.93	3.21	18.18	13.52	0.00	14.74	0.05	0.27	0.21	9.56	94.67	0.03	0.00
K4-99,1BtProfil1	35.85	3.70	17.35	13.62	0.03	15.14	0.01	0.24	0.18	9.64	95.74	0.00	0.00
K4-99,1BtProfil1	35.69	3.71	17.45	12.64	0.01	15.59	0.00	0.34	0.20	9.62	95.25	0.01	0.00
K4-99,1BtProfil1	34.78	3.30	18.89	13.08	0.01	14.98	0.02	0.42	0.22	9.62	95.30	0.01	0.00
K4-99,1BtProfil1	34.99	3.38	18.24	13.58	0.00	15.10	0.02	0.40	0.22	9.60	95.52	0.00	0.00
K4-99,1BtProfil1	35.24	3.58	17.74	13.64	0.07	15.03	0.03	0.27	0.17	9.47	95.24	0.01	0.00
K4-105_2Bt1	37.11	4.21	15.13	15.64	0.03	13.33	0.00	0.19	0.09	9.62	95.34	0.00	0.00
K4-105_2Bt2	36.98	4.29	15.10	15.34	0.07	13.29	0.04	0.24	0.09	9.67	95.10	0.00	0.00
K4-105_2Bt3	37.10	4.03	15.25	15.90	0.08	13.14	0.08	0.13	0.08	9.66	95.44	0.00	0.00
K4-105_2Bt4	36.91	3.76	16.05	15.00	0.06	13.47	0.04	0.14	0.14	9.45	95.02	0.00	0.00
K4-105_2Bt5	37.22	4.14	15.12	15.48	0.03	13.27	0.02	0.19	0.11	9.61	95.18	0.00	0.00
K4-106/1Phg1	50.80	0.05	3.57	0.05	3.16	27.20	0.01	0.61	0.23	10.98	96.65	0.03	0.00
K4-106/1Phg2	52.47	0.02	4.45	0.01	2.88	24.72	0.01	0.95	0.20	10.71	96.40	0.01	0.00
K4-106/1Phg3	42.43	0.07	10.69	0.01	12.73	18.96	0.02	1.06	1.68	8.06	95.72	1.05	0.00
K4-106/1Phg4	50.65	0.05	3.68	0.00	2.97	26.73	0.00	0.77	0.34	10.65	95.84	0.01	0.00
K4-117,1PhgProfil1 [230]	48.41	0.72	29.73	4.39	0.10	1.10	0.01	0.20	0.19	10.67	95.52	0.00	0.00
K4-117,1PhgProfil1	48.03	0.71	29.38	4.54	0.04	1.16	0.00	0.26	0.22	10.60	94.95	0.01	0.00
K4-117,1PhgProfil1	48.16	0.69	29.09	4.61	0.00	1.30	0.01	0.29	0.27	10.73	95.15	0.00	0.00
K4-117,1PhgProfil1	48.26	0.69	29.47	4.76	0.05	1.25	0.00	0.17	0.27	10.65	95.56	0.00	0.00
K4-117,1PhgProfil1	48.29	0.71	29.17	4.50	0.03	1.21	0.00	0.28	0.20	10.70	95.08	0.00	0.00
K4-117,1PhgProfil1	48.28	0.73	29.23	4.50	0.08	1.15	0.02	0.22	0.15	10.68	95.03	0.00	0.00
K4-117,1PhgProfil1	48.23	0.71	29.37	4.63	0.05	1.30	0.00	0.19	0.24	10.68	95.40	0.00	0.00
K4-117,1PhgProfil1	48.44	0.74	29.13	4.68	0.05	1.31	0.00	0.17	0.23	10.65	95.40	0.00	0.00
K4-117,1PhgProfil1	48.27	0.70	29.37	4.47	0.07	1.29	0.00	0.15	0.25	10.61	95.18	0.00	0.00
K4-117,1PhgProfil1	48.47	0.70	29.17	4.55	0.04	1.34	0.00	0.21	0.28	10.72	95.48	0.02	0.00
K4-117,1PhgProfil1	48.18	0.75	29.45	4.42	0.01	1.30	0.02	0.16	0.25	10.60	95.13	0.00	0.00
K4-117,1PhgProfil1	48.27	0.71	29.17	4.52	0.05	1.26	0.00	0.17	0.25	10.63	95.03	0.01	0.00
K4-117,1PhgProfil1	48.02	0.77	29.51	4.55	0.05	1.30	0.00	0.21	0.24	10.64	95.30	0.00	0.00
K4-117,1PhgProfil1	48.03	0.73	29.32	4.40	0.08	1.35	0.00	0.18	0.27	10.71	95.06	0.00	0.00
K4-117,1PhgProfil1	48.35	0.75	28.77	4.46	0.01	1.44	0.00	0.19	0.27	10.58	94.81	0.01	0.00
K4-117,1PhgProfil1	48.14	0.76	28.99	4.55	0.04	1.41	0.01	0.23	0.23	10.52	94.89	0.00	0.00
K4-117,1PhgProfil1	48.06	0.72	28.73	4.60	0.04	1.41	0.00	0.17	0.31	10.56	94.59	0.00	0.00
K4-117,1PhgProfil1	47.54	0.74	27.65	4.75	0.07	1.48	0.00	0.14	0.25	10.52	93.12	0.01	0.00
K4-117,1PhgProfil1	48.30	0.76	28.70	4.66	0.06	1.55	0.01	0.24	0.24	10.35	94.86	0.00	0.00
K4-117,1PhgProfil1	48.34	0.79	29.05	4.56	0.03	1.37	0.02	0.12	0.24	10.49	95.02	0.01	0.00
K4-117,1PhgProfil1	48.33	0.77	29.13	4.56	0.04	1.40	0.00	0.18	0.27	10.65	95.30	0.01	0.00
K4-117,1PhgProfil1	48.74	0.75	28.67	4.59	0.03	1.45	0.01	0.26	0.21	10.61	95.33	0.01	0.00
K4-117,1PhgProfil1	48.19	0.83	29.12	4.57	0.04	1.33	0.00	0.15	0.28	10.64	95.15	0.00	0.00
K4-117,1PhgProfil1	48.60	0.84	28.76	4.50	0.04	1.47	0.01	0.30	0.26	10.53	95.32	0.00	0.00
K4-117,1PhgProfil1	48.34	0.87	28.72	4.52	0.06	1.40	0.00	0.21	0.31	10.58	95.01	0.02	0.00
K4-117,1PhgProfil1	48.19	0.83	28.78	4.48	0.04	1.43	0.02	0.26	0.24	10.58	94.84	0.01	0.00
K4-117,1PhgProfil1	45.62	0.81	31.20	4.26	0.00	0.78	0.01	0.26	0.28	10.39	93.63	0.00	0.00
K4-117,1PhgProfil2 [150]	45.85	0.77	31.99	4.15	0.03	0.72	0.00	0.21	0.36	10.52	94.60	0.01	0.00
K4-117,1PhgProfil2	48.50	0.68	28.72	4.70	0.03	1.40	0.00	0.19	0.31	10.37	94.89	0.01	0.00
K4-117,1PhgProfil2	48.93	0.71	28.86	4.60	0.03	1.49	0.00	0.26	0.28	10.59	95.73	0.00	0.00
K4-117,1PhgProfil2	48.54	0.69	28.10	4.72	0.03	1.57	0.00	0.20	0.27	10.54	94.65	0.00	0.00
K4-117,1PhgProfil2	48.74	0.66	28.56	4.82	0.06	1.46	0.00	0.25	0.26	10.56	95.37	0.01	0.00
K4-117,1PhgProfil2	48.65	0.66	28.68	4.64	0.07	1.35	0.01	0.08	0.26	10.48	94.88	0.00	0.00
K4-117,1PhgProfil2	48.34	0.66	28.61	4.59	0.07	1.48	0.00	0.18	0.32	10.60	94.86	0.00	0.00
K4-117,1PhgProfil2	48.08	0.65	29.04	4.61	0.09	1.44	0.00	0.22	0.31	10.64	95.07	0.01	0.00
K4-117,1PhgProfil2	48.80	0.63	28.70	4.65	0.07	1.52	0.00	0.23	0.27	10.58	95.45	0.00	0.00
K4-117,1PhgProfil2	48.61	0.65	28.87	4.59	0.08	1.34	0.00	0.18	0.30	10.62	95.24	0.00	0.00
K4-117,1PhgProfil2	48.20	0.67	28.40	4.61	0.02	1.41	0.00	0.21	0.24	10.41	94.18	0.00	0.00
K4-117,1PhgProfil2	48.62	0.70	29.03	4.50	0.08	1.40	0.00	0.17	0.28	10.54	95.32	0.01	0.00
K4-117,1PhgProfil2	47.54	0.69	29.71	4.35	0.02	1.16	0.01	0.20	0.31	10.31	94.29	0.01	0.00
K4-117,1PhgProfil2	46.28	0.75	30.91	4.28	0.03	0.81	0.00	0.31	0.40	10.56	94.33	0.02	0.00
K4-118b2PhgProfil1 [100]	49.91	0.56	27.69	3.82	0.00	2.49	0.00	0.09	0.41	10.13	95.09	0.00	0.00
K4-118b2PhgProfil1	50.36	0.50	26.47	3.81	0.01	2.89	0.00	0.14	0.36	10.27	94.80	0.00	0.00
K4-118b2PhgProfil1	50.75	0.58	25.67	4.50	0.00	3.04	0.01	0.21	0.32	10.21	95.30	0.00	0.00
K4-118b2PhgProfil1	50.82	0.59	25.45	4.60	0.00	3.08	0.00	0.15	0.27	10.32	95.29	0.01	0.00
K4-118b2PhgProfil1	50.76	0.56	25.48	4.60	0.02	3.10	0.00	0.08	0.31	10.25	95.16	0.02	0.00
K4-118b2PhgProfil1	50.30	0.56	26.04	4.72	0.04	2.96	0.00	0.11	0.31	10.39	95.43	0.00	0.00
K4-118b2PhgProfil1	50.44	0.53	25.84	4.46	0.00	3.10	0.00	0.06	0.32	10.25	94.99	0.01	0.00
K4-118b2PhgProfil1	50.51	0.48	26.36	4.30	0.00	2.90	0.01	0.10	0.32	10.29	95.28	0.01	0.00

K4-118b2PhgProfil1	50.35	0.46	26.98	4.12	0.00	2.85	0.00	0.12	0.37	10.26	95.48	0.01	0.00
K4-118b1Bt1	36.31	1.88	17.20	20.19	0.05	10.27	0.02	0.00	0.22	8.87	94.99	0.01	0.48
K4-118b1Bt2	36.43	1.86	17.30	20.62	0.11	10.49	0.03	0.03	0.17	9.21	96.23	0.00	0.46
K4-118b1Phg1	50.27	0.78	25.68	4.64	0.01	3.13	0.01	0.22	0.36	10.48	95.58	0.00	0.00
K4-118b1Phg2	50.50	0.54	26.68	3.95	0.01	2.84	0.00	0.09	0.38	10.20	95.20	0.00	0.00
K4-119,1PhgProfil1 [780]	46.26	1.16	27.75	4.74	0.00	1.86	0.01	0.25	0.24	10.27	92.53	0.03	0.00
K4-119,1PhgProfil1	48.39	1.16	27.11	4.47	0.00	2.55	0.00	0.38	0.22	10.72	95.01	0.01	0.00
K4-119,1PhgProfil1	48.79	0.68	25.97	4.48	0.02	2.80	0.02	0.31	0.22	10.61	93.89	0.03	0.00
K4-119,1PhgProfil1	49.55	0.71	25.56	4.61	0.00	2.97	0.00	0.33	0.23	10.65	94.61	0.01	0.00
K4-119,1PhgProfil1	50.29	0.58	26.13	4.56	0.02	3.07	0.01	0.24	0.22	10.57	95.68	0.00	0.00
K4-119,1PhgProfil1	50.04	0.62	26.20	4.60	0.03	2.95	0.01	0.26	0.23	10.63	95.57	0.00	0.00
K4-119,1PhgProfil1	49.70	0.65	26.17	4.61	0.00	3.07	0.00	0.28	0.24	10.60	95.32	0.00	0.00
K4-119,1PhgProfil1	49.73	0.62	26.22	4.70	0.00	3.03	0.01	0.26	0.23	10.72	95.51	0.01	0.00
K4-119,1PhgProfil1	49.01	0.67	26.06	4.43	0.02	2.85	0.00	0.27	0.23	10.64	94.18	0.00	0.00
K4-119,1PhgProfil1	49.56	0.66	26.13	4.63	0.02	3.10	0.01	0.27	0.26	10.84	95.47	0.01	0.00
K4-119,1PhgProfil1	49.70	0.64	26.16	4.75	0.03	2.92	0.03	0.34	0.24	10.84	95.64	0.00	0.00
K4-119,1PhgProfil1	49.77	0.61	26.28	4.58	0.02	2.88	0.01	0.31	0.23	10.67	95.36	0.00	0.00
K4-119,1PhgProfil1	50.05	0.66	26.05	4.75	0.02	2.91	0.00	0.38	0.21	10.63	95.67	0.00	0.00
K4-119,1PhgProfil1	50.16	0.68	26.26	4.56	0.06	2.88	0.00	0.37	0.22	10.69	95.86	0.01	0.00
K4-119,1PhgProfil1	49.51	0.74	25.83	4.80	0.03	3.03	0.02	0.35	0.25	10.63	95.19	0.00	0.00
K4-119,1PhgProfil1	49.52	0.72	26.11	4.62	0.00	2.96	0.00	0.31	0.22	10.64	95.11	0.01	0.00
K4-119,1PhgProfil1	49.91	0.63	26.03	4.63	0.00	2.97	0.00	0.34	0.27	10.79	95.57	0.01	0.00
K4-119,1PhgProfil1	49.55	0.68	25.89	4.61	0.01	2.90	0.01	0.28	0.22	10.67	94.80	0.01	0.00
K4-119,1PhgProfil1	50.01	0.64	26.02	4.55	0.00	3.00	0.00	0.33	0.21	10.68	95.44	0.02	0.00
K4-119,1PhgProfil1	49.85	0.68	25.93	4.61	0.00	2.98	0.00	0.22	0.21	10.82	95.29	0.01	0.00
K4-119,1PhgProfil1	49.82	0.62	25.93	4.75	0.02	3.01	0.00	0.34	0.26	10.55	95.30	0.00	0.00
K4-119,1PhgProfil1	50.05	0.66	25.71	4.71	0.06	2.97	0.01	0.28	0.23	10.71	95.38	0.01	0.00
K4-119,1PhgProfil1	50.25	0.65	25.79	4.86	0.01	3.20	0.00	0.42	0.20	10.64	96.01	0.00	0.00
K4-119,1PhgProfil1	49.95	0.67	25.77	4.83	0.00	2.94	0.01	0.39	0.22	10.57	95.35	0.00	0.00
K4-119,1PhgProfil1	49.89	0.69	25.99	4.81	0.00	2.94	0.00	0.38	0.21	10.74	95.65	0.00	0.00
K4-119,1PhgProfil1	49.76	0.68	26.34	4.82	0.00	2.96	0.00	0.35	0.27	10.68	95.87	0.00	0.00
K4-119,1PhgProfil1	49.65	0.70	25.71	4.86	0.01	2.95	0.01	0.18	0.22	10.84	95.12	0.00	0.00
K4-119,1PhgProfil1	49.88	0.72	25.99	4.87	0.03	2.95	0.01	0.25	0.26	10.74	95.68	0.01	0.00
K4-119,1PhgProfil1	49.99	0.65	25.88	4.86	0.03	2.94	0.00	0.19	0.24	10.71	95.48	0.00	0.00
K4-119,1PhgProfil1	50.17	0.72	25.84	4.74	0.01	2.99	0.01	0.28	0.22	10.69	95.67	0.00	0.00
K4-119,1PhgProfil1	49.52	0.69	25.98	4.84	0.00	3.00	0.01	0.27	0.24	10.67	95.22	0.00	0.00
K4-119,1PhgProfil1	50.20	0.71	25.96	4.83	0.00	3.02	0.01	0.27	0.28	10.65	95.94	0.00	0.00
K4-119,1PhgProfil1	50.29	0.67	25.80	4.67	0.02	3.05	0.01	0.32	0.21	10.57	95.60	0.00	0.00
K4-119,1PhgProfil1	49.97	0.68	26.04	4.71	0.03	2.94	0.00	0.41	0.25	10.65	95.68	0.01	0.00
K4-119,1PhgProfil1	49.71	0.55	26.18	4.71	0.02	2.98	0.00	0.34	0.26	10.73	95.48	0.00	0.00
K4-119,1PhgProfil1	49.75	0.75	26.21	4.84	0.02	2.85	0.01	0.36	0.16	10.72	95.65	0.01	0.00
K4-119,1PhgProfil2 [670]	49.67	0.47	26.39	4.56	0.00	2.94	0.00	0.38	0.19	10.97	95.58	0.01	0.00
K4-119,1PhgProfil2	49.71	0.54	26.24	4.58	0.00	2.92	0.00	0.44	0.20	10.81	95.44	0.00	0.00
K4-119,1PhgProfil2	50.47	0.58	26.32	4.55	0.00	2.99	0.00	0.35	0.19	10.78	96.23	0.00	0.00
K4-119,1PhgProfil2	50.31	0.48	26.16	4.63	0.00	3.03	0.00	0.21	0.21	10.85	95.88	0.00	0.00
K4-119,1PhgProfil2	49.73	0.44	26.25	4.55	0.02	2.94	0.01	0.21	0.20	10.66	95.01	0.02	0.00
K4-119,1PhgProfil2	49.96	0.49	26.38	4.47	0.02	3.04	0.02	0.37	0.18	10.67	95.60	0.00	0.00
K4-119,1PhgProfil2	49.55	0.50	26.38	4.64	0.02	2.95	0.00	0.29	0.22	10.93	95.48	0.00	0.00
K4-119,1PhgProfil2	49.70	0.55	26.21	4.51	0.03	3.03	0.03	0.40	0.22	10.88	95.55	0.00	0.00
K4-119,1PhgProfil2	45.25	1.19	26.87	8.03	0.00	3.16	0.02	0.21	0.23	10.48	95.44	0.01	0.00
K4-119,1PhgProfil2	49.57	0.64	26.20	4.38	0.00	3.10	0.00	0.31	0.19	11.01	95.40	0.00	0.00
K4-119,1PhgProfil2	49.37	0.75	26.83	4.58	0.00	2.90	0.00	0.34	0.18	10.74	95.67	0.00	0.00
K4-119,1PhgProfil2	50.14	0.58	25.97	4.66	0.03	3.18	0.00	0.25	0.24	10.81	95.87	0.00	0.00
K4-119,1PhgProfil2	50.35	0.61	25.99	4.41	0.00	3.11	0.00	0.36	0.16	10.84	95.83	0.00	0.00
K4-119,1PhgProfil2	49.75	0.71	25.92	4.49	0.02	3.07	0.00	0.23	0.17	10.90	95.26	0.00	0.00
K4-119,1PhgProfil2	49.50	0.59	26.17	4.50	0.03	3.04	0.00	0.34	0.20	10.88	95.25	0.01	0.00
K4-119,1PhgProfil2	49.15	0.73	26.37	4.77	0.04	2.95	0.00	0.20	0.22	10.87	95.28	0.00	0.00
K4-119,1PhgProfil2	49.54	0.72	26.23	4.69	0.06	2.91	0.00	0.36	0.21	10.74	95.46	0.00	0.00
K4-119,1PhgProfil2	48.64	0.77	26.02	4.75	0.02	2.88	0.02	0.39	0.19	10.50	94.17	0.03	0.00
K4-119,1PhgProfil2	49.29	0.71	26.12	4.81	0.00	2.94	0.00	0.38	0.26	10.74	95.25	0.01	0.00
K4-119,1PhgProfil2	49.29	0.74	26.27	4.82	0.01	2.87	0.00	0.09	0.26	10.80	95.15	0.00	0.00
K4-119,1PhgProfil2	49.05	0.72	26.40	4.78	0.02	2.91	0.00	0.31	0.24	10.88	95.31	0.00	0.00
K4-119,1PhgProfil2	49.68	0.75	26.39	4.76	0.03	2.99	0.00	0.30	0.22	10.91	96.02	0.01	0.00
K4-119,1PhgProfil2	49.40	0.73	26.06	4.85	0.00	2.83	0.00	0.35	0.20	10.69	95.12	0.00	0.00
K4-119,1PhgProfil2	49.16	0.73	26.19	5.01	0.00	2.79	0.00	0.34	0.26	10.69	95.17	0.01	0.00
K4-119,1PhgProfil2	49.14	0.76	26.16	4.82	0.02	2.85	0.00	0.41	0.24	10.73	95.12	0.00	0.00
K4-119,1PhgProfil2	49.44	0.66	26.12	4.95	0.00	2.74	0.01	0.32	0.29	10.85	95.38	0.00	0.00
K4-119,1PhgProfil2	49.48	0.78	26.09	4.88	0.00	2.92	0.01	0.30	0.26	10.71	95.43	0.01	0.00
K4-119,1PhgProfil2	49.25	0.76	26.22	4.83	0.03	2.90	0.00	0.32	0.24	10.74	95.28	0.01	0.00
K4-119,1PhgProfil2	49.49	0.78	25.87	4.88	0.02	2.88	0.00	0.20	0.26	10.64	95.01	0.02	0.00
K4-119,1PhgProfil2	49.66	0.79	26.09	4.87	0.04	2.93	0.00	0.25	0.24	10.80	95.68	0.00	0.00
K4-119,1PhgProfil2	49.71	0.76	26.23	4.78	0.00	2.94	0.00	0.14	0.23	10.89	95.67	0.00	0.00
K4-119,1PhgProfil2	49.40	0.75	26.10	4.95	0.05	2.98	0.01	0.34	0.28	10.77	95.62	0.00	0.00
K4-119,1PhgProfil2	49.27	0.73	25.97	4.95	0.01	2.94	0.00	0.24	0.23	10.81	95.15	0.01	0.00
K4-119,1PhgProfil2	48.41	0.78	25.89	5.04	0.02	2.85	0.00	0.31	0.23	10.53	94.05	0.01	0.00
K4-119,1PhgProfil2	49.20	0.76	26.06	5.10	0.03	2.95	0.00	0.42	0.25	10.57	95.33	0.00	0.00

K4-119,1PhgProfil2	49.31	0.77	26.26	4.79	0.02	2.91	0.01	0.30	0.22	10.71	95.32	0.00	0.00
K4-119,1PhgProfil2	49.04	0.72	26.21	4.93	0.01	2.91	0.00	0.23	0.21	10.77	95.04	0.00	0.00
K4-119,1PhgProfil2	49.07	0.79	25.84	4.77	0.02	2.98	0.00	0.39	0.22	10.81	94.90	0.00	0.00
K4-119,1PhgProfil2	49.33	0.73	26.13	4.85	0.03	2.95	0.00	0.28	0.26	10.65	95.19	0.00	0.00
K4-119,1PhgProfil2	49.28	0.72	26.23	4.88	0.03	2.93	0.01	0.44	0.28	10.73	95.53	0.00	0.00
K4-119,1PhgProfil2	49.29	0.74	26.18	4.91	0.00	2.98	0.02	0.26	0.26	10.76	95.40	0.00	0.00
K4-119,1PhgProfil2	49.38	0.74	26.23	4.83	0.00	2.92	0.00	0.44	0.24	10.87	95.65	0.01	0.00
K4-119,1PhgProfil2	48.90	0.77	26.19	4.90	0.03	2.87	0.00	0.37	0.22	10.74	94.99	0.01	0.00
K4-119,1PhgProfil2	49.75	0.72	26.28	4.69	0.03	2.90	0.00	0.15	0.21	10.85	95.58	0.00	0.00
K4-119,1PhgProfil2	49.13	0.76	25.82	4.89	0.01	2.94	0.00	0.40	0.23	10.80	94.97	0.00	0.00
K4-119,1PhgProfil2	48.96	0.72	25.79	4.88	0.03	2.97	0.00	0.34	0.22	10.81	94.73	0.01	0.00
K4-119,1PhgProfil2	49.45	0.71	25.85	4.93	0.02	2.98	0.00	0.32	0.20	10.91	95.37	0.00	0.00
K4-119,1PhgProfil2	49.63	0.71	25.70	4.77	0.00	3.01	0.00	0.41	0.21	10.52	94.95	0.00	0.00
K4-119,1PhgProfil2	49.55	0.71	25.70	4.77	0.02	3.18	0.00	0.31	0.20	10.69	95.13	0.00	0.00
K4-119-Gl1 embedded [100]	50.18	0.71	26.73	4.27	0.00	2.92	0.00	0.37	0.26	10.68	96.13	0.00	n.d.
K4-119-Gl1	49.98	0.65	26.67	4.56	0.01	2.86	0.00	0.25	0.23	10.73	95.94	0.00	n.d.
K4-119-Gl1	50.29	0.63	26.77	4.58	0.00	2.90	0.00	0.29	0.25	10.46	96.17	0.00	n.d.
K4-119-Gl1	50.05	0.66	26.61	4.62	0.00	2.92	0.00	0.28	0.27	10.59	96.00	0.00	n.d.
K4-119-Gl1	49.86	0.66	26.64	4.38	0.03	2.89	0.00	0.25	0.26	10.58	95.55	0.00	n.d.
K4-119-Gl1	49.90	0.70	26.57	4.82	0.01	2.87	0.00	0.26	0.22	10.60	95.97	0.00	n.d.
K4-119-Gl1	49.91	0.75	26.81	4.59	0.03	2.80	0.00	0.30	0.24	10.60	96.03	0.00	n.d.
K4-119-Gl1	49.85	0.70	26.70	4.61	0.02	2.88	0.00	0.27	0.26	10.76	96.06	0.00	n.d.
K4-119-Gl1	49.55	0.69	26.71	4.59	0.02	2.82	0.00	0.14	0.23	10.71	95.46	0.00	n.d.
K4-119-Gl1	49.42	0.67	27.09	4.55	0.00	2.88	0.00	0.23	0.23	10.70	95.77	0.00	n.d.
K4-119-Gl2 embedded [110]	50.20	0.63	26.47	4.45	0.00	3.04	0.00	0.28	0.28	10.49	95.84	0.00	n.d.
K4-119-Gl2	50.12	0.60	26.18	4.44	0.01	3.18	0.00	0.39	0.17	10.72	95.80	0.01	n.d.
K4-119-Gl2	49.97	0.68	26.72	4.48	0.01	3.00	0.02	0.36	0.28	10.42	95.91	0.00	n.d.
K4-119-Gl2	50.27	0.63	26.39	4.41	0.00	3.09	0.00	0.36	0.23	10.77	96.15	0.00	n.d.
K4-119-Gl2	50.16	0.65	26.48	4.29	0.04	3.08	0.00	0.34	0.21	10.51	95.76	0.00	n.d.
K4-119-Gl2	50.26	0.65	26.59	4.53	0.04	2.96	0.00	0.22	0.26	10.65	96.18	0.00	n.d.
K4-119-Gl2	50.23	0.66	26.47	4.45	0.02	3.04	0.00	0.33	0.28	10.73	96.20	0.00	n.d.
K4-119-Gl2	50.23	0.62	26.73	4.37	0.00	3.08	0.00	0.43	0.24	10.57	96.26	0.00	n.d.
K4-119-Gl2	50.45	0.58	26.29	4.44	0.08	3.09	0.00	0.26	0.24	10.59	96.02	0.02	n.d.
K4-119-Gl2	49.83	0.64	26.39	4.51	0.05	2.96	0.00	0.36	0.22	10.58	95.53	0.01	n.d.
K4-119-Gl3 embedded [110]	48.44	0.51	25.71	4.14	0.00	2.92	0.00	0.19	0.23	10.22	92.35	0.02	n.d.
K4-119-Gl3	50.15	0.57	26.92	4.52	0.00	2.88	0.00	0.39	0.23	10.65	96.31	0.02	n.d.
K4-119-Gl3	49.89	0.64	26.86	4.63	0.00	2.96	0.02	0.36	0.20	10.64	96.20	0.00	n.d.
K4-119-Gl3	48.55	0.66	26.40	4.55	0.01	2.85	0.00	0.31	0.20	9.89	93.42	0.02	n.d.
K4-119-Gl3	49.98	0.64	27.13	4.63	0.00	2.86	0.00	0.29	0.25	10.63	96.41	0.00	n.d.
K4-119-Gl3	49.42	0.64	26.82	4.37	0.02	2.89	0.01	0.33	0.24	10.21	94.95	0.01	n.d.
K4-119-Gl3	46.97	0.62	25.45	4.25	0.01	2.71	0.01	0.25	0.22	10.03	90.52	0.04	n.d.
K4-119-Gl3	49.69	0.68	26.69	4.54	0.00	2.83	0.00	0.22	0.23	10.74	95.60	0.01	n.d.
K4-119-Gl4 embedded [80]	49.46	0.62	27.07	4.31	0.03	2.92	0.00	0.30	0.22	10.66	95.58	0.01	n.d.
K4-119-Gl4	50.07	0.67	26.59	4.48	0.00	2.85	0.04	0.18	0.21	10.51	95.60	0.02	n.d.
K4-119-Gl4	50.13	0.66	26.81	4.30	0.00	2.95	0.00	0.34	0.22	10.70	96.11	0.00	n.d.
K4-119-Gl4	50.05	0.65	26.75	4.38	0.00	2.92	0.00	0.37	0.26	10.61	95.98	0.01	n.d.
K4-119-Gl4	50.36	0.67	26.76	4.42	0.01	2.95	0.00	0.25	0.22	10.61	96.24	0.00	n.d.
K4-119-Gl4	50.00	0.64	26.56	4.56	0.00	2.92	0.00	0.40	0.24	10.63	95.94	0.01	n.d.
K4-119-Gl4	49.92	0.60	26.94	4.41	0.00	2.94	0.01	0.27	0.20	10.41	95.71	0.01	n.d.
K4-119-Gl4	50.08	0.60	26.96	4.45	0.06	2.94	0.00	0.17	0.21	10.66	96.11	0.00	n.d.
K4-119-Gl5 embedded [40]	49.78	0.57	26.40	4.57	0.01	2.90	0.04	0.34	0.24	10.23	95.07	0.00	n.d.
K4-119-Gl5	49.82	0.55	26.49	4.48	0.00	2.98	0.00	0.21	0.20	10.50	95.23	0.01	n.d.
K4-119-Gl5	50.37	0.59	26.72	4.37	0.01	2.95	0.03	0.32	0.21	10.62	96.19	0.00	n.d.
K4-120b2Phg1	51.81	0.83	25.64	3.31	0.03	3.94	0.00	0.27	0.28	10.69	96.78	0.00	0.00
K4-120b2Phg2	51.60	0.63	25.84	3.35	0.00	3.80	0.00	0.26	0.36	10.67	96.49	0.01	0.00
K4-120b2Phg3	51.97	0.53	26.14	3.04	0.00	3.85	0.00	0.34	0.31	10.63	96.80	0.01	0.00
K4-120b3Phg	51.70	0.88	25.45	3.39	0.00	3.87	0.02	0.24	0.27	10.64	96.45	0.00	0.00
K4-120b5Phg1	51.32	0.90	25.36	3.39	0.00	3.88	0.00	0.20	0.29	10.66	96.00	0.01	0.00
K4-120b5PhgProfil1 [ca 1000]	43.34	0.81	27.88	8.57	0.04	4.89	0.21	0.26	0.31	8.49	94.81	0.01	0.00
K4-120b5PhgProfil1	49.50	0.46	27.83	3.88	0.06	2.78	0.00	0.21	0.33	10.70	95.74	0.00	0.00
K4-120b5PhgProfil1	49.43	0.36	27.21	3.84	0.05	2.86	0.01	0.36	0.37	10.64	95.13	0.01	0.00
K4-120b5PhgProfil1	50.31	0.34	27.11	3.47	0.00	3.13	0.00	0.25	0.45	10.55	95.61	0.00	0.00
K4-120b5PhgProfil1	50.38	0.50	26.99	3.49	0.02	3.19	0.00	0.26	0.42	10.47	95.71	0.01	0.00
K4-120b5PhgProfil1	49.70	0.73	25.29	3.12	0.08	3.43	0.00	0.22	0.31	9.99	92.84	0.02	0.00
K4-120b5PhgProfil1	51.04	0.79	25.71	3.19	0.01	3.69	0.00	0.34	0.33	10.60	95.68	0.00	0.00
K4-120b5PhgProfil1	49.91	0.87	25.19	3.46	0.02	3.70	0.07	0.24	0.35	10.44	94.25	0.05	0.00
K4-120b5PhgProfil1	50.08	0.44	27.22	3.56	0.03	3.27	0.00	0.35	0.31	10.80	96.05	0.02	0.00
K4-120b5PhgProfil1	51.08	0.62	25.96	3.40	0.01	3.64	0.00	0.27	0.29	10.67	95.94	0.01	0.00
K4-120b5PhgProfil1	50.83	0.81	25.43	3.16	0.02	3.63	0.00	0.26	0.28	10.60	95.01	0.01	0.00
K4-120b5PhgProfil1	51.12	0.75	25.76	3.29	0.01	3.73	0.00	0.27	0.30	10.73	95.96	0.01	0.00
K4-120b5PhgProfil1	51.26	0.82	25.42	3.23	0.00	3.71	0.00	0.34	0.29	10.85	95.91	0.00	0.00
K4-120b5PhgProfil1	51.09	0.85	25.55	3.37	0.00	3.72	0.00	0.25	0.29	10.78	95.90	0.00	0.00
K4-120b5PhgProfil1	50.82	0.79	25.29	3.41	0.01	3.67	0.00	0.27	0.26	10.58	95.10	0.01	0.00
K4-120b5PhgProfil1	50.99	0.85	25.61	3.29	0.01	3.70	0.00	0.27	0.28	10.78	95.78	0.00	0.00
K4-120b5PhgProfil1	51.03	0.86	25.68	3.37	0.00	3.71	0.00	0.39	0.29	10.72	96.04	0.00	0.00
K4-120b5PhgProfil1	49.14	0.80	25.08	3.31	0.02	3.56	0.00	0.22	0.27	10.06	92.46	0.00	0.00

K4-120d2PhgProfil1Vers2 [ca 260]	51.92	0.59	26.19	3.24	0.04	3.56	0.00	0.26	0.24	10.89	96.92	0.01	0.00
K4-120d2PhgProfil1Vers2	51.59	0.66	25.99	3.33	0.00	3.67	0.00	0.18	0.22	10.78	96.41	0.02	0.00
K4-120d2PhgProfil1Vers2	51.59	0.71	25.74	3.45	0.00	3.63	0.00	0.19	0.23	10.91	96.45	0.01	0.00
K4-120d2PhgProfil1Vers2	51.61	0.71	25.80	3.25	0.04	3.74	0.00	0.22	0.28	10.83	96.48	0.00	0.00
K4-120d2PhgProfil1Vers2	51.75	0.69	25.43	3.33	0.01	3.82	0.00	0.19	0.28	10.57	96.07	0.00	0.00
K4-120d2PhgProfil1Vers2	51.73	0.75	25.85	3.40	0.01	3.68	0.00	0.21	0.30	10.77	96.71	0.01	0.00
K4-120d2PhgProfil1Vers2	52.08	0.67	25.57	3.20	0.02	3.72	0.03	0.28	0.29	10.79	96.64	0.01	0.00
K4-120d2PhgProfil1Vers2	51.85	0.72	25.39	3.26	0.03	3.90	0.00	0.20	0.31	10.74	96.38	0.00	0.00
K4-120d2PhgProfil1Vers2	51.72	0.62	25.69	3.52	0.01	3.96	0.01	0.27	0.29	10.43	96.51	0.03	0.00
K4-120d2PhgProfil1Vers2	51.80	0.68	25.40	3.22	0.02	3.91	0.00	0.16	0.30	10.74	96.22	0.01	0.00
K4-120d2PhgProfil1Vers2	51.85	0.67	25.35	3.41	0.01	3.79	0.00	0.13	0.29	10.76	96.25	0.00	0.00
K4-120d2PhgProfil1Vers2	51.77	0.80	25.40	3.23	0.00	3.94	0.00	0.25	0.30	10.68	96.37	0.00	0.00
K4-120d2PhgProfil1Vers2	51.74	0.74	25.43	3.27	0.00	3.85	0.00	0.24	0.27	10.59	96.13	0.00	0.00
K4-120d2PhgProfil1Vers2	51.44	0.80	25.49	3.46	0.02	3.80	0.00	0.29	0.28	10.61	96.18	0.00	0.00
K4-120d2PhgProfil1Vers2	51.35	0.71	25.37	3.25	0.04	3.83	0.00	0.35	0.26	10.73	95.89	0.02	0.00
K4-120d2PhgProfil1Vers2	51.64	0.75	25.87	3.54	0.01	3.72	0.00	0.32	0.26	10.79	96.91	0.01	0.00
K4-120d2PhgProfil1Vers2	51.57	0.72	25.89	3.33	0.00	3.80	0.00	0.28	0.27	10.79	96.64	0.00	0.00
K4-120d2PhgProfil1Vers2	51.79	0.81	25.61	3.33	0.04	3.86	0.00	0.29	0.27	10.53	96.54	0.02	0.00
K4-120d2PhgProfil1Vers2	50.50	0.67	25.37	3.37	0.00	3.50	0.00	0.35	0.25	10.59	94.60	0.03	0.00
K4-120d2PhgProfil1Vers2	51.61	0.82	25.73	3.26	0.05	3.81	0.00	0.30	0.28	10.78	96.63	0.01	0.00
K4-120d2PhgProfil1Vers2	51.53	0.81	25.56	3.33	0.01	3.93	0.00	0.33	0.27	10.69	96.46	0.02	0.00
K4-120d2PhgProfil1Vers2	51.44	0.80	25.51	3.27	0.04	3.94	0.00	0.36	0.25	10.95	96.56	0.02	0.00
K4-120d2PhgProfil1Vers2	51.48	0.82	25.61	3.40	0.00	3.70	0.00	0.32	0.26	10.61	96.20	0.00	0.00
K4-120d2PhgProfil1Vers2	51.41	0.85	25.54	3.25	0.01	3.85	0.01	0.27	0.25	10.65	96.08	0.02	0.00
K4-120d2PhgProfil1Vers2	51.34	0.82	25.55	3.21	0.04	3.83	0.00	0.24	0.27	10.89	96.19	0.00	0.00
K4-120d2PhgProfil1Vers2	50.99	0.80	25.11	3.74	0.00	4.32	0.05	0.20	0.22	10.53	95.96	0.00	0.00
K4-120d2PhgProfil1Vers2	51.24	0.79	25.80	3.30	0.00	3.79	0.13	0.32	0.24	10.71	96.32	0.01	0.00
K4-120d2PhgProfil1 [ca 260]	51.60	0.56	25.55	4.19	0.00	4.90	0.04	0.20	0.21	10.02	97.26	0.00	0.00
K4-120d2PhgProfil1	52.47	0.71	27.01	3.22	0.00	3.77	0.00	0.23	0.21	10.78	98.39	0.01	0.00
K4-120d2PhgProfil1	52.03	0.77	26.70	3.24	0.01	3.79	0.00	0.17	0.26	10.81	97.79	0.00	0.00
K4-120d2PhgProfil1	52.22	0.66	26.73	3.49	0.03	3.92	0.02	0.30	0.23	10.74	98.34	0.00	0.00
K4-120d2PhgProfil1	52.10	0.73	26.69	3.36	0.00	3.89	0.02	0.21	0.28	10.71	97.99	0.00	0.00
K4-120d2PhgProfil1	52.27	0.71	26.93	3.48	0.02	3.90	0.00	0.24	0.26	10.60	98.41	0.00	0.00
K4-120d2PhgProfil1	51.97	0.74	26.59	3.43	0.00	3.89	0.00	0.21	0.25	10.72	97.79	0.01	0.00
K4-120d2PhgProfil1	52.15	0.69	26.47	3.43	0.03	3.93	0.00	0.19	0.29	10.79	97.98	0.01	0.00
K4-120d2PhgProfil1	52.22	0.73	26.32	3.49	0.03	4.13	0.00	0.24	0.27	10.69	98.12	0.01	0.00
K4-120d2PhgProfil1	52.35	0.80	26.09	3.45	0.01	4.31	0.00	0.21	0.28	10.78	98.27	0.01	0.00
K4-120d2PhgProfil1	52.09	0.65	26.81	3.55	0.03	3.83	0.00	0.26	0.32	10.86	98.39	0.01	0.00
K4-120d2PhgProfil1	52.22	0.83	26.36	3.52	0.00	4.18	0.00	0.27	0.29	10.72	98.39	0.00	0.00
K4-120d2PhgProfil1	52.31	0.78	26.36	3.44	0.00	4.14	0.00	0.31	0.29	10.70	98.33	0.00	0.00
K4-120d2PhgProfil1	52.31	0.76	26.15	3.30	0.02	4.17	0.00	0.22	0.27	10.73	97.93	0.01	0.00
K4-120d2PhgProfil1	52.48	0.83	25.82	3.43	0.03	4.27	0.00	0.27	0.28	10.73	98.15	0.00	0.00
K4-120d2PhgProfil1	51.33	0.77	25.96	3.42	0.00	3.95	0.00	0.27	0.25	10.32	96.28	0.01	0.00
K4-120d2PhgProfil1	52.05	0.72	26.59	3.37	0.00	3.93	0.00	0.24	0.25	10.84	97.98	0.01	0.00
K4-120d2PhgProfil1	52.42	0.80	26.45	3.45	0.04	4.14	0.00	0.18	0.24	10.65	98.38	0.00	0.00
K4-120d2PhgProfil1	51.99	0.65	26.96	3.46	0.00	4.00	0.00	0.30	0.25	10.78	98.39	0.01	0.00
K4-120d2PhgProfil1	52.07	0.82	26.44	3.36	0.03	4.05	0.00	0.32	0.26	10.81	98.16	0.00	0.00
K4-120d2PhgProfil1	52.28	0.80	26.29	3.33	0.00	4.10	0.00	0.30	0.29	10.76	98.14	0.00	0.00
K4-120d2PhgProfil1	52.10	0.80	26.39	3.27	0.01	4.15	0.01	0.30	0.23	10.68	97.94	0.01	0.00
K4-120d2PhgProfil1	52.20	0.78	26.44	3.43	0.03	4.06	0.01	0.30	0.25	10.67	98.17	0.01	0.00
K4-120d2PhgProfil1	51.99	0.78	26.42	3.34	0.02	4.15	0.01	0.26	0.26	10.74	97.97	0.01	0.00
K4-120d2PhgProfil1	52.01	0.83	26.37	3.42	0.01	4.02	0.01	0.31	0.27	10.67	97.91	0.01	0.00
K4-120d2PhgProfil1	50.83	0.81	25.59	4.40	0.03	4.74	0.07	0.31	0.25	10.40	97.44	0.01	0.00
K4-120d2PhgProfil1	52.30	0.83	26.53	3.38	0.01	3.93	0.11	0.26	0.28	10.71	98.33	0.00	0.00
K4-120d2PhgProfil2 [ca 230]	51.68	0.73	26.24	3.92	0.01	4.19	0.02	0.22	0.29	10.57	97.87	0.00	0.00
K4-120d2PhgProfil2	52.08	0.87	25.89	3.63	0.02	3.87	0.00	0.31	0.29	10.74	97.70	0.00	0.00
K4-120d2PhgProfil2	52.05	0.80	26.42	3.58	0.00	3.92	0.01	0.29	0.35	10.65	98.06	0.02	0.00
K4-120d2PhgProfil2	52.16	0.89	26.27	3.48	0.00	3.98	0.00	0.25	0.29	10.78	98.09	0.00	0.00
K4-120d2PhgProfil2	52.29	0.85	26.17	3.67	0.02	3.92	0.01	0.29	0.31	10.47	98.00	0.00	0.00
K4-120d2PhgProfil2	52.00	0.83	26.67	3.56	0.04	3.84	0.00	0.25	0.28	10.65	98.11	0.00	0.00
K4-120d2PhgProfil2	51.92	0.84	26.54	3.69	0.00	3.82	0.00	0.37	0.26	10.60	98.03	0.01	0.00
K4-120d2PhgProfil2	52.20	0.87	26.33	3.43	0.01	4.03	0.00	0.23	0.24	10.70	98.03	0.01	0.00
K4-120d2PhgProfil2	52.21	0.86	26.45	3.62	0.01	3.91	0.00	0.27	0.26	10.70	98.29	0.03	0.00
K4-120d2PhgProfil2	52.08	0.86	26.31	3.51	0.02	3.88	0.00	0.30	0.27	10.73	97.97	0.01	0.00
K4-120d2PhgProfil2	52.20	0.90	26.22	3.56	0.00	4.08	0.00	0.25	0.26	10.73	98.19	0.00	0.00
K4-120d2PhgProfil2	51.98	0.89	26.30	3.40	0.02	4.07	0.00	0.27	0.27	10.80	98.00	0.01	0.00
K4-120d2PhgProfil2	52.02	0.88	26.16	3.66	0.00	3.90	0.01	0.22	0.28	10.42	97.56	0.04	0.00
K4-120d2PhgProfil2	52.24	0.85	26.49	3.42	0.03	3.90	0.00	0.23	0.31	10.91	98.37	0.01	0.00
K4-120d2PhgProfil2	52.10	0.89	26.47	3.58	0.01	3.84	0.00	0.27	0.26	10.64	98.06	0.02	0.00
K4-120d2PhgProfil2	51.95	0.91	26.51	3.52	0.00	3.84	0.00	0.31	0.31	10.75	98.11	0.00	0.00
K4-120d2PhgProfil2	51.84	0.86	26.22	3.47	0.00	3.83	0.00	0.27	0.31	10.71	97.51	0.02	0.00
K4-120d2PhgProfil2	51.90	0.82	26.53	3.40	0.03	3.78	0.02	0.26	0.32	10.44	97.48	0.03	0.00
K4-120d2PhgProfil2	52.10	0.74	26.49	3.47	0.00	3.87	0.00	0.23	0.32	10.60	97.81	0.00	0.00
K4-120d2PhgProfil2	52.18	0.81	26.35	3.46	0.00	3.90	0.00	0.34	0.32	10.69	98.05	0.01	0.00
K4-120d2PhgProfil2	52.19	0.79	26.51	3.55	0.00	3.86	0.00	0.18	0.33	10.75	98.15	0.02	0.00
K4-120d2PhgProfil2	51.75	0.73	26.22	3.35	0.03	3.87	0.00	0.32	0.32	10.73	97.32	0.01	0.00
K4-120d2PhgProfil2	52.11	0.49	26.70	3.40	0.00	3.94	0.01	0.28	0.33	10.68	97.94	0.01	0.00
K4-120d2PhgProfil2	51.68	0.53	26.44	3.58	0.05	4.03	0.00	0.51	0.35	10.46	97.63	0.00	0.00

K4-120d2PhgProfil2	51.36	0.45	26.41	3.40	0.04	3.83	0.01	0.25	0.44	10.28	96.48	0.00	0.00
JNar2,3PhgProfil1 [290]	50.37	0.60	29.51	1.58	0.00	3.20	0.09	n.d.	0.29	10.11	95.75	0.01	0.00
JNar2,3PhgProfil1	50.65	0.63	30.24	1.64	0.00	3.24	0.00	n.d.	0.39	10.57	97.36	0.00	0.00
JNar2,3PhgProfil1	50.71	0.53	30.90	1.44	0.00	3.02	0.01	n.d.	0.32	10.66	97.58	0.00	0.00
JNar2,3PhgProfil1	51.23	0.63	28.98	1.37	0.05	3.68	0.03	n.d.	0.37	10.46	96.80	0.02	0.00
JNar2,3PhgProfil1	51.77	0.60	28.11	1.47	0.00	3.57	0.40	n.d.	0.32	9.96	96.19	0.00	0.00
JNar2,3PhgProfil1	51.20	0.64	28.45	1.55	0.00	3.82	0.04	n.d.	0.38	10.55	96.62	0.01	0.00
JNar2,3PhgProfil1	51.39	0.62	28.46	1.77	0.04	3.87	0.02	n.d.	0.35	10.62	97.13	0.02	0.00
JNar2,3PhgProfil1	51.24	0.60	28.16	1.84	0.01	3.96	0.02	n.d.	0.37	10.28	96.48	0.02	0.00
JNar2,3PhgProfil1	51.56	0.66	28.26	1.86	0.00	3.82	0.04	n.d.	0.33	10.44	96.96	0.02	0.00
JNar2,3PhgProfil1	51.37	0.72	28.32	1.59	0.00	3.79	0.03	n.d.	0.34	10.63	96.78	0.02	0.00
JNar2,3PhgProfil1	51.14	0.65	28.27	1.54	0.00	3.88	0.04	n.d.	0.30	10.41	96.22	0.00	0.00
JNar2,3PhgProfil1	51.35	0.66	28.37	1.68	0.00	3.78	0.03	n.d.	0.32	10.50	96.69	0.02	0.00
JNar2,3PhgProfil1	51.47	0.70	28.45	1.63	0.01	3.72	0.05	n.d.	0.35	10.50	96.88	0.02	0.00
JNar2,3PhgProfil1	50.07	0.59	30.18	1.49	0.01	3.08	0.18	n.d.	0.37	10.54	96.51	0.03	0.00
JNar2,3PhgProfil1	50.32	0.55	30.63	1.62	0.02	2.97	0.04	n.d.	0.34	10.68	97.16	0.02	0.00
JNar2,3PhgProfil1	49.37	0.50	31.15	1.51	0.00	2.81	0.09	n.d.	0.34	10.51	96.27	0.04	0.00
JNar2,3PhgProfil1	50.27	0.52	30.84	1.50	0.00	2.94	0.03	n.d.	0.29	10.74	97.12	0.01	0.00
JNar2,2PhgProfilInCzo1 [80]	52.09	0.66	30.14	2.19	0.04	3.31	0.12	0.34	0.41	8.89	98.19	0.01	0.00
JNar2,2PhgProfilInCzo1	54.98	0.51	27.30	1.98	0.01	4.31	0.04	0.39	0.34	8.93	98.79	0.01	0.00
JNar2,2PhgProfilInCzo1	55.01	0.53	27.39	1.94	0.01	4.40	0.06	0.41	0.34	9.01	99.09	0.01	0.00
JNar2,2PhgProfilInCzo1	54.64	0.50	26.99	2.02	0.00	4.33	0.02	0.45	0.37	8.96	98.27	0.00	0.00
JNar2,2PhgProfilInCzo1	54.02	0.56	27.55	2.03	0.01	4.34	0.01	0.32	0.38	9.02	98.22	0.00	0.00
JNar2,2PhgProfilInCzo1	53.74	0.58	28.12	1.89	0.00	4.08	0.01	0.30	0.38	9.04	98.14	0.01	0.00
JNar2,2PhgProfilInCzo1	52.82	0.62	27.98	1.85	0.00	4.00	0.03	0.25	0.36	9.06	96.97	0.00	0.00
JNar2,2PhgProfilInCzo1	50.99	0.57	30.51	1.93	0.00	3.12	0.05	0.39	0.44	9.03	97.02	0.01	0.00
JNar2,2PhgProfilInCzo1	51.26	0.55	30.86	1.87	0.01	3.10	0.04	0.22	0.34	8.89	97.14	0.00	0.00
JNar2,2PhgProfilInCzo1	52.79	0.54	29.88	1.82	0.01	3.61	0.05	0.34	0.38	9.10	98.50	0.00	0.00
JNar2,2PhgProfilInCzo1	51.95	0.54	29.32	1.82	0.00	3.68	0.04	0.34	0.35	8.99	97.04	0.00	0.00
JNar2,2PhgProfilInCzo1	52.84	0.53	29.27	1.87	0.01	3.90	0.02	0.32	0.35	8.92	98.02	0.00	0.00
JNar2,2PhgProfilInCzo1	53.87	0.54	28.72	1.86	0.01	3.91	0.09	0.37	0.38	8.53	98.28	0.01	0.00
JNar2,2PhgProfilInCzo1	53.33	0.50	29.63	1.75	0.00	3.65	0.11	0.34	0.31	7.90	97.50	0.01	0.00
JNar2,2PhgProfilInCzo1	54.05	0.50	28.20	1.99	0.01	4.25	0.03	0.31	0.36	9.00	98.71	0.00	0.00
JNar2,2PhgProfilInCzo1	53.82	0.50	28.17	1.95	0.04	4.15	0.09	0.45	0.37	8.62	98.14	0.00	0.00
JNar2,2PhgProfilInCzo1	54.02	0.50	27.72	2.05	0.00	4.28	0.03	0.26	0.36	9.01	98.23	0.01	0.00
JNar2,2PhgProfilInCzo1	54.49	0.49	27.46	2.07	0.01	3.95	0.00	0.28	0.37	8.74	97.86	0.01	0.00
JNar2,2PhgProfilInCzo1	54.29	0.50	27.92	2.09	0.01	4.11	0.07	0.38	0.35	8.49	98.20	0.02	0.00
JNar2,2PhgProfilInCzo2 [ca 20]	52.34	0.60	30.74	2.13	0.00	3.30	0.11	0.43	0.40	9.10	99.14	0.01	0.00
JNar2,2PhgProfilInCzo2	50.91	0.49	30.79	1.96	0.00	3.09	0.05	0.25	0.42	8.81	96.77	0.01	0.00
JNar2,2PhgProfilInCzo2	53.74	0.60	28.04	2.02	0.00	3.96	0.04	0.44	0.38	8.86	98.09	0.00	0.00
JNar2,2PhgProfilInCzo2	54.25	0.53	27.39	1.94	0.07	4.13	0.01	0.42	0.41	9.03	98.17	0.00	0.00
JNar2,2PhgProfilInCzo2	52.84	0.60	29.23	2.05	0.00	3.63	0.06	0.57	0.39	9.07	98.44	0.01	0.00
JNar2,3PhgProfilInGrt1 [20]	50.89	0.72	31.39	2.00	0.02	2.73	0.20	0.45	0.56	9.14	98.08	0.00	0.00
JNar2,3PhgProfilInGrt1	51.19	0.66	31.04	1.98	0.00	2.95	0.03	0.23	0.55	9.06	97.69	0.01	0.00
JNar2,3PhgProfilInGrt1	51.57	0.62	30.96	2.01	0.03	3.02	0.04	0.25	0.65	9.10	98.24	0.01	0.00
JNar2,3PhgProfilInGrt2 [40]	50.82	0.61	30.61	2.01	0.01	2.76	0.05	0.47	0.56	10.11	98.01	0.01	0.00
JNar2,3PhgProfilInGrt2	51.36	0.56	30.26	1.98	0.04	2.95	0.03	0.35	0.57	9.93	98.02	0.00	0.00
JNar2,3PhgProfilInGrt2	51.17	0.55	30.63	1.88	0.00	2.84	0.06	0.28	0.62	9.89	97.93	0.00	0.00
JNar2,3PhgProfilInGrt2	51.55	0.53	30.68	1.87	0.00	2.96	0.02	0.34	0.57	9.92	98.44	0.02	0.00
JNar2,3PhgProfilInGrt2	51.79	0.54	30.42	2.03	0.02	2.99	0.04	0.49	0.58	10.10	98.99	0.00	0.00
JNar2,1PhgProfilInGrt1 [100]	55.85	0.15	11.58	4.85	0.01	7.71	13.36	0.08	7.23	0.00	100.82	0.00	0.00
JNar2,1PhgProfilInGrt1	56.31	0.13	12.18	4.61	0.04	7.61	12.94	0.00	7.43	0.01	101.25	0.00	0.00
JNar2,1PhgProfilInGrt1	56.25	0.12	12.02	4.77	0.04	7.83	13.13	0.00	7.32	0.00	101.48	0.00	0.00
JNar2,1PhgProfilInGrt1	56.25	0.14	12.13	4.87	0.01	7.54	12.86	0.17	7.57	0.03	101.57	0.01	0.00
JNar2,1PhgProfilInGrt1	56.44	0.08	12.04	4.91	0.02	7.75	13.17	0.01	7.30	0.01	101.74	0.01	0.00
JNar2,1PhgProfilInGrt1	56.35	0.13	12.03	4.93	0.00	7.65	13.11	0.05	7.25	0.00	101.51	0.00	0.00
JNar2,1PhgProfilInGrt1	56.38	0.13	12.05	4.68	0.04	7.76	13.11	0.00	7.53	0.01	101.69	0.00	0.00
JNar2,1PhgProfilInGrt1	56.44	0.15	11.66	4.76	0.00	7.81	13.38	0.00	7.28	0.00	101.49	0.00	0.00
JNar2,1PhgProfilInGrt1	56.10	0.10	11.37	4.88	0.00	7.97	13.55	0.00	6.96	0.01	100.93	0.02	0.00
JNar2,1PhgProfilInGrt1	56.01	0.14	11.37	5.18	0.06	7.92	13.93	0.00	7.10	0.02	101.73	0.01	0.00
JNar2,1PhgProfilInGrt2 [70]	56.30	0.22	11.43	4.86	0.01	7.88	13.40	0.00	7.14	0.00	101.23	0.00	0.00
JNar2,1PhgProfilInGrt2	55.97	0.13	12.00	4.80	0.03	7.68	13.48	0.00	7.26	0.00	101.35	0.00	0.00
JNar2,1PhgProfilInGrt2	56.59	0.08	12.42	4.40	0.08	7.43	12.56	0.02	7.82	0.00	101.40	0.00	0.00
JNar2,1PhgProfilInGrt2	56.33	0.12	12.39	4.42	0.03	7.37	12.75	0.01	7.54	0.02	100.97	0.01	0.00
JNar2,1PhgProfilInGrt2	56.38	0.08	11.97	4.87	0.08	7.60	12.92	0.09	7.40	0.00	101.38	0.00	0.00
JNar2,1PhgProfilInGrt2	55.79	0.15	12.14	4.94	0.06	7.75	13.11	0.13	7.28	0.00	101.35	0.00	0.00
PK2-4cBt3	36.81	3.40	18.71	14.39	0.01	14.43	0.02	n.d.	0.32	9.32	97.40	0.01	0.00
PK2-4cBt4	37.12	3.39	19.20	13.87	0.02	14.49	0.03	n.d.	0.40	9.34	97.86	0.01	0.00
PK2-4cBt5	36.52	3.02	19.24	13.87	0.00	14.25	0.05	n.d.	0.35	9.13	96.43	0.00	0.00
PK2-4cBt6	37.63	3.21	17.86	13.14	0.03	14.89	0.08	n.d.	0.37	9.41	96.62	0.01	0.00
PK2-4cBt7	43.00	2.29	20.69	9.82	0.00	11.27	2.14	n.d.	2.30	7.26	98.78	0.01	0.00
PK2-4cBt8	39.06	2.81	19.40	11.99	0.04	14.18	0.57	n.d.	0.99	8.82	97.85	0.01	0.00
PK2-4cBt9	38.22	2.87	18.95	11.99	0.03	14.47	0.29	n.d.	0.81	9.20	96.83	0.00	0.00

Table A6. Microprobe analyses of epidote minerals

Sample [Profile length in μm]	SiO_2	TiO_2	Al_2O_3	FeO	MnO	MgO	CaO	BaO	Na_2O	K_2O	Sum
K4-35,2CpxInCzoProfil1 [70]	40.50	0.05	32.03	1.12	0.00	0.36	23.35	0.16	0.04	0.05	97.66
K4-35,2CpxInCzoProfil1	39.65	0.04	32.46	1.19	0.00	0.05	24.65	0.03	0.04	0.00	98.11
K4-35,2CpxInCzoProfil1	40.10	0.04	32.57	1.18	0.01	0.06	24.63	0.00	0.03	0.02	98.62
K4-35,2CpxInCzoProfil1	40.15	0.05	32.65	1.23	0.00	0.07	24.70	0.13	0.00	0.00	98.98
K4-53,3Ep1	38.77	0.19	27.81	7.27	0.03	0.15	23.02	n.d.	0.01	0.01	97.26
K4-53,3Ep2	38.90	0.17	27.82	7.13	0.04	0.14	23.15	n.d.	0.02	0.01	97.39
K4-118b1alla3	37.75	0.17	24.42	11.21	0.04	0.07	22.93	n.d.	n.d.	n.d.	96.58
K4-118b1alla4	36.90	0.11	22.79	11.79	0.02	0.21	20.67	n.d.	n.d.	n.d.	92.48
K4-118b1alla2	38.11	0.12	23.80	11.88	0.03	0.05	22.91	n.d.	n.d.	n.d.	96.90
K4-120c2EpProfil [50]	38.12	0.13	23.62	11.63	0.02	0.22	23.01	n.d.	0.00	0.00	96.75
K4-120c2EpProfil	38.30	0.15	23.62	11.61	0.05	0.22	23.09	n.d.	0.04	0.01	97.08
K4-120c2EpProfil	38.02	0.16	23.62	11.98	0.09	0.24	23.09	n.d.	0.03	0.01	97.24
PK2-4g,2Ep1	38.95	0.13	27.96	7.27	0.00	0.22	23.28	n.d.	0.01	0.00	97.81
PK2-4g,2Ep2	38.85	0.07	27.86	7.30	0.05	0.25	23.20	n.d.	0.00	0.01	97.59
PK2-4g,2Ep3	39.29	0.11	28.33	6.72	0.04	0.21	23.33	n.d.	0.01	0.00	98.04
PK2-4g,1Ep1	38.73	0.12	27.32	7.88	0.01	0.25	23.17	n.d.	0.01	0.00	97.49
PK2-4g,1turmalin2a	39.21	0.09	28.15	6.72	0.02	0.14	23.41	n.d.	0.00	0.01	97.74
PKL2ep1	38.37	0.12	24.60	11.24	0.03	0.18	22.86	0.10	0.04	0.00	97.54
PKL2ep2	38.36	0.10	24.32	11.89	0.02	0.11	23.06	0.05	0.00	0.01	97.91
JNar2,2CpxInCzoProfil2 [80]	39.82	0.03	31.56	1.91	0.00	0.04	23.83	0.01	0.06	0.01	97.27
JNar2,2CpxInCzoProfil2	39.77	0.09	31.78	1.84	0.01	0.03	23.50	0.11	0.01	0.01	97.15
JNar2,2CpxInCzoProfil2	40.60	0.05	30.52	2.27	0.00	0.51	23.26	0.06	0.40	0.00	97.66
JNar2,2CpxInCzoProfil2	39.88	0.09	31.77	1.62	0.00	0.04	23.65	0.04	0.07	0.00	97.16
JNar2,2CpxInCzoProfil2	39.94	0.10	31.79	1.49	0.05	0.04	23.53	0.06	0.06	0.00	97.04
JNar2,2CpxInCzoProfil2	39.83	0.09	31.73	1.73	0.00	0.04	23.71	0.09	0.03	0.00	97.24
JNar2,1czoProfil [80]	39.88	0.11	31.45	1.86	0.00	0.10	23.71	0.01	0.04	0.00	97.15
JNar2,1czoProfil	39.81	0.08	31.69	1.95	0.00	0.02	23.81	0.08	0.00	0.00	97.44
JNar2,1czoProfil	39.97	0.09	31.77	1.66	0.00	0.03	23.48	0.00	0.02	0.00	97.02
JNar2,1czoProfil	39.95	0.07	31.91	1.48	0.01	0.02	23.57	0.09	0.00	0.00	97.09
JNar2,1czoProfil	40.08	0.07	31.92	1.50	0.00	0.03	23.52	0.00	0.04	0.01	97.18
JNar2,1czoProfil	40.09	0.09	31.42	1.78	0.00	0.06	23.12	0.09	0.03	0.05	96.73

Table A7. Microprobe analyses of feldspar/plagioclase

	SiO_2	TiO_2	Al_2O_3	FeO	CaO	BaO	Na_2O	K_2O	Sum
PK2-4cBt1	60.86	0.02	23.87	0.18	4.88	n.d.	9.71	0.08	99.60
PK2-4cBt2	60.81	0.02	23.43	0.35	6.56	n.d.	8.87	0.11	100.15
PK2-4	62.64	0.02	23.56	0.29	3.91	n.d.	9.96	0.22	100.60
PK2-4	60.05	0.01	25.32	0.24	6.97	n.d.	8.29	0.08	100.96
JNar2,3Alb1	64.34	0.01	21.90	0.21	3.04	0.01	10.58	0.17	100.26
JNar2,3Alb2	62.00	0.03	23.38	0.12	4.98	0.03	9.42	0.18	100.14
JNar2,3Alb3	64.13	0.04	21.83	0.11	2.87	0.02	10.96	0.14	100.12
K4-76Plag1	64.52	0.01	22.48	0.13	3.69	0.01	10.35	0.22	101.40
K4-76PlagTwin1	63.48	0.00	22.30	0.06	3.75	0.03	10.19	0.22	100.04
K4-76Plag2	64.19	0.05	22.48	0.09	3.70	0.01	10.56	0.24	101.32
K4-76PlagTwin2	64.54	0.01	22.62	0.10	3.62	0.01	10.37	0.23	101.50
K4-57,2Bt7	62.32	0.01	23.29	0.22	4.51	n.d.	9.73	0.26	100.33
K4-57,2Bt8	62.21	0.01	23.52	0.15	4.68	n.d.	9.82	0.26	100.65
K4-57,2Alb1	62.50	0.02	23.96	0.31	5.36	0.00	9.30	0.28	101.74
K4-57,2Alb2	63.30	0.04	23.49	0.23	5.08	0.03	9.36	0.32	101.85
K4-57,2albInSymp1	59.57	0.00	25.04	0.21	7.31	0.01	7.84	0.19	100.16
K4-57,2albInSymp2	59.03	0.44	22.80	2.36	4.77	0.06	7.92	1.31	98.68
K4-58,1alb2	65.97	0.01	21.93	0.16	2.79	0.00	10.70	0.27	101.83
K4-58,1alb3	66.72	0.00	21.25	0.16	2.26	0.02	10.94	0.36	101.70
K4-58,1bt1	64.59	0.02	21.68	0.20	2.50	n.d.	10.73	0.36	100.08
K4-58,1bt3	64.47	0.00	21.76	0.26	2.56	n.d.	10.85	0.32	100.21
K4-58,1bt5	64.55	0.05	22.22	0.43	2.85	n.d.	10.76	0.25	101.12
K4-58,1bt6	64.50	0.00	21.71	0.15	2.53	n.d.	10.91	0.31	100.11
K4-58,1bt7	64.76	0.01	21.75	0.26	2.53	n.d.	10.86	0.32	100.48

Table A8. Whole rock geochemistry

sample/wt%	SiO_2	TiO_2	Al_2O_3	Fe_2O_3(tot)	MnO	MgO	CaO	Na_2O	K_2O	P_2O_5	CO_2	H_2O	Sum
K4-120B	43.96	3.18	14.33	16.31	0.21	5.32	11.79	2.40	0.64	0.47	0.68	0.49	99.77
K4-120C	43.78	3.02	13.87	16.58	0.21	5.80	12.39	2.09	0.39	0.31	0.99	0.28	99.71
K4-105	44.80	2.21	15.36	15.03	0.24	6.67	11.74	2.08	0.68	0.13	0.81	0.11	99.86
K4-100	41.64	3.76	12.48	22.00	0.20	6.50	10.46	1.74	0.01	0.15			99.67

ppm	Ba	Cr	Nb	Rb	Sr	V	Y	Zn	Zr	Ga	Ni	Sc
K4-120B	194	136	18	12	134	393	48	129	229	22	93	
K4-120C	128	137	20	10	364	411	36	129	208	21	87	
K4-105	188	266	17	12	198	322	52	121	263	19	86	
K4-100	<20	96	5	<3	78	950	28	134	98	22	227	42

ppm	Y	La	Ce	Pr	Pr korr.	Nd	Sm	Eu	Gd	Tb	Dy	Ho
K4-100	20.5	1.8	6.9	1.6	1.2	6.5	3.0	1.4	4.3	0.5	4.1	0.8

ppm	Er	Tm	Yb	Lu	Sc	Ba
K4-100	2.3	0.3	1.9	0.3	42.3	7.8

Table A9. Ar-Ar geochronology

Laser output	$^{40}Ar/^{39}Ar$		$^{37}Ar/^{39}Ar$		$^{36}Ar/^{39}Ar$ (x10^{-3})		K/Ca	$^{40}Ar^*$ (%)	^{39}ArK fraction (%)	$^{40}Ar^*/^{39}ArK$		Age(±1s) (Ma)	
K4-4	C08057	white mica											
J=	0.00196												
0.014	300.67	± 2.68	0.1844	± 0.3736	950.30	± 11.56	3.19	6.61	0.05	19.89	± 2.48	69.05	± 8.46
0.018	39.14	± 0.14	0.0068	± 0.0240	95.47	± 1.04	86.64	27.92	0.64	10.93	± 0.30	38.27	± 1.04
0.02	12.64	± 0.03	0.0022	± 0.0007	5.27	± 0.05	263.50	87.67	12.11	11.08	± 0.03	38.82	± 0.19
0.022	12.47	± 0.02	0.0003	± 0.0005	3.61	± 0.02	1753.24	91.44	21.13	11.40	± 0.02	39.90	± 0.17
0.024	9.07	± 0.01	0.0011	± 0.0002	0.90	± 0.01	512.14	97.08	23.57	8.81	± 0.01	30.91	± 0.13
0.026	7.33	± 0.02	0.0015	± 0.0002	0.51	± 0.01	391.04	97.94	18.01	7.18	± 0.02	25.22	± 0.12
0.028	7.34	± 0.02	0.0061	± 0.0044	1.03	± 0.05	97.15	95.85	5.29	7.03	± 0.02	24.72	± 0.13
0.03	7.33	± 0.02	0.0074	± 0.0041	1.23	± 0.06	79.66	95.05	3.67	6.96	± 0.03	24.48	± 0.14
0.034	7.15	± 0.01	0.0058	± 0.0074	0.56	± 0.02	101.15	97.69	8.62	6.99	± 0.01	24.56	± 0.11
0.044	7.30	± 0.00	0.0021	± 0.0043	0.51	± 0.03	279.77	97.93	6.90	7.15	± 0.01	25.13	± 0.10
K4-61	C08067	white mica											
J=	0.00200												
0.014	83.00	± 0.91	0.1289	± 0.1716	241.42	± 6.34	4.56	14.06	0.23	11.67	± 1.88	41.59	± 6.62
0.018	14.33	± 0.05	0.0008	± 0.0015	17.15	± 0.12	703.58	64.64	8.35	9.27	± 0.05	33.09	± 0.23
0.02	9.31	± 0.05	0.0000	± 0.0003	2.07	± 0.03	19380.81	93.42	29.73	8.70	± 0.05	31.07	± 0.21
0.022	8.75	± 0.04	0.0000	± 0.0003	0.71	± 0.02	15171.46	97.60	23.28	8.54	± 0.04	30.51	± 0.20
0.024	8.76	± 0.05	0.0035	± 0.0009	0.51	± 0.02	168.64	98.29	16.54	8.61	± 0.05	30.76	± 0.21
0.026	8.78	± 0.02	0.0071	± 0.0017	0.48	± 0.04	82.30	98.39	8.08	8.63	± 0.02	30.86	± 0.14
0.03	8.57	± 0.02	0.0073	± 0.0016	0.44	± 0.04	80.81	98.50	7.93	8.44	± 0.02	30.16	± 0.14
3.6-5	9.09	± 0.03	0.0099	± 0.0018	0.78	± 0.09	59.70	97.49	5.86	8.86	± 0.04	31.67	± 0.18
K4-70H	C08064	biotite											
J=	0.00200												
0.02	148.11	± 0.09	0.0027	± 0.0027	482.68	± 1.16	221.50	3.70	14.79	5.47	± 0.34	19.60	± 1.22
0.022	13.66	± 0.02	0.0005	± 0.0005	18.82	± 0.14	1303.77	59.31	21.98	8.10	± 0.04	28.95	± 0.19
0.024	11.21	± 0.01	0.0000	± 0.0001	10.32	± 0.05	11805.21	72.80	17.76	8.16	± 0.02	29.16	± 0.13
0.026	9.98	± 0.02	0.0006	± 0.0020	6.10	± 0.03	1004.76	81.93	14.37	8.18	± 0.02	29.21	± 0.13
0.028	10.00	± 0.04	0.0035	± 0.0018	6.09	± 0.09	170.21	82.01	8.98	8.20	± 0.04	29.28	± 0.19
0.03	10.06	± 0.02	0.0065	± 0.0042	7.04	± 0.12	90.87	79.31	4.80	7.97	± 0.04	28.49	± 0.19
0.032	10.31	± 0.03	0.0076	± 0.0100	7.11	± 0.13	77.18	79.64	4.08	8.22	± 0.05	29.34	± 0.20
0.036	10.14	± 0.04	0.1961	± 0.0133	6.29	± 0.08	3.00	81.89	5.75	8.30	± 0.04	29.65	± 0.20
4-4.4	10.24	± 0.02	0.0902	± 0.0065	7.42	± 0.08	6.52	78.69	7.50	8.05	± 0.03	28.77	± 0.16

K4-117 C08073

J= 0.00199

0.014	117.86	±	0.88	0.0699	±	0.1019	302.66	±	2.62	8.42	24.13	0.70	28.44	±	0.63	99.06	±	2.18
0.018	16.79	±	0.02	0.0179	±	0.0111	26.79	±	0.22	32.82	52.86	12.42	8.87	±	0.07	31.50	±	0.27
0.02	10.29	±	0.03	0.0048	±	0.0050	5.03	±	0.03	123.65	85.56	26.17	8.80	±	0.03	31.24	±	0.16
0.022	9.61	±	0.03	0.0059	±	0.0063	2.54	±	0.04	99.00	92.20	21.11	8.86	±	0.03	31.45	±	0.16
0.024	9.26	±	0.02	0.0086	±	0.0099	2.75	±	0.09	68.02	91.24	11.99	8.45	±	0.03	30.01	±	0.16
0.028	10.04	±	0.03	0.0080	±	0.0087	4.03	±	0.06	73.13	88.17	21.77	8.86	±	0.03	31.44	±	0.17
0.03	10.32	±	0.03	0.0179	±	0.0031	1.50	±	0.14	32.79	95.71	5.84	9.88	±	0.05	35.03	±	0.23

K4-118 C08058 phengite

J= 0.00197

0.014	235.66	±	1.93	0.1389	±	0.2459	679.70	±	7.20	4.23	14.78	0.24	34.83	±	1.45	119.50	±	4.84
0.016	32.66	±	0.14	0.0462	±	0.0281	60.25	±	0.37	12.72	45.51	1.27	14.86	±	0.12	51.96	±	0.47
0.018	18.10	±	0.02	0.0066	±	0.0049	18.93	±	0.06	89.37	69.09	8.95	12.50	±	0.02	43.81	±	0.19
0.02	12.10	±	0.03	0.0002	±	0.0005	2.64	±	0.02	3228.91	93.55	28.70	11.32	±	0.03	39.70	±	0.18
0.024	11.56	±	0.04	0.0007	±	0.0009	1.33	±	0.02	807.28	96.59	36.24	11.17	±	0.04	39.18	±	0.21
0.024	11.59	±	0.02	0.0046	±	0.0050	1.36	±	0.02	127.64	96.55	19.24	11.19	±	0.02	39.27	±	0.18
0.026	16.17	±	0.06	0.0069	±	0.0142	3.59	±	0.21	84.95	93.44	2.21	15.11	±	0.08	52.81	±	0.35
0.03	23.04	±	0.06	0.0343	±	0.0354	3.97	±	0.24	17.14	94.92	1.78	21.87	±	0.09	75.95	±	0.44
0.034	56.56	±	0.11	0.7150	±	0.0866	7.43	±	0.50	0.82	96.28	1.37	54.49	±	0.18	183.61	±	0.91

K4-120b C08063 phengite

J= 0.00198

0.016	45.45	±	0.08	0.0012	±	0.0027	100.82	±	0.76	496.95	34.45	3.91	15.65	±	0.22	55.07	±	0.80
0.018	23.78	±	0.04	0.0059	±	0.0066	22.99	±	0.36	100.46	71.43	6.81	16.99	±	0.11	59.68	±	0.45
0.02	20.53	±	0.01	0.0002	±	0.0004	6.82	±	0.07	3400.67	90.18	26.76	18.52	±	0.02	64.96	±	0.27
0.022	20.14	±	0.03	0.0025	±	0.0020	5.34	±	0.05	231.21	92.17	37.42	18.56	±	0.03	65.11	±	0.28
0.024	22.59	±	0.04	0.0081	±	0.0064	4.88	±	0.11	72.77	93.62	11.78	21.15	±	0.05	74.02	±	0.34
0.026	26.05	±	0.08	0.0203	±	0.0334	5.86	±	0.11	29.00	93.36	6.65	24.32	±	0.08	84.84	±	0.43
0.03	28.34	±	0.07	0.0346	±	0.0889	6.10	±	0.21	16.99	93.65	2.75	26.55	±	0.09	92.42	±	0.48
0.036	21.27	±	0.17	0.0543	±	0.0597	3.97	±	0.23	10.84	94.52	3.91	20.11	±	0.17	70.43	±	0.66

K4-120d C08056 phengite

J= 0.00198

0.014	72.15	±	1.19	0.2373	±	0.2831	181.43	±	6.34	2.48	25.73	0.42	18.57	±	1.70	65.13	±	5.86
0.018	21.97	±	0.02	0.0133	±	0.0091	12.55	±	0.09	44.34	83.14	48.84	18.27	±	0.03	64.10	±	0.27
0.02	19.73	±	0.02	0.0005	±	0.0010	2.85	±	0.11	1259.43	95.73	38.17	18.89	±	0.04	66.25	±	0.29
0.022	19.12	±	0.08	0.0843	±	0.0488	4.70	±	0.49	6.98	92.80	2.36	17.74	±	0.17	62.29	±	0.62
0.026	24.55	±	0.12	0.1355	±	0.0809	18.13	±	0.97	4.34	78.25	1.47	19.21	±	0.31	67.35	±	1.08
0.03	21.03	±	0.07	0.0424	±	0.0315	7.11	±	0.45	13.88	90.03	8.74	18.93	±	0.15	66.39	±	0.57

Table A10. Calculation of zeta

sample	serial no.	zeta	error	locality of apatite
UP30-20	1	388.4	24.4	Durango
UP30-21	2	377.2	23.2	Durango
UP43-1	3	374.6	22.5	Durango
UP65-3	4	387.2	30.8	Fish Canyon Tuff
UP65-4	5	382.6	33.1	Fish Canyon Tuff
UP7-28	6	357.4	23.6	Fish Canyon Tuff
UP7-29	7	363.6	23.7	Mount Dromedary
UP43-4	8	382.9	21.8	Mount Dromedary
UP43-5	9	381.2	20.9	Mount Dromedary

Calculation of zeta

arithmetic mean	=	(sum Xi) / i	X = value
weighted arithmetic mean	=	sum (Xi/(Si squared)) / sum ((1/ Si) squared)	S = error
error on weighted mean	=	1/ (sqrt (sum (1/ Si squared))	i = ith value in series
simple mean error	=	(sum Si) / i	

arithmetic mean	**weighted arithmetic mean**	error on weighted mean	simple mean error
377.2	**376.6**	8.0	24.9